
**Faculty of Medicine and Health Sciences**

# THE ROLE OF CASPASE-ACTIVATED DNase (CAD) IN CHROMOSOME BREAKS DURING OXIDATIVE STRESS-INDUCED APOPTOSIS

Boon Siaw Shi

Master of Science
(Cancer Molecular Biology)
2009

## ACKNOWLEDGEMENTS

I would like to take this opportunity to express my utmost appreciation to my supervisor, Associate Professor Dr. Samirah Abdullah@Sim Sai Peng for guidance, patience and continuous support throughout my study. I have been given the freedom to explore in the area of my study. Without her encouragement and guidance, this thesis would not be completed or written. Besides, my co-supervisor, Miss Chin Mei Yieng has also been very caring and supportive. Not forgetting my fun yet supportive labmates (Peter, Cynthia, Grace, Sang Nee, Bing Ling, Shen Chuen, Hui Chong, David, Wilson, Angela, Sunita, Royston, Cyrus, Paul, Siti, Suzie and Hartini). They have lightened up my life and given me their moral support. Most of all, I would like to express my billions and trillions of thanks my parents and siblings who have been given me invaluable support, care and love. I also wish to thank Professor Shigekazu Nagata (University of Osaka, Japan) for providing us the plasmids; Associate Professor Dr. Edmund Sim Ui Hang (Universiti Malaysia Sarawak) for providing us the HeLa cell line; as well as Professor Sam Choon Kook (Nanyang Technology of University) for providing us the NPC cell line. I would like to acknowledge financial support from UNIMAS via Postgraduate Student Fellowship (Zamala), research grants from Malaysian Government, namely Intensification of Research in Priority Areas (IRPA) Grants No. 09-02-09-1017, E14008/F07/08/06-02-09-1020 and Science Fund (E14088)-02-01-09-SF0014. Last but not least, I would like to thank personal who involved directly and indirectly in helping in this study.

## ABSTRACT

Chromosomal rearrangement, such as additions, deletions, translocations and inversions are phenomena commonly observed in various types of cancers including leukaemia and nasopharyngeal carcinoma (NPC). In leukaemia, structural rearrangements of the Mixed Lineage Leukaemia (MLL) gene at 11q23 have been reported extensively. In NPC, chromosomal deletions and additions are observed where one of the common deletion sites is at 11q23. However, the precise site of deletion has not been mapped to the gene level. Furthermore, mechanism leading to chromosome rearrangements in NPC is unknown. In the case of leukaemia, there are various mechanisms being proposed where apoptotic nuclease is one of them. Harmful or mutated cells undergo autonomous elimination through programmed cell death or apoptosis. However, dysregulation of apoptosis can result in many diseases such as cancer. Morphologically, apoptotic cells are characterised by cells dislodgement, membrane blebbing, condensation of cytoplasm and nucleus, as well as cellular fragmentation into membrane apoptotic bodies. In addition, apoptotic cells DNA integrity is changed where chromatin loop domains are released and may be followed by internucleosomal cleavage. This leads to DNA ladder formation typically seen on agarose gel. During apoptosis, there are a few DNases responsible for DNA fragmentation, in which one of them is the Caspase-activated DNase (CAD). In normal growing cells, CAD co-exists with its inhibitor, ICAD, and remains inactive. ICAD also functions as a chaperone for CAD and is essential for the correct folding of CAD protein. When triggered by apoptotic stimuli, ICAD is cleaved by caspase-3, releasing the active CAD. Activated CAD will then cleave the genomic DNA. Mutation of CAD and ICAD may result in reduction of internucleosomal cleavage. This is because mutated CAD does not form stable complex with the DNA. Moreover, mutated

ICAD, which is resistant to caspase-3 cleavage, is bound to CAD permanently, thus, in spite of the presence of apoptotic stimuli, CAD does not become activated. *In vitro* studies showed that a variety of cells, including tumour cell lines and normal cell types undergo apoptosis when they are exposed to oxidative stress. Oxidative stress occurs when cells are injured due to elevated production of reactive oxygen species (ROS), such as hydrogen peroxide, $H_2O_2$. Excessive ROS production leads to direct DNA damage, which can result in induction of apoptosis in severely damaged cells. We hypothesized that, during stress-induced apoptosis, CAD may cause the initial chromosome break which eventually leads to result in chromosomal rearrangement of the MLL breakpoint cluster region (bcr). Our dose response experiments showed that, NPC (SUNE1) and cervical cancer (HeLa) cell line treated with 50 μM and 100 μM $H_2O_2$ respectively for 20 hours showed apoptotic features. Cleavage within the MLL bcr was further confirmed via Inverse Polymerase Chain Reaction (IPCR). In order to study the role of CAD and ICAD, these genes were expressed transiently and stably in mammalian cell lines. Human and murine CAD genes as well as murine ICAD genes were subcloned into 2 expression vectors, namely pcDNA and pTracer. The role of CAD was studied by using four approaches. Firstly, CAD was overexpressed in mammalian cell line but the result was inconclusive. This may be due to the CAD expressed was not functional. Secondly, mutant ICAD was overexpressed to inhibit CAD directly. Mutant ICAD which was resistant to caspase-3 cleavage bound to endogenous CAD and hence CAD could not execute its DNase activity. However, the IPCR result showed that mutant ICAD did not reduce cleavage within the MLL bcr. Therefore, third approach was designed where CAD was inhibited indirectly by using caspase inhibitor. Caspase inhibitor should block the activation of caspase-3 and thus block CAD activation. However, our result showed no significant difference between cells with and without caspase inhibition. This could be due to

inefficient uptake of caspase inhibitor into the cells. There might be other DNase responsible to DNA cleavage within the MLL bcr, such as Endonuclease G (Endo G), Apoptosis-induced Factor (AIF) and so on. Chromosomal breakage within the MLL bcr might not solely dependent on the caspase pathway upon oxidative stress-induced apoptosis. In the last approach, CAD and/or ICAD was overexpressed. As confirmed by Western blotting, co-expression of CAD and ICAD resulted in CAD expression. Overexpression of ICAD alone was sufficient to induce high levels of endogenous CAD expression. From the IPCR result, it showed that CAD expression enhances cleavage within the MLL bcr upon oxidative stress. In conclusion, oxidative stress can induce apoptosis in mammalian cell lines. CAD may be involved directly in the cleavage of the MLL bcr. Chromosome rearrangements via the apoptotic process may be dependent on the chromatin structure. In order to further strengthen the hypothesis, involvement of CAD in the cleavage of other genes should also be studied.

## ABSTRAK

*Penyusunan semula kromosom, seperti penambahan, delesi, translokasi dan songsangan adalah phenomena yang biasanya dijumpai dalam pelbagai jenis kanser, seperti leukemia dan kanser nasofaringeal (NPC). Dalam leukaemia, penyusunan semula struktur bagi gen Mixed Lineage Leukaemia (MLL) pada lokasi kromosom 11q23 telah dilaporkan secara ekstensif. Dalam NPC, delesi dan penambahan kromosom diperhatikan di mana salah satu tapak delesi biasanya berlaku pada kromosom 11q23. Walau bagaimanapun, tapak delesi yang tepat belum dipetakan pada tahap gen. Lagipun, mekanisma yang mengakibatkan penyusunan semula kromosom dalam NPC belum diketahui. Dalam kes leukemia, terdapat pelbagai jenis mekanisma yang dicadangkan di mana nuklease apoptotik adalah salah satu daripadanya. Sel-sel yang bahaya atau mengalami mutasi akan disingkirkan secara automatic melalui proses apoptosis atau kematian sel diprogramkan. Walau bagaimanapun, disregulasi dalam apoptosis akan mengakibatkan pelbagai penyakit seperti kanser. Secara morfologi, sel-sel yang apoptotik boleh dicirikan oleh penanggalan sel, "blebbing" membran, kondensasi bagi nukleus dan sitoplasma dan fragmentasi selular kepada badan apoptotik membrane. Tambahan pula, DNA integrasi bagi sel yang apoptotik ditukarkan di mana domain loop kromatin dilonggarkan dan boleh diikuti oleh belahan internukleosom. Ini akan mengakibatkan pembentukan tangga DNA yang dijumpai pada gel agaros. Semasa apoptosis, terdapat beberapa DNase yang bertanggungjawab kepada fragmentasi DNA, di mana salah satu daripadanya adalah Caspase-activated DNase (CAD). Dalam sel-sel bertumbuh yang normal, CAD wujud bersama dengan perencatnya, ICAD, dan kekal inaktif. ICAD juga berfungsi sebagai pengiring bagi CAD dan adalah amat penting bagi pembentukan protein CAD yang betul. Apabila dirangsang oleh stimuli apoptotik, ICAD dibelah oleh caspase-3, membebaskan CAD yang aktif. CAD yang diaktifkan seterusnya akan membelah DNA*

*genomik. CAD dan ICAD yang mengalami mutasi akan mengakibatkan pengurangan dalam belahan internukleosom. Ini adalah disebabkan oleh CAD yang mengalami mutasi tidak membentuk compleks tetap dengan DNA. Tambahan pula, ICAD yang mengalami mutasi di mana ia adalah tahan terhadap belahan caspase-3, terikat kepada CAD secara kekal. Dengan demikian, walaupun dengan kewujudan rangsangan apoptosis, CAD tidak diaktifkan. Kajian in vitro menunjukkan bahawa pelbagai sel, termasuk sel-sel tumor dan sel yang normal mengalami apoptosis apabila terdedah kepada tekanan pengoksidaan. Tekanan pengoksidaan berlaku apabila sel-sel tercedera disebabkan oleh penghasilan spesis reaktif oksigen (ROS) yang meningkat, seperti hidrogen peroksida ($H_2O_2$). Penghasilan ROS yang berlebihan akan mengakibatkan DNA dihancur secara langsung, yang mana akan menyebabkan rangsangan apoptosis dalam sel-sel yang mengalami penghancuran yang teruk. Kami mengandaikan bahawa, semasa apopsis dirangsangkan oleh tekanan, CAD boleh mengakibatkan permulaan bagi pemutusan kromosom yang mana akhirnya akan menyebabkan penyusunan semula kromosom bagi MLL breakpoint cluster region (bcr). Menurut uji kaji tindakbalas sukatan kami, NPC (SUNE1) dan kanser serviks (HeLa) sel dirawat dengan 50 μM dan 100 μM $H_2O_2$ masing-masing selama 20 jam menunjukkan ciri-ciri apoptosis. Pembelahan dalam MLL bcr seterusnya disahkan melalui Reaksi Rantaian Polimerasi Tersongsang (IPCR). Demi mengaji peranan CAD dan ICAD, gen-gen ini diekpres secara sementara atau tetap dalam sel-sel mamalia. Gen-gen CAD bagi manusia dan tikus dan juga gen ICAD bagi tikus disubklonkan ke dalam 2 vektor ekspressi, iaitu pcDNA dan pTracer. Peranan CAD dikaji dengan menggunakan 4 cara. Pertama, CAD diekspress secara berlebihan dalam sel mamalia tetapi keputusan tidak dapat disimpulkan. Ini mungkin disebabkan oleh CAD yang diekspress tidak berfungsi. Kedua, ICAD yang mengalami mutasi secara berlebihan bagi merencat CAD secara langsung. ICAD mutan,*

*yang mana tahan terhadap belahan caspase-3 terikat kepada CAD endogenius, maka CAD tidak dapat menjalani fungsi aktiviti DNasenya. Walau bagaimanapun, keputusan IPCR menunjukkan bahawa ICAD mutan tidak mengurangkan pembelahan dalam MLL bcr. Dengan demikian, cara ketiga dilakarkan di mana CAD direncatkan secara tidak langsung dengan menggunakan perencat caspase. Perencat caspase sepatutnya menghalang pengaktifan caspase-3 dan seterusnya menghalang pengaktifan CAD. Walau bagaimanapun, keputusan kami menunjukkan bahawa, tiada perbezaan yang jelas di antara sel-sel dirawat dengan atau tanpa perencat caspase. Ini mungkin disebabkan oleh ketidakefisien. Terdapat kemungkinan juga terdapat DNase lain bertanggungjawab kepada pembelahan DNA dalam MLL bcr, seperti Endonuclease G (Endo G), Apoptosis-induced Factor (AIF) dan sebagainya. Pemutusan kromosom dalam MLL bcr mungkin tidak bergantung sepenuhnya kepada caspase pathway di atas apoptosis yang dirangsangkan oleh tekanan oksidatif. Dalam cara yang terakhir, CAD dan/atau ICAD diekspress secara berlebihan. Seperti yang disahkan oleh Western blotting, keputusan ekspressi CAD bersama dengan ICAD mengakibatkan ekspressi CAD. Pengekspressan ICAD secara berlebihan sahaja adalah memadai untuk mendorong ekspressi CAD endogenius pada tahap yang tinggi. Daripada keputusan IPCR, ditunjukkan bahawa ekspressi CAD menambahkan pembelahan dalam MLL bcr semasa mengalami tekanan oksidasi. Kesimpulannya, tekanan oksidatif boleh mendorong apoptosis dalam sel-sel mamalia. CAD mungkin terlibat dalam pembelahan MLL bcr secara langsung. Penyusunan semula kromosom melalui proses apoptosis mungkin bergantung kepada struktur kromatin. Selanjutnya, bagi mengukuhkan hipotesis, penglibatan CAD dalam pembelahan gen-gen yang lain harus dikaji.*

## TABLE OF CONTENTS

## LIST OF TABLES

## LIST OF FIGURES

## LIST OF ABBREVIATIONS

| Abbreviation | Description |
|---|---|
| % | percentage |
| γ | gamma |
| μ | micro |
| β | beta |
| AIF | Apoptotic-inducing factor |
| ALL | acute lymphoblastic leukaemia |
| AML | acute myeloid leukaemia |
| APS | ammonium persulfate |
| Asp | Aspartate |
| Bam | Bacillus amyloliquefaciens |
| bcr | breakpoint cluster region |
| *Bgl* | *Bacillus globigii* |
| bp | base pairs |
| BSA | bovine serum albumin |
| $Ca^{2+}$ | calcium ion |
| CAD | caspase-activated DNase |
| cm | centimetre |
| $CO_2$ | carbon dioxide |
| dATP | deoxyadenosine triphosphate |
| DFF | DNA Fragmentation Factor |
| DFF35 | DNA Fragmentation Factor 35 |
| DFF40 | DNA Fragmentation Factor 40 |
| DFF45 | DNA Fragmentation Factor 45 |
| DMEM | Dulbecco's Modified Eagle Medium |
| DMSO | dimethyl sulfoxide |
| DNA | deoxyribonucleic acid |
| dNTPs | deoxyribonucleoside triphosphates |
| DSB | Double-stranded break |
| *E. coli* | *Eschericia coli* |
| EBV | Epstein-Barr virus |
| EDTA | ethylene diamine tetracetic acid |
| Endo G | Endonuclease G |
| FBS | fetal bovine serum |
| GAPDH | glyceraldehyde 3-phosphate dehydrogenase |
| GFP | Green fluorescence protein |
| Gln | Glutamine |
| GSH | reduced form of glutathione |
| $H_2O_2$ | hydrogen peroxide |
| hCAD | human strain CAD |
| HCl | hydrochloric acid |
| *Hind* | Haemophilus influenza Rd |
| HMW | high molecular weight |
| hr | hour |
| HRP | Horseradish peroxidase |
| ICAD | inhibitor of CAD |

| | |
|---|---|
| ICE | interleukin (IL-1b)-converting enzyme |
| IPCR | Inverse Polymerase Chain Reaction |
| K | amino acid Lysine |
| kb | kilobases |
| kDa | kilodalton |
| *Kpn* | *Klebsiella pneumonia* |
| kV | kilovolt |
| LB | Luria-Bertani |
| M | molar |
| MARs | Matrix attachment regions |
| mCAD | mouse strain of CAD |
| MDR | minimal deletion region |
| MDS | myelodysplastic syndrome |
| ME | mercaptoethanol |
| $Mg^{2+}$ | magnesium ion |
| MgSO4 | magnesium sulphate |
| mICAD | mouse strain of ICAD |
| mICAD-L | long form of mICAD |
| mICAD-Ldm | double mutated long form of mICAD |
| min | minute |
| ml | millilitre |
| MLL | Mixed Lineage Leukaemia |
| mM | milimolar |
| Msc | Micrococcus |
| mtDNA | mitochondrial DNA |
| Na3C6H5O7 | sodium citrate |
| NaCl | sodium chloride |
| NaOH | sodium hydroxide |
| NCBI | National Center for Biotechnology Information |
| NEB | New England Biolabs |
| ng | nanogram |
| NHEJ | Non-homologous End Joining |
| nm | nanometre |
| NPC | Nasopharyngeal carcinoma |
| O.D. | optical density |
| $O_2^-$ | superoxide anion |
| $^oC$ | degree Celcius |
| OH· | hydroxyl radical |
| PBS | phosphate buffer saline |
| PBST | phosphate buffer saline –Tween 20 |
| PCR | Polymerase Chain Reaction |
| pg | picogram |
| pmol | picomole |
| PMSF | phenylmethylsulfonyl fluoride |
| Q | amino acid Glutamine |
| RCmICAD-Ldm | reverse compliment of mICAD-Ldm |
| RNA | ribonucleic acid |
| ROS | reactive oxygen species |

| | |
|---|---|
| rpm | revolution per minute |
| SARs | scaffold attachment regions |
| SDS | Sodium dodecyl sulphate |
| *Sma* | *Serratia marcescens* |
| SOD | superoxide dismutase |
| sUPW | sterilised ultra pure water |
| t-AML | therapy-related acute myeloid leukaemia |
| TBE | tracheobronchial epithelial |
| TBE | Tris Boric Acid-EDTA |
| TE | Tris-EDTA |
| V | volumes |
| WHO | World Health Organisation |
| X | times |
| x g | multiples of earth's gravitational force |
| *Xba* | *Xanthomonas badrii* |
| µg | microgram |
| µl | microlitre |
| µM | micromolar |

# CHAPTER 1

# INTRODUCTION AND LITERATURE REVIEW

## 1.1 Carcinogenesis and Chromosome Rearrangements

Cancer is a complex disease, which can arise from all tissue types. Carcinogenesis involves multiple genes in diverse pathways involving initiation, progression, invasion and metastasis of the affected cells. In fact, it is widely accepted that, there is sequential accumulation of mutations that activates oncogenes and disrupts tumour suppressor genes. This event, in combination with multiple cycles of clonal selection and evolution facilitate the process of carcinogenesis. It has been estimated that disruption of about six cellular processes are required for transformation from normal to cancerous cells. Cancer patients often present with a wide range of clinical manifestations (Hanahan and Weinberg, 2000) with genetic anomalies. Cancer cells often exist as a group of neoplastic cells which proliferate uncontrollably with several hallmarks, namely mutations, genetic instability and gaining of unlimited replication potential (Aplan, 2006; Meza-Junco *et al.*, 2006). Genomic instability has been proposed to play an important role in cancer by accelerating the accumulation of genetic mutations for cancer cells evolution (Murnane, 2006).

Genomic instability is one of the hallmarks of cancer (Hanahan and Weinberg, 2000). Studies showed that, telomere attrition triggers genomic instability in epithelial carcinogenesis (Artandi and DePinho, 2000). Genomic instability, ranging from gross aberration to limited DNA alteration is a commonly observed event in cancer cells. Typical DNA alteration involves one or a few base pairs. Microsatellite instability, particularly somatic microsatellite instability, which involves the genomic fragility in tandemly repeated DNA is an example.

Microsatellites occur frequently in the human genome. Their high degree of polymorphism makes them useful as markers for genetic linkage analysis (Hearne *et al.*, 1992). The polymorphism arises from DNA replication errors and misalignment between template and daughter DNA strands in the region(s) containing repetitive sequences (Gonzalez-Zulueta *et al.*, 1993; Burks *et al.*, 1994; Merlo *et al.*, 1994). It had also been found that, exogenously introduced DNA into cultured tumour cells results in chromosomal instability where their gene equilibrium was disturbed (ter Elst *et al.*, 2006).

Chromosomal rearrangements (Mitelman *et al.*, 1997), such as additions, deletions, translocations, inversions, chromosome breakage or loss, and gene amplification are commonly found in several types of cancers (Koeffler *et al.*, 1991; Smith *et al.*, 2004; Umanskaia *et al.*, 2005). These include leukaemia, nasopharyngeal carcinoma, colorectal carcinoma, ovarian carcinoma, hepatocellular carcinoma, thyroid carcinoma, breast carcinoma, renal carcinoma, pancreatic carcinoma and so on (Johansson *et al.*, 1992; Jen *et al.*, 1994; Fang *et al.*, 1995; Samuli Hemmer *et al.*, 1999; Simon *et al.*, 2000; Rennstam *et al.*, 2001; Crawley and Furge, 2002; Leroy *et al.*, 2002; Betti *et al.*, 2003). Many molecular studies had been conducted to look at breakpoints from specific aberrations. It has been found that deletions often lead to loss of a tumour-suppressor gene. Translocations or inversions can be specific to tumour type and idiopathic (Rabbitts, 1994).

## 1.2 Leukaemia and Chromosomal Rearrangement

Leukaemia is a very heterogenous disease. It can be classified to *de novo* acute myeloid leukaemia (AML), acute lymphoblastic leukaemia (ALL), biphenotypic leukaemia, and secondary acute myeloid leukaemias (Heim and Mitelman, 1987). Some of the chromosomal translocations identified include the t(4; 11) and t( 11; 19) found in ALL and the t(9; 11), t(6; 11 ) **,** and t(11; 19) found in *de novo* AML (Kaneko *et al.*, 1988; Raimondi, 1993). Clonal chromosomal rearrangements in at least 70 to 80% were detected through molecular diagnosis (Burmeister and Thiel, 2001). These chromosomal rearrangements occur in a non-random manner. Certain types of rearrangements are often associated with the particular leukaemia subtype (Heim and Mitelman, 1995; Super *et al.*, 1997). This suggests that chromosomal changes could contribute to the etiology and pathogenesis of the associated leukaemia subtypes (Burmeister and Thiel, 2001).

*De novo* acute myeloid or lymphoid leukaemias are observed particularly common in infant below one year of age (Kaneko *et al.*, 1986; Hayashi *et al.*, 1988; Kaneko *et al.*, 1988). In this disease, chromosomal rearrangements, namely translocations and deletions, at location 11q23 are common events (Hunger *et al.*, 1993). In has been found that, in acute myeloid leukaemias (AML), the most common chromosomal translocations are t(9;11)(p21-24;q23) and t(11;19)(q23;p13) (Kaneko *et al.*, 1986; Hayashi *et al.*, 1988; Kaneko *et al.*, 1988; Hudson *et al.*, 1991). Translocations at 11q23 acute lymphoblastic leukaemias (ALL) are usually undifferentiated and often display mixed-lineage characteristics (Kaneko *et al.*, 1986; Mirro *et al.*, 1986; Kaneko *et al.*, 1988; Raimondi *et al.*, 1989; Gibbons *et al.*, 1990; Raimondi *et al.*, 1989). For lymphoma and myelodysplastic syndrome (MDS), chromosomal rearrangements at locus 11q23 were also observed even through rarely (Heim and Mitelman,

1995). Studies found that 11q23 contains the Mixed Lineage Leukaemia (MLL) gene. The involvement of this gene in leukaemia has been studied extensively (Dimartino and Cleary, 1999; DeVore *et al.*, 1989). The name MLL is given to this gene due to its indiscriminate rearrangements found in myeloid, lymphocytic and biphenotypic leukaemias. In most of the chromosomal translocations identified in leukaemia, each gene has a specific partner gene (Collins and Rabbitts, 2002). The MLL gene was found to translocate with more than 50 other genes (Pais *et al.*, 2005; Meyer *et al.*, 2006). Rearrangement of the MLL gene has been implicated in therapy-related leukaemia patients who had been treated with topoisomerase II poison during their primary malignancy (DeVore *et al.*, 1989; Ratain and Rowley, 1992; Super *et al.*, 1993; Ratain and Rowley, 1992). In addition, secondary leukaemias or therapy-related AML (t-AML) could also arise from chemotherapy of unrelated malignancies (Le Beau *et al.*, 1986; Zulian *et al.*, 1993). This addresses the involvement of 11q23 in tumourigenesis of leukaemias and its association with other type of malignancies.

### 1.3 Nasopharyngeal Carcinoma (NPC) and Chromosomal Rearrangement

Nasopharyngel carcinoma (NPC) is a rare malignancy throughout most parts of the world (Parkin and Muir, 1992). However, high prevalence of NPC case was found in Guangdong Province and several other regions in Southern China as well as Southeast Asia (Jeannel *et al.*, 1999; Chien and Chen, 2003). Therefore, NPC is regarded as a malignancy with striking geographical and ethnic distribution (Lo and Huang, 2002). According to the World Health Organisation (WHO) classifications, 3 histopathological types are being recognised in NPC. NPC can be classified into Type I, II and III. Squamous cell carcinoma with varying degrees of differentiation are classified as Type I. Type II is characterised by non-keratinising

carcinoma, whereas Type III is undifferentiated carcinoma. Type II and III can be considered as undifferentiated carcinoma of NPC (Shanmugaratnam and Sobin, 1993).

Carcinogenesis of NPC is believed to be contributed by multiple factors, namely environmental, Epstein-Barr virus (EBV) infection and genetic factors (Ho, 1971; Hildesheim and Levine, 1993; Yu and Henderson, 1996; McDermott *et al.*, 2001; Jia *et al.*, 2003). Other contributing factors, such as dietary factors (consumption of salted and preserved foods), cigarette smoking, occupational exposures to wood dust, formaldehyde and chemical fumes as well as use of Chinese herbs are also associated with NPC (Ho, 1972; Chien and Chen, 2003). EBV infection is closely associated with WHO types II and III carcinoma (Pearson *et al.*, 1978; Pearson *et al.*, 1983; Pearson *et al.*, 1984; Hu *et al.*, 1996). From emigration and dialect studies, it was suggested that genetic alteration could contribute to the development of NPC (Jia *et al.*, 2003; Lo and Huang, 2002).

Somatic gene aberrations, such as allelic loss, chromosomal gains or losses, and specific gene alterations had been reported in NPC extensively (Jia *et al.*, 2003). Study of loss of heterozygosity (LOH) and the use of Comparative Genome Hybridisation (CGH) had identified various chromosomal regions involved (Li *et al.*, 2006). Common additions were identified at 1q, 2q, 3q, 4q, 6q, 8q, 11q, 12p, 12q, 17p, 17q, 18q, 19 and 20 (Hui *et al.*, 1999; Chien *et al.*, 2001; Fang *et al.*, 2001; Li *et al.*, 2006). These include chromosome 3p (Lo *et al.*, 1994; Sung *et al.*, 2000; Hu *et al.*, 1996), 9p (Huang *et al.*, 1994), 11q (Hui *et al.*, 1996), 13q (Mutirangura *et al.*, 1996; Shao *et al.*, 2002) and 14q (Mutirangura *et al.*, 1998; Shao *et al.*, 2002). In addition, the minimal deletion regions (MDRs) had also been identified (Jia *et al.*, 2003). These include chromosomes 1p34 and 1p36, 3p14-21, 3p24-26, 3q25-26 and

3q27, 5q15-21 and 5q32-33, 9p21-23 and 9q33-34, 11p12-14 and 11q21-23, 13q12-14 and 13q31-32, 14q11-13 and 14q24-32 and 16q22-23 (Lo *et al.*, 2000; Shao *et al.*, 2000; Shao *et al.*, 2001). These MDRs are believed to contain tumour suppressor genes that are involved in tumourigenesis of NPC (Lo *et al.*, 2000).

Deletion of chromosome 11q is one of the major genetic changes in NPC (Mutirangura *et al.*, 1997; Hui *et al.*, 1999; Fan *et al.*, 2000; Lo *et al.*, 2000; Shao *et al.*, 2000; Chien *et al.*, 2001; Fang Y. *et al.*, 2001; Shao *et al.*, 2001). From LOH studies, it indicates that there are more than one target genes located on chromosome 11q (Hui *et al.*, 1996; Lo *et al.*, 2000). There are two tumour suppressor loci identified on 11q13.3-22 and at 11q22-24. Example of the tumour suppressor genes mapped in these regions are MLL, ATM and TSLC1 (Hui *et al.*, 2002). The TSLC1 gene at 11q23 may be a NPC-associated tumour suppressor (Hui *et al.*, 2003). However, in some of the NPC tumours with deletion at chromosome 11q, alteration of the TSLC1 was not observed. The carcinogenesis of NPC at molecular level remains to be elucidated (Lo and Huang, 2002).

### 1.4 Mixed Lineage Leukaemia (MLL) gene breakpoint cluster region (bcr)

The expression of the normal Mixed Lineage Leukaemia (MLL) gene is crucial for the regulation of HOX genes in haematopoisis during fetal development. In leukaemia, the function of this gene is compromised as the result of cleavage, recombination and chimeric fusion with more than 50 partner genes (Pais *et al.*, 2005; Meyer *et al.*, 2006). Structural rearrangements of MLL gene at 11q23 is commonly observed in both *de novo* and t-AML (Rowley, 1993). The most common 11q23 translocations are the t(4;11) and t(11;19) in ALL and the t(9;11), t(6;11) and t(11;19) in *de novo* AML (Kaneko *et al.*, 1998; Raimondi, 1993).

The MLL gene spans approximately 100 kb and contains at least 21 small exons that code for a protein of approximate molecular mass of 430 kDa (Bernard, 1995). The majority of the MLL translocations occur within an 8.3 kb region of the MLL, defined by *Bam*H I restriction sites, which is designated as the breakpoint cluster region (bcr). The MLL bcr contains 8 Alu repetitive elements, 2 scaffold-associated regions (SARs) which colocalised with 6 of 7 topoisomerase II consensus cleavage sites (Broeker *et al.*, 1996).

Studies found that, in therapy-related leukaemia, breakpoints were found clustered within the telomeric region (3' end) of the bcr, a location which happen to colocalise with a DNase hypersensitivity site and is also the target for site-specific apoptotic cleavage (Stanulla *et al.*, 1997; Betti *et al.*, 2001; Strissel *et al.*, 1998). The controlling mechanism of such nuclease sensitivity is not well illustrated. It has been found that the earliest detectable apoptotic fragmentation occurs at sites of DNA attachment to the nuclear matrix may relate to such mechanism (Khodarev *et al.*, 2000; Oberhammer *et al.*, 1993). The telomeric region of the MLL contains an experimentally defined nuclear matrix attachment regions (MARs) or scaffold attachment regions (SARs) which is AT-rich (Broeker *et al.*, 1996). The chromatin structure of the MLL bcr is shown in Figure 1.1. Apoptotic nucleases may therefore cleave the MLL by targeting specific DNA structures found at the nuclear matrix (Khodarev *et al.*, 2000; Broeker *et al.*, 1996).

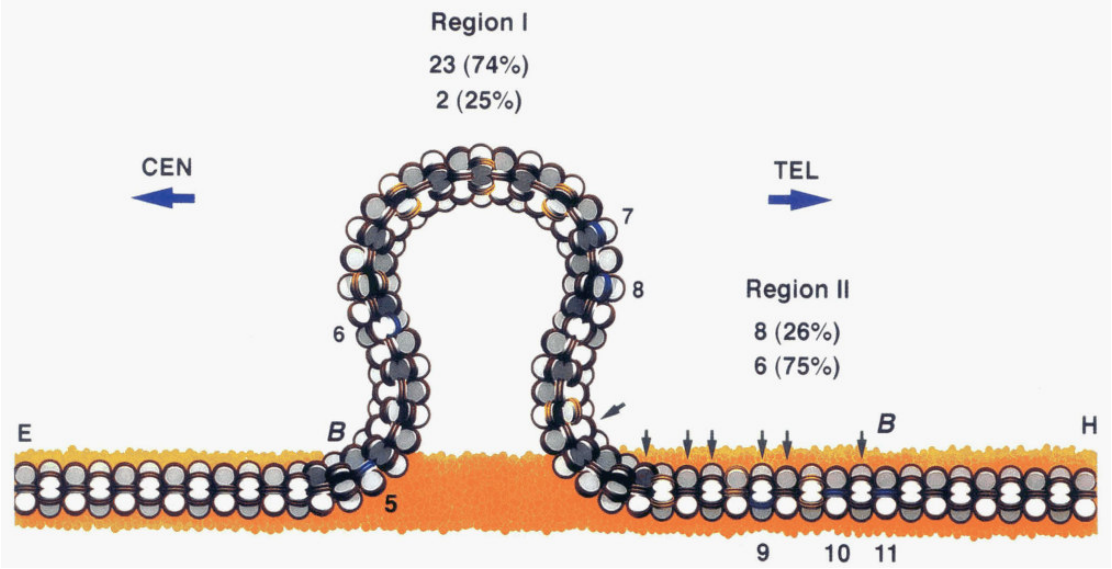


Figure 1.1: Proposed model of the chromatin structure of the MLL breakpoint cluster region. This figure presents a three-dimensional DNA drawing summarising the relationship of patient breakpoints to SARs, high stringency *in vitro* vertebrate topo II consensus sites. and Alu sequences in the MLL 8.3 kb breakpoint cluster region. The DNA (thick red coil) is wrapped around the histone core proteins (grey discs). Then coiled upon itself representing the 30 nm fiber. Scaffold proteins (melon color at the base of DNA) which form the chromosomal axis are schematically drawn along the bases of the loop domain end are shown binding to the centromeric low- and telomeric high-affinity SARs. The map represents 12.9 kb of *MLL,* including portions centromeric, within, and telomeric to the *Bam*H I restriction sites (*Bam*H I = B sites in italics). Note that the 30-nm fiber (6 nucleosomes/turn) is not drawn to scale. The loop represents Region 1, in which 74% of our *de novo* (top numbers) and 25% of our t-AML (bottom numbers) patient breakpoints mapped. The flanking regions adjacent to the loop represent the centromeric portion 5' of the breakpoint cluster region and the telomeric half of the breakpoint cluster region, Region II, in which 26% of our *de novo* (top numbers) and 75% of our t-AML (bottom numbers) patient breakpoints mapped. MLL exons 5-11 are represented as blue along the DNA fiber. Alu repeats are represented as yellow along the DNA fiber, topo II consensus sites are represented by green arrows above the DNA fiber at Region II (Taken from: Broeker *et al.*, 1996).

Betti *et al.* (2001) showed that, after exposure to pro-apoptotic stimuli, cells may either undergo apoptosis and be eliminated or regain their survival. These surviving cells managed to escape apoptosis. One possible mechanism could be that the cleaved MLL is joined to other breakage via Non-Homologous End Joining (NHEJ) repair system (Betti *et al.*, 2001). This is commonly observed in therapy-related leukaemias in which cells failed to execute apoptosis (Felix *et al.*, 1993).

### 1.5 Apoptosis

Apoptosis or programmed cell death is a cell autonomous and complex phenomenon which vary with tissues and cell types (Zakeri *et al.*, 1995). This naturally occuring process eliminates harmful cells during cell development or aging in animals (Vaux and Korsmeyer, 1999; Jacobson *et al.*, 1997). Apoptosis can also be triggered by cytotoxins, anti-cancer drugs, death factors and the transcriptional activation of genes involved in apotosis (Green, 1998; Raff, 1998; Nagata, 1997).

Cells undergo apoptosis through several apoptotic pathways. Among them, the two major apoptotic pathways are the death-receptor pathway and the mitochondrial pathway (Green, 2000; Wang, 2001). The death receptor pathway is triggered by death factors such as Fas ligand, TNF, and Apo3 ligand, leads to activation of caspase 8 by receptor aggregation at the plasma membrane. This subsequently results in activation of other downstream caspases (Ashkenazi and Dixit, 1998; Nagata, 1997). On the other hand, the mitochondrial pathway is triggered by DNA-damaging agents such as γ radiation and anti-cancer drugs involving the mechanism that is dependent on the p53 tumour suppressor gene product (Clarke *et al.*, 1993; Evan and Littlewood, 1998). Cell death as the result of deprivation of survival factors from

factor-dependent cells, causes the dephosphorylation of Bad, which is a pro-apoptotic member of the Bcl-2 family. This mode of apoptosis acts through the mitochondrial pathway (Raff, 1998).

Apoptosis is characterised by specific morphological and biochemical features (Wyllie *et al.*, 1980). Morphologically, apoptotic cells are characterised by a series of structural changes such as blebbing of the plasma membrane, condensation of the cytoplasm and nucleus, and cellular fragmentation into membrane apoptotic bodies (Wyllie *et al.*, 1980; Steller, 1995). Biochemical changes of apoptosis include the degradation of chromatin (Oberhammer *et al.*, 1993; Wyllie *et al.*, 1980; Susin *et al.*, 1999), degradation of death substrates by caspases (Budihardjo *et al.*, 1999; Zhang and Xu., 2000; Nagata *et al.*, 2003), increased levels of the protein clusterin (Pearse *et al.*, 1992) and activation of the enzyme type-II transglutaminase (Fesus, 1991). During apoptosis, chromatin degradation occurs at 2 levels. It is first cleaved into large fragments of 50 – 300 kilobases (kb), known as the High Molecular Weight (HMW) DNA. These large fragments are subsequently degraded into smaller fragments, that are monomers and multimers of 200 base pairs (bps) (Oberhammer *et al.*, 1993; Wyllie *et al.*, 1980; Susin *et al.*, 1999). In addition of chromatin degradation into the HMW DNA is believed to occur at the nuclear scaffold (Sakahira *et al.*, 1999). DNA sequences at the nuclear scaffolds are rich in AT-residues. DNase such as CAD prefers to cut at this AT-rich region. When apoptosis is being triggered, CAD is activated. This DNase first cleaves this region, which may unfold the chromatin structure, and leads to exposure of the spacer regions of nucleosomes. Subsequently, CAD attacks the exposed region and causes nucleosomal DNA fragmentation (Nagata, 2000). In dying cells, CAD is involved in DNA fragmentation

and lysosomal DNase II also plays a role after the apoptotic cells are phagocytosed (Nagata *et al.*, 2003).

## 1.6 Caspase-activated DNase (CAD) and its inhibitor, ICAD

### 1.6.1 Family of Caspases

Early studies concentrated on the role of nucleases in causing apoptosis, especially on interleukin-1β (IL-1β)-converting enzyme (ICE)-like proteases. Horvitz and colleagues worked extensively to understand the programmed cell death by using nematode *Caenorhabditis elegans* (*C. elegans*) as model. They found that, during development, 131 cells of the 1090 cells became apoptotic (Ellis *et al.*, 1991). The two genes, *ced-3* and *ced-4* genes are important in the cell death of *C. elegans*. Ced-3 protein is identical to the mammalian ICE. Overexpression of ICE causes cells to become apoptotic (Yuan *et al.*, 1993). A further nine ICE-like proteases had later been identified. As a result of isolating the same proteases by different groups which caused confusion, a unified nomenclature had been suggested (Alnemri *et al.*, 1996). The name proposed for all family members is caspase; the "c" denoting a cysteine protease and "aspase" referring to the ability of these enzymes to cleave after an Aspartic acid residue.

In proliferating cells, caspases are synthesised as inactive proenzymes, which are activated following their cleavage at specific Aspartatic acid cleavage sites. From the phylogenetic analysis of the caspases, it reveals that there are 3 subfamilies: an ICE subfamily, comprising of caspases-1, -4 and -5, a ced-3 family protease, the CPP32 (32 kDa cysteine protease) subfamily, comprising of caspases-3, -6, -7, -8, -9 and -10, and an ICH-1 (where ICH is *Ice* and *ced-3* homologue)/Nedd2 subfamily (Thornberry, 1998; Garcia-Calvo *et al.*, 1998). The

mammalian caspase gene (Alnemri *et al.*, 1996) family consists of 14 members, of which 12 of them have been identified (Alnemri *et al.*, 1996; Salvesen and Dixit, 1997; Van de *et al.*, 1997). Caspases can be classified according to their function, namely initiator and executor. The initiator caspases (Caspase -1, -2, -4, -5, -8, -9, -10, -11 and -12) possess long prodomains. Among the initiator caspases, Caspase -1, -5 and -11 fall into the subclass that control both apoptosis and certain inflammatory responses (Thornberry *et al.*, 1997) as shown in Figure 1.2. Besides, caspases-8, -9, and -10 are also involved in apoptosis. These caspases function as initiator element. They are activated by oligomerisation at the plasma membrane or by apoptosomes in mitochondria (Stroh and Schulze-Osthoff, 1998). The downstream caspases are the executor caspases (Caspase -3, -6 and -7) which contain short prodomain (Thornberry *et al.*, 1997). They are activated by initiator caspases and are responsible for the cleavage of at least 60 death related substrates (Stroh and Schulze-Osthoff, 1998). Beside Caspase-3, Caspase-7 but not caspase-1, -2, -4, -5, -6 and 8 cleaves ICAD (McIlroy *et al.*, 1999; Wolf *et al.*, 1999).

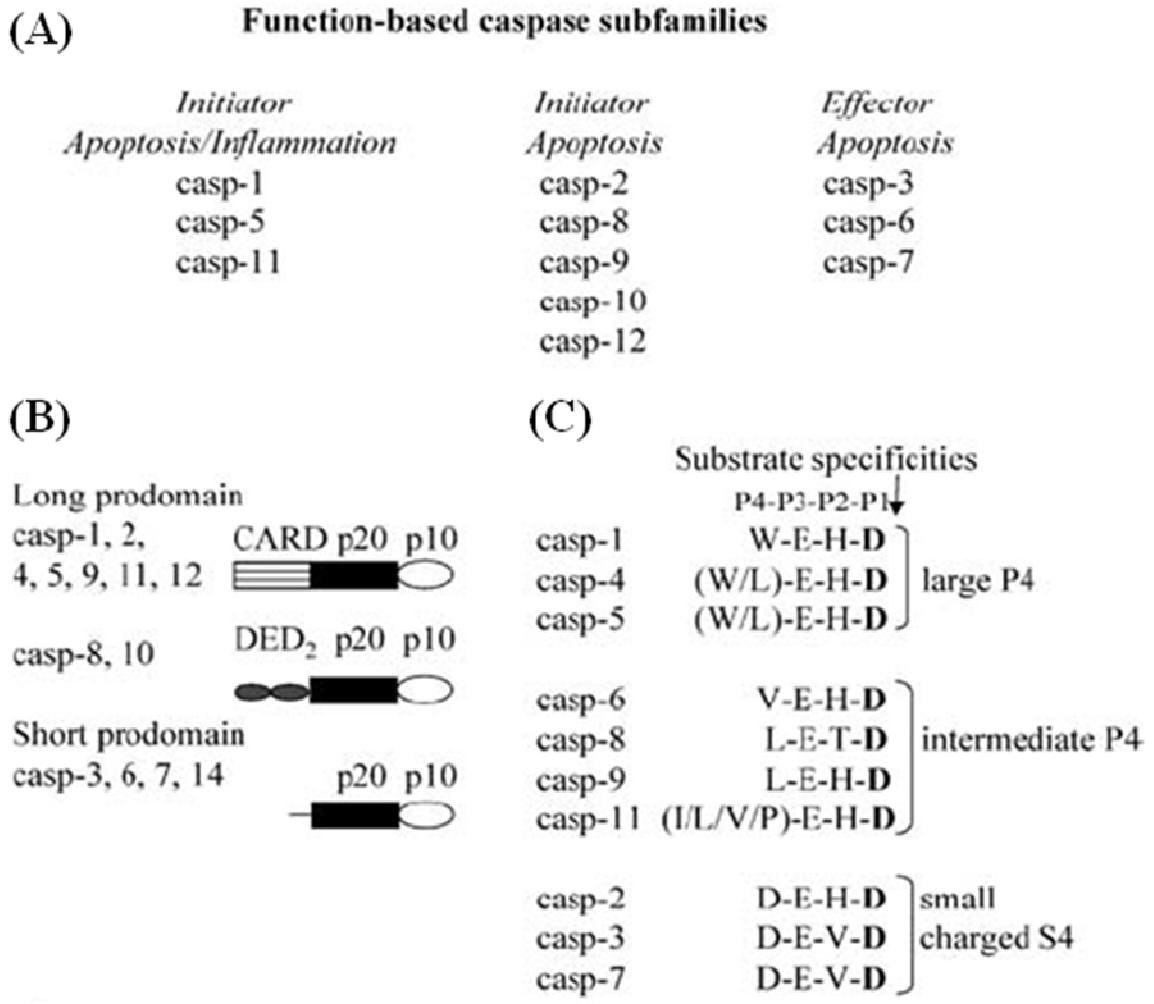


Figure 1.2: Classification of caspases. (A) Classification of the caspase family based on reported functions. (B) General structure of caspases and classification based on the prodomain length. (C) Caspase substrate specificities. Data are based on Thornberry *et al.* (1997). Preferred amino acids in P4-P1 positions are shown. Based on the size of the S4 subsite and P4 residue, caspases can be divided into three subfamilies (Taken from: Degterev Alexie *et al.*, 2003).

### 1.6.2 Caspase-activated DNase (CAD) and its function

Caspase-activated DNase (CAD), also called DNA Fragmentation Factor 40 (DFF40) (Liu *et al.*, 1998) has been identified in human and murine. Human and murine CADs (designated as hCAD and mCAD respectively) are 40 kDa proteins which consist of 344 and 338 amino acids respectively. They are the basic proteins with respective pI of 9.7 and 9.3. Their amino acid sequences are well conserved (75.9% identity) (Enari *et al.*, 1998; Halenbeck *et al.*, 1998). CAD requires magnesium ion ($Mg^{2+}$) for its DNase activity, and functions at neutral pH. The specific DNase activity of CAD is comparable to other DNases, such as DNase I and II. CAD has intrinsic DNase (endonuclease) activity, but it does not cleave ribonucleic acid (RNA) (Liu *et al.*, 1999). CAD does not generate single stranded nicks when cleaving double-stranded DNA. Instead, this endonuclease introduces double-stranded breaks which create either blunt ends or one-base 5'-overhangs with 5'-phosphate and 3'-hydroxyl groups. This characteristic of CAD excludes the possibility for single strand repair enzymes to rejoin the broken ends. Double-stranded DNA break is an apoptotic signal. The cleavage of genomic DNA by CAD may trigger an amplification cycle which is an irreversible step for apoptosis (Liu *et al.*, 1998). Study showed that when CAD is injected into cells, chromatins condense quickly and are fragmented (Susin *et al.*, 2000). The involvement of CAD in DNA fragmentation is illustrated in Figure 1.3.

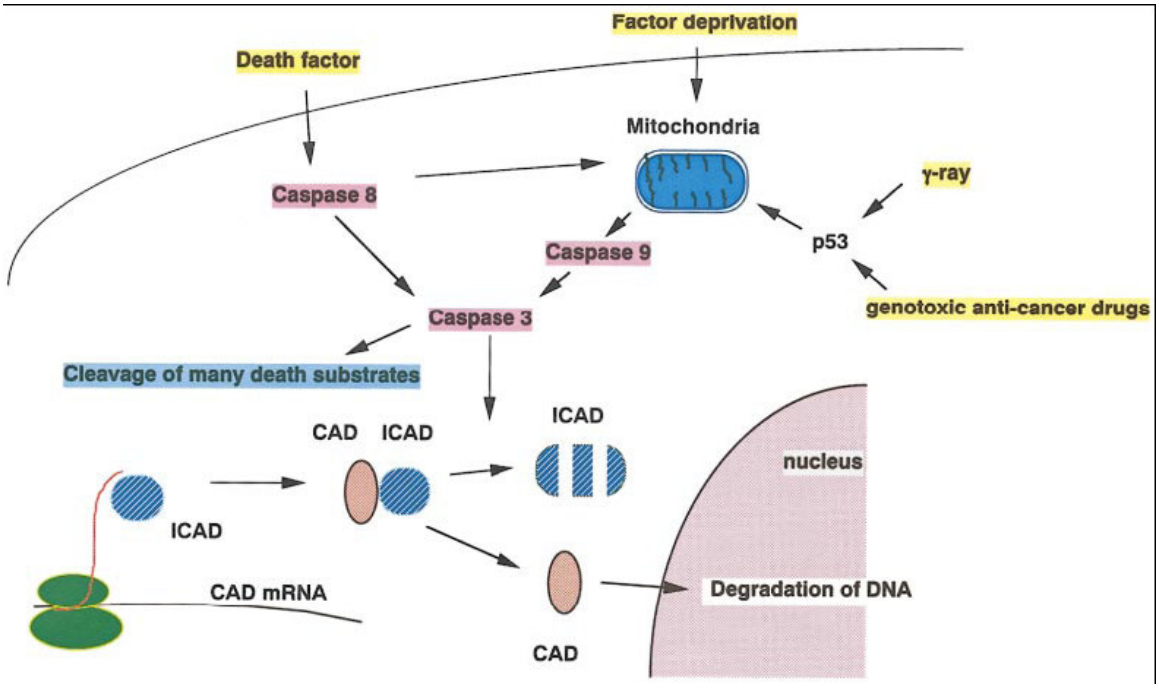


Figure 1.3: CAD-mediated DNA fragmentation during apoptosis. When CAD is synthesised, ICAD helps in the correct folding of CAD. CAD thus exists as an inactive enzyme complexed with ICAD in proliferating cells. Various apoptotic signals such as death factors, factor-deprivation, or genotoxic agents activate the caspase cascade. Caspase-3 downstream of the cascade cleaves ICAD at two positions and inactivates its CAD-inhibitory activity. CAD, thus released from ICAD, degrades chromosomal DNA. CAD degrades chromatin during apoptosis by attacking phosphodiester bonds of DNA in the linker region between nucleosomes (Enari *et al.*, 1998; Liu *et al.*, 1997). During apoptosis, DNA laddering observed is due to cleavage restricted to the internucleosomal DNA in chromatin (Taken from: Widlak *et al.*, 2000).

### 1.6.3 Inhibitor of Caspase-activated DNase (ICAD) and its function

ICAD has two isoforms, namely a $M_r$ 45,000 isoform (ICAD-L or DNA Fragmentation Factor 45, DFF45) and a $M_r$ 35,000 isoform (ICAD-S or DNA Fragmentation Factor 35, DFF35) (Enari *et al.*, 1998;Gu *et al.*, 1999). The full-length form of ICAD, ICAD-L, is a 45-kDa protein. It consists of 331 amino acids with a pI of 4.5. A short form of ICAD, ICAD-S, consists of amino acids 1–265. ICAD-S is generated by alternative splicing of ICAD-L and is expressed in a number of different human and murine cells (Enari *et al.*, 1998; Gu *et al.*, 1999; Kawane *et al.*, 1999) at a level similar to ICAD-L. Despite their difference in length, both ICAD-L and ICAD-S carry two caspase-3 putative recognition sites at amino acid positions 117 and 224 in both human and murine ICAD. Caspase-3 can cleave recombinant human and murine ICAD at these 2 positions (Talanian *et al.*, 1997; Thornberry *et al.*, 1997). Sakahira and colleagues (1999) showed that recombinant ICAD-L and ICAD-S protein expressed in *Escherichia coli,* insect cells, and mammalian cells are relatively stable to high temperature (at 90°C for 5 min), and strong denaturation agents (6 M guanidine hydrochloride, 8 M urea, 0.1% SDS). Both forms bind to CAD to inhibit its DNase and DNA fragmentation activity efficiently (Sakahira *et al.*, 1999). Its inhibitory property ensures that DFF will only become activated through the cleavage by caspases, upon receiving apoptotic signals (Cryns and Yuan, 1998). The involvement of ICAD in inhibiting and activating CAD is illustrated in Figure 1.4.

Besides functioning as inhibitor of CAD, ICAD-L or DNA Fragmentation Factor 45 (DFF45) also works as its chaperone by binding to its nascent chain polypeptide during its synthesis and facilitates its proper folding. ICAD-L remains complexed with CAD after CAD synthesis is completed to form CAD/ICAD complex (Enari *et al.*, 1998; Halenbeck *et al.*, 1998; Zhang

*et al.*, 1998). However, ICAD-S does not function in this way. Once stimulated by apoptotic stimuli, caspase-3 is activated which in turn activates downstream of the caspase cascade. Caspase-3 cleaves ICAD-L, releasing active CAD to degrade the chromosomal DNA. ICAD-S may further regulate the CAD DNase at this point, by binding to the activated CAD (Sakahira *et al.*, 1998; Nagata, 2000). ICAD-L also enhances the renaturation of chemically denatured CAD, confirming its chaperone-like function (Sakahira *et al.*, 2000). This shows that ICAD is important for the expression and activity of CAD. Patients with esophageal carcinoma whose ICAD expression was found low, were diagnosed with poor prognosis (Konishi *et al.*, 2002). Zhang *et al.* (1998) showed that cell extracts prepared from DFF45 knockout mice, the DNA fragmentation activity is completely abolished (Zhang *et al.*, 1998). However, ICAD-S (DFF35) and ICAD-L (DFF45) can inhibit DNase activity of CAD but not the DNA binding capacity of CAD (Korn *et al.*, 2005).

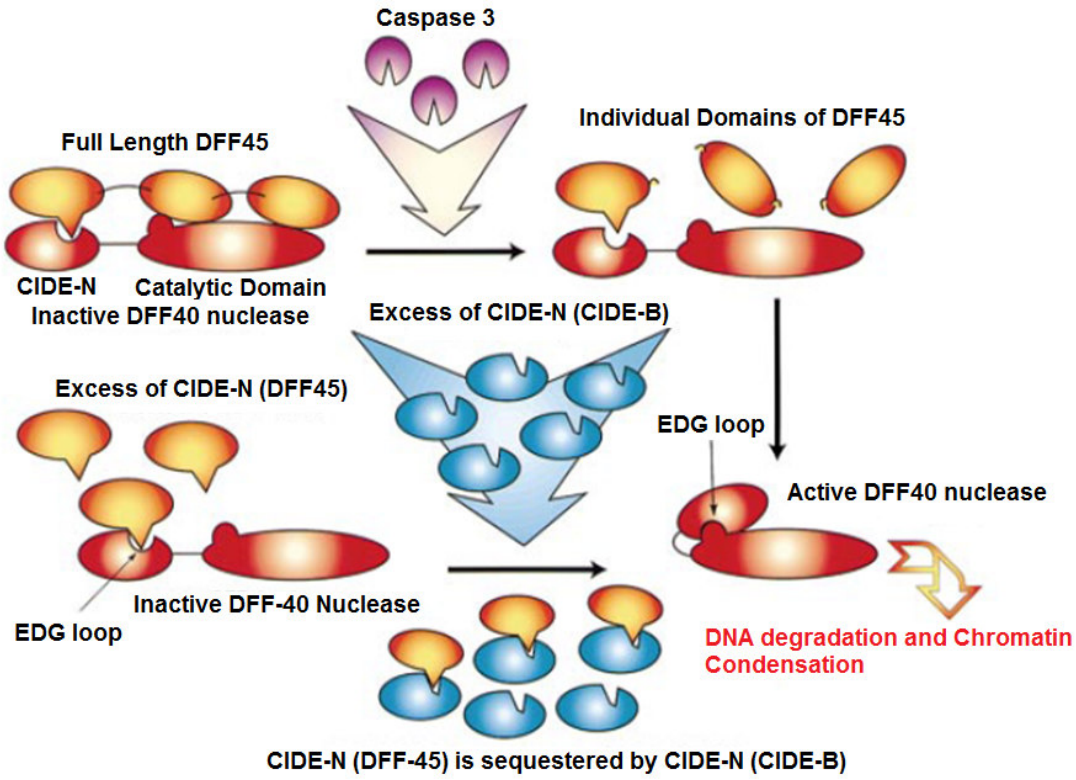


Figure 1.4: A model for the inhibition and activation of DFF40 nuclease. Caspase-3 cleaves DFF45 into three domains that dissociate from the DFF40/DFF45 complex (top). Subsequently, the EDG loop of the CIDE-N domain of DFF40 interacts with the catalytic domain of nuclease, triggering DNA degradation and chromatin condensation. DFF40 can be inhibited by an excess of CIDE-N (DFF45). However, excess CIDE-N (CIDE-B) can sequester the CIDE-N domain of DFF45, making the EDG loop of DFF40 available for the interaction with nuclease catalytic domain (bottom) (Taken from: Lugovskoy *et al.*, 1999).

### 1.6.4 Interaction of CAD and ICAD

CAD and ICAD share a homologous domain (the CAD/CIDE domain) of about 80 amino acids at the N-terminal (Inohara *et al.*, 1998; Mukae *et al.*, 1998). CAD domain is a protein-protein interaction domain involved in the formation of CAD-ICAD complex (Uegaki *et al.*, 2000). Amino acid portion 3 to 329 at N-terminal of CAD is sufficient for the DNase activity of CAD. Its C-terminal residues (amino acids 330–344) are important for nuclear transport. C-terminal of both CAD and ICAD is essential for nuclear targeting of CAD/ICAD complex (Lechardeur *et al.*, 2000; Scholz *et al.*, 2002; Samejima and Earnshaw, 1998). However, it has also been found that several histidine residues clustered in the C-terminal half of the CAD protein may constitute an active site for CAD DNase as found in other DNases (Nagata, 2000).

ICAD is not only an inhibitor, but is also essential for generating properly folded CAD as illustrated in Figure 1.5. This was shown in both *in vitro* and *in vivo* studies (Sakahira *et al.*, 1998; Zhang *et al.*, 1998; Sakahira *et al.*, 2000). Co-translational folding of protein is an important mechanism to avoid intramolecular misfolding as this error could lead to aggregation (Netzer and Hartl, 1998). Proteins which are misfolded and aggregated could be cytotoxic and cause apoptosis (Kakizuka, 1998). *In vitro* cotranslation experiment using truncated CAD mRNAs indicated that ICAD assisted the folding of CAD by binding to the CAD/CIDE domain of the nascent CAD polypeptide on ribosomes (Sakahira and Nagata, 2002). These domains interact with each other to form the heterodimeric complex. This interaction has been suggested to be essential for the correct folding of CAD (Otomo *et al.*, 2000). Sakahira and Nagata (2002) showed that Hsp70 and Hsp40 are essential for the refolding of chemically denatured CAD. They could co-operatively suppress the aggregation

of CAD in an ATP-dependent manner in the absence of ICAD. But they do not assist in restoring the CAD DNase activity. These proteins assist in the partial refolding of CAD at its C-terminal. In addition, chemically denatured CAD can be renatured in the presence of ICAD and reticulocyte lysates. This suggests that ICAD is involved in the second step of refolding of CAD to form complete and functional CAD protein (Sakahira and Nagata, 2002).

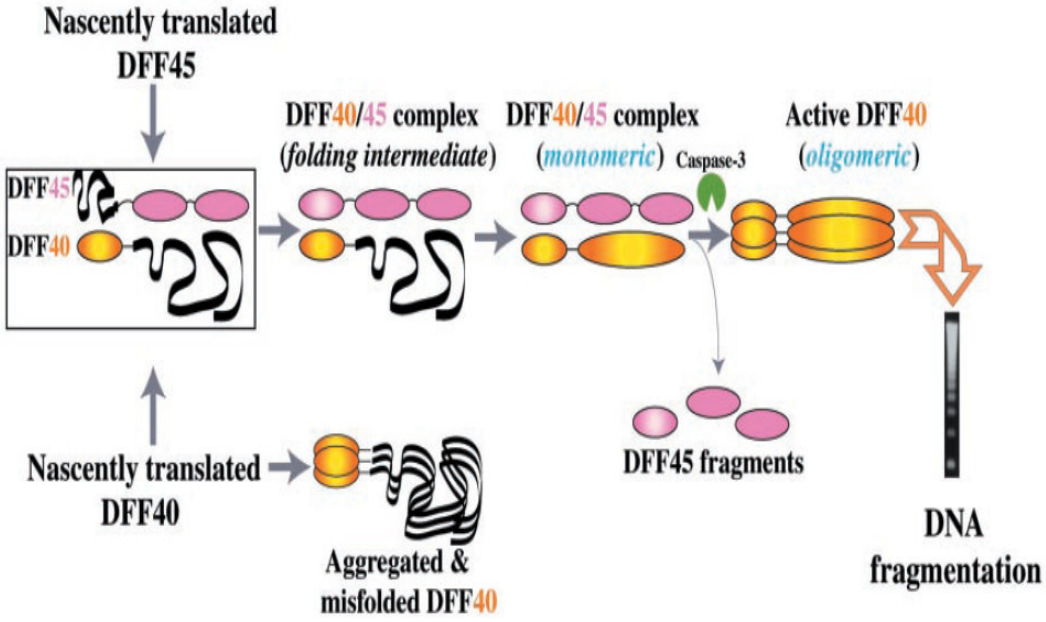


Figure 1.5: Model of the mutual chaperoning of DFF40 and DFF45 (Taken from: Zhou *et al.*, 2001).

Besides Hsp70 and Hsp40, the activity of DFF40 can be markedly stimulated by the abundant chromatin-associated proteins such as histone H1, HMG-1, and HMG-2 (Liu *et al.*, 1998; Toh *et al.*, 1998). These are the structural supporting proteins which are located in the internucleosomal linker regions of chromatin (Bustin, 1996; van Holde, 1989). Interestingly, histone H1 has the ability to stimulate the nuclease activity of DFF (CAD/ICAD complex) more than 10-fold (Liu *et al.*, 1998). It is likely that histone, a basic protein, removes both of the cleaved ICAD-L and ICAD-S fragments (acidic proteins) from CAD. This in turn, enhances the CAD DNase activity (Nagata, 2000).

In normal growing cells, CAD remains complexed with ICAD and hence stays inactive (Enari *et al.*, 1998; Liu *et al.*, 1997). DFF migrates on a gel filtration column as a heterodimer with a molecular mass of 85 kDa (Liu *et al.*, 1997). It has been shown that in HeLa cells, endogenous DFF is detected almost entirely located in the nucleus (Korn *et al.*, 2005). Structurally, both CAD and ICAD are composed of 1 α-helix and 5 β-strands. These proteins belong to the ubiquitin-superfold family. When exist as complex, CAD and ICAD aligned side by side through ionic interactions between basic residues in CAD and acidic residues in ICAD (Otomo T *et al.*, 2000). Therefore, ICAD mutants are not able to associate with CAD. As a result, it could not facilitate the correct folding of CAD (Sakahira *et al.*, 2001; Zhang *et al.*, 1998).

The CAD molecule can be divided into three distinct domains, namely Domain C1 (1 – 85), Domain C2 (residues 86 – 131) and Domain C3 (132 – 328). Similarly, ICAD is also divided into three distinct domains, designated as Domain I1 (residues 1 – 117), Domain I2 (residues 118 – 224) and Domain I3 (residues 225 – 331). Domain C1 interacts with Domain I1;

Domain C2 binds with Domain I2; whereas Domain C3 interacts with Domain I3. When CAD monomer dimerised, the C3 domains exist as a large and deep crevice resemble the shape of the two blades of an open pair of scissors. The width of the crevice is the right size to accommodate double-stranded DNA. During apoptosis, ICAD-L is cleaved by caspase-3 at its two putative recognition sites, releasing free ICAD-L into three domains from the latent CAD monomer. Domain I2 appears to be required to disassemble the CAD dimmer. Hence, dissociation of Domain I2 unlocked the Domain C2 leading to the assembly of CAD monomers to form active CAD dimmers (Woo *et al.*, 2004). The involvement of CAD in cleaving chromosomal DNA is shown in Figure 1.6.

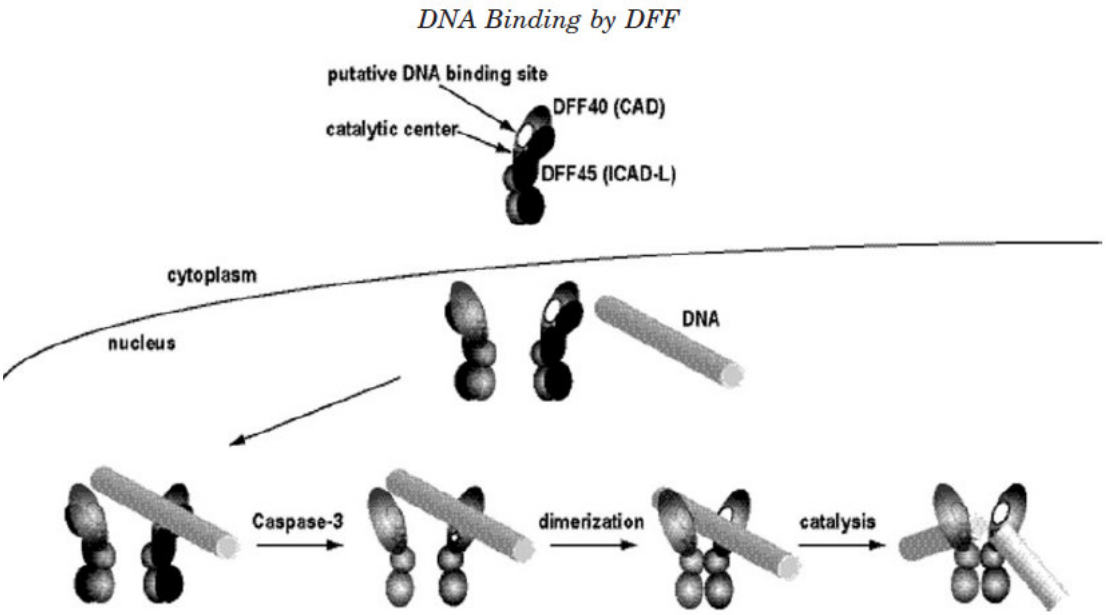


Figure 1.6: Model of involvement of CAD in chromosomal DNA cleavage. DFF can be found in the cytoplasm and nuclei of mammalian cells, dependent on the cell line. According to our results, DFF directly binds to DNA via the nuclease subunit. Preformation of DFF-DNA complexes, *i.e.* the interaction of DFF40 (CAD) with DNA in the inhibited state, facilitates access of the DNA substrate to the catalytic center at the bottom of a deep active site cleft seen in dimeric CAD, probably by dimer assembly around the DNA. Interaction of DFF with DNA reveals an unprecedented mechanism for nuclear inhibition and suggests that DFF can be activated in a DNA-bound state (Taken from: Korn *et al.*, 2005).

### 1.6.5 Mutation of CAD

In many tumour types, genes encoding for CAD are not well-regulated and expressed. In addition, the abnormalities in this gene are associated with poor prognosis in cancer patients (Ohira *et al.*, 2000; Konishi *et al.*, 2002; Hsieh *et al.*, 2003). Disregulation of CAD gene expression results in increased frequency of DNA damage-induced chromosomal instability *in vivo* and *in vitro*. This shows that, apoptotic DNA fragmentation is an important step to maintain genetic stability and suppress cellular transformation in carcinogen-induced tumuorigenesis (Yan *et al.*, 2006). This suggests that CAD activity is required to maintain genomic stability and prevent tumourigenesis.

Similar to RNase T1, DNase I and S1 nuclease, CAD is grouped as one of the members of the histidine nuclease family (Meiss *et al.*, 2001; Sakahira *et al.*, 2001; Korn *et al.*, 2002; Korn *et al.*, 2005;). Mutation of several histidine, lysine and tyrosine residues in the C-terminal half of CAD (Sakahira *et al.*, 2001; Meiss *et al.*, 2001) affect its DNase activity ( Meiss *et al.*, 2001; Sakahira *et al.*, 2001; Korn *et al.*, 2002; Korn *et al.*, 2005;). Amino acid of CAD at position 155, Lysine, $Lys^{155}$ in murine or at 157, $Lys^{157}$ in human, is not an active site residue but this residue is closer to the CAD/CIDE-N-domain of the protein. This site appears to be involved in maintaining the protein structure and/or DNA binding (Meiss *et al.*, 2001; Widlak *et al.*, 2003; Woo *et al.*, 2004) as shown in Figure 1.7. Human CAD which carries mutation at position 157, from Lysine (K) to Glutamine (Q), the K157Q mutant, does not form stable DNA complexes. Crystal structure of murine CAD showed that $Lys^{155}$ is a buried residue involved in stabilising the N-terminal end of the α-helix 4 of CAD, where this structure presumably binds in the major groove of the DNA (Woo *et al.*, 2004).

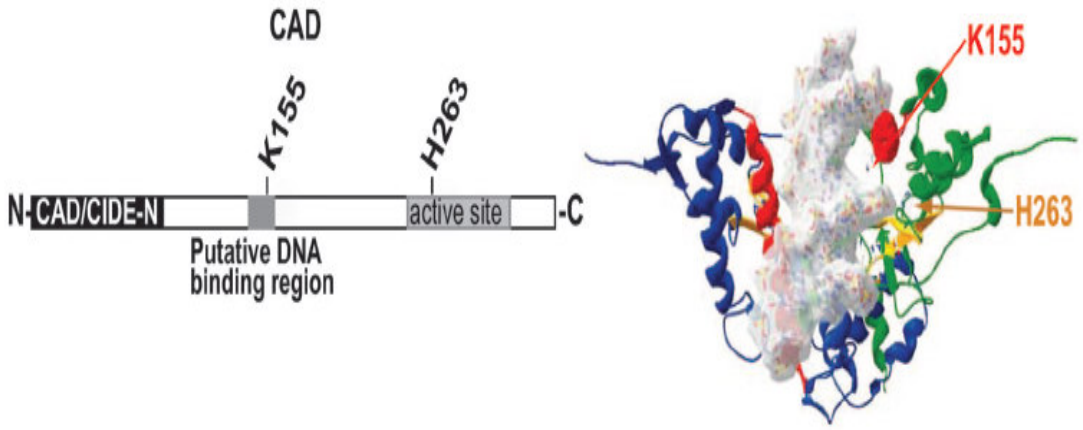


Figure 1.7: Schematic diagram of CAD (murine DFF40) showing the positions of two critical amino acid residues (*K155* and *H263*) (*left panel*) and model for the CAD-DNA complex based on the crystal structure of active CAD. His263 is located in the catalytic center (*highlighted in orange*) while Lys155 is buried at the N terminus of α-helix 4 (*highlighted in red*) that fits into the major groove of the DNA (CAD-DNA model has been adapted from Woo *et al.*, 2004). The two identical subunits of the CAD dimer are highlighted in *blue* and *green*, respectively (*right panel*) (Taken from: Korn *et al.*, 2005).

### 1.6.6 Mutation of ICAD

Mutation of ICAD-L and ICAD-S (replacement of Asp by Glu) at either or both caspase recognition sites (amino acid position 117 and 224) does not affect their ability in inhibiting CAD DNase function (Sakahira *et al.*, 1998). Apoptotic stimulus via caspase treatment does not affect the inhibitory activity of the ICAD-L double mutant. Mutants carrying a single mutation of either at 117 or 224 still show significant CAD inhibiting activity. This suggests that both of the ICAD caspase recognition sites must be cleaved to release activate CAD (Enari *et al.*, 1998; McCarty *et al.*, 1999). However, when Jurkat cells with ICAD double mutant (ICAD-Ldm) expression were treated with etoposide for 24 hours, DNA fragmentation was observed. Similar observation was found in TF-1 cells with ICAD-Ldm overexpression. This suggested that besides CAD, other DNase(s) might mediate the chromosomal DNA fragmentation. It could also indicate that DNA fragmentation is not a prerequisite event for cell death. When cells were transfected with mICAD-Ldm, the transfected mICAD-Ldm did not inhibit caspase-3 to cleave endogenous human ICAD. They also did not work as competitive inhibitor of caspase-3 and is able to bind to active CAD released from endogenous CAD:ICAD complexes quick enough to inhibit its DNase activity (McIlroy *et al.*, 1999).

## 1.7 Oxidative Stress-induced Apoptosis

During oxidative stress, cells exhibit diverse responses against it, including proliferation (Brar *et al.*, 2002), differentiation (Steinbeck *et al.*, 1998; Katoh *et al.*, 1999), and cell demise (apoptosis and/or necrosis) (Gorman *et al.*, 1997; Kanno *et al.*, 1999), depending on the cell types or levels of oxidative stress. Oxidative stress is defined as a condition whereby there is

an excess of reactive oxygen species (ROS), a decrease in anti-oxidant level, or both (http://www.biochem.northwestern.edu/holmgren/Glossary/Definitions/Def-O/oxidative_ stress.html). ROS are produced during oxygen metabolism via a series of one electron reduction (Klebanoff, 1988). ROS include hydrogen peroxide ($H_2O_2$), superoxide anion ($O_2^-$) and hydroxyl radical (OH·). ROS have been implicated in aging, apoptosis and numerous diseases (Chandra and Samali, 2000; Finkel, 2000). Under normal physiological condition, ROS are continuously produced as by-products of aerobic metabolism, in which the estimated number is at 10,000 per day. Its production is related to normal cell proliferation process through the activation of growth-related signaling pathways (Benhar *et al.*, 2002). ROS are generated from respiration, cell injury, drug metabolism and infection (Floyd, 1995). These oxidant by-products can cause significant damage to DNA (Burdon, 1995), protein and lipid (Cadet and Berger, 1985; Hutchinson, 1985). The DNA damages generated includes single and double-stranded breaks as well as a mixture of nucleotide modifications (Cadet and Berger, 1985; Hutchinson, 1985). There are DNA repairing enzymes and anti-oxidants that remove most of these damaging agents from our body (Ames and Shigenaga, 1991), such as superoxide dismutase (SOD), catalase, glutathione peroxide, vitamin C and E as well as reduced form of glutathione (GSH). These anti-oxidants could eliminate or reduce injury efficiently through oxidative mechanism (Rhee, 1999). However, this anti-oxidative mechanism may not work perfectly (Meneghini, 1993). DNA repair enzymes could remove most, but not all of the lesions formed (Ames and Shigenaga, 1991).

When cells experience oxidative stress, they could become apoptotic (Chandra and Samali, 2000; Finkel, 2000). In an *in vitro* study, it has been found that a variety of cells, including tumuor cell lines (Lennon *et al.*, 1991; Lennon *et al.*, 1992), and normal cell types, like

endothelium (Abello *et al.*, 1994), vascular smooth muscle cells (Li *et al.*, 1997), and renal epithelial cells (Ueda and Shah, 1992), underwent apoptosis when exposed to oxidative stress inducers, where $H_2O_2$ was one of them. $H_2O_2$ has been shown to induce apoptosis in many cell types, including lymphocytes (Hansson *et al.*, 1996; Kasai *et al.*, 1998), blastocyts (Pierce *et al.*, 1991), neutrophils (Lundqvist-Gustafsson and Bengtsson, 1999), HL-60 cells (DiPietrantonio *et al.*, 1999), monocytes (Li and Zong, 1999) and tracheobronchial epithelial (TBE) cells (DiPietrantonio *et al.*, 1999).

Cells experienced oxidative stress upon exposure to high level of exogenous and endogenously produced ROS (Parman *et al.*, 1999). It was also shown that BHK-21 cells became apoptotic when exposed to high concentration of $H_2O_2$ (Burdon *et al.*, 1995). This occurs due to a disturbance in the redox balance of the cells. As a consequence, cellular functions are affected. Intracellular proteins and lipids are being modified and may cause direct DNA damage (Parman *et al.*, 1999), including mitochondrial DNA (mtDNA) damage. Such mutation causes dysfunction of the mitochondrial respiratory chain. This in turn, leads to further increase in ROS production, causing a continuation of such faulty cycles of mtDNA damage, amplifying ROS production (Spitz *et al.*, 2004; Wallace, 1992).

Studies using animal models showed that, oxidative lesions increased with age (Ames and Shigenaga, 1991; Branda *et al.*, 1993). The human genome is potentially vulnerable to damage (or mutation) by $H_2O_2$. Although $H_2O_2$ by itself is not sufficient to attack DNA (Meneghini, 1993), the $H_2O_2$-derived hydroxyl radical ($OH\cdot$) or another hydroxyl-derived product can react with cellular DNA to produce DNA damage (Halliwell and Aruoma, 1991; Ueda and Shah, 1992). This radicals are capable in causing DNA double-stranded breaks

(DSBs) in mammalian cells following induction of apoptosis (Birnboim, 1986) as well as base modification. The apoptotic induction does not only relate to the chemical nature of the DNA damage (Halliwell and Aruoma, 1991). Burdon *et al.* (1996) showed that exposure to various concentrations of exogenously added $H_2O_2$ resulted in DNA damage in a sequence specific manner, which is in the AT-rich region (Burdon *et al.*, 1996). However, it has also been proposed that, oxygen free radicals preferentially damage nucleotide C. The most frequent mutation observed is nucleotide C to T transition (Tkeshelashvili *et al.*, 1992). The second most frequent mutations involved transversion of nucleotide G to C. The next commonly observed mutation involved nucleotide G to T transversion (Ames *et al.*, 1993).

Cellular membrane is highly permeable to $H_2O_2$ (Chance *et al.*, 1979). $H_2O_2$ uptake by the cells in culture occurs within a few minutes (Antunes and Cadenas, 2000). However, full apoptotic execution may only follow a few hours later (Antunes *et al.*, 2001). Study done by Li *et al.* (1999) showed that, U937 cells treated with $H_2O_2$ for less than a minute could lead to the formation of HMW DNA fragments (Li *et al.*, 1999) of several hundred kb (Sestili *et al.*, 1995; Li *et al.*, 1999). These HMW fragments were reversible upon $H_2O_2$ removal. However, as treatment time was increased, the HMW was processed into smaller fragments that were not reversible (Li *et al.*, 1999). The transition from reversible to irreversible chromosome breaks was unclear but nuclease activation was suggested to be involved (Sun and Cohen, 1994; Huang *et al.*, 1997; Krieser and Eastman, 1998). Besides nucleases, exposure to $H_2O_2$ may lead to influx of calcium ions and cause increased intracellular calcium concentration. As a result, endonucleases are activated and lead to subsequent DNA fragmentation (Halliwell and Aruoma, 1991; Ueda and Shah, 1992). HMW DNA fragments

are then further digested by nucleases into smaller DNA fragments, which can be revealed as nucleosomal DNA ladders.

## 1.8 Objective of Study

Chromosome rearrangement is commonly observed in NPC. To date, the mechanism of chromosomal rearrangement in NPC remains to be elucidated. On the other hand, the apoptotic nuclease has been implicated in chromosome rearrangement in leukaemia, especially in translocation of the MLL gene. The MLL gene locates at chromosome 11q23, which is a common deletion site in NPC. Therefore, it is possible that chromosome rearrangement in NPC at 11q23 occur via a similar mechanism where apoptotic nuclease is believed to play a role.

ROS are the by-products of normal metabolism processes. The level of ROS increased during oxidative stress. Oxidative stress is well implicated in cancer development and is known to cause apoptosis. Hence, we hypothesise that, during oxidative stress, cells undergo apoptosis, where chromosomal DNA are fragmented. Upon erroneous repair, the cells survive with rearranged chromosome. The current study focuses on the MLL bcr because the MLL bcr gene is commonly translocated in leukaemia and it is also situated at chromosome 11q23 which is a common deletion site in NPC.

The specific objectives of this study are:

1. To assess the involvement of CAD in cleavage of the MLL bcr by CAD overexpression and CAD/ICAD co-expression.

2. To investigate the role of CAD in the MLL bcr cleavage by inhibiting CAD directly and indirectly.

In this study, the cervical cancer cell line, HeLa and nasopharyngeal carcinoma (NPC) cell line, SUNE1 were used as experimental model. Four approaches were employed. Firstly, CAD alone was overexpressed in cell lines, followed by treatment with $H_2O_2$ to induce apoptosis. Genomic DNA was extracted and IPCR was performed to detect breaks within the MLL bcr. Secondly, ICAD double mutant, ICAD-Ldm was overexpressed to inhibit CAD directly. Cells were also treated with $H_2O_2$ and cleavage within the MLL bcr was detection via IPCR. In the third approach, CAD activation was inhibited indirectly using Caspase Inhibitor (CI) prior to $H_2O_2$ treatment. Genomic DNA was extracted and IPCR was also performed. In the fourth approach, CAD was co-expressed with ICAD and treated with $H_2O_2$. Expression of CAD and ICAD was detected by Western Blotting. Subsequently, genomic DNA was isolated from these transfectants and IPCR was carried out.

# CHAPTER TWO

# OVEREXPRESSION OF CAD

## 2.1 Introduction

When cells are insulted, they undergo apoptosis and are eliminated. Apoptosis is also a naturally occurring process. At molecular level, this scenario is mediated by a family of cysteine-aspartate proteases, the caspases, which are involved in both the signalling and the execution phase of cell death (Nicholson, 1999). Even though there are several nucleases responsible for the degradation of genomic DNA, Caspase-activated DNase (CAD) is believed to be the major nuclease in causing chromosomal DNA fragmentation (Nagata, 2005).

CAD, a protein of 40 kDa, is also known as DNA Fragmentation Factor 40 (DFF40). Human (hCAD) and murine CAD (mCAD) consist of 344 and 338 amino acids, respectively (Enari *et al.*, 1998; Halenbeck *et al.*, 1998; Liu *et al.*, 1997). Under normal physiological condition, CAD forms a complex with its inhibitor, ICAD, and remains inactive (Liu *et al.*, 1997; Enari *et al.*, 1998). During apoptosis, caspase-3 is activated. The activated caspase-3 in turn, cleaves ICAD and hence releases CAD. CAD is then activated and able to execute its DNase activity (Sakahira *et al.*, 1998; Nagata, 2000). CAD cleaves double-stranded DNA; it creates either blunt end or one-base 5'-overhangs with 5'-phosphate and 3'-hydroxyl group. It does not generate single-strand nick and does not cleave RNA (Liu *et al.*, 1998; Liu *et al.*, 1999). There are two levels of apoptotic execution, in which the first stage involves high molecular weight (HMW) DNA fragmentation and later internucleosomal DNA cleavage. It was suggested that CAD is involved in HMW DNA cleavage in the early stage of apoptosis

(Samejima *et al.*, 2001) as well as the internucleosomal DNA cleavage (Enari *et al.*, 1998; Nagata, 2000). Internucleosomal DNA cleavage is a hallmark of apoptosis (Wyllie *et al.*, 1980).

Reactive oxygen species (ROS) are natural by-products of aerobic metabolism. Under normal physiological condition, ROS are produced during cell proliferation through the activation of growth-related signaling pathways (Benhar *et al.*, 2002). Cells produce oxidant by-products from normal metabolism, in which the estimated number is at 10,000 per day. ROS production is increased when cells undergo oxidative stress. These include hydrogen peroxide ($H_2O_2$), superoxide anion ($O_2^-$) and hydroxyl radical ($OH\cdot$) (Chandra and Samali, 2000; Finkel, 2000). ROS can cause damage to DNA, protein and lipid. There are DNA repairing enzymes and anti-oxidants that remove most of these damaging agents from our body (Ames and Shigenaga, 1991). Several laboratory results had shown that $H_2O_2$ can cause damage or mutation of human genome (Meneghini, 1993). Studies done by Burdon *et al.* (1996) showed that DNA extracted from HeLa cells that were exposed to various concentrations of exogenously added $H_2O_2$ caused DNA damage in AT-rich region (Burdon *et al.*, 1996). It was also shown that BHK-21 cells became apoptotic when exposed to high concentration of $H_2O_2$ (Burdon *et al.*, 1995).

In order to study the role of CAD in oxidative stress-induced chromosomal cleavage, the first approach was to overexpress CAD in mammalian cell lines, namely NPC cell line (SUNE1) and cervical cancer cell line (HeLa). HeLa cells were chosen to overexpress CAD because of its known low endogenous expression of CAD (Mukae *et al.*, 1998; Shiokawa and Tanuma,

2001). Studies done by Mukae *et al.* (1998) showed that overexpression of CAD in HeLa cells resulted in DNA fragmentation when treated with anti-Fas antibody. It was also shown that high level of CAD expression in Jurkat cells, when treated with staurosporine resulted in rapid DNA fragmentation (Mukae *et al.*, 1998). CAD at amino acid position of 157 in human and 155 in murine, was found to be involved in maintaining protein structure and/or DNA binding of CAD. Even though it is not an active site mutation, CAD mutated at this amino acid position caused the protein to bind to DNA in a different manner, such that it could not bind to the major groove of the DNA. As a result, CAD was unable to form stable complex with DNA (Woo *et al.*, 2004).

We hypothesised that when CAD is overexpressed, upon oxidative stress-activated apoptosis induction, CAD may cause initial chromosomal break of the MLL bcr. Therefore, overexpression of CAD in mammalian cells should show enhanced cleavage within the MLL bcr. Meanwhile, CAD mutant, hCAD(K157Q) expression in the cells should show a decrease in the MLL bcr cleavage as compared to cells overexpressing CAD. In this experiment, hCAD, mCAD and hCAD mutant, hCAD(K157Q) genes were subcloned into plasmid vector, pTracer. The recombinant plasmids, namely pTracer-hCAD, pTracer-mCAD and pTracer-hCAD(K157Q) were transfected into mammalian cells. As controls, transfection with vector and mock transfection were also performed. Cleavage within the MLL bcr was detected via optimised nested IPCR method. In this experiment, CAD alone was expressed because Enari *et al.* (1998) showed that, when CAD was expressed alone, chromosomal DNA fragmentation was observed (Enari *et al.*, 1998).

## 2.2 Materials And Methods

### 2.2.1 Subcloning

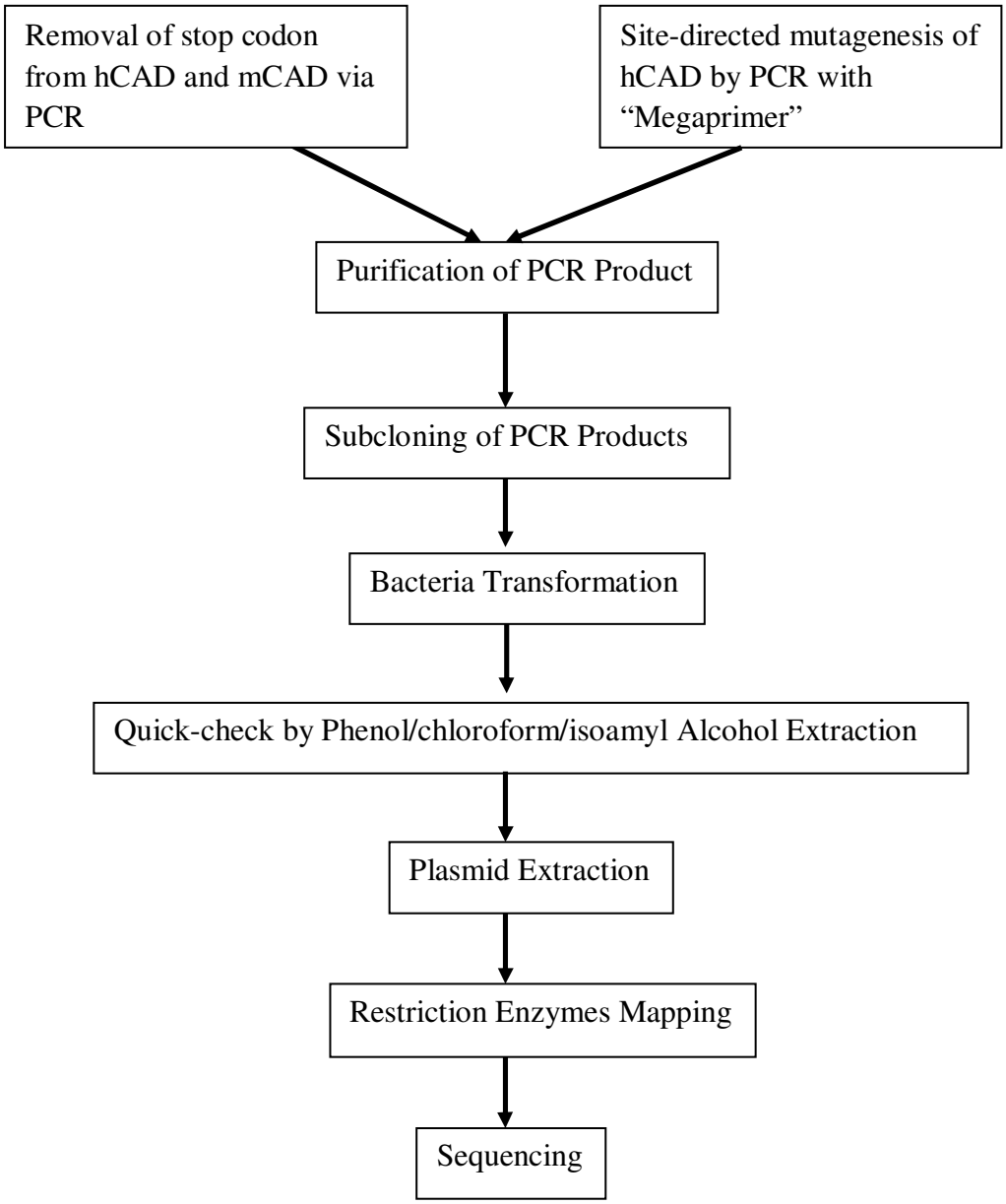


Figure 2.1: General flow of subcloning of pTracer-hCAD, pTracer-mCAD and pTracer-hCAD(K157Q).

For transfection purpose, plasmid pTracer-EF/V5-His B as shown in Appendix A was used as the plasmid vector. The genes for mCAD, hCAD and its mutant, hCAD(K157Q) as mentioned in Section 2.2.1.1 and 2.2.1.2 were produced via conventional polymerase chain reaction (PCR) method. Subsequently, these genes were subcloned into plasmid vector pTracer-EF/V5-His B (Invitrogen, USA). In order to express each protein with a V5 epitope at the C-terminal, the stop codon at the 3' end of each gene was removed, as described in Section 2.2.1.1. Thus expression of the genes can be detected by Anti-V5 antibody (Invitrogen, USA) as discussed in Chapter Five. Subcloning method is summarised in Figure 2.1.

### 2.2.1.1 Removal of Stop Codon from hCAD and mCAD via PCR

Plamid pBS-hCAD and pBS-mCAD were used as DNA template. These plasmids were kindly provided by Professor Shigekazu Nagata from University of Osaka, Japan. A pair of primers was designed according to hCAD (GenBank accession number AB013918) and mCAD (GenBank accession number AB009377) sequences reported, as showed in Appendix B.

For amplification of hCAD without stop codon, forward primer, designated as hCAD(F) (5' – CG**GGTACC**ATGCTCCAGAAG – 3') which carries a *Kpn* I restriction site (GGTACC) at the 5' end as shown in bold and reverse primer, designated as hCAD(R) (5' – CG**TCTAGA**CTGGCGTTTCCG – 3') which carries an *Xba* I restriction site (TCTAGA) as shown in bold were used. Primer hCAD(R) was designed to exclude the stop codon at the 3'

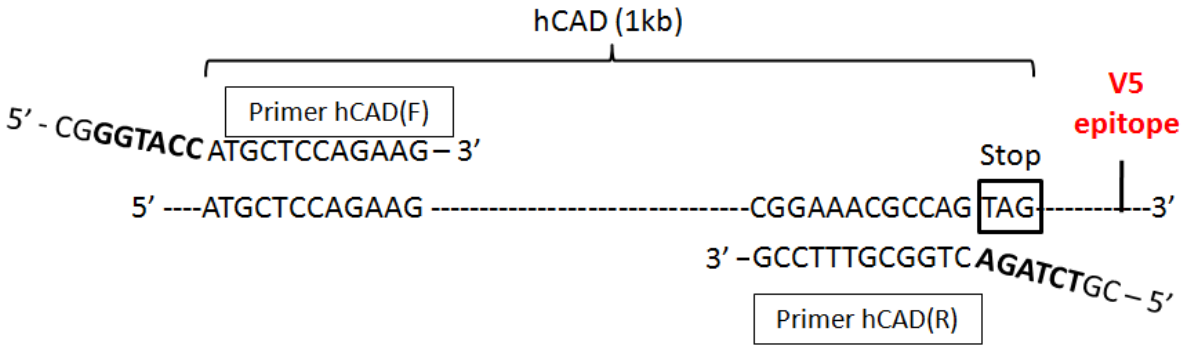


Figure 2.2: Schematic diagram showing the binding position of primers for hCAD amplification. Forward primer, hCAD(F) contains a *Kpn* I restriction site (GGTACC). Reverse primer, hCAD(R) contains an *Xba* I restriction site (TCTAGA). Amplification by using these primers produced a 1 kb fragment of hCAD which included the start codon (ATG) and excluded the stop codon (TAG). This fragment carries a *Kpn* I restriction site at its 5' end and an *Xba* I restriction site at its 3' end. By omitting the stop codon, hCAD will be expressed as a fusion protein with V5 epitope at the C-terminal.

end of hCAD gene as shown in Figure 2.2. By excluding the stop codon, hCAD will be expressed with V5 epitope at the C-terminal.

Amplification of mCAD without stop codon was performed by using mCAD(F) (5' – CT**GATATC**ATGTGCGCGGTG – 3') which contains an *Eco*R V restriction site (GATATC in bold) and reverse primer, designated as mCAD(R) (5' – CC**TCTAGA**GCGCTTCCGAGC – 3') which carries an *Xba* I restriction site (TCTAGA in bold) at the 3' end. Primer mCAD(R) was designed purposely to exclude the stop codon (TAG) as shown in Figure 2.3. Since the stop codon was omitted, subsequent nucleotides were read and expressed, including the V5 epitope.

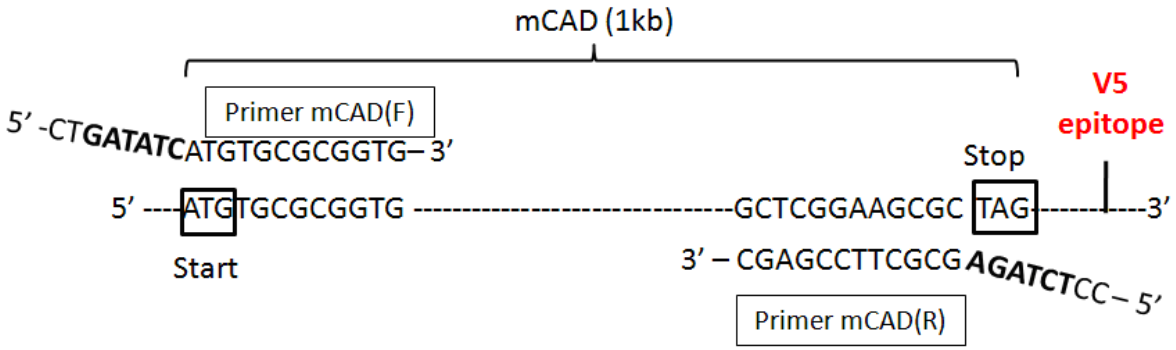


Figure 2.3: Schematic diagram showing the binding position of primers for mCAD amplification. Forward primer, mCAD(F) contains an *Eco*R V restriction site (GATATC). Reverse primer, mCAD(R) contains an *Xba* I restriction site (TCTAGA). Amplification by using these primers produced a 1 kb fragment of mCAD which included the start codon (ATG) and excluded the stop codon (TAG). This fragment carries an *Eco*R V restriction site at its 5' end and an *Xba* I restriction site at its 3' end. By omitting the stop codon, mCAD will be expressed as fusion protein with V5 epitope at the C-terminal.

PCR was carried out with 10 ng of DNA template as recommended together with 1X Phusion HF Buffer (Finnzyme, Finland), 200 µM of each of the deoxynucleotide triphosphate, dNTP (Promega, USA), 0.5 µM of each of the primers, 0.4 U of Phusion DNA polymerase and sterile ultra pure water (sUPW) in a final volume of 20 µl in 0.2 ml PCR tubes (Eppendorf, USA). PCR was performed in optimised condition with 30 seconds of initial denaturation at 98$^{o}$C for 1 cycle, followed by 30 cycles of denaturation at 98$^{o}$C for 10 seconds, annealing of primers at 67.9$^{o}$C for 30 seconds, extension at 72$^{o}$C for 15 seconds, followed by single cycle of final extension step at 72$^{o}$C for 10 min as shown in Table 2.1 by using MJ Research PT-200 Peltier Thermal Cycler, USA. The annealing temperatures were calculated based on the nearest-neighbour method suggested for Phusion DNA Polymerase (www.finnzymes.com).

Table 2.1: PCR condition for amplification of hCAD and mCAD without stop codon.

| **Step** | **Temperature ($^{o}$C)** | **Time** |
|---|---|---|
| Hot start | 80 | Forever |
| Initial denaturation | 98 | 30s |
| Denaturation | 98 | 10s |
| Annealing | 67.9 | 30s |
| Extension | 72 | 15s |
| | Go to Denaturation step and repeat for 29 cycles | |
| Final extension | 72 | 10 minutes |
| Cooling | 20 | Forever |

### 2.2.1.2 Site-directed Mutagenesis of hCAD by Polymerase Chain Reaction with "Megaprimer"

#### 2.2.1.2.1 Amplification of "Megaprimer"

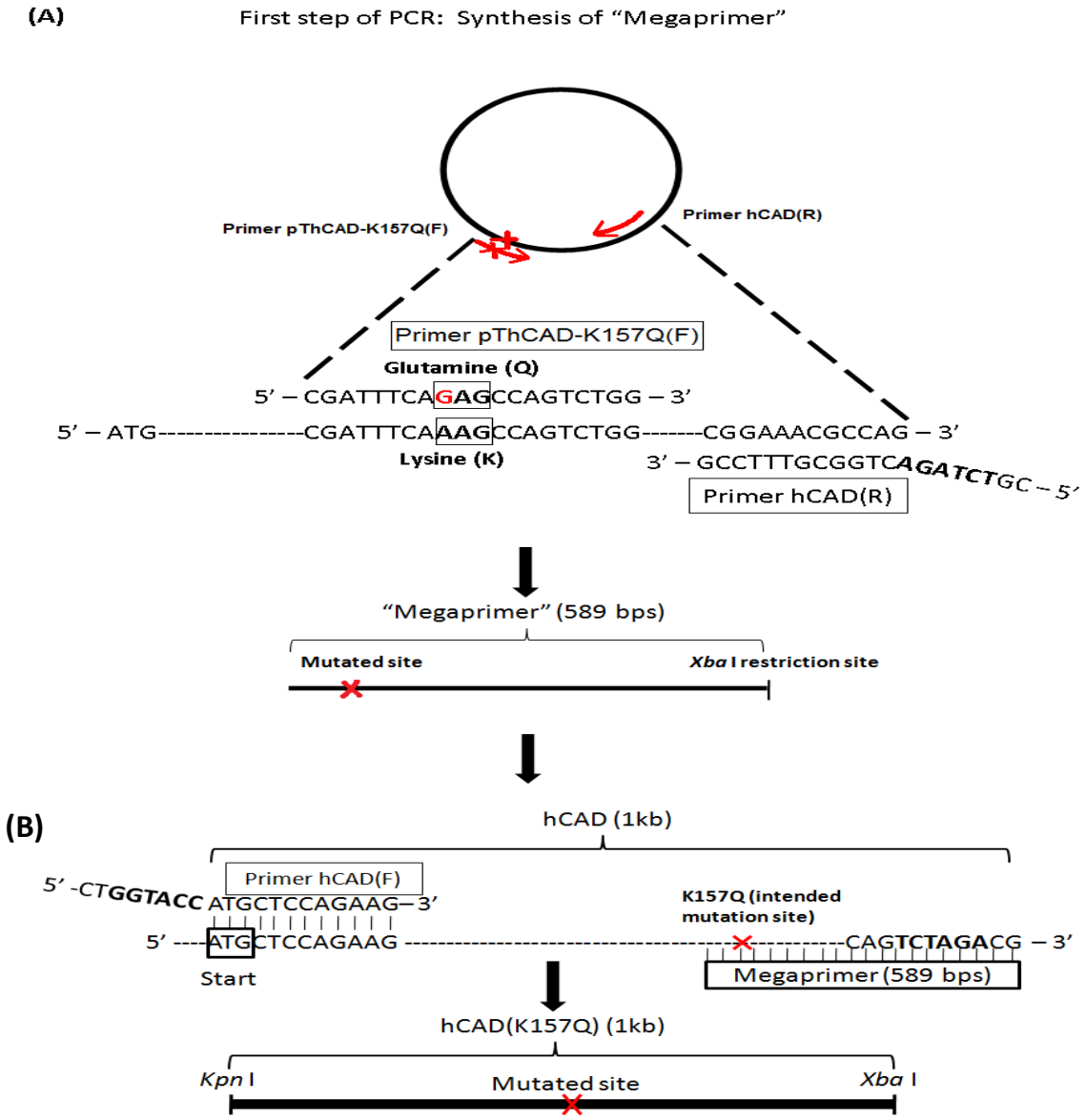


Figure 2.4: Schematic diagram showing amplification of mutant hCAD, hCAD(K157Q). (A) In the first step of PCR, plasmid pTracer-hCAD without stop codon was used as DNA template. Forward primer, pThCAD-K157Q(F) was designed to carry a mutation from Lysine (K), AAG to Glutamine (Q), GAG whereas reverse primer, hCAD(R) was designed to carry an *Xba* I restriction site. K157 is the intended mutation site. After amplification via conventional PCR method, a "Megaprimer" of size 589 bps was synthesised which carries the mutated site (red cross) at its 5' end and *Xba* I restriction site at 3' end. (B) In second step of PCR, "Megaprimer" synthesised in the first step of PCR was used as reverse primer. Primer hCAD(F) which carries a *Kpn* I restriction site was used as forward primer. One kb of mutant

hCAD, hCAD(K157Q) fragment was amplified, carrying a *Kpn* I restriction site at its 5' end and *Xba* I restriction site at its 3' end.

A PCR-based method was used to mutate human CAD at amino acid position 157, from Lysine (K) to Glutamine (Q), designated as hCAD(K157Q). This method involved the amplification of "Megaprimer". The purpose of amplifying "Megaprimer" is to produce a primer carrying the mutation as well as the desired restriction sites. This "Megaprimer" was produced for use in the second step of PCR to produce the hCAD(K157Q) (refer Section 2.2.1.2.2). This method was employed because there is no convenient restriction site near the intended mutation site which can be used for direct subcloning upon completion of site-directed mutagenesis. A pair of primers, pThCAD-K157Q(F) and hCAD(R) were designed according to hCAD sequence (GenBank accession number AB013918) to synthesise a "Megaprimer" of 589 bps. Forward primer pThCAD-K157Q(F) (5' – CGATTTCA**GAG**CCAGTCTGG – 3') was designed specifically to carry the mutation from Lysine (K), AAG to Glutamine (Q), GAG as indicated in bold. Meanwhile, reverse primer hCAD(R) (5' – CG**TCTAGA**CTGGCGTTTCCG – 3') was designed at the 3' end of hCAD and carries an *Xba* I restriction site (TCTAGA) as indicated in bold as mentioned in Section 2.2.1.1. PCR was performed by using 100 ng of pTracer-hCAD without stop codon as DNA template under the same PCR condition as mentioned in Section 2.2.1.1, except the annealing temperature for this set of primers was 65$^{o}$C as shown in Table 2.2. The PCR product ("Megaprimer") obtained which carries mutation at the desired site was analysed via gel electrophoresis. DNA fragment of size around 589 bps was excised and purified by using QIAquick Gel Extraction Kit (Qiagen), following the manufacturer's instruction. Briefly, PCR products were analysed on 1% agarose gel and product of size of 589 bps was excised with clean and sharp scarpel. Empty 1.7 ml microcentrifuge tube (Axygen, USA) was

weighed. Excised gel slice was added into the sterile empty microcentrifuge tube and weighed. Gel was dissolved with 3 Volumes (V) of Buffer QG to 1 Volume of gel at 50$^{o}$C for approximately 10 minutes until gel slice dissolved completely. At the same time, QIAquick spin column was placed inside the 2 ml collection tube provided. The sample was applied to the QIAquick column and centrifuged at 18,000x g (Eppendorf 5417R) for 1 minute at room temperature and the flow through was discarded. Five hundred µl of Buffer QG was added to QIAquick column placed in the same collection tube to remove all traces of agarose. Centrifugation was performed at 18,000x g for 1 minute and flow through was discarded. Sample was washed by adding 0.75 ml of Buffer PE into the column and let the column stand for 2 to 5 minutes before centrifugation at 18,000x g (Eppendorf 5417R) for 1 minute at room temperature. Flow through was discarded and additional centrifugation at 13,000x g for 1 minute was done. QIAquick column was placed into a clean 1.5 ml microcentrifuge tube. DNA was eluted by adding 50 µl of Buffer EB into the center of the column and centrifuged at 13,000x g for 1 minute. Purification of DNA fragment from agarose gel by using QIAquick Gel Extraction Kit (Qiagen) is simplified in flowchart in Appendix C.

Table 2.2: PCR condition for amplification of "Megaprimer" of mutant hCAD, hCAD(K157Q).

| **Step** | **Temperature ($^{o}$C)** | **Time** |
|---|---|---|
| Hot start | 80 | Forever |
| Initial denaturation | 98 | 30s |
| Denaturation | 98 | 10s |

| | | |
|---|---|---|
| Annealing | 65 | 30s |
| Extension | 72 | 15s |
| | Go to Denaturation step and repeat for 29 cycles | |
| Final extension | 72 | 10 minutes |
| Cooling | 20 | Forever |

#### 2.2.1.2.2 Amplification of 1 kb of Mutant hCAD, hCAD(K157Q)

The ""Megaprimer"" synthesised (refer to Section 2.2.1.2.1) (40 ng) was then used as the reverse primer together with the forward primer, hCAD(F) (5' – CG**GGTACC**ATGCTCCAGAAG – 3') which contains a *Kpn* I restriction site (GGTACC) for second step of PCR to amplify 1 kb of insert which is hCAD(K157Q). As mentioned before, "Megaprimer" carries an *Xba* I restriction site (TCTAGA). Second step of PCR was performed under the same condition as first step of PCR in producing "Megaprimer", except the annealing temperature was increased to 71$^{o}$C instead of 65$^{o}$C as shown in Table 2.3. This produced the full length hCAD(K157Q) with a *Kpn* I restriction site at the 5' end and an *Xba* I restriction site at the 3' end as shown in Figure 2.4(B). The synthesis of "Megaprimer" and hCAD(K157Q) are simplified in Figure 2.4.

Table 2.3: PCR condition for amplifying full length (approximately 1 kb) of mutant hCAD, hCAD(K157Q).

| Step | Temperature ($^{o}$C) | Time |
|---|---|---|
| Hot start | 80 | Forever |
| Initial denaturation | 98 | 30s |
| Denaturation | 98 | 10s |
| Annealing | 71 | 30s |
| Extension | 72 | 15s |
| | Go to Denaturation step and repeat for 29 cycles | |
| Final extension | 72 | 10 minutes |
| Cooling | 20 | Forever |

### 2.2.1.3 Purification of PCR Products: mCAD, hCAD and hCAD(K157Q)

PCR products were analysed by gel electrophoresis and subsequently purified by using QIAquick Gel Extraction Kit (Qiagen) as described in Section 2.2.1.2.1.

### 2.2.1.4 Subcloning of PCR Products

Purified PCR products [mCAD, hCAD and its mutant hCAD(K157Q)] were subcloned by ligating with plasmid pTracer upon restriction digest with their respective restriction enzymes as mentioned in Section 2.2.1.1 and 2.2.1.2. Plasmid pTracer digested with restriction

enzymes *Kpn* I and *Xba* I was ligated with hCAD and its mutant hCAD(K157Q) which were also digested with the same restriction enzymes. As for mCAD, it was digested with restriction enzymes *Eco*R V and *Xba* I, and ligated with pTracer which was digested with the same restriction enzymes. Ligation was carried out at an insert to vector ratio of 10 to 1 by using 40 units of T4 DNA ligase, 1X T4 DNA ligase buffer (NEB, England) and sUPW in a final volume of 20 µl at 16$^{o}$C overnight. The process is summarised in Figure 2.5.

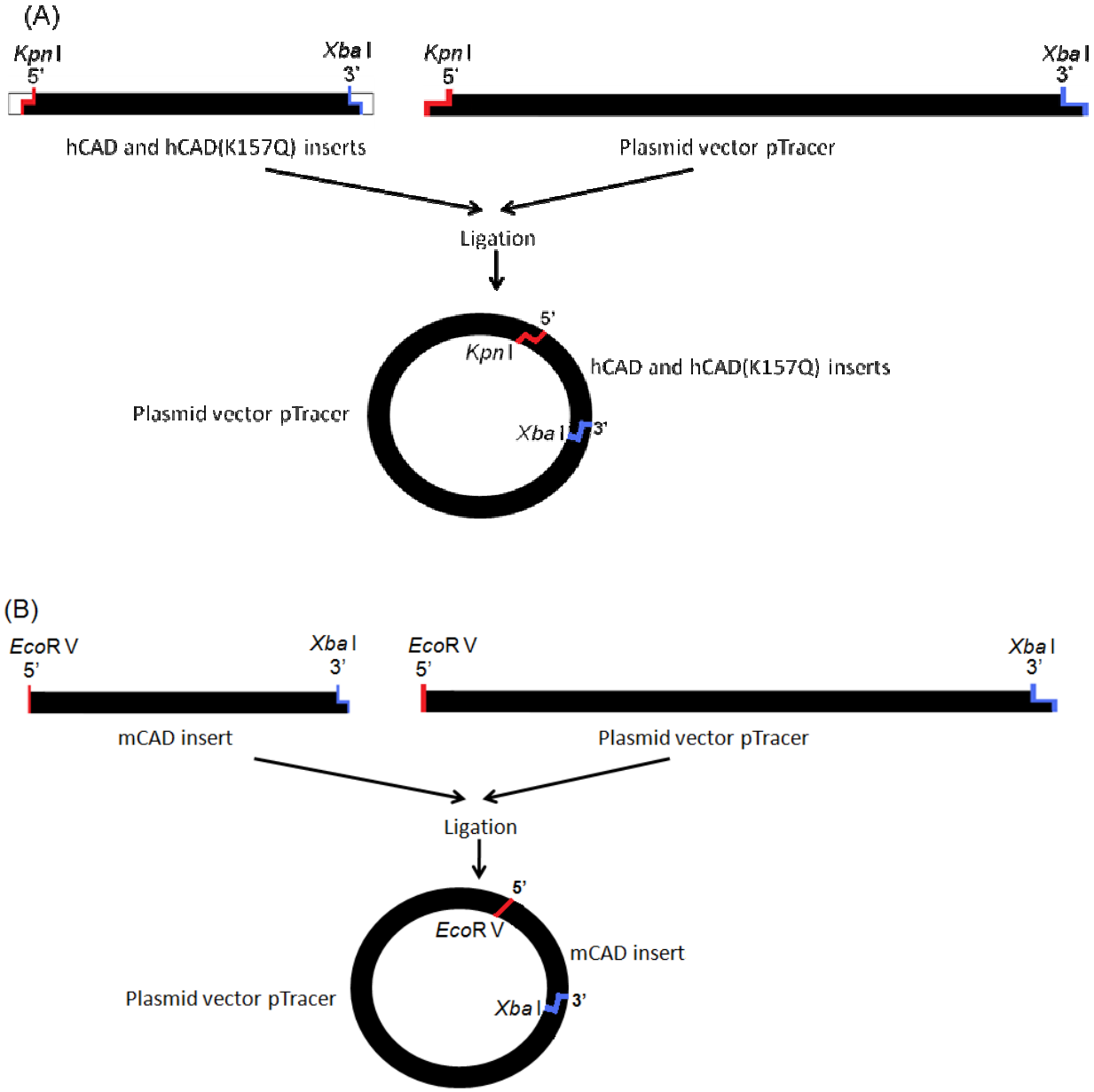


Figure 2.5: Schematic diagram showing the generation of recombinant plasmids carrying hCAD, hCAD(K157Q) and mCAD. (A) Amplified inserts, hCAD and its mutant, hCAD(K157Q) as well as plasmid vector, pTracer were digested with *Kpn* I and *Xba* I. Ligation was then carried out to generate recombinant plasmid carrying either hCAD or hCAD(K157Q). (B) For subcloning of mCAD into plasmid vector pTracer, both mCAD and pTracer were digested with *Eco*R V and *Xba* I.

### 2.2.1.5 Bacteria Transformation

Bacteria transformation was carried out by using electroporation method. Electrocompetent cells *Escherichia coli* (*E. coli*) HB101 were prepared as described in Appendix D. Electroporation was carried out by using Eppendorf Electroporator 2510 at charging voltage of 2000V, fired strength of 20 kV/cm and pulse length of 5 – 6 mili second. Subsequently, bacteria transformants were suspended with S.O.C media (Invitrogen, USA) which was pre-warmed at 37$^{o}$C for approximately 30 minutes and transferred to Snap Cap tube (Fisherbrand, UK). Incubation at 37$^{o}$C was carried out for 1 hour 15 minutes with agitation at a speed of 220 rpm. Bacteria culture was spreaded on LB agar plates containing 50 µg/ml of Ampicillin (GIBCO, USA) and incubated at 37$^{o}$C overnight. Bacteria colonies were picked randomly and each was cultured in 2 ml of LB broth containing 50 µg/ml Ampicillin overnight. The electroporation protocol is summarised in Appendix E. Clones were then checked by performing Quick-check using phenol/chloroform/isoamyl alcohol extraction as described in Section 2.2.1.6.

### 2.2.1.6 Quick-check by Phenol/chloroform/Isoamyl Alcohol Extraction

Picked colonies were checked by extraction with phenol/chloroform/isoamyl alcohol (Ratio 25:24:1). Approximately 900 µl of bacteria culture was taken and bacteria cells collected by centrifuging at 4000x g for 3 minute (Eppendorf 5415 C, Germany). Eight hundred µl of supernatant was discarded. The remaining 100 µl of supernantant together with bacteria cells was suspended gently. Phenol/chloroform/isoamyl alcohol was thawed and centrifuged at 2,000x g for 3 minutes (Eppendorf 5810, Germany). One hundred µl of phenol/chloroform/isoamyl alcohol was added to the bacteria suspension and vortexed

vigorously at 2,200 rpm for 1 minute until homogenous. Mixture was further centrifuged at 14,000x g (Eppendorf 5415 C) for 5 minutes. Ten µl of aqueous phase containing the DNA was taken and analysed on 1% agarose gel with 0.5X TBE buffer. Bacteria culture for clone which was suspected to carry the desired plasmid was then grown in 10 ml of LB broth with 50 µg/ml Ampicilllin. The culture was then agitated at a speed of 220 rpm overnight at 37$^{o}$C. The quick-check protocol is simplified in Appendix F.

#### 2.2.1.7 Plasmid Extraction

Plasmid was extracted from transformant by using S.N.A.P Miniprep Kit (Invitrogen, USA) following the manufacturer's protocol. Briefly, approximately 1 to 3 ml of bacteria culture was taken and loaded into 1.5 ml centrifuge tube (Axygen, USA). Bacteria cells were collected by centrifugation at 14,000x g (Eppendorf 5415 C) for 1 minute. Cell pellet was suspended in 150 µl of Suspension Buffer. Subsequently, cells were lysed by adding 150 µl of Lysis Buffer, mixed gently and incubated at room temperature for 3 minutes. Lysate was then precipitated by adding 150 µl of ice-cold precipitation salt and inverted 6 to 8 times to ensure thorough mixing. Mixture was centrifuged at 14,000x g (Eppendorf 5415 C) for 5 minutes at room temperature. At the same time, S.N.A.P Miniprep column was placed inside the 2 ml collection tube provided. After the centrifugation, supernatant was pipetted into a sterile microcentrifuge tube, followed by addition of 600 µl of Binding Buffer and mixed by inverting 5 to 6 times. The mixture was then pipetted into the S.N.A.P Miniprep Column/Collection tube and centrifuged at 1,000x g for 10 to 30 seconds at room temperature. Column flow through was discarded and 500 µl of Wash Buffer was added into the column. Column/collection tube was centrifuged at room temperature at the speed of

1,000x g for 30 seconds (Eppendorf 5417R). Flow through was discarded and 900 µl of 1X Final Wash buffer was added into the column. Column/collection tube was centrifuged at room temperature at the speed of 1,000x g for 30 seconds (Eppendorf 5417R). Flow through was discarded. Additional centrifugation was done by centrifuging the column/collection tube at room temperature at maximum speed for 1 minute to dry the resin. In order to elute and collect the extracted plasmid, S.N.A.P Miniprep Column was transferred to a sterile 1.5 microcentrifuge tube (Axygen). Fifty µl of TE Buffer (pH 8.0) was added to the resin and incubated for 3 minutes at room temperature. Plasmid was eluted by centrifuging the column and microcentrifuge tube at maximum speed (Eppendorf 5417R) at room temperature for 1 minute. Plasmid extraction by using S.N.A.P Miniprep Kit is summarised in Appendix G.

#### 2.2.1.8 Restriction Enzymes Mapping

Suspected clones were further checked via restriction mapping using various restriction enzymes. Approximately 200 to 500 ng of plasmids were isolated from the selected clones and digested with 10 – 20 units of each of the restriction enzymes. Plasmid pTracer-hCAD and pTracer-hCAD(K157Q) were checked by using restriction enzymes *Kpn* I and *Xba* I, *Bam*H I, *Sma* I as well as *Eco*R V. Meanwhile, plasmid pTracer-mCAD was checked with restriction enzymes *Eco*R V and *Xba* I, *Eco*R I, *Kpn* I as well as *Sma* I. All restriction enzymes used were purchased from NEB except *Eco*R I (Fermentas, USA) and *Eco*R V (Promega). Restriction mapping was carried out as illustrated in Table 2.4. Plasmids extracted were sent for sequencing for further confirmation and checked for possible mismatching introduced by PCR as explained in Section 2.2.1.9.

Table 2.4: Restriction mapping reactions for pTracer-hCAD, pTracer-mCAD and pTracer-hCAD(K157Q) and the expected size of fragments produced.

| Samples | pTracer-hCAD / pTracer-hCAD(K157Q) | | | | pTracer-mCAD | | | |
|---|---|---|---|---|---|---|---|---|
| Restriction enzyme (RE), unit | *Kpn* I (10U) and *Xba* I (20U) | *Bam*H I (20 U) | *Sma* I (20 U) | *Eco*R V (20 U) | *Eco*R V (20 U) and *Xba* I (20 U) | *Eco*R I (50U) | *Kpn* I (10U) | *Sma* I (20U) |
| sUPW, µl | 4 | 5 | 6 | | | | | |
| RE buffer, µl | 1 (10X NE Buffer 2 | 1 (10X *Bam*H I Buffer 2 | 1 (10XNE Buffer 4 | 1 (10X Buffer D) | 1 (10X NE Buffer 2 | 1 (10X Buffer *Eco*R I) | 1 (10XNE Buffer 1 | 1 (10XNE Buffer 4 |
| 10X BSA, µl | 1 | 1 | 1 | 0.8 | 1 | - | 1 | - |
| Plasmid, µl | 2 | 2 | 2 | 2 | 2 | 2 | 2 | 2 |
| Total reaction, µl | 10 | 10 | 10 | 10 | 10 | 10 | 10 | 10 |
| Temperature, $^{o}$C | 37 | 37 | 25 | 37 | 37 | 37 | 37 | 25 |
| Duration | 2 hours | 2 hours | 2 hours | 2 hours | 2 hours | 2 hours | 2 hours | 2 hours |
| Expected size of fragments | 5.867 kb and 1.016 kb | 5.03 kb, 1.853 kb and 261 bps | 4.414 kb and 2.469 kb | No restriction site (circularised plasmid) | 5.91 kb and 1.039 kb | 6.049 kb (linearised) | 6.186 kb and 863 bps | 4.247 kb, 2.481 kb and 221 bps |

#### 2.2.1.9 Sequencing

For further confirmation, extracted plasmids were sent for sequencing. Sequencing reactions were prepared according to recommended protocol by DYEnamic ET Termination Cycle Sequencing Kit (Amersham Biosciences, US) following the manufacturer's protocol as summarised in Appendix H.

Briefly, for each of the sequencing reaction, 0.1 – 0.2 pmol of DNA template, 5 pmol each of primers (forward or reverse primer), 8 µl of sequencing reagent premix and sUPW were added to a total volume of 20 µl. Primers were designed at locations approximately 50 to 100 bps from the region to be sequenced. Forward primer, pTracer(KX-F) (5' – TTCAGGTGTCGTGAGGAATT – 3') was used to sequence the sense strand whereas primer pTracer(KX-R) (5' – ATGGTGATGGTGATGATGAC – 3') was used to sequence anti-sense strand of the plasmids pTracer-hCAD, pTracer-hCAD(K157Q) and pTracer-mCAD. Amplification was carried out using thermal cycler (MJ Research). Twenty-five cycles of PCR was carried out at 95$^{o}$C for 20 seconds, followed by 50$^{o}$C for 15 seconds and 60$^{o}$C for 1 minute in 0.2 ml PCR tubes (Eppendorf). When cycling completed, 2 µl (1/10 Volume) of sodium acetate (1.5 M, pH>8)/EDTA (250 mM) buffer was added to each tube. Subsequently, 80 µl of 95% ethanol was added to each reaction and mixed well by vortexing. Reaction mixture was transferred to 1.5 ml microcentrifuge tubes and centrifuged at 15,000x g (Eppendorf 5417R) for 15 minutes at room temperature. As much as possible of the supernatant was removed by aspiration from each microcentrifuge tube to prevent dye blobs. DNA pellets were washed with 1 ml of 70% ethanol. Supernatant was removed by aspiration and pellet was air-dried for 5 minutes without overdrying the pellets and sent for sequencing. Sequencing results obtained as shown in Appendix I were analysed by using DNASTAR

software. This software was founded by University of Wisconsin Professor of Genetics Frederick Blattner and his student colleague John Schroeder in the early 1980s. The centrifuge used for this protocol was Eppendorf Centrifuge 5417R.

### 2.2.2 Mammalian Cell Culture

HeLa cell line was obtained from Dr. Edmund Sim Ui Hang from Universiti Malaysia Sarawak. HeLa was derived from an adenocarcinoma of the cervix in 1952 and was the first human epithelial cancer cell line established in long-term culture (Gey *et al.*, 1952). The cells have a hypertriploid chromosome number. This cell line was selected as transfection host due to its known low endogenous level of CAD as shown by RT-PCR and Northern blot analysis, and little internucleosomal DNA fragmentation was detected by various apoptotic stimuli, although they died by apoptosis (Shiokawa *et al.*, 2001). HeLa cells are also adherent monolayer cells. On the other hand, the NPC cell line, SUNE1, was generously provided by Professor Dr. Sam Choon Kook previously from Universiti Malaya, Kuala Lumpur. This cell line was established from a poorly differentiated non-keratinizing nasopharyngeal carcinoma cell from a Chinese (Gu *et al.*, 1983). Morphologically, the cells have well-defined cell margins, stratified or pavemented and not syncytial. SUNE1 grows as adherent epitheloid cells forming a monolayer.

HeLa cells were maintained in Dulbecco's Modified Eagle Medium (DMEM), which contains low glucose (1X), 1g/L D-glucose, L-glutamine (2 mM) and 100 mg/L sodium pyruvate, supplemented with 10% heat-inactivated fetal bovine serum (FBS), penicillin (100 U/ml) and streptomycin (100 µg/ml). Meanwhile, NPC cells (SUNE1) were maintained in RPMI 1640 medium supplemented with 10% heat-inactivated fetal bovine serum (FBS), L-glutamine (2

mM), penicillin (100 U/ml) and streptomycin (100 µg/ml). TrypLE Express (Invitrogen) was used to detach cells from the T25 tissue culture flask (Nalgene) during passaging. The above mentioned items were purchased from GIBCO, Invitrogen. Cells were kept in a humidified incubator with an atmosphere of 95% air and 5% $CO_2$ at 37°C. Upon reaching confluency of about 70%, cells were passaged and grown in new flask. Confluency of cells was estimated by observing the cells at approximately 5 to 7 microscope field.

### 2.2.3 Dose Response Test of SUNE1 and HeLa Cells to Hydrogen Peroxide, $H_2O_2$

SUNE1 cells in T25 flask at 70% confluency were trypsinised with 0.7 ml of TrypLE Express (Invitrogen) and suspended with 4.5 ml of complete culture medium. From a total of 5.0 ml, 0.2 ml of cell suspension was seeded into 8 60 mm dishes where each of the dishes was pre-added with 4 ml of complete culture medium. Cells were grown to 50 to 60% confluency. These cells were then treated with 0, 10, 50, 100, 500, 1000 and 10,000 µM of $H_2O_2$ for 20 hours. In addition, as a positive control, 1 ml of cells was seeded to a separate 60 mm dish containing 3 ml of complete medium to allow the cells to overgrow to more than 100% confluency upon collection. This sample was named as the apoptotic sample. Cells were collected, genomic DNA extracted and breakpoint within the MLL bcr for each sample was analysed using IPCR method as described in section 2.2.5.

### 2.2.4 Transient Overexpression of CAD in Mammalian Cell Lines

#### 2.2.4.1 Plasmid Extraction for Transfection

For transfection purpose, plasmid pTracer-hCAD, pTracer-mCAD and pTracer-hCAD(K157Q) were each extracted from single colony streaked from glycerol stock by using

QIAfilter Plasmid Maxi Kits (Qiagen) following manufacturer's instruction. Plasmid yield obtained by using this kit was approximately 300 – 500 µg. In order to obtain single colony, the desired clones were streaked on LB agar plates, which contained 50 µg/ml Ampicillin. Single colony was picked and inoculated into starter culture containing 2 ml of LB Broth with 50 µg/ml Ampicillin and grown for 8 hours. Fifty µl of bacteria culture was then further inoculated into 100 ml of LB Broth containing 50 µg/ml Ampicillin and grown overnight. Bacteria cells were harvested by centrifugation at 6,000x g (Eppendorf 5810R) for 15 minutes at 4$^{o}$C. Supernatant was discarded. For lysis of bacteria cells, 10 ml of Buffer P1 was added and mixed by vortexing or pippeting up and down. Subsequently, 10 ml of Buffer P2 was added and mixed thoroughly by inverting 4 to 6 times. Subsequently, the mixture was incubated at room temperature for 5 minutes. Ten ml of chilled Buffer P3 was added and mixed throroughly by inverting 4 to 6 times. Lysate was poured into the barrel of QIAfilter cartridge which was capped at the nozzle and incubated for 10 minutes at room temperature. Meanwhile, QIAGEN-tip 500 was equilibrated by applying 10 ml of Buffer QBT and emptied by gravity flow. Cap was removed from QIAfilter Catridge outlet nozzle. Plunger was inserted gently into the QIAfilter Maxi Catridge to create the pressure. The cell lysate was filtered into the equilibrated QIAGEN-tip 500. Approximately 25 ml of cleared lysate was filtered into the resin. QIAGEN-tip was washed with 30 ml of Buffer QC twice. DNA was eluted by adding 15 ml of QF buffer into QIAGEN-tip. In order to precipitate DNA from the elution buffer, 10.5 ml (0.7 Volume) of isopropanol at room temperature was added. Solution was mixed and centrifuged at 15,000x g (Eppendorf 5810R), 4$^{o}$C for 30 minutes. Supernatant was removed. DNA pellet was then washed with 5 ml of 70% Ethanol at room temperature and centrifuged at 15,000x g. Supernatant was removed and further centrifuged at 15,000x g

(Eppendorf 5810R), 4°C for 10 minutes. DNA pellet was air-dried for about 5 to 10 minutes. DNA pellet was redissolved in 100 µl of Buffer TE, pH 8.0.

#### 2.2.4.2 Transient Transfection of CAD into SUNE1 Cells

Subcloned plasmid pTracer-hCAD, pTracer-mCAD and pTracer-hCAD(K157Q) were overexpressed in SUNE1 cells transiently to study the overexpression of CAD in inducing chromosomal break. As controls, plasmid vector pTracer was transfected as well as mock transfection where cells underwent transfection process without DNA. Cells were maintained at 70% confluency in T25 flask. TrypLE Express was added to detach the cells. The cells were diluted 10 fold to a total of 5 ml and suspended. One ml of suspended cells was seeded into each of the 60 mm dishes containing 3 ml of seeding medium 24 hours prior to transfection. Seeding medium used was plain RPMI medium supplemented with 20% FBS and without antibiotics. During the transfection process, 2 µg of DNA to be transfected was mixed with 8 µl of PLUS reagent (Invitrogen) and transfection medium was added to a final volume of 250 µl. Transfection medium used was plain RPMI medium (without FBS, Penicillin/Streptomycin and L-glutamine). Subsequently, the mixture was incubated for 15 minutes to allow formation of DNA-PLUS complex. Meanwhile, 12 µl of Lipofectamine (Invitrogen) was diluted with transfection medium to a total volume of 250 µl. After 15 minutes, 250 µl of diluted Lipofectamine was added to 250 µl of DNA-PLUS complexes and incubated for another 15 minutes. Seeding medium in the 60 mm dishes was replaced with 2 ml of transfection medium. Subsequently, DNA-PLUS-Lipofectamine complex mixture was added. After 3 and 5 hours of transfection for SUNE1 and HeLa cells respectively, transfection medium was replaced with fresh complete medium containing RPMI 1640

medium supplemented with 10% FBS, L-glutamine (2 mM), penicillin (100 U/ml) and streptomycin (100 µg/ml). Transfected cells were then subjected to oxidative stress-induced apoptosis 17 hours post transfection.

### 2.2.5 Inverse Polymerase Chain Reaction (IPCR)

#### 2.2.5.1 Genomic DNA Extraction for IPCR

Genomic DNA was extracted using Blood and Cell Culture DNA Mini Kit (Qiagen) as described in Appendix J according to manufacturer's instruction. In brief, the collected cells were washed with 1 ml of cold PBS. The cells were centrifuged at 4ºC for 10 minutes at 1,500x g (Eppendorf 5810R). The supernatant was discarded. Three ml of cold PBS was added to the cell pellet and vortexed before being centrifuged at 4ºC for 10 minutes at 1,500 x g. The supernatant was discarded. The pellet was resuspended in 0.5 ml of cold PBS. One Volume of ice-cold Buffer C1 and 3 Volumes of ice-cold distilled water were added. The tubes were inverted several times to mix, followed by 10 minutes incubation on ice. The lysed cells were centrifuged at 4ºC for 15 minutes at 1,300x g (Eppendorf 5810R). The supernatant was discarded, 0.25 ml of ice-cold Buffer C1 and 0.75 ml of ice-cold distilled water were added. The pelleted nuclei were resuspended by vortexing before being centrifuged again at 4ºC for 15 minutes at 1,300x g (Eppendorf 5810R). The supernatant was discarded. One ml of Buffer G2 containing RNase A (200 µg/ml) was added and mixed thoroughly by vortexing for 10 to 30 seconds at maximum speed. Twenty-five µl of QIAGEN Protease was then added to the nuclei, followed by incubation at 50ºC for 1 hour. QIAGEN Genomic-tip 20/G was equilibrated with 2 ml of Buffer QBT, and the tip was allowed to empty by gravity flow. The clear lysate was vortexed for 10 seconds at maximum speed and was applied to the

equilibrated QIAGEN Genomic-tip. The sample was allowed to enter the QIAGEN Anion-Exchange Resin by gravity flow. The QIAGEN Genomic-tip was washed with l ml of Buffer QC for 3 times. The genomic DNA was eluted with 0.9 ml of pre-warmed Buffer QF for 2 times. The DNA was precipitated by addition of 0.7 Volume of room-temperature isopropanol followed by inverting the tube 10 to 20 times, and subsequently centrifuged at 8,000x g (Eppendorf 5417R) for 15 minutes at 4ºC. The supernatant was carefully removed. The DNA pellet was washed with 1 ml of cold 70% ethanol, vortexed briefly and centrifuged again at 8,000x g (Eppendorf 5417R) for 10 minutes at 4ºC. The supernatant was carefully removed and the pellet was air-dried for 10 minutes. The extracted DNA was dissolved in 125 µl of Tris-EDTA (10 mM Tris.Cl, 1 mM EDTA, pH 8.0) at 55ºC for 2 hours.

The extracted genomic DNA was digested with *Bam*H I enzyme to obtain the MLL bcr fragments. *Bam*H I restriction enzyme defines the 8.3 kb of the intact MLL bcr. Ethanol precipitation was then carried out as described in Appendix K. Genomic DNA was then modified prior to nested IPCR. Nested IPCR was performed based on the modified version from Bowtell Lab Manual from the Peter MacCallum Cancer Institute, Australia. Figure 2.6 showed the simplified diagram of genomic DNA modification and nested IPCR protocol.

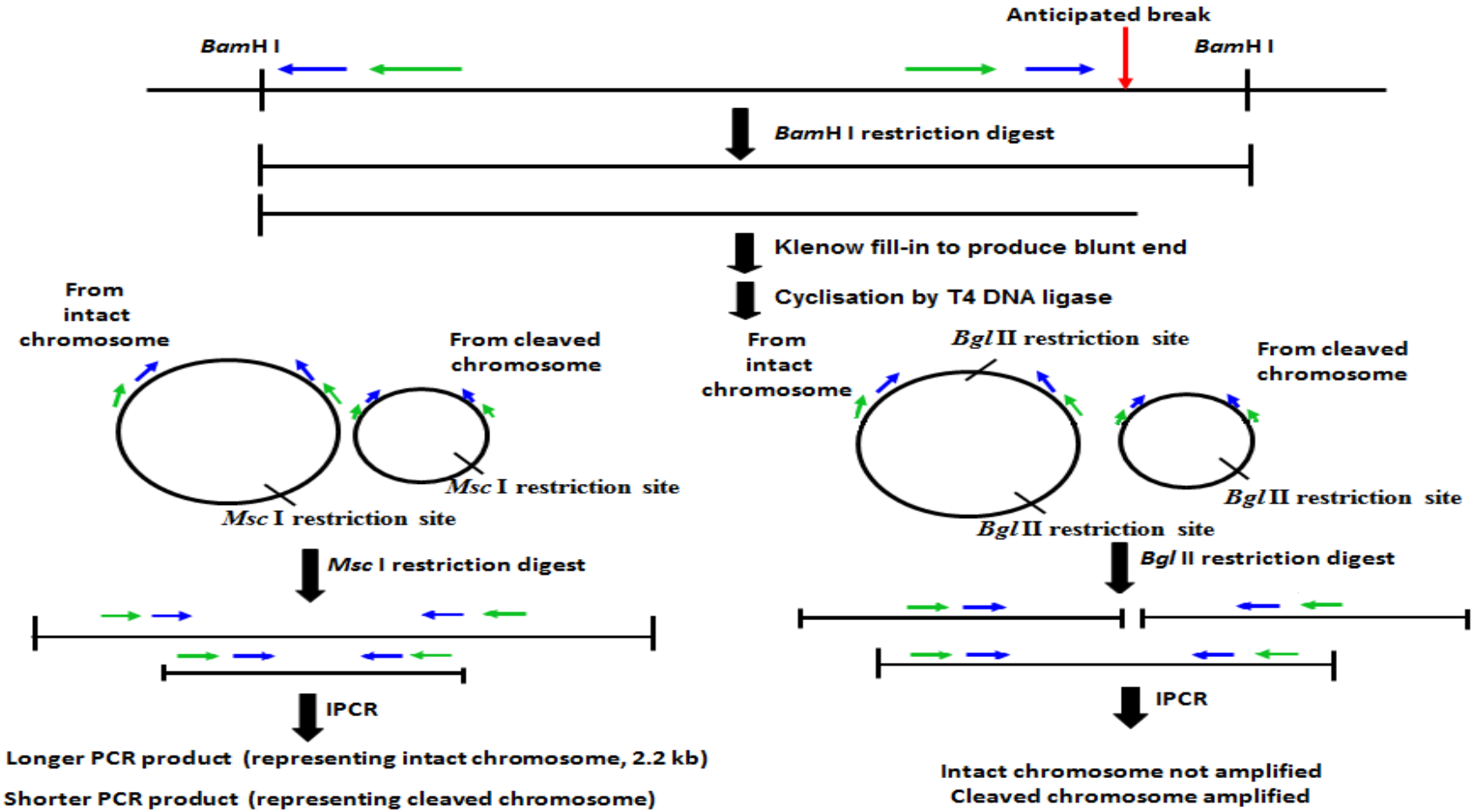


Figure 2.6: Genomic DNA modifications prior to nested IPCR. Genomic DNA was digested with *Bam*H I. Digested DNA was klenow filled-in to create blunt ends which were then cyclised and ligated. DNA was then purified. The circularised MLL bcr fragments underwent second enzyme, *Msc* I digestion to linearise the fragments before nested IPCR was performed. Longer IPCR product (2.2 kb) represents the intact MLL bcr fragments while the shorter one (less than 2.2kb) represents the cleaved MLL bcr fragments. At the same time, the circularised DNA was digested with third enzyme, *Bgl* II to eliminate the amplification of the intact MLL bcr fragments. Hence, only the cleaved fragments were amplified. Nest 1 IPCR primers were represented with green arrows whereas blue arrows represent primers used in Nest 2 IPCR. Red arrow represents possible DNA breakpoint.

### 2.2.5.2 Klenow Fill-In and Cyclisation of The MLL bcr Fragments

Genomic DNA digested with 100 units of *Bam*H I (NEB) enzyme produced 5' overhangs of 4 base pairs, while apoptotic nuclease such as CAD has preference to create blunt ends at 3' end. In order to obtain ligatable blunt ends, klenow fill-in was performed using DNA Polymerase I (Large) Klenow Fragment (NEB). Prior to klenow fill-in, DNA was quantified where absorbance reading was taken. Subsequently, 2 µg of extracted DNA was filled-in with 2 units of Klenow Fragment in 1X NE Buffer 2 supplemented with 33 µM of each of the dNTP (Finnzymes) at 25$^{o}$C for 15 minutes in a total reaction volume of 50 µl. The reaction was terminated by adding EDTA to a final concentration of 10 mM and heating at 75$^{o}$C for 20 minutes to inactivate the enzyme. The blunt-ended DNA was then circularised by using T4 DNA ligase (NEB). Ligation was performed at 16$^{o}$C by using 2,000 units of T4 DNA Ligase (NEB) with its 1X T4 DNA Ligase Buffer in a total reaction volume of 300 µl. Ligation reaction was carried out in a large reaction volume so as to favor the intra-molecular ligation rather than the intermolecular ligation.

### 2.2.5.3 Removal of Free Nucleotides

The excessive amount of unincorporated dNTP remained in the samples subsequent to the klenow fill-in reaction needed to be removed to avoid interference with the absorbance reading during DNA quantification. Therefore, the QIAquick Nucleotide Removal Kit (Qiagen) was used. The clean-up steps were performed according to the manufacturer's protocol as simplified in Appendix L. All the centrifugations were performed using a bench-top microcentrifuge. Briefly, 10 Volumes of Buffer PN was added to 1 Volume of the reaction sample and mixed. The sample was applied to the QIAquick column inserted in a 2

ml collection tube and followed by centrifugation for 1 minute at 6,000x g (Eppendorf 5417R). The flow through was discarded and the QIAquick column was washed with 750 µl of Buffer PE by centrifugation at 6,000x g (Eppendorf 5417R) for 1 minute. The flow through was discarded and the QIAquick column was placed back into the empty collection tube. An additional centrifugation at 13,000x g (Eppendorf 5417R) for 1 minute was done to remove the residual Buffer PE before the QIAquick column was placed into a clean 1.5 ml microcentrifuge tube. The DNA was eluted with 50 µl of Buffer EB.

#### 2.2.5.4 DNA Quantification, Second and Third Enzymes Restriction Digest

Purified DNA was quantified by measuring absorbance at 260 nm and 280 nm. The purified DNA was then subjected to second enzyme digestion with *Msc* I (NEB) to linearise the circularised DNA. *Msc* I restriction enzyme was chosen because it has unique restriction site in the entire MLL bcr at location 1121 according to the GenBank sequences (accession number U04737). Besides, digestion occurs outside the amplification range of Nest 1 IPCR primer pair. *Msc* I digests at centromeric end of the MLL bcr, between the two Nest 1 primers. Hence, circularised fragment could be linearised without affecting the polymerisation during IPCR. Digestion was carried out using 15 units of *Msc* I in 1X NEBuffer 4 in a total volume of 40 µl at 37$^{o}$C for approximately 3 hours. The enzyme was inactivated by heating at 65ºC for 20 minutes.

The DNA extracted may exist as heterogenous population containing mixture of the intact and cleaved MLL bcr. The cleaved MLL bcr exists in a smaller population, whereas the intact MLL bcr exists in a larger population. In order to avoid the competition during amplification,

*Bgl* II was used to eliminate amplification of the intact MLL bcr. Therefore, the cleaved MLL bcr could be amplified efficiently. In the cyclised intact MLL bcr fragments, there are 3 *Bgl* II restriction sites at positions 2253, 8234 and 8302 based on the GenBank sequences (accession number U04737). After circularisation, *Bgl* II digestion at position 2252 will linearise both the intact and cleaved MLL bcr fragment. However, *Bgl* II digestion at position 8234 and 8302 will disable amplification of the intact fragment (refer Figure 2.6).

Restriction digest reaction was performed using 20 units of *Bgl* II in 1X NEBuffer 3 in a total volume of 40 µl at 37$^{o}$C for approximately 3 hours. After restriction digest by using either *Msc* I or *Bgl* II, DNA was purified by using QIAquick Nucleotide Removal Kit as described in section 2.2.5.3 before quantification. Absorbance reading was taken for each of the samples and calculation was done to determine the amount of DNA template for nested IPCR.

#### 2.2.5.5 Nested IPCR

During the amplification, MLL 6261 (5'-GAGAATCGCTTGAACCCAACAG-3') and MLL 302 (5' – CTTGTGGGTCAGCAATTCCTTC – 3') were used in Nest 1 while MLL 6479 (5'-CCACTCCTTTATATTCCCATAGC-3') and MLL 274 (5' – TCCTCCACTCACCTGATTC – 3') were used in Nest 2 IPCR. Annealing temperature in Nest 1 was 63$^{o}$C while in Nest 2 the annealing temperature was 59$^{o}$C. Nest 1 IPCR was carried out by using approximately 100 to 150 ng of DNA template, 50 pmol of each of the MLL bcr primers (MLL302 and MLL6261), 200 µM of each of the dNTP (Promega), 0.4 unit of Phusion DNA polymerase (Finnzymes), 1X of Phusion HF Buffer (Finnzymes) and sterile Ultra Pure Water (sUPW) in a final volume of 20 µl in a 0.2 ml PCR tube (Eppendorf). The PCR was performed in

optimised condition with 30 seconds of initial denaturation at 98ºC for 1 cycle, followed by 30 cycles of 98ºC denaturation for 10 seconds, 59$^{o}$C annealing for 30 seconds, 72$^{o}$C extension for 15 seconds, followed by one cycle of 72$^{o}$C final extension for 10 minutes. Nest 1 product was then diluted 10 fold and 2 µl were used as DNA template for Nest 2 IPCR. The inner MLL 274 and MLL 6479 primers together with other reagents similar in Nest 1 IPCR were used in Nest 2. PCR cycle condition for Nest 2 was similar to Nest 1 except the annealing temperature was reduced to 54$^{o}$C and the 72$^{o}$C extension time was reduced to 11 seconds during the 30 cycles of amplification as summarised in Table 2.5. The annealing temperatures were calculated based on the nearest-neighbour method suggested for Phusion DNA Polymerase (www.finnzymes.com).

Table 2.5: Nested IPCR condition for detection of cleavage within the MLL bcr.

| **Step** | **Temperature ($^{o}$C)** | **Time** |
|---|---|---|
| Hot start | 80 | Forever |
| Initial denaturation | 98 | 30s |
| Denaturation | 98 | 10s |
| Annealing | 59 (Nest 1); 54 (Nest 2) | 30s |
| Extension | 72 | 15s (Nest 1); 11s (Nest 2) |
| | Go to Denaturation step and repeat for 29 cycles | |
| Final extension | 72 | 10 minutes |
| Cooling | 20 | Forever |

## 2.3 Result

In order to study the role of CAD, CAD was overexpressed in HeLa and SUNE1 cells. Transfected cells were then subjected to oxidative stress-induced apoptosis by using $H_2O_2$. Prior to this, dose response of HeLa and SUNE1 to $H_2O_2$ was performed.

### 2.3.1 Dose Response Test of HeLa and SUNE1 Cells to Hydrogen Peroxide, $H_2O_2$

Dose response of HeLa and SUNE1 cells to $H_2O_2$ was carried out to determine the concentration of $H_2O_2$ that was sufficient to induce both SUNE1 and HeLa cells to undergo apoptosis. HeLa cells were treated with 10 μM, 50 μM, 100 μM, 500 μM, 1 mM and 10 mM of $H_2O_2$ for 20 hours. Morphologically, for cells treated with 10 μM and 50 μM $H_2O_2$ for 20 hours, 70% of HeLa cells remained healthy and attached as monolayer cells. For cells treated with 100 μM of $H_2O_2$, 70% of them remained attached while 5% of the cells floated and blebbed. 60% of the cells remain attached and 15% of floating and blebbing cells were observed when treated with 500 μM of $H_2O_2$. However, 20% of attached cells appeared to be slightly enlarged morphologically in the 100 μM and 500 μM treatment. For cells treated with 1 mM of $H_2O_2$, the cell confluency was only 40% with 80% of the attached cells appeared to be normal morphologically and 20% of floating, clumping and blebbing cells was found. When treated with 10 mM of $H_2O_2$, all cells became apoptotic (data not shown).

IPCR was used to detect chromosome breaks within the MLL bcr. Based on the primer position, amplification of the intact MLL bcr produced a 2.2 kb band. Amplification of the

cleaved MLL bcr gave rise to band(s) of size smaller than 2.2 kb. Positive and negative controls for IPCR were included to ensure that the PCR reaction worked. In this experiment, the DNA template used for the positive control for IPCR was the DNA extracted from SUNE1 cells transfected with pTracer-hCAD and digested with *Msc* I. This DNA was used because in previous experiment, clear intact and cleaved bands were detected. As negative control for IPCR, DNA template was not added. As shown in Figure 2.7(A), a 2.2 kb band was detected in all of the samples. Bands of sizes smaller than 2.2 kb were also detected in all samples (Lanes 3 – 10). Relatively, cells treated with 10 mM of $H_2O_2$ showed increased cleavage of the MLL bcr (Lane 10) as compared to other samples. Treatment with 10 µM of $H_2O_2$ was sufficient to induce cleavage within the MLL bcr (Lane 5). Very minimal cleavage was found in cells grew at optimal density (Lane 4), which served as negative control in this experiment as compared to other samples. From the morphological observation, cells treated with 10 µM, 50 µM and 100 µM of $H_2O_2$ remained at confluency of 70%. Ninety percent of the attached cells remained healthy and 10% were rounded up and bright. Treatment with 100 µM of $H_2O_2$ was hence chosen to treat HeLa cells in the subsequent experiment because majority of the HeLa cells remained healthy and cleavage within the MLL bcr was detected. For this experiment, positive control and negative control were included. As positive control, HeLa cells were overgrown. This sample was named as apoptotic sample (Lane 3). As negative control for the experiment, cells were grown at optimal density (Lane 4), where cells were healthy and grew to 70% confluency.

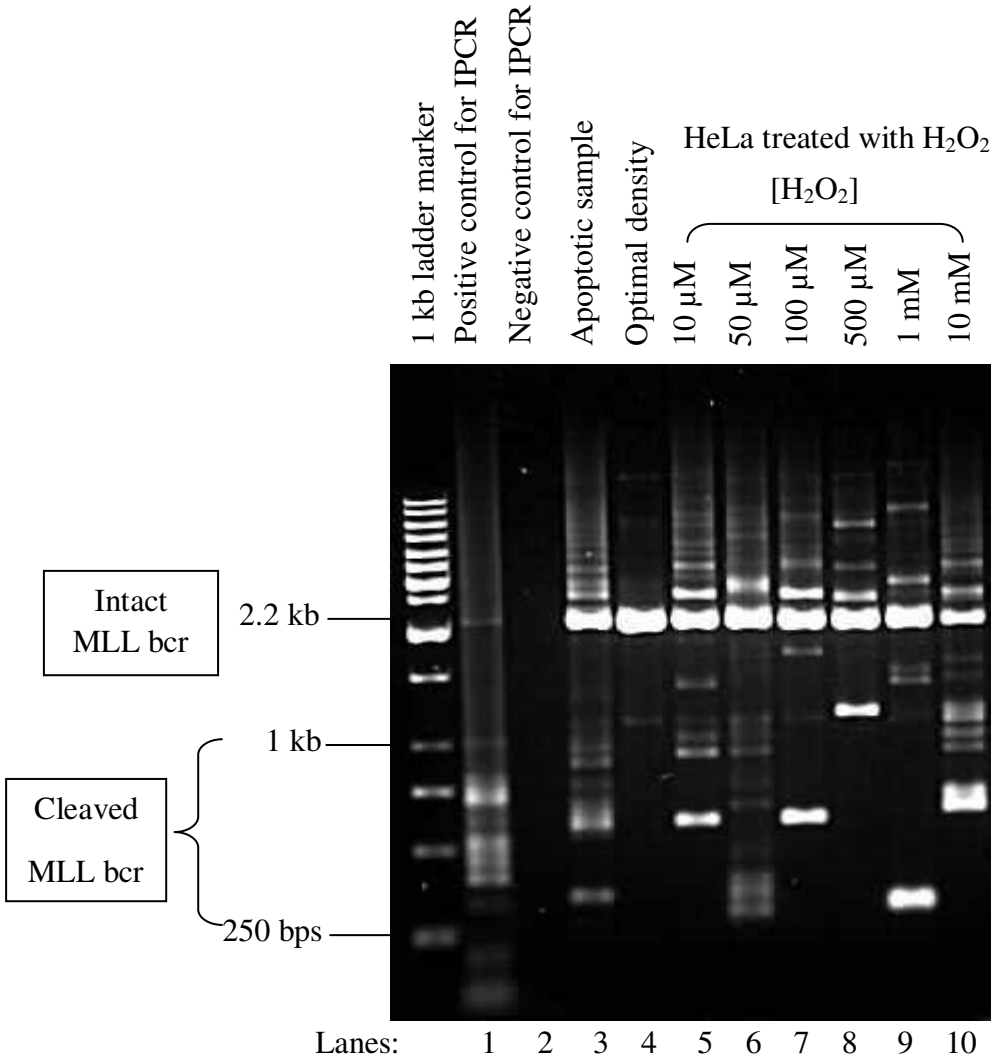


**Figure 2.7(A): Nested IPCR result of HeLa cells treated with various concentrations of $H_2O_2$ for 20 hours.** HeLa cells were either grown to optimal cell density (approximately 70%) (Lane 4) or overgrown (Lane 3) to induce apoptosis with high cell density (>100% confluency) in 60 mm dishes. Optimally growing cells were also treated with 10 µM (Lane 5), 50 µM (Lane 6), 100 µM (Lane 7), 500 µM (Lane 8), 1 mM (Lane 9) and 10 mM (Lane 10) of $H_2O_2$ for 20 hours. Genomic DNA was extracted and processed for IPCR. DNA was digested with restriction enzyme *Msc* I prior to IPCR. The 2.2 kb band represents the intact MLL bcr whereas smaller fragments of sizes ranging from 250 bps to 1 kb represent the cleaved MLL bcr. As positive control for IPCR, DNA extracted from SUNE1 cells transfected with pTracer-hCAD and digested with *Msc* I enzyme was used. As negative control for IPCR, DNA template was not added.

Similarly, SUNE1 cells were treated with 10 µM, 50 µM, 100 µM, 500 µM, 1 mM and 10 mM of $H_2O_2$ for 20 hours. From the morphological observation, approximately 80% of SUNE1 cells remained healthy and attached to the flask when treated with 10 µM to 50 µM of $H_2O_2$. For cells treated with 100 µM, 80% of the cells remained attached and 10% of the cells floated and blebbed. These attached cells became slightly enlarged with slight heavy granulation in the cytoplasm. Approximately 30% of the cells remained attached and 50% of floating and blebbing cells were observed when treated with 500 µM of $H_2O_2$. When cells were treated with 1 mM and 10 mM of $H_2O_2$, all of them appeared to be rounded up, became brighter and blebbing even though they were still attaching to the bottom of the flasks (data not shown).

From the IPCR result shown in Figure 2.7(B), cells treated with 50 µM (Lane 6), 100 µM (Lane 7) and 500 µM (Lane 8) of $H_2O_2$ showed clear and distinct cleaved MLL bcr fragments. Size of cleaved MLL bcr fragments became smaller from 50 µM to 500 µM of $H_2O_2$. There was no band detected when cells were treated with 1 mM (Lane 9) and 10 mM (Lane 10) of $H_2O_2$. Treatment using 1 mM and 10 mM of $H_2O_2$ might be too high. This could possibly lead to cleavage within the MLL bcr was too extensive, such that priming regions of the primers were cleaved. This could cause the amplification process inefficient. From the morphological observation, cells treated with 10 µM, 50 µM and 100 µM of $H_2O_2$ remained at confluency of 70%. Approximately 90% of the attached cells remained healthy while 10% of attached cells appeared to be rounded up and bright. From the combination of morphological observation and IPCR result, 50 µM of $H_2O_2$ was chosen to treat SUNE1 cells in subsequent experiments. As positive control, SUNE1 cells were overgrown. This sample was named as

apoptotic sample (Lane 3). Cells at optimal density (Lane 4), where cells were healthy and grew to 70% confluency was used as negative control.

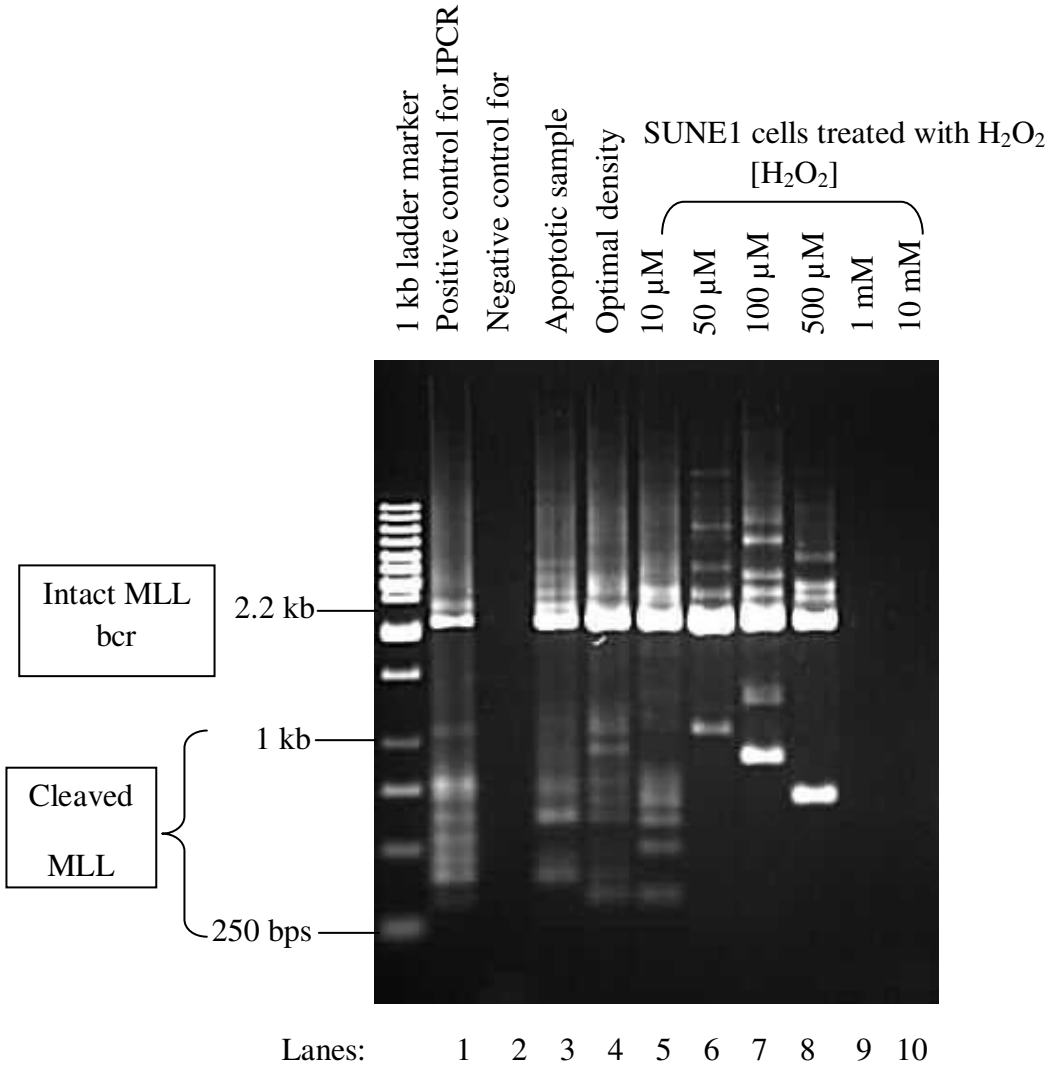


**Figure 2.7(B): Nested IPCR result of SUNE1 cells treated with various concentrations of $H_2O_2$ for 20 hours.** SUNE1 cells were either grown to optimal cell density (approximately 70%) (Lane 4) or overgrown (Lane 3) to induce apoptosis with high cell density (>100% confluency) in 60 mm dishes. Optimally growing cells were also treated with 10 µM (Lane 5), 50 µM (Lane 6), 100 µM (Lane 7), 500 µM (Lane 8), 1 mM (Lane 9) and 10 mM (Lane 10) of $H_2O_2$ for 20 hours. Genomic DNA was extracted and modified for IPCR. DNA was digested with restriction enzyme *Msc* I prior to IPCR. The 2.2 kb band represents the intact MLL bcr whereas smaller fragments of sizes ranging from 250 bps to 1 kb represent the cleaved MLL bcr. As positive control for IPCR, DNA extracted from SUNE1 cells transfected with pTracer-hCAD and digested with *Msc* I enzyme was used. As negative control for IPCR, DNA template was not added.

### 2.3.2 Transient Overexpression of CAD and Its Mutant in HeLa and SUNE1 Cells

Studies showed that various types of cells, such as tumour cell lines (Lennon *et al.*, 1992) and normal cell types including endothelium (Abello *et al.*, 1994; Li *et al.*, 1997; Ueda *et al.*, 1992) underwent apoptosis when treated with oxidative stress *in vitro*. In the first approach to study the role of CAD, HeLa cells were transiently transfected with hCAD, mCAD, mutant hCAD and the vector. Subsequently, cells underwent oxidative stress-induced apoptosis by treatment with 50 µM of $H_2O_2$ for 8 hours as being optimised. Prior to this experiment, optimisation was performed. Based on the dose response test, as shown in Figure 2.7(A), for HeLa cells, and 2.7(B) for SUNE1 cells, 100 µM and 50 µM of $H_2O_2$ were decided to be used in treatment of transfected HeLa and SUNE1 cells, respectively. After 3 hours of transfection, cells were grown for another 17 hours. Treatment of transiently transfected cells was then performed for different period of time (2, 4, 6, 8, 10 and 12 hours) for both cell lines. The morphological result showed that, HeLa and SUNE1 cells treated with 100 µM of $H_2O_2$ and 50 µM of $H_2O_2$ respectively for 8 hours was sufficient to cause cells to present with apoptotic features, like floating, blebbing and fragmentation into apoptotic bodies. Treatment longer than 8 hours was found to be too stressful for the cells. At least 30% of cells were floating, blebbing and apoptotic bodies were also observed. Thus, 8 hours was chosen as the treatment time for both cell lines. It was expected to see elevated DNA cleavage in hCAD and mCAD transfected cells as compared to vector (pTracer only), mutant hCAD and non-DNA transfected cells when apoptosis was triggered.

Transfection was performed within 24 hours after seeding when cells were growing at their exponential phase. At the time of transfection, HeLa cells were healthy and at confluency of about 70%. Approximately 5% of attaching cells were rounded up and bright while 5% of floating and blebbing cells were observed (data not shown). At 17 hours post transfection,

before the transfected cells were treated with 50 μM of $H_2O_2$, morphology of the cells were observed as shown in Table 2.6. Most of the cells transfected with pTracer, pTracer-mCAD and pTracer-hCAD(K157Q) were at a confluency of 80 to 90%, and appeared to be healthy. However, about 10% of attaching cells were rounded up and bright, and 10% of cells floating and blebbing. Majority of HeLa cells transfected with pTracer-hCAD and cells underwent mock transfection appeared to be healthy, at confluency of 70%. Approximately 95% of attached cells were healthy. Under fluorescence light emission, no fluorescence was observed in cells underwent mock transfection. It was estimated that about 70% of the cells transfected with pTracer were fluorescing, 60% in pTracer-hCAD(K157Q), 50% in both pTracer-hCAD and pTracer-mCAD transfected cells. In average, approximately 60% of transfected cells fluoresced. This indicated that plasmid carrying the GFP gene was transfected successfully at transfection efficiency of approximately 60%.

Transiently transfected HeLa cells were then treated with 50 μM of $H_2O_2$ for 8 hours. From the morphological observation as shown in Table 2.7, the cells showed similar cell morphology as before treatment, except that there was a slight increased in apoptotic cells. Approximately 20% of attaching cells appeared rounded up and bright. In addition, 20% of floating, blebbing cells and apoptotic bodies were also found. However, cells were emitting stronger fluorescence light than before. Cell confluency for pTracer-hCAD and mock transfected cells increased to 80%. Approximately 60% of attaching cells fluoresced with relatively weaker intensity than before treatment. Microscopic observation of cell morphology is as shown in Table 2.6 and 2.7. Healthy cells are shown by black arrows; red arrows indicate the attached but rounded up cells; whereas blue arrows pointed to floating and blebbing cells.

Table 2.6: Microscopic morphology of transiently transfected HeLa cells (non-treated). Magnification of 100X under bright field and fluorescence light emission. Black arrow indicates healthy cells; red arrow indicates attached but rounded up cells; and blue arrow indicates floating cells.

| **DNA transfected** | **Cell morphology** | |
|---|---|---|
| | **Bright Field** | **Fluorescence Light** |
| pTracer | 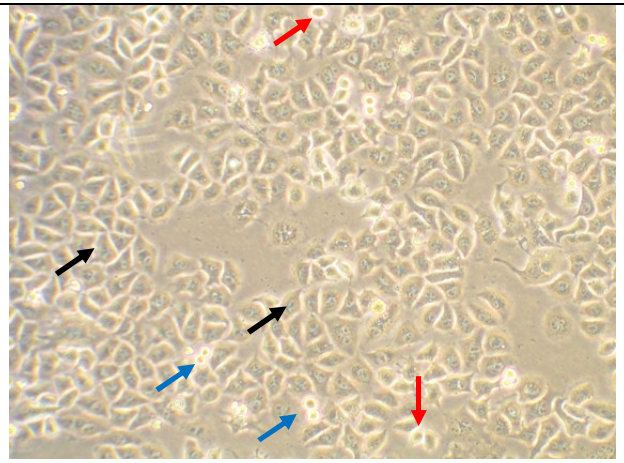 | 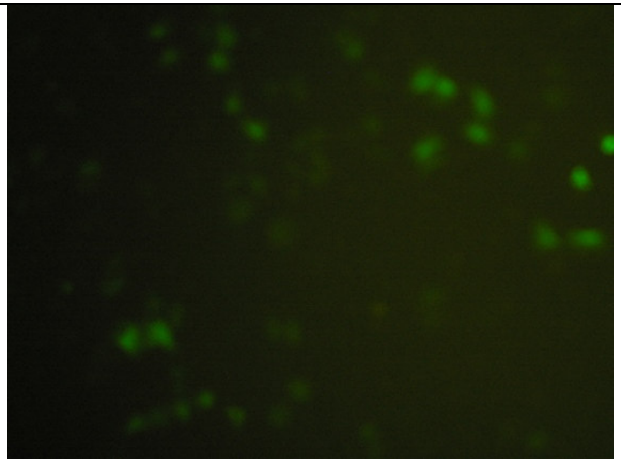 |
| pTracer-hCAD | 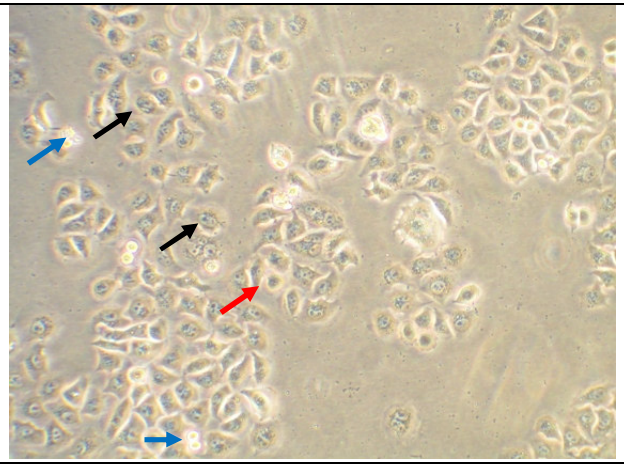 | 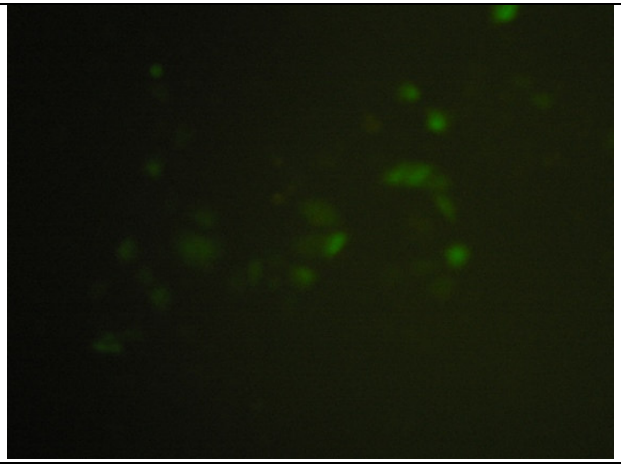 |

| | | |
|---|---|---|
| pTracer-mCAD | 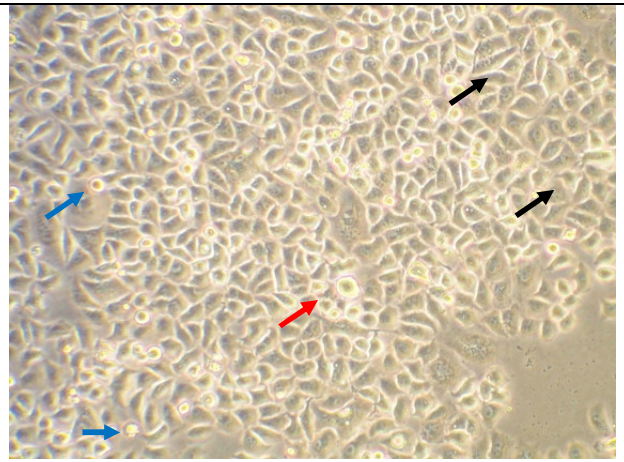 | 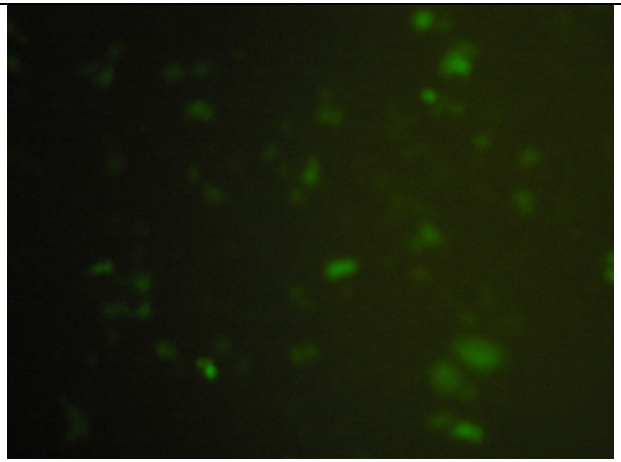 |
| pTracer-hCAD(K157Q) | 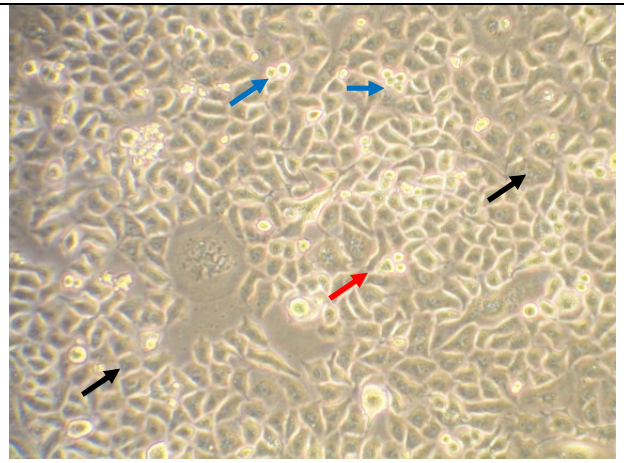 | 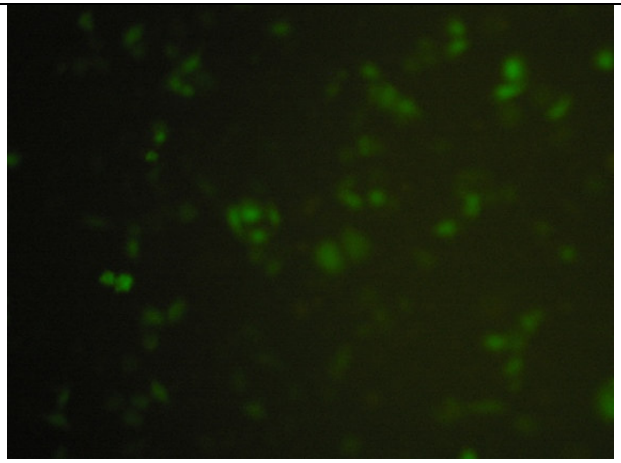 |

| | | |
|---|---|---|
| No DNA (Mock Transfection) | 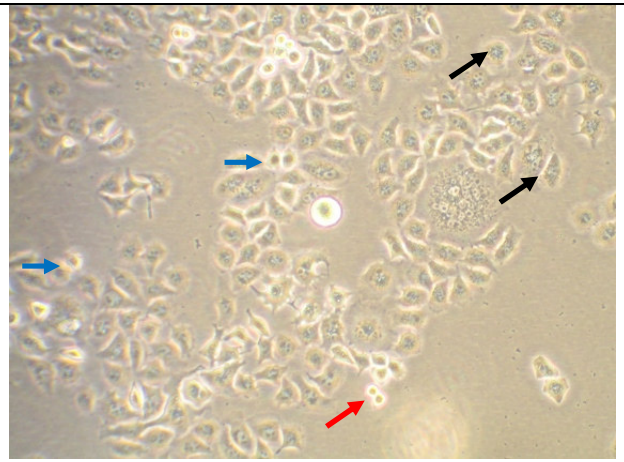 |  |

Table 2.7: Microscopic morphology of HeLa transiently transfected cells treated with 50 µM of $H_2O_2$ for 8 hours. Magnification of 100X under bright field and fluorescence light emission. Black arrow indicates healthy cells; red arrow indicates attached but rounded up cells; and blue arrow indicates floating cells.

| **DNA transfected** | **Cell morphology** | |
|---|---|---|
| | **Bright Field** | **Fluoresence Light Emission** |
| pTracer | 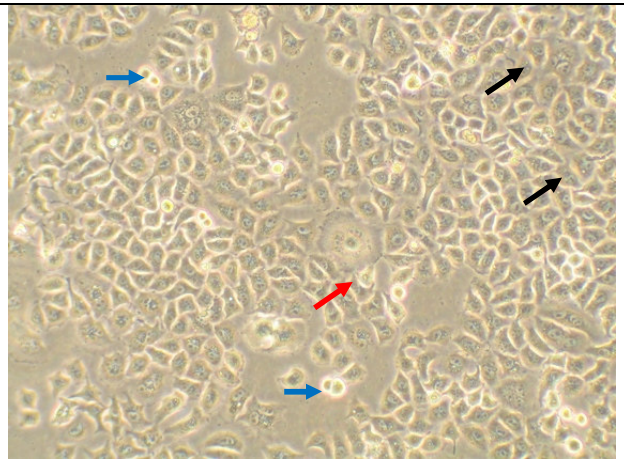 | 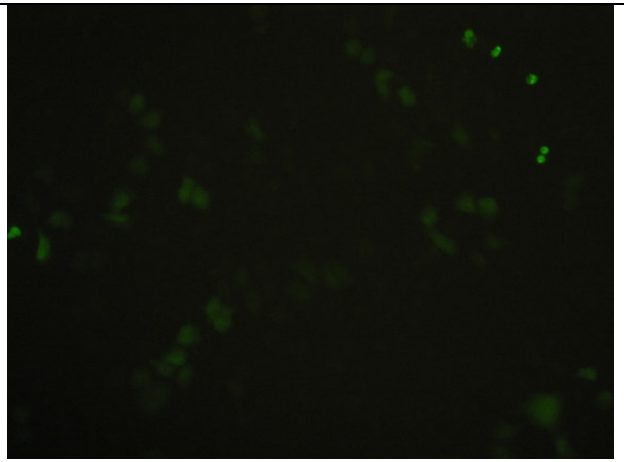 |

| | | |
|---|---|---|
| pTracer-hCAD | 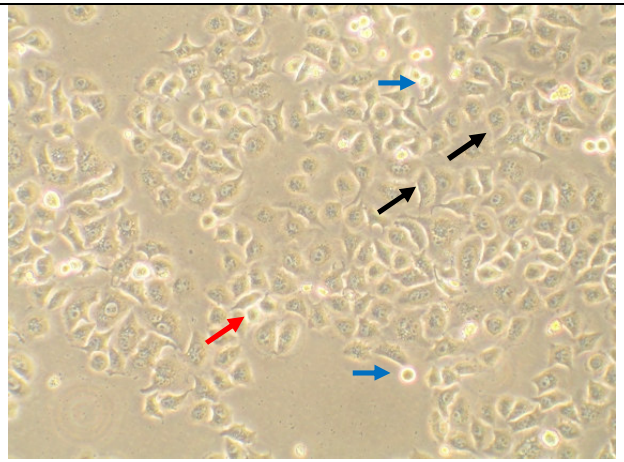 | 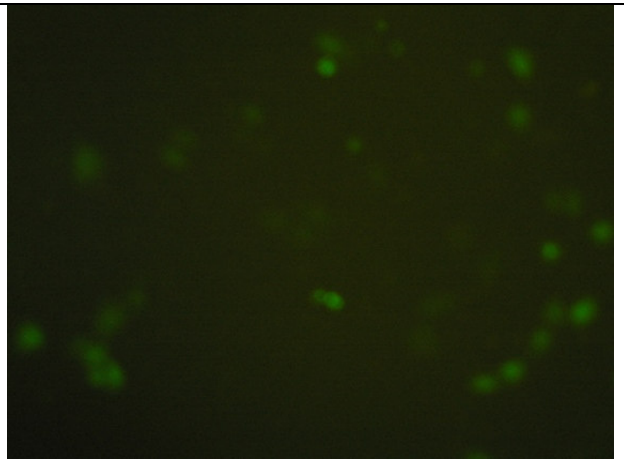 |
| pTracer-mCAD | 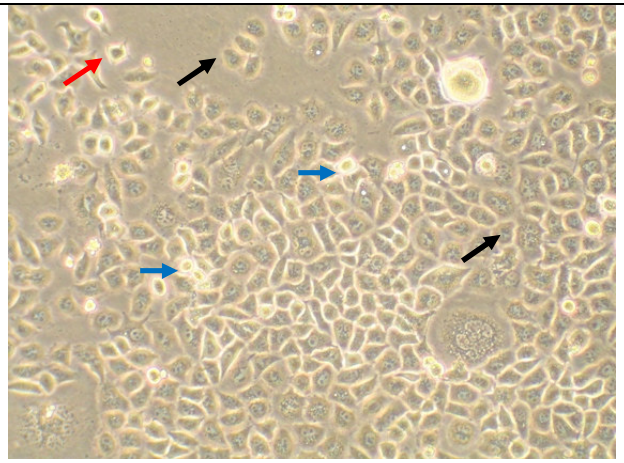 | 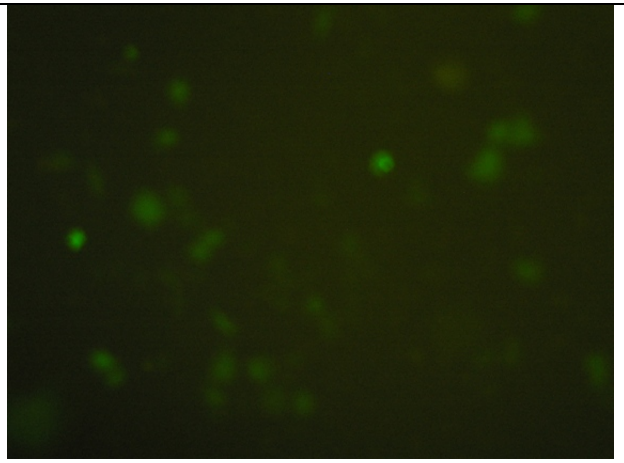 |

| | | |
|---|---|---|
| pTracer-hCAD(K157Q) | 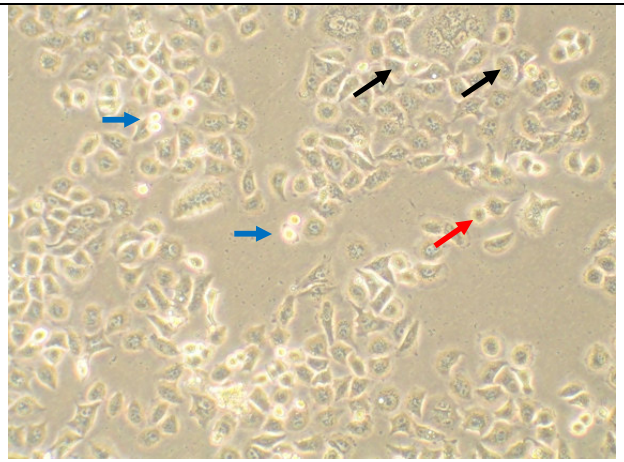 | 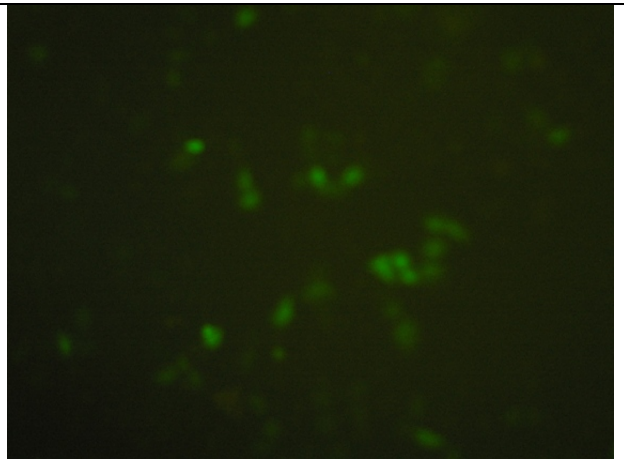 |
| No DNA (Mock Transfection) | 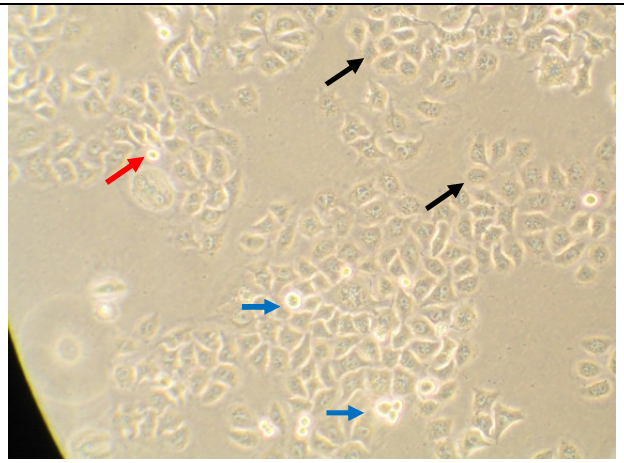 |  |

IPCR was performed to detect the intact band of 2.2 kb and cleaved MLL bcr fragments of sizes smaller than 2.2 kb. It was expected that cells transfected with hCAD and mCAD should show enhanced cleavage within the MLL bcr compared to pTracer, hCAD mutant and mock transfected cells in both non-treated and treated samples. For each of the transfectants, treatment with 50 μM of $H_2O_2$ was expected to enhance cleavage within the MLL bcr as compared to those without treatment. However, as shown in Figure 2.8(A), there was no significant difference between the transfected HeLa cells which were not treated (Lanes 3 – 7) and those treated (Lanes 8 – 12) with 50 μM of $H_2O_2$. Both set of samples showed cleavage within the MLL bcr as indicated by smaller fragments of sizes ranging from 250 bps to 1 kb. In non-treated samples, HeLa cells transfected with hCAD (Lane 4) and mCAD (Lane 5) did not show increased cleavage within the MLL bcr as compared to CAD mutant (Lane 6), vector (Lane 3) and cells underwent mock transfection (Lane 7). Similarly, upon treatment with 50 μM of $H_2O_2$, hCAD (Lane 9) and mCAD (Lane 10) also did not show clear increased cleavage within the MLL bcr as compared to CAD mutant (Lane 11), vector (Lane 8) and cells underwent mock transfection (Lane 12).

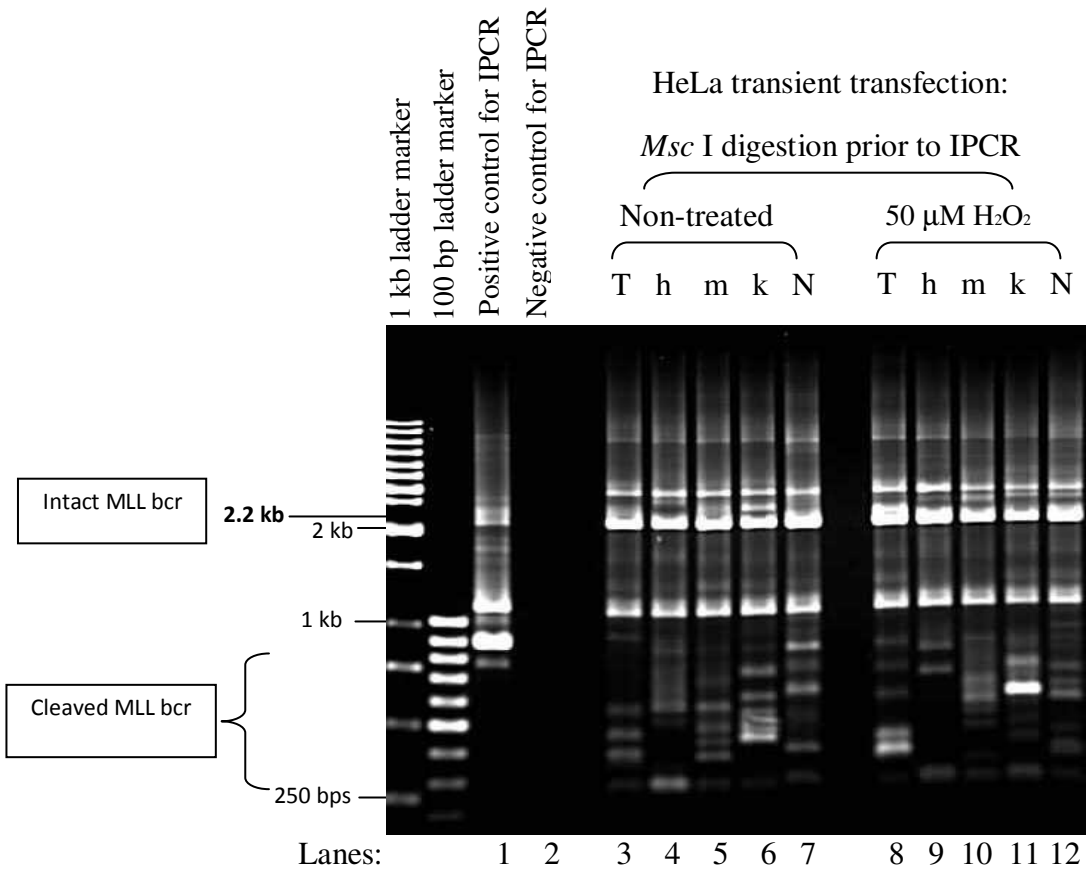


**Figure 2.8(A): Nested IPCR with *Msc* I-digested DNA from transiently transfected HeLa cells non-treated and treated with 50 µM of $H_2O_2$.** HeLa cells were transiently transfected with either pTracer, T (Lanes 3 and 8); pTracer-hCAD, h (Lanes 4 and 9); pTracer-mCAD, m (Lanes 5 and 10) or pTracer-hCAD(K157Q), k (Lanes 6 and 11). A mock transfection (no DNA), N (Lanes 7 and 12) was included as control. The cells were either non-treated (Lanes 3 – 7) or treated (Lanes 8 – 12) with 50 µM of $H_2O_2$ for 8 hours at 17 hours post-transfection. Genomic DNA extracted was digested with *Bam*H I, modified and digested with *Msc* I prior to IPCR. *Msc* I-digested DNA from HeLa cells transiently transfected with pTracer-hCAD was used as DNA template in positive control for IPCR. As for negative control for IPCR, no DNA template was included. The 2.2 kb band represents the intact MLL bcr whereas smaller fragments of sizes ranging from 250 bps to 1 kb represent the cleaved MLL bcr.

In order to eliminate amplification of the intact MLL bcr, the modified DNA was digested with *Bgl* II instead of *Msc* I prior to IPCR. Elimination of intact was believed to favour amplification of the cleaved MLL bcr. As shown in Figure 2.8(B), fragment of size 2.2 kb representing the intact MLL bcr was not observed on 1% agarose gel. There was a general increase in the number and intensity of smaller bands representing the cleaved MLL bcr. However, the expected difference between the transfectants was not observed. Both of the non-treated cells (Lanes 3 – 7) and cells treated with 50 µM of $H_2O_2$ (Lanes 8 – 12) showed similar cleavage within the MLL bcr. In non-treated samples, cells transfected with hCAD (Lane 4) and mCAD (Lane 5) did not show increased cleavage within the MLL bcr as compared to cells transfected with CAD mutant (Lane 6), vector (Lane 3) and cells underwent mock transfection (Lane 7). Even with 50 µM of $H_2O_2$ treatment, cells transfected with hCAD (Lane 9) and mCAD (Lane 10) also did not show clear increased cleavage within the MLL bcr as compared to CAD mutant (Lane 11), vector (Lane 8) and cells underwent mock transfection (Lane 12). This result tallied with the result obtained from DNA subjected to *Msc* I restriction enzymes digestion as shown in Figure 2.8(A).

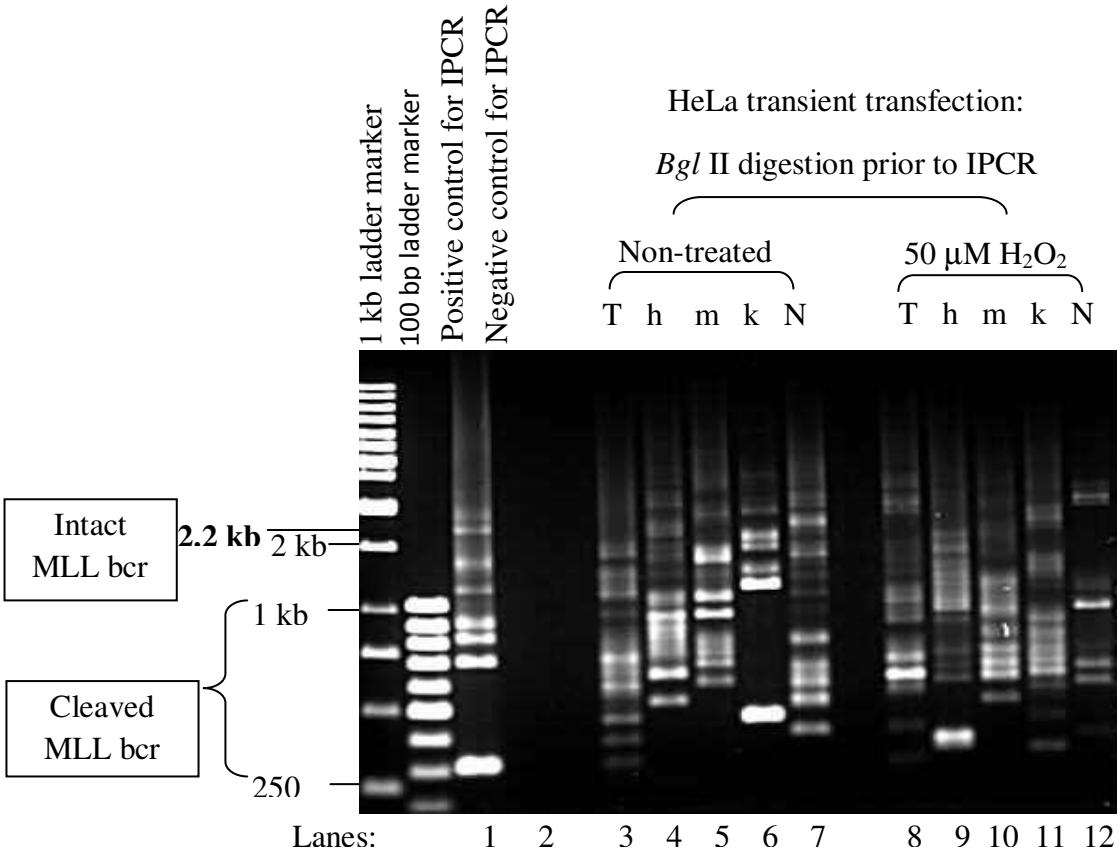


**Figure 2.8(B): Nested IPCR with *Bgl* II-digested DNA from transiently transfected HeLa cells non-treated and treated with 50 µM of $H_2O_2$.** HeLa cells were transiently transfected with either pTracer, T (Lanes 3 and 8); pTracer-hCAD, h (Lanes 4 and 9); pTracer-mCAD, m (Lanes 5 and 10) or pTracer-hCAD(K157Q), k (Lanes 6 and 11). A mock transfection (no DNA), N (Lanes 7 and 12) was included as control. The cells were either non-treated (Lanes 3 – 7) or treated (Lanes 8 – 12) with 50 µM of $H_2O_2$ for 8 hours at 17 hours post-transfection. Genomic DNA extracted was digested with *Bam*H I, modified and digested with *Bgl* II prior to IPCR. *Msc* I-digested DNA from HeLa cells transiently transfected with pTracer-hCAD was used as DNA template in positive control for IPCR. As for negative control for IPCR, no DNA template was included. The 2.2 kb band represents intact the MLL bcr whereas smaller fragments of sizes ranging from 250 bps to 1 kb represent the cleaved MLL bcr.

In addition to HeLa, SUNE1 (NPC cell) was also used in this experiment. As being confirmed by dose-response test of SUNE1 to $H_2O_2$, 50 μM was sufficient to induce apoptosis in SUNE1 cells. Our previous laboratory result also showed that $H_2O_2$ concentration of above 100 μM may induce cells to undergo necrosis instead of apoptosis. Healthy cells are shown by black arrows; red arrows indicate the attached but rounded up cells whereas blue arrows show floating and blebbing cells. Transient transfection of two sets of SUNE1 cells were carried out within 24 hours after cell seeding. Upon transfection, cell confluency reached 70%. Ninety-five percent of the attaching cells were healthy while 5% of the cells were rounded up and bright. Approximately 5% of cells were floating and blebbing (data not shown). At 17 hours post transfection, cell confluency reached 90% with 90% of the cells healthy, 10% of the attaching cells rounded up and bright, with 10% of floating and blebbing cells. Seventy percent to eighty percent of transfected cells fluoresced strongly, as shown in Table 2.8. This observation was similar between the 2 sets of transiently transfected SUNE1 cells.

One set of the transiently transfected cells was treated with 50 μM of $H_2O_2$ while the other set remains non-treated. After 8 hours of treatment, the morphology of treated cells was similar to before treatment as shown in Table 2.9. For pTracer and mock transfected cells, they retained a confluency of 90% where 90% of them appeared healthy while 10% of them rounded up and bright, 10% of the cells were floating and blebbing. Confluency of the cells transfected with pTracer-hCAD, pTracer-mCAD and pTracer-hCAD(K157Q) was 85%. Majority of the cells appeared healthy. More floating, blebbing and apoptotic cells were found in these samples as compared to pTracer and mock transfected cells. Approximately 25%, 30% and 15% of apoptotic cells were found in pTracer-hCAD, pTracer-mCAD and pTracer-hCAD(K157Q) transfected cells respectively. It was estimated that 80 to 90% of cells fluoresced strongly.

Table 2.8: Microscopic morphology of transiently transfected SUNE1 cells (non-treated). Magnification of 100X under bright field and fluorescence light emission. Black arrow indicates healthy cells; red arrow indicates attached but rounded up cells; and blue arrow indicates floating cells.

| **DNA transfected** | **Cell Morphology** | |
|---|---|---|
| | **Bright Field** | **Fluorescence Light** |
| pTracer | 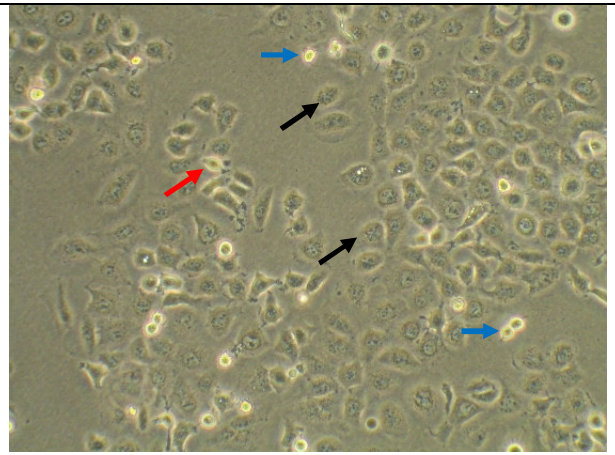 | 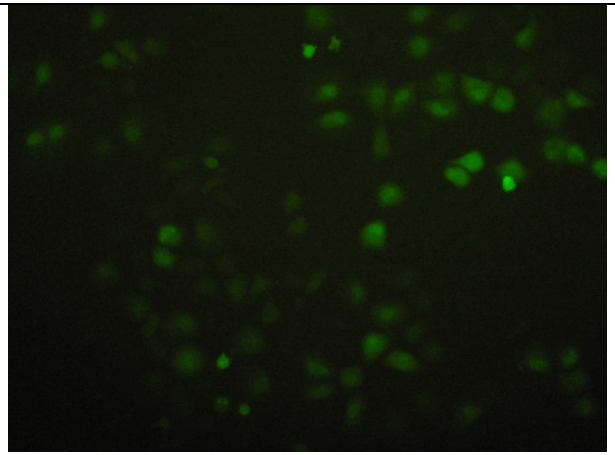 |

| | | |
|---|---|---|
| pTracer-hCAD | 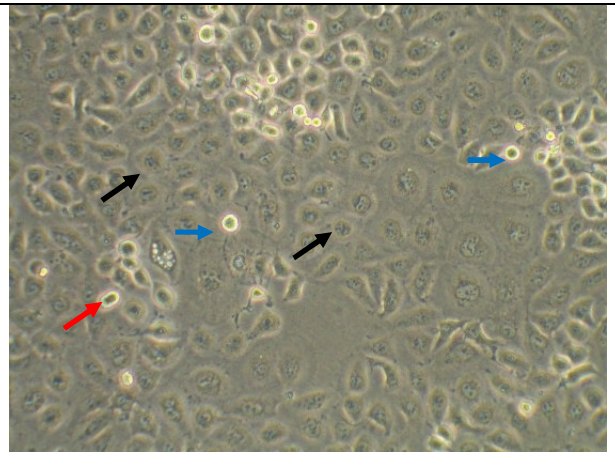 | 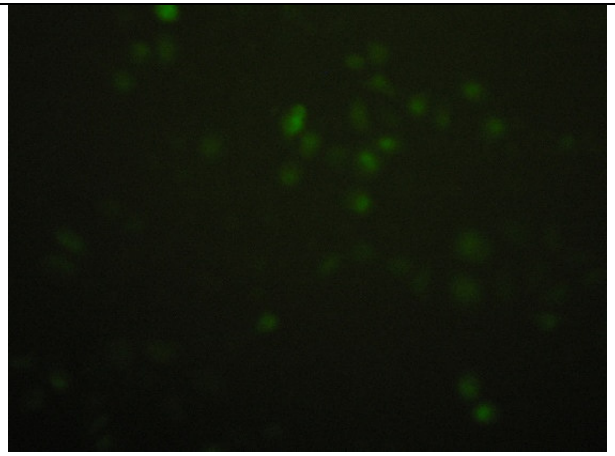 |
| pTracer-mCAD | 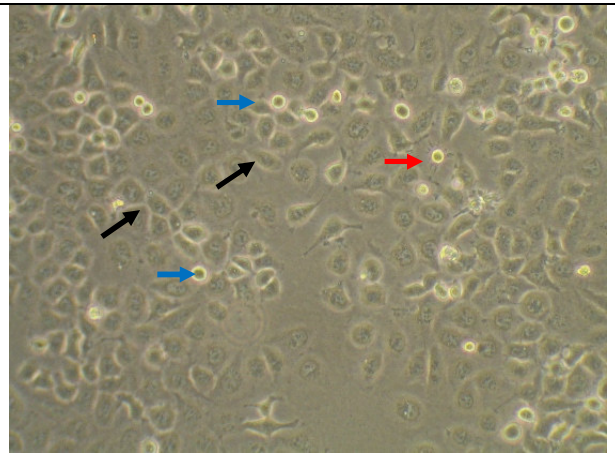 | 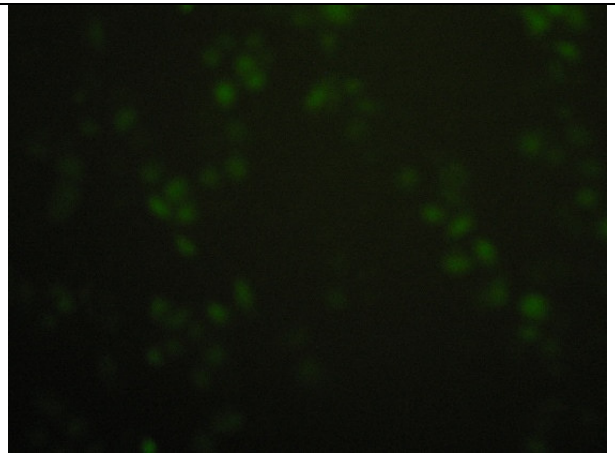 |

| | | |
|---|---|---|
| pTracer-hCAD(K157Q) | 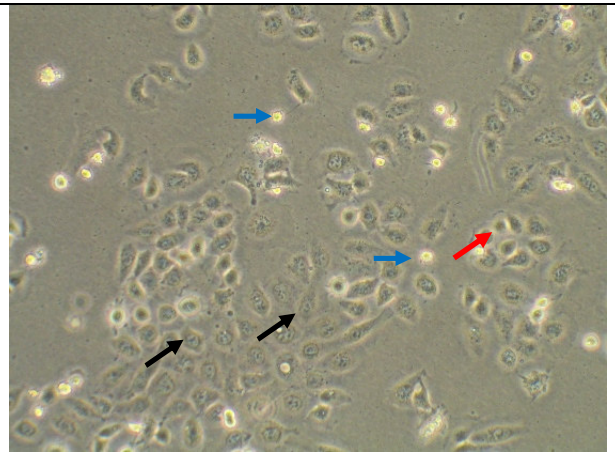 | 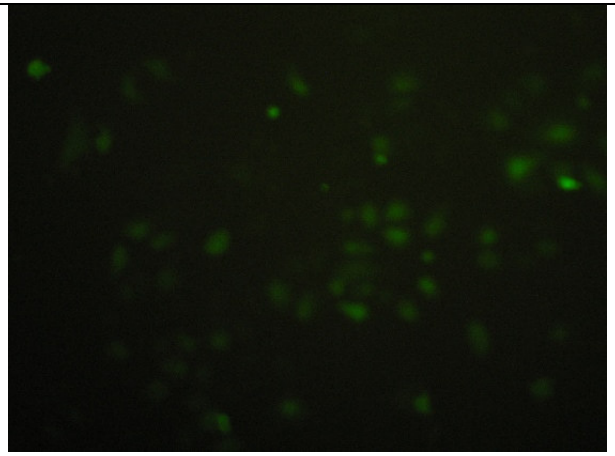 |
| No DNA (Mock transfection) | 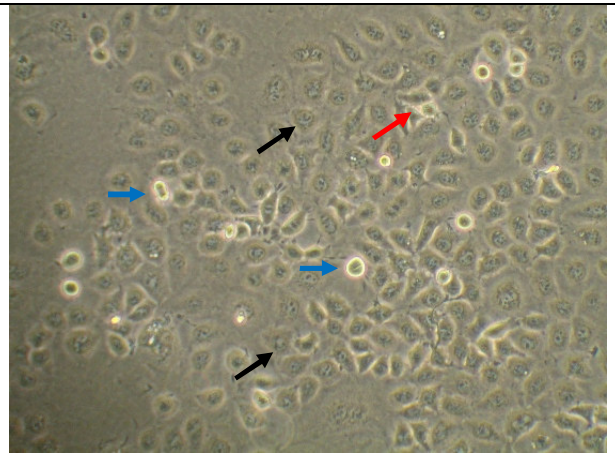 |  |

Table 2.9: Microscopic morphology of transiently transfected SUNE1 cells treated with 50 µM of $H_2O_2$ for 8 hours. Magnification of 100X under bright field and fluorescence light emission. Black arrow indicates healthy cells; red arrow indicates attached but rounded up cells; and blue arrow indicates floating cells.

| **DNA transfected** | **Cell Morphology** | |
|---|---|---|
| | **Bright Field** | **Fluorescence Light** |
| pTracer | 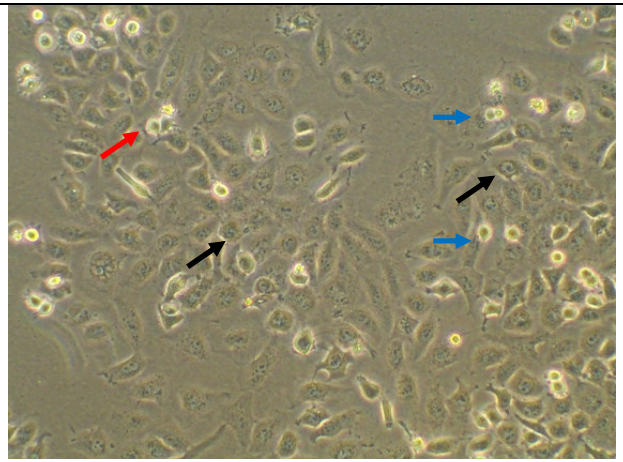 | 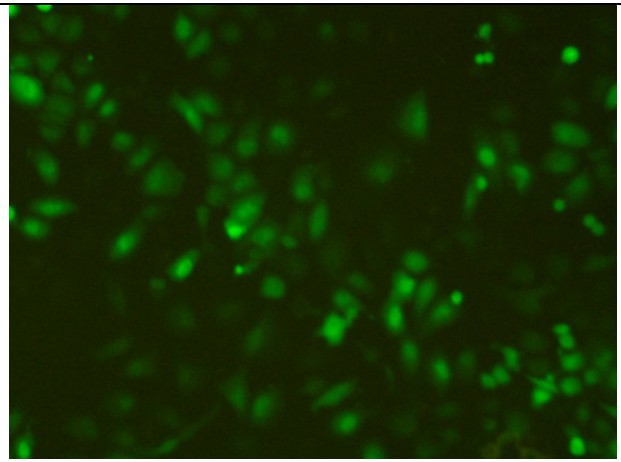 |

| | | |
|---|---|---|
| pTracer-hCAD | 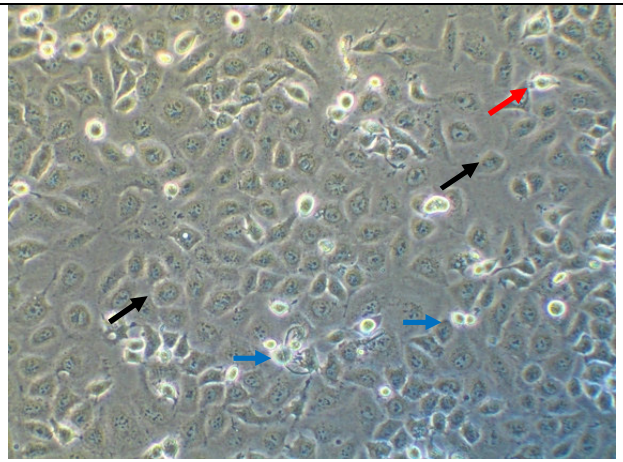 | 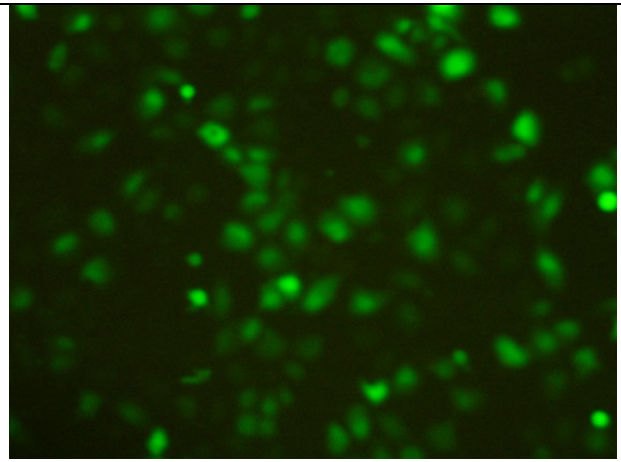 |
| pTracer-mCAD | 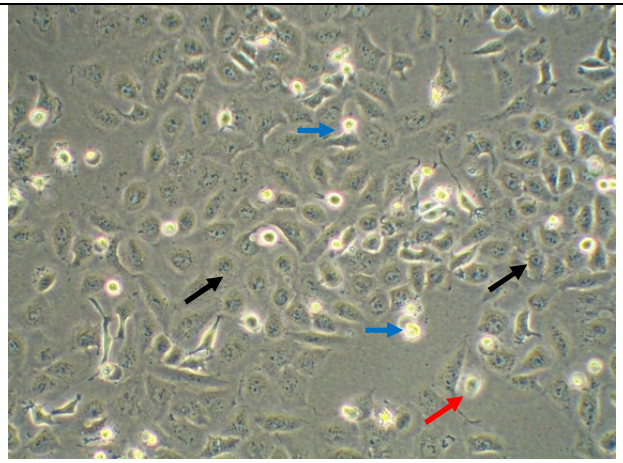 | 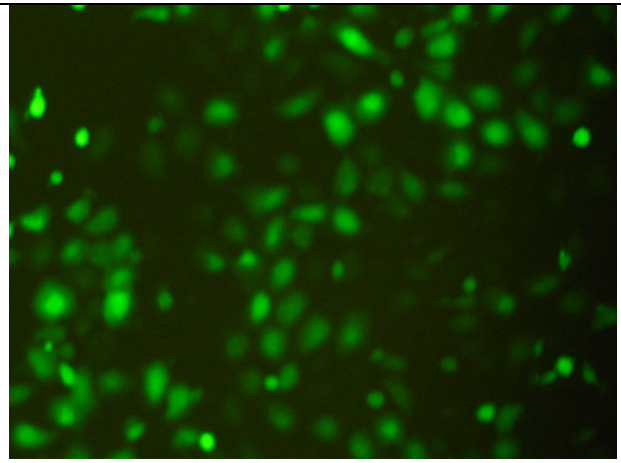 |

| | | |
|---|---|---|
| pTracer-hCAD(K157Q) | 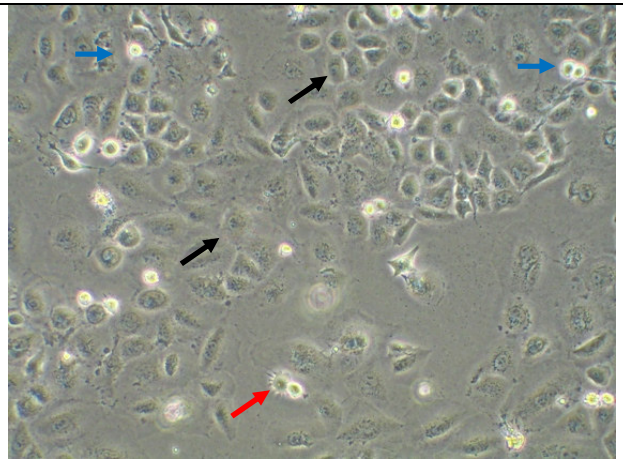 | 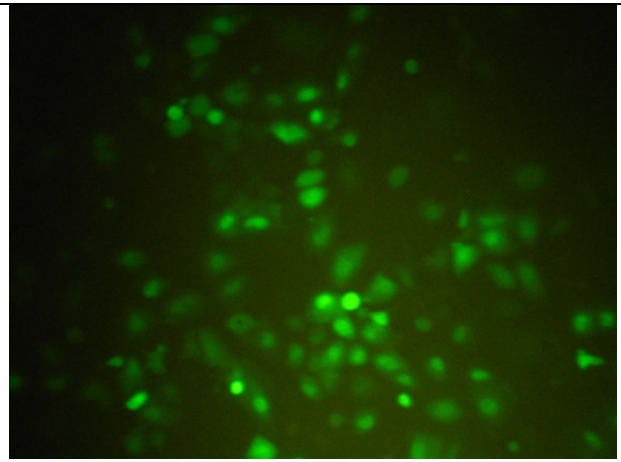 |
| No DNA (Mock Transfection) | 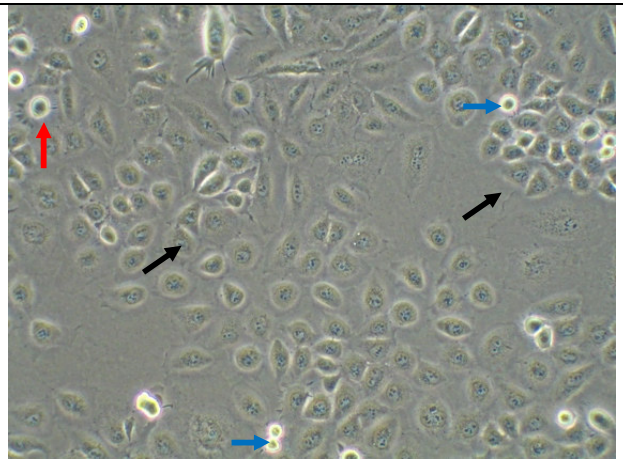 |  |

IPCR was carried out to detect intact and/or the cleaved MLL bcr. Amplified fragment of size 2.2 kb representing the intact MLL bcr while fragments of sizes smaller than 2.2 kb representing the cleaved MLL bcr. With overexpression of CAD in SUNE1 cells in both non-treated and treated samples, it was thought to see enhancement of cleavage within the MLL bcr as compared to other transfectants. After treatment with 50 μM of $H_2O_2$, it was expected that the overexpressed CAD will cleave the MLL bcr more extensively compared to non-treated samples.

From the IPCR result, as shown in Figure 2.9(A), both SUNE1 cells which were non-treated (Lanes 3 – 7) and treated (Lanes 8 – 12) with 50 μM of $H_2O_2$ showed cleavage within the MLL bcr. However, cleaved fragments observed were fuzzy for both sets of samples. In non-treated samples, SUNE1 cells transfected with hCAD (Lane 4) and mCAD (Lane 5) did not show increased cleavage within the MLL bcr as compared to CAD mutant (Lane 6), vector (Lane 3) and mock transfected cells (Lane 7). After transfected cells were treated with 50 μM of $H_2O_2$, mCAD (Lane 10) showed a very intense band of size approximately 1 kb. This might be an indication of enhanced cleavage within the MLL bcr as compared to cells transfected with CAD mutant (Lane 11), vector (Lane 8) and cells underwent mock transfection (Lane 12). Cells transfected with hCAD (Lane 9) did not show enhanced cleavage as compared to cells transfected with vector (Lane 8). However, there was a slight increased cleavage for this transfectant as compared to cells transfected with CAD mutant (Lane 11) and mock transfected (Lane 12) cells. Fuzzy bands were observed. This complicated our analysis.

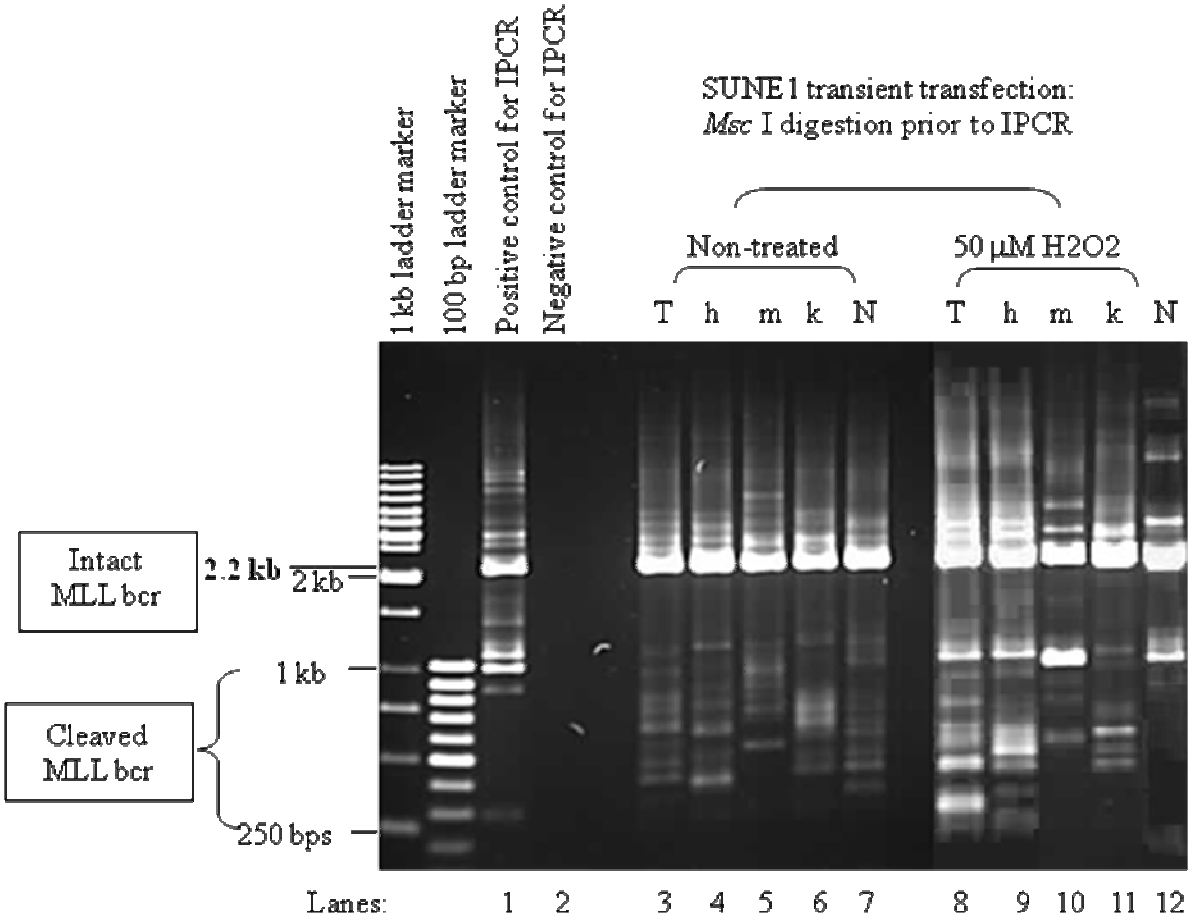


**Figure 2.9(A): Nested IPCR with *Msc* I-digested DNA from transiently transfected SUNE1 cells non-treated and treated with 50 µM of $H_2O_2$.** SUNE1 cells were transiently transfected with either pTracer, T (Lanes 3 and 8); pTracer-hCAD, h (Lanes 4 and 9); pTracer-mCAD, m (Lanes 5 and 10) or pTracer-hCAD(K157Q), k (Lanes 6 and 11). A mock transfection (no DNA), N (Lanes 7 and 12) was included as control. The cells were either non-treated (Lanes 3 – 7) or treated (Lanes 8 – 12) with 50 µM of $H_2O_2$ for 8 hours at 17 hours post-transfection. Genomic DNA extracted was digested with *Bam*H I, modified and digested with *Msc* I prior to IPCR. *Msc* I-digested DNA from HeLa cells transiently transfected with pTracer-hCAD was used as DNA template in positive control for IPCR. As for negative control for IPCR, no DNA template was included. The 2.2 kb band represents the intact MLL bcr whereas smaller fragments of sizes ranging from 250 bps to 1 kb represent the cleaved MLL bcr.

Again, *Bgl* II was used to eliminate amplification of the intact MLL bcr in order to favour amplification of the cleaved MLL bcr. As shown in Figure 2.9(B), band of size 2.2 kb representing the intact MLL bcr was not detected. In general, the number and intensity of the smaller bands representing the cleaved MLL bcr seemed to increase as compared to the *Msc* I digestion. However, there was no significant difference between the various transfectants. The non-treated cells (Lanes 3 – 7) and cells treated with 50 μM of $H_2O_2$ (Lanes 8 – 12) both showed cleavage within the MLL bcr and there was no significant difference among them. In addition, in the absence of $H_2O_2$ treatment, SUNE1 cells transfected with hCAD (Lane 4) and mCAD (Lane 5) did not show increased cleavage within the MLL bcr as compared to cells transfected with CAD mutant (Lane 6), vector (Lane 3) and cells underwent mock transfection (Lane 7). When transfected cells were treated with 50 μM of $H_2O_2$, cells transfected with hCAD (Lane 9) and mCAD (Lane 10) also did not show clear increased cleavage within the MLL bcr as compared to CAD mutant (Lane 11), vector (Lane 8) and cells underwent mock transfection (Lane 12). Therefore, this result did not tally with result obtained from DNA digested with *Msc* I where cells transfected with mCAD showed enhanced cleavage as shown in Figure 2.9(A).

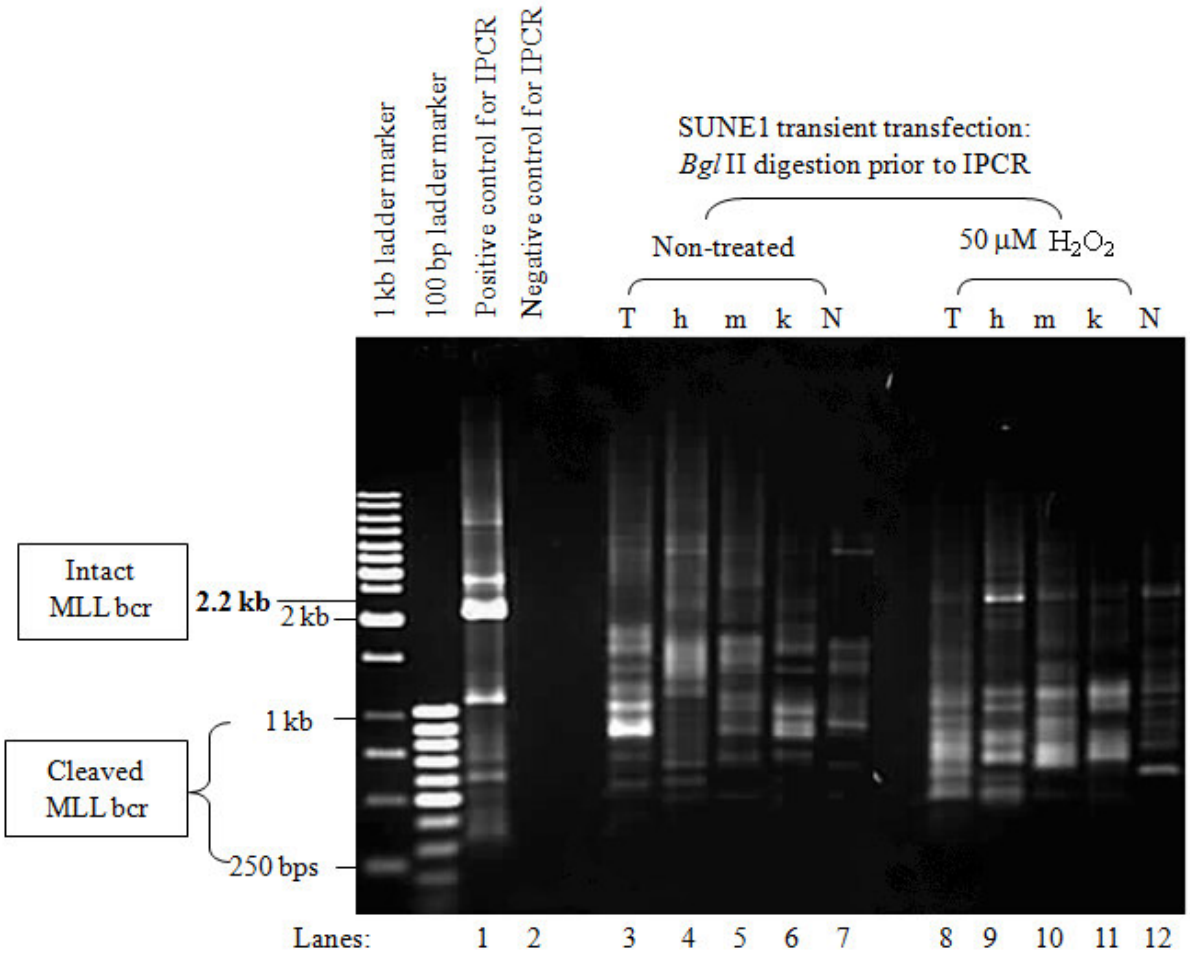


**Figure 2.9(B): Nested IPCR with *Bgl* II-digested DNA from transiently transfected SUNE1 cells non-treated and treated with 50 µM of $H_2O_2$.** SUNE1 cells were transiently transfected with either pTracer, T (Lanes 3 and 8); pTracer-hCAD, h (Lanes 4 and 9); pTracer-mCAD, m (Lanes 5 and 10) or pTracer-hCAD(K157Q), k (Lanes 6 and 11). A mock transfection (no DNA), N (Lanes 7 and 12) was included as control. The cells were either non-treated (Lanes 3 – 7) or treated (Lanes 8 – 12) with 50 µM of $H_2O_2$ for 8 hours at 17 hours post-transfection. Genomic DNA extracted was digested with *Bam*H I, modified and digested with *Bgl* II prior to IPCR. *Msc* I-digested DNA from HeLa cells transiently transfected with pTracer-hCAD was used as DNA template in positive control for IPCR. As for negative control for IPCR, no DNA template was included. The 2.2 kb band represents the intact MLL bcr whereas smaller fragments of sizes ranging from 250 bps to 1 kb represent the cleaved MLL bcr.

## 2.4 Discussion

The role of CAD in DNA fragmentation has been studied extensively (Enari *et al.*, 1998; Sakahira *et al.*, 1998; Mukae *et al.*, 1998; Nagata *et al.*, 2003). This nuclease has been shown to be a key player in internucleosomal DNA ladder formation (Enari *et al.*, 1998; Nagata *et al.*, 2003). CAD was also suggested to be the cultprit that caused chromosomal breaks within the MLL bcr in leukaemic cells (Sim and Liu, 2001; Hars *et al.*, 2006). It has also been suggested to play an important role in chromosomal translocations in leukaemia (Hars *et al.*, 2006). However, the role of CAD in chromosomal breaks resulted from stress-induced apoptosis is yet to be established. Thus, in this chapter, we looked into this aspect by overexpressing CAD. CAD alone was overexpressed because it had been shown that, when CAD was overexpressed in HeLa cells, chromosomal DNA ladder was formed (Lechardeur *et al.*, 2004; Korn *et al.*, 2005). In this experiment, $H_2O_2$ was chosen as the apoptotic inducer because it is a ROS which is generated during oxidative stress and is known to induce apoptosis (Stangel *et al.*, 1996).

In the current study, cells were treated with $H_2O_2$ for 8 hours as optimised. From the morphological observation, cells appeared healthy before 8 hours of treatment. Although significant morphological changes were only observed at and beyond 8 hours of treatment, the actual insult could have occurred earlier. $H_2O_2$ is known to be consumed within minutes upon addition into a cell culture (Antunes and Cadenas, 2000). It is also known to diffuse across the cellular compartments easily (Chance *et al.*, 1979). Thus 8 hours of treatment may seem to be unnecessarily long. However, it has been shown that uptake of $H_2O_2$ into a cells will lead to cell apoptosis hours later. It was found that exposure of cells to $H_2O_2$ for only a few

minutes were sufficient to cause cells to become apoptotic. However, the process of apoptotic induction by $H_2O_2$ treatment took several hours to develop fully (Antunes *et al.*, 2001). Studies done by Li *et al.* (1999) showed that U937 cells treated with $H_2O_2$ for less than a minute could lead to DNA fragmentation resulting in high molecular weight (HMW) DNA formation (Li *et al.*, 1999). Changes in cells morphology after 8 hours of $H_2O_2$ treatment in our experiment agreed to these previous studies.

It was expected to see an enhanced chromosome breaks within the MLL bcr but this was not observed even when CAD was overexpressed. It could be possible that the exogenous CAD expressed was not functional. *In vitro* expression of CAD, done by Enari *et al.* (1998) showed that CAD, in the absence of ICAD was inactive. It became functional when co-expressed with ICAD and activated by caspase-3 (Enari *et al.*, 1998). ICAD is known to be the chaperon for CAD (Sakahira *et al.*, 2000). Lechardeur *et al.* (2004) showed that majority of endogenous CAD coupled with endogenous ICAD, where folding of exogenously expressed CAD was severely impaired without ICAD (Lechardeur *et al.*, 2004). Moreover, overexpression of CAD together with ICAD in human 293 cells showed clear enhanced internucleosomal DNA cleavage after treatment with staurosporine. This was not observed in cells transfected with CAD or ICAD alone (Cao *et al.*, 2001). So, it is possible that there was insufficient endogenous ICAD available for proper folding of the exogenously expressed CAD. This improperly folded CAD could be degraded (Sakahira and Nagata, 2002). Major difficulties were encountered during result analysis, mainly due to combination of complications contributed by the transfection process, which was somehow cytotoxic (Cartier *et al.*, 2003) and the effect of free hydroxyl radicals ($OH\cdot$) from $H_2O_2$ which is known to cause direct DNA strand breaks.

From our IPCR result, fuzzy bands and background cleavage were observed, even in mock transfected cells. This might be due to the process of transient transfection. In non-viral gene delivery system, DNA complexes are transferred through endocytic pathway. Cartier *et al.* (2003) demonstrated the peptide-mediated gene transfer by using human cancer cells *in vitro* (Dalluge *et al.*, 2002). They performed the ultrastructural analysis of DNA complexes during transfection and intracellular transport process. The cationic polymer/DNA complexes (polyplexes) formed was stained with uranyl acetate on a formvar-coated grid (Bremer and Rasquin, 1998). Process of formation and movement of these complexes were observed under electron microscope. Formation of these polyplexes during the transfection process is a critical issue. The main concern was on the physicochemical properties of transfection active complexes as well as the internalisation process. In the transfection process, calcium ion is an essential factor. However, it was found that calcium ion exerts a cytotoxic effect at the later stages of the gene transfer process. This lead to elevated number of damaged mitochondria regardless of presence or absence of DNA complexes (Cartier *et al.*, 2003). Sakurai *et al.* (2001) showed that mitochondrial damage resulted in apoptosis as indicated by DNA ladder formation and externalisation of phosphatidylserine of plasma membrane (Sakurai *et al.*, 2001). Thus, the elevated number of damaged mitochondria seen during gene transfer may indicate that the transfer process could exert certain level of damage to the cells.

## 2.5 Conclusion

From the result, $H_2O_2$ induced apoptosis in mammalian cell lines, namely HeLa and SUNE1. However, overexpression of CAD did not show enhanced cleavage within the MLL bcr. Besides, overexpression of CAD mutant, hCAD(K157Q) did not show decreased cleavage of

the MLL bcr, suggesting that in the absence of exogenous ICAD, CAD is not functional. However, this does not rule out the role of CAD in the cleavage of the MLL bcr.

# CHAPTER THREE

# OVEREXPRESSION OF MURINE INHIBITOR OF CASPASE-ACTIVATED DNase MUTANT (mICAD-Ldm)

## 3.1 Introduction

The natural inhibitor of CAD, ICAD, exists in two isoforms, namely the full length form, ICAD-L and the short form, ICAD-S, of molecular weight 45 kDa and 35 kDa respectively (Enari *et al.*, 1998; Gu *et al.*, 1999). ICAD-L consists of 331 amino acids, whereas ICAD-S contains 265 amino acids. ICAD-S which is generated by alternative splicing of ICAD-L, was found to be expressed in numerous cell types in human and mouse (Enari *et al.*, 1998; Kawane *et al.*, 1999; Sabol *et al.*, 1999; Gu *et al.*, 1999). Under normal physiological condition, ICAD dimerises with CAD (Liu *et al.*, 1997; Enari *et al.*, 1998) and inhibits the DNase activity of CAD. Besides, it also works as a specific molecular chaperone for CAD to ensure its proper folding (Enari *et al.*, 1998; Halenbeck *et al.*, 1998; Zhang *et al.*, 1998).

Even though ICAD-L and ICAD-S are different in length and molecular weight, both contain two putative cleavage sites of caspase-3 at amino acid positions 117 and 224 (Wyllie *et al.*, 1980; Talanian *et al.*, 1997; Thornberry *et al.*, 1997). Mutation of the murine ICAD-L, mICAD-L at these two sites causes the ICAD to be resistant to caspase-3 cleavage and hence stays as complex with CAD. Studies done by McIlroy *et al.* (1999) also showed that overexpression of double mutant, ICAD-Ldm in Jurkat cells and TF-1 cells abolished DNA fragmentation upon various apoptotic induction, even though cells eventually died (McIlroy *et*

*al.*, 1999). Interestingly, overexpression of the wild-type ICAD-L in Jurkat cells also eliminated DNA fragmentation upon apoptotic induction by staurosporine (Sakahira *et al.*, 1998).

In Chapter Two, we have discussed the first approach to study the role of CAD in the MLL bcr cleavage induced by oxidative stress. Here, we described the second approach, which is to overexpress ICAD-Ldm in NPC (SUNE1) cells. It was expected to see less cleavage within the MLL bcr upon oxidative stress-induced apoptosis. This is because, when cells undergo apoptosis, caspase-3 will cleave endogenous ICAD and release activated endogenous CAD. High abundance of exogenous mICAD-Ldm expressed in the cells should bind to these activated endogenous CAD and hence inhibits their DNase activity. Since the ICAD-Ldm cannot be inactivated through cleavage by caspase-3, thus CAD will not be released from ICAD-Ldm. Therefore, there should be less active CAD available to cleave the MLL bcr. In this experiment, pTracer-mICAD-Ldm was transfected into NPC (SUNE1) cells. As controls, cells were transfected with vector pTracer and the reverse compliment of mICAD-Ldm (pTracer-RCmICAD-Ldm). Mock transfection was also carried out where cells underwent transfection without DNA. In order to detect cleavage within the MLL bcr, nested IPCR was performed.

## 3.2 Materials and Methods

### 3.2.1 Subcloning of pTracer-mICAD-Ldm and pTracer-RCmICAD-Ldm

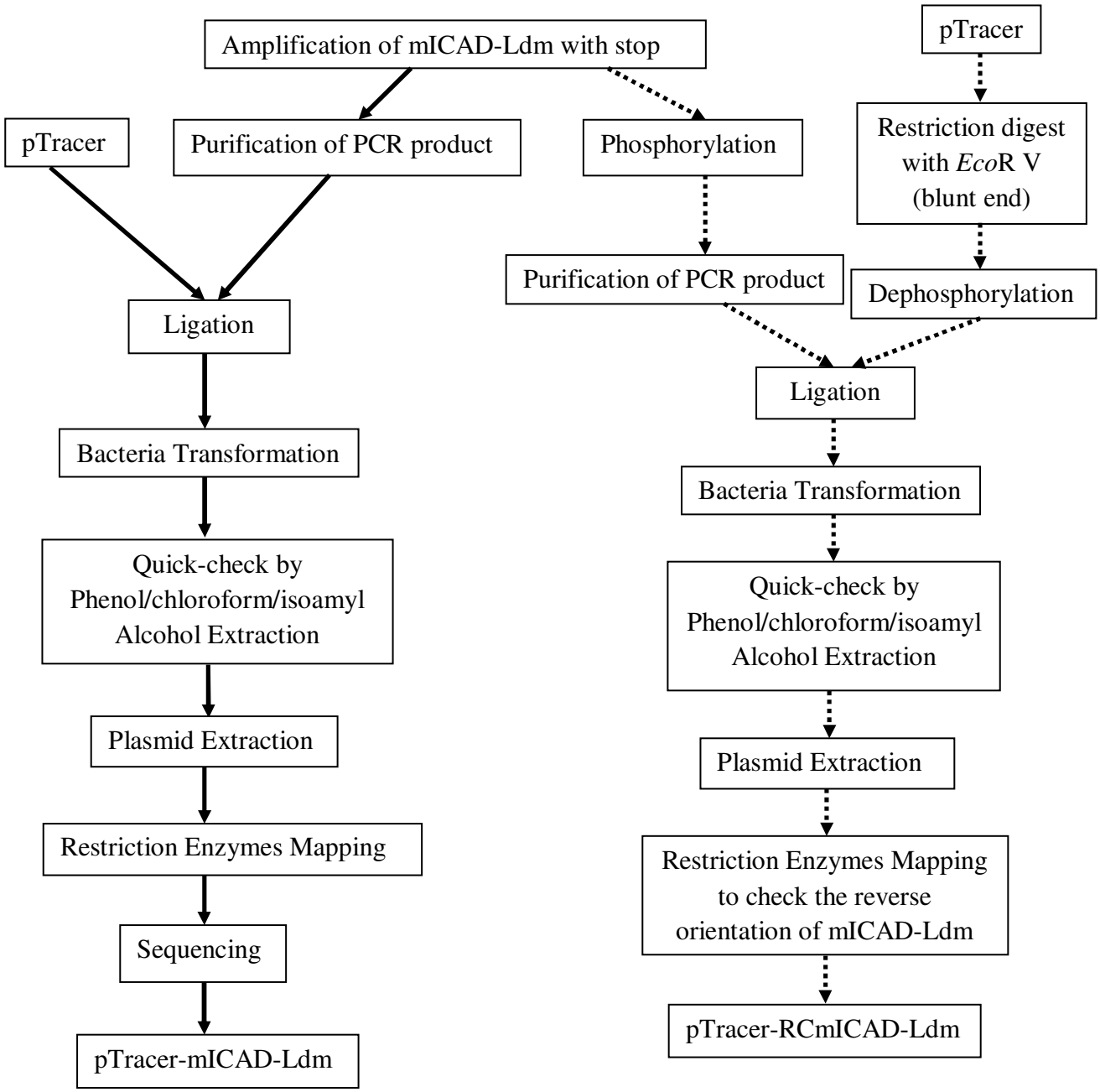


Figure 3.1: General flow of subcloning of pTracer-mICAD-Ldm and pTracer-RCmICAD-Ldm.

Plasmid pEF-FL-mICAD-Ldm carrying the mICAD-Ldm, the generous gift from Professor Dr. Shigekazu Nagata of University of Osaka, Japan, was sent as lyophilised plasmid. Plasmid DNA was dissolved in 10 µl of TE buffer (pH 8). One ng of each plasmid was transformed into 50 µl of electrocompetent *E. coli* HB101 cells as described in Section 2.2.1.5. The selected clone was cultured and kept as stock at -80$^{o}$C in 50% sterilised glycerol. The plasmid was also extracted from the culture for subcloning purpose.

Plasmid vector pTracer-EF/V5-His B was used because it carries the green fluorescence protein (GFP) gene as shown in Appendix A. The mICAD-Ldm gene without stop codon was obtained via conventional PCR method. When the gene was subcloned into plasmid vector pTracer-EF/V5-His B, recombinant plasmid pTracer-mICAD-Ldm was produced. When this gene was subcloned in a reverse orientation, recombinant plasmid pTracer-RCmICAD-Ldm was produced. pTracer-RCmICAD-Ldm was needed to assess the background cleavage resulted from transfection and expression of a gene, as indicated by the fuzzy background bands shown in Figure 2.8 and 2.9 in Chapter Two. When these recombinant plasmids were being expressed in mammalian cells, GFP will be expressed simultaneously and can be observed under fluorescence microscope (Olympus IX70). GFP expression was used to estimate the transfection efficiency. The subcloning procedure is summarised in Figure 3.1.

#### 3.2.1.1 Amplification of The mICAD-Ldm Gene Without Stop Codon.

Plasmid pEF-FL-mICAD-Ldm was used as DNA template in the amplification of the mutant mICAD double mutant, mICAD-Ldm gene for subcloning. Information about the sequence of ICAD mutant, mICAD-Ldm was amended from mICAD-L sequence according to the

information reported by Sahakira *et al.* (1998) (Sakahira *et al.*, 1998). The mICAD-Ldm carries double mutations at amino acid positions 117 and 224. The mutation was GAC (for Aspartate) to GAA (for Glutamate) at both positions. The forward primer, mICAD-K/X(F) (5' – GA**GGTACC**ATGGAGCTGTC – 3') was used. This primer contained a *Kpn* I (GGTACC) restriction site as indicated in bold. In order to produce mICAD-Ldm gene without the stop codon at its 3' end, the reverse primer, mICAD(R-K/X)2 (5' – CATCTAGACGAGGAGTCTCG – 3'), was designed according to the mICAD-L sequence reported (GenBank accession number AB009375) as shown in Appendix B. Positions of these primers were shown in Figure 3.2.

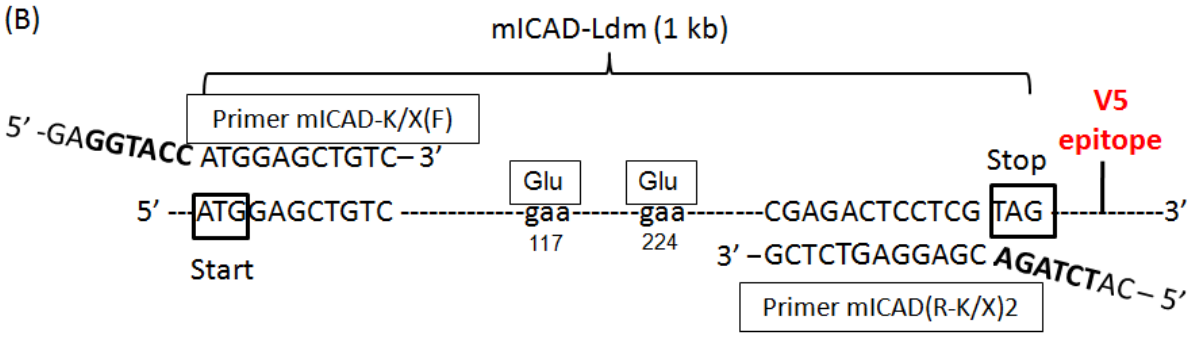


Figure 3.2: Schematic diagram showing the positions of primers used in the amplification of ICAD double mutant, mICAD-Ldm without stop codon. Forward primer, mICAD-K/X(F) contains a *Kpn* I restriction site (GGTACC) as indicated in bold. Reverse primer, mICAD(R-K/X)2 contains an *Xba* I restriction site (TCTAGA) as indicated in bold. Amplification by using these primers produces a 1 kb fragment of the mICAD-Ldm gene which includes the start codon (ATG) but without the stop codon (TAG). The mICAD-Ldm gene carries mutation at amino acid position 117 and 224. This fragment also carries a *Kpn* I restriction site at its 5' end and an *Xba* I restriction site at its 3' end. By omitting the stop codon, mICAD-Ldm will be expressed as fusion protein with V5 epitope at the C-terminal.

PCR was carried out with 10 ng of DNA template as recommended together with 1X Phusion HF Buffer (Finnzyme), 200 µM of each of the dNTP (Promega), 0.5 µM of each of the primers, 0.4 U Phusion DNA polymerase and sterile ultra pure water (sUPW) in a final volume of 20 µl in 0.2 ml PCR tubes (Eppendorf). PCR was performed under optimised condition with 30 seconds of initial denaturation at 98$^{o}$C for 1 cycle, followed by 30 cycles of denaturation at 98$^{o}$C for 10 seconds, annealing of primers at 61.2$^{o}$C for 30 seconds, extension at 72$^{o}$C for 15 seconds, followed by single cycle of final extension step at 72$^{o}$C for 10 min as shown in Table 3.1. The annealing temperatures were calculated based on the nearest-neighbour method suggested for Phusion DNA Polymerase (www.finnzymes.com).

Table 3.1: PCR condition for amplification of mICAD-Ldm without stop codon.

| **Step** | **Temperature ($^{o}$C)** | **Time** |
|---|---|---|
| **Hot start** | **80** | **Forever** |
| **Initial denaturation** | **98** | **30s** |
| **Denaturation** | **98** | **10s** |
| **Annealing** | **61.2** | **30s** |
| **Extension** | **72** | **15s** |
| | **Go to Denaturation step and repeat for 29 cycles** | |

| | | |
|---|---|---|
| **Final extension** | **72** | **10 minutes** |
| **Cooling** | **20** | **Forever** |

### 3.2.1.2 Phosphorylation of PCR Product and Dephosphorylation of Plasmid Vector

PCR product generated was blunt-ended and did not contain phosphate group at its 5' end. Therefore, T4 Polynucleotide Kinase (Invitrogen) was used to phosphorylate the PCR product following standard protocol. Briefly, 3 µl of gamma-phosphate ATP ([$\gamma$-$^{32}$P ] ATP, (10 µCi/µl, 3000 Ci/mmol)) was used to phosphorylate 5 pmol of PCR product in the presence of 10 units of T4 Polynucleotide Kinase, 6 µl of 5X Forward reaction buffer, and sUPW in a final volume of 30 µl. Meanwhile, 2 µg of plasmid vector pTracer was digested with 50 units of *Eco*R V (Promega) together with 1X *Eco*R V buffer, 0.1 mg/ml of acetyl BSA and sUPW in a total volume of 20 µl. In order to prevent self-ligation of the plasmid vector, 2 units of Shrimp Alkaline Phosphatase (SAP) was used to catalyse the dephosphorylation process. Dephosphorylation was carried out in 1X SAP Buffer and sUPW in a final volume of 30 µl. These pTracer and mICAD-Ldm were then purified (Section 3.2.1.3) and ligated (Section 3.2.1.4).

### 3.2.1.3 Purification of PCR Product, mICAD-Ldm

PCR product was analysed on 1% agarose gel and product of size of 1 kb was excised with clean and sharp scarpel. DNA was purified by using QIAquick Gel Extraction Kit (Qiagen) as described in Section 2.2.1.3.

### 3.2.1.4 Ligation of PCR Product with pTracer to Generate pTracer-mICAD-Ldm and pTracer-RCmICAD-Ldm

Purified PCR product, mICAD-Ldm was subcloned into plasmid vector pTracer. Both plasmid vector pTracer and mICAD-Ldm were digested with *Kpn* I (NEB) and *Xba* I (NEB) restriction enzymes and subsequently ligated. Restriction enzymes digestion was carried out in 1X NE Buffer 4 (NEB), 1X BSA (NEB), 10 U of *Kpn* I, 20 U *Xba I* and sUPW in a final volume of 10 µl at 37$^{o}$C for 2 hours. Ligation was done at an insert to vector ration of 10 to 1 by using 40 units of T4 DNA ligase, 1X T4 DNA ligase buffer (NEB) and sUPW in a final volume of 20 µl at 16$^{o}$C overnight as simplified in Figure 3.3(A). This generated recombinant plasmid pTracer-mICAD-Ldm.

As for subcloning of the reverse complementary strand of mICAD-Ldm, the phosphorylated insert and dephosphorylated plasmid vector were ligated. Ligation was carried out at an insert to vector ratio of 10 to 1 by using 40 units of T4 DNA ligase, 1X T4 DNA ligase buffer (NEB) and sUPW in a final volume of 20 µl at 16$^{o}$C overnight. This procedure is simplified in Figure 3.3(B). This generated recombinant plasmid pTracer-RCmICAD-Ldm.

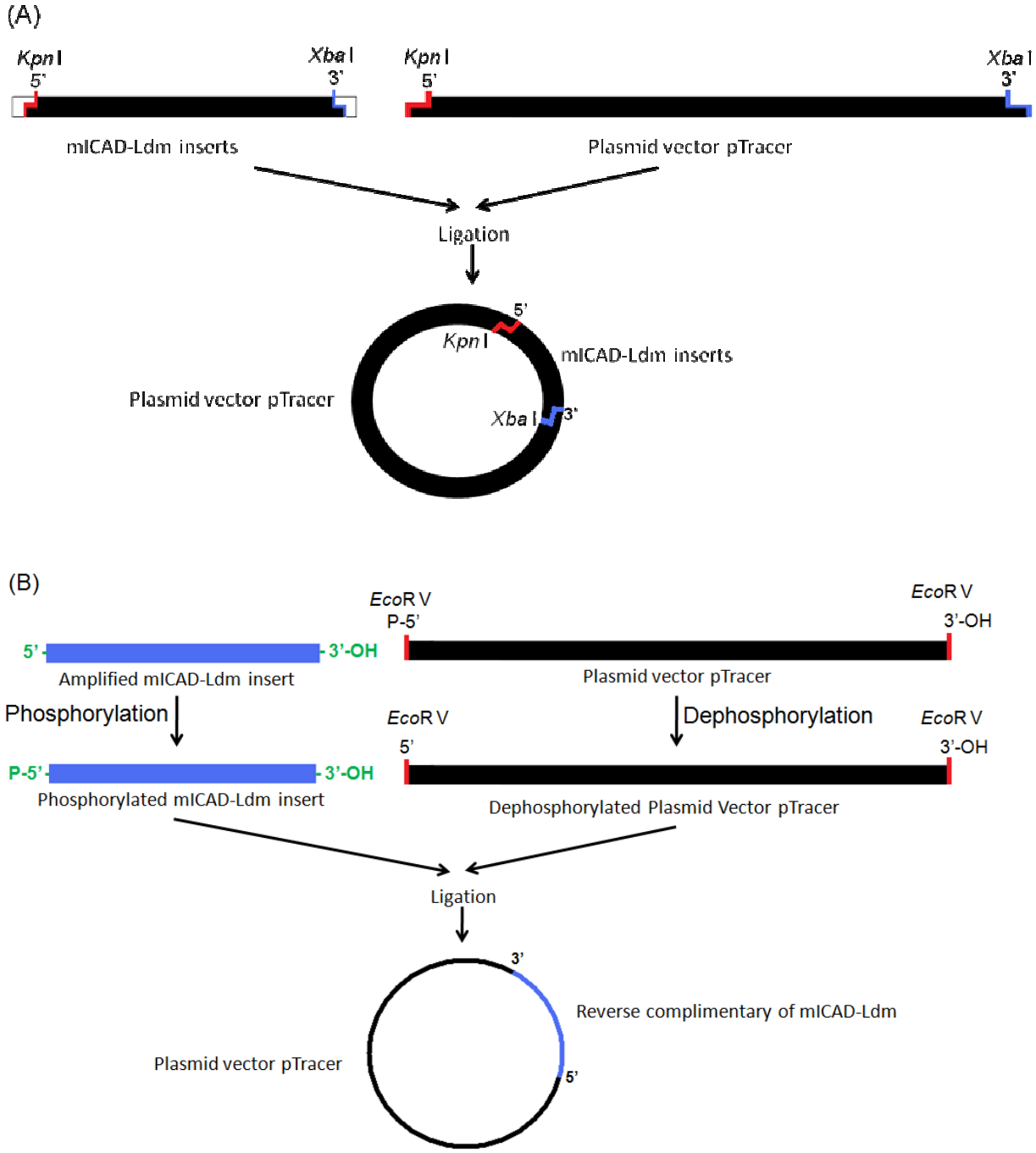


Figure 3.3: Schematic diagram showing the generation of recombinant plasmids, pTracer-mICAD-Ldm and pTracer-RCmICAD-Ldm. (A) Amplified insert, mICAD-Ldm as well as plasmid vector, pTracer were digested with *Kpn* I and *Xba* I. Ligation was then carried out to generate recombinant plasmid carrying mICAD-Ldm. (B) Amplified insert, mICAD-Ldm was phosphorylated and plasmid vector, pTracer was dephosphorylated. Ligation was carried out. Insertion of mICAD-Ldm in the reverse orientation resulted in recombinant plasmid carrying the reverse complimentary strand of mICAD-Ldm.

### 3.2.1.5 Bacteria Transformation

Recombinant plasmids, pTracer-mICAD-Ldm and pTracer-RCmICAD-Ldm were transformed into electrocompetent cells, *E. coli* HB101 via electroporation method as described in Section 2.2.1.5.

### 3.2.1.6 Quick-check by Phenol/chloroform/Isoamyl Alcohol Extraction

Randomly picked colonies were checked by extraction with phenol/chloroform/isoamyl alcohol (Ratio 25:24:1) as described in Section 2.2.1.6. Suspected clones, which might carry the plasmid of interest, were grown and plasmids were extracted for further confirmation by restriction enzymes mapping as elaborated in Section 3.2.1.8.

### 3.2.1.7 Plasmid Extraction

After the quick-check, plasmids were isolated from suspected clones by using S.N.A.P Miniprep Kit according to manufacturer's instruction as described in Section 2.2.1.7 for further checking.

### 3.2.1.8 Restriction Enzymes Mapping

Recombinant plasmids pTracer-mICAD-Ldm and pTracer-RCmICAD-Ldm were checked using restriction enzymes mapping. Approximately 200 to 500 ng of these plasmids isolated from selected clones were digested with various restriction enzymes. Plasmid pTracer-mICAD-Ldm was checked by using *Kpn* I and *Xba* I, *Bgl* II, *Bam*H I, *Bst*X I (all NEB) as

well as *Eco*R V (Promega) restrictions enzymes. Meanwhile, plasmid pTracer-RCmICAD-Ldm was checked by using restriction enzymes *Bam*H I, *Bst*X I, *Kpn* I (all from NEB) as well as *Eco*R I (Fermentas). Restriction enzymes digestion was carried out as simplified in Table 3.2. The restriction mapping allows us to check the orientation of the insert. The one inserted in a 5' → 3' manner produced the pTracer-mICAD-Ldm. While the one inserted in the opposite orientation produced the pTracer-RCmICAD-Ldm. In addition, based on the fragment size, the clone containing the correct plasmid could be identified.

Table 3.2: Restriction mapping reactions for pTracer-mICAD-Ldm and pTracer-RCmICAD-Ldm and the expected size of the fragments produced.

| Samples | pTracer-mICAD-Ldm | | | | | pTracer-RCmICAD-Ldm | | | |
|---|---|---|---|---|---|---|---|---|---|
| Restriction enzyme (RE), unit | *Kpn* I (10U) and *Xba* I (20U) | *Bgl* II (10 Units) | *Bam*H I (20 U) | *Bst*X I (10 U) | *Eco*R V (50 U) | *Bam*H I (20U) | *Bst*X I (10 U) | *Eco*R I (50U) | *Kpn* I (10U) |
| sUPW, µl | 4 | 6 | 5 | 6 | 3 | 5 | 6 | 6 | 5 |
| RE buffer, µl | 1 µl of 10X NE Buffer 2 | 1 µl of 10X NE Buffer 3 | 1 µl 10X *Bam*H I Buffer 2 | 1 µl of 10X NE Buffer 4 | 1 µl 10X Buffer D) | 1 µl 10X *Bam*H I Buffer 2 | 1 µl of 10X NE Buffer 4 | 1 (10X Buffer *Eco*R I) | 1 (10XNE Buffer 1 |
| 10X BSA, µl | 1 | - | 1 | - | - | 1 | - | - | 1 |
| Plasmid, µl | 2 | 2 | 2 | 2 | 3 | 2 | 2 | 2 | 2 |
| Total reaction, µl | 10 | 10 | 10 | 10 | 10 | 10 | 10 | 10 | 10 |
| Temperature, $^{o}$C | 37 | 37 | 37 | 55 | 37 | 37 | 55 | 37 | 37 |
| Duration | 2 hours | 2 hours | 2 hours | 2 hours | 2 hours | 2 hours | 2 hours | 2 hours | 2 hours |
| Expected size of fragments | 5.867 kb and 995 bps | 4.877 kb, 1.078 kb and 907 bps | 5.097 kb and 1.783 kb | 6.862 kb (linearised) | No restriction site (circularised plasmid) | 4.288 kb, 2.424 kb and 234 bps | 5.911 kb, 824 bps and 211 bps | 6.946 kb (linearised) | 5.897 kb and 1.049 kb |

### 3.2.1.9 Sequencing

In order to confirm the sequence of plasmid pTracer-mICAD-Ldm, the plasmid was sent for sequencing as described in Section 2.2.1.9. However, the sequencing primers used were different. Forward primer, pT-LdmSeq-F (5' – CACGACACCTGAAATGGAAG – 3') was used to sequence the sense strand whereas reverse primer, pT-LdmSeq-R (5' – CCCCTGGACAGTGGCACAGC – 3') was used to sequence the anti-sense strand of pTracer-mICAD-Ldm. Sequencing results obtained, as shown in Appendix I, was analysed by using DNASTAR software.

## 3.2.2 Mammalian Cell Culture

SUNE1 grows as adherent epitheloid cells forming a monolayer. SUNE1 cells were maintained in RPMI 1640 medium supplemented with 10% heat-inactivated fetal bovine serum (FBS), L-glutamine (2 mM), penicillin (100 U/ml) and streptomycin (100 μg/ml). TrypLE Express was used to dislodge the NPC cells from the T25 tissue culture flask (Nalgene) during subculturing and cell seeding. The above mentioned items were purchased from GIBCO, Invitrogen. Cells were kept in a humidified incubator with an atmosphere of 95% air and 5% $CO_2$ at 37$^{o}$C. Upon reaching confluency of about 70%, cells were subcultured and grew in new T25 flask.

### 3.2.3 Transfection of Mammalian Cells

#### 3.2.3.1 Plasmid Extraction for Transfection

For transfection purpose, high concentration of plasmid pTracer-mICAD-Ldm and pTracer-RCmICAD-Ldm were extracted from fresh culture of bacteria by using QIAfilter Plasmid Maxi Kits (Qiagen) according to manufacturer's instruction as described in Section 2.2.4.1.

#### 3.2.3.2 Transient Transfection

Subcloned plasmid pTracer-mICAD-Ldm was overexpressed transiently in SUNE1 cells to study the effect of direct inhibition of CAD. As controls, plasmid vector pTracer and pTracer-RCmICAD-Ldm were also transfected. For negative control, cells underwent mock transfection where no DNA was used during the transfection process. Transient transfection was carried out as elaborated in Section 2.2.4. After 3 hours of transfection, the transfection medium was replaced with fresh complete medium consisting of RPMI 1640 medium supplemented with 10% heat-inactivated fetal bovine serum (FBS), L-glutamine (2 mM), penicillin (100 U/ml) and streptomycin (100 µg/ml). Two sets of cells were transfected, one to be treated with 50 µM of $H_2O_2$ for 8 hours while the other set remained untreated as a control.

### 3.2.4 Oxidative Stress-induced Apoptosis of Transiently Transfected SUNE1 Cells

After 17 hours of culturing in complete media, the transiently transfected SUNE1 cells were induced to undergo apoptosis via oxidative stress. The cells which were transfected with

pTracer, pTracer-mICAD-Ldm, pTracer-RCmICAD-Ldm as well as mock transfected cells were either treated with 50 μM of $H_2O_2$ for 8 hours or left untreated. Subsequently, genomic DNA was extracted, modified and IPCR was carried out to detect cleavage within the MLL bcr as described in Section 2.2.5.

## 3.3 Result

In the second approach of studying the role of CAD, ICAD mutant was overexpressed. This is to inhibit CAD directly. As discussed in Section 2.3.1, treatment with 50 μM of $H_2O_2$ for 8 hours was chosen. SUNE1 cells were transiently transfected with plasmid vector pTracer, pTracer-mICAD-Ldm and pTracer-RCmICAD-Ldm. A mock transfection was included as control. Reverse complimentary strand of ICAD was used to compare the effect of overexpression of an unknown protein with that of ICAD.

For transfection purpose, SUNE1 cells were seeded 24 hours before transfection being carried out. The cell confluency reached 70% before transfection. Among the attached cells, 95% of them were healthy and 5% were rounded up. Approximately 5% of floating and blebbing cells were also observed (data not shown). After 3 hours of transfection, cells in all of the samples reached a confluency of 80 to 90%. Morphologically, 90% of the attached cells were healthy whereas 10% were rounded and bright. Approximately 5 to 10% of the cells were floating and blebbing. It was estimated that 60 to 70% of SUNE1 cells transfected with pTracer, pTracer-mICAD-Ldm and pTracer-RCmICAD-Ldm were fluorescing strongly. These plasmids carry the GFP gene. With the guide of GFP expression, transfection

efficiency could be estimated. In this case, transfection efficiency was estimated to be 60 to 70%. For SUNE1 cells which underwent mock transfection, there was no fluorescence observed, as shown in Table 3.4. After 8 hours of treatment with 50 μM of $H_2O_2$, cell morphology was observed, as shown in Table 3.4. Cell confluency for all of the samples reached 90%. All of the attached cells appeared rounded up and blebbing. For SUNE1 cells transfected with pTracer, pTracer-RCmICAD-Ldm and mock transfected cells, 20 to 30% of the cells were floating and blebbing with observation of apoptotic bodies. Forty percent of floating and blebbing cells containing apoptotic bodies were found in pTracer-mICAD-Ldm transfected cells. Under the fluorescence light, approximately 70% of these attached and rounded up cells fluoresced strongly. Healthy cells are shown by black arrows; red arrows indicate the attached but rounded up cells; whereas blue arrows pointed to show floating and blebbing cells.

Table 3.3: Microscopic morphology of transiently transfected SUNE1 cells (non-treated). Magnification of 100X under bright field and fluorescence light emission. Black arrow indicates healthy cells; red arrow indicates attached but rounded up cells; and blue arrow indicates floating cells.

| DNA transfected | Cell Morphology | |
|---|---|---|
| | Bright Field | Fluorescence Light |
| pTracer | 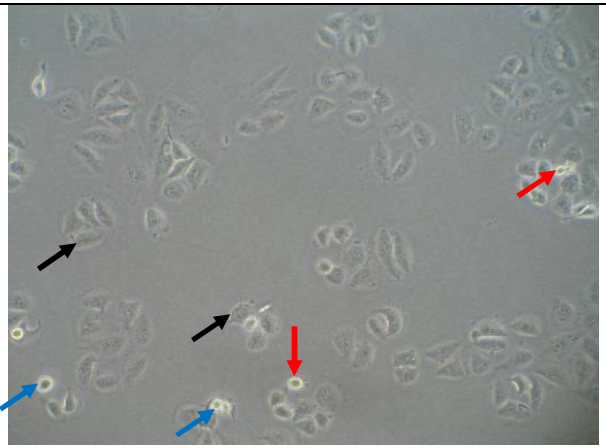 | 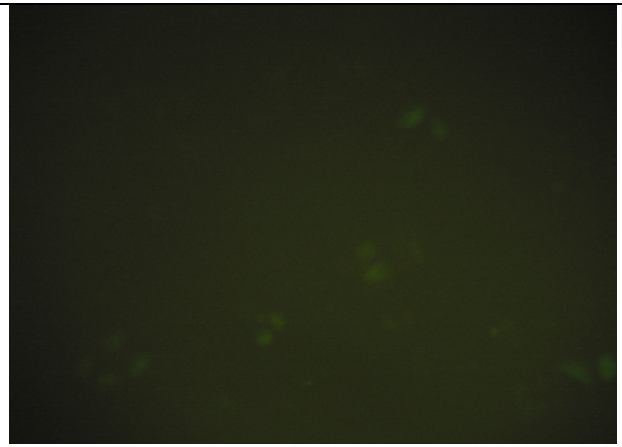 |

| | | |
|---|---|---|
| pTracer-mICAD-Ldm | 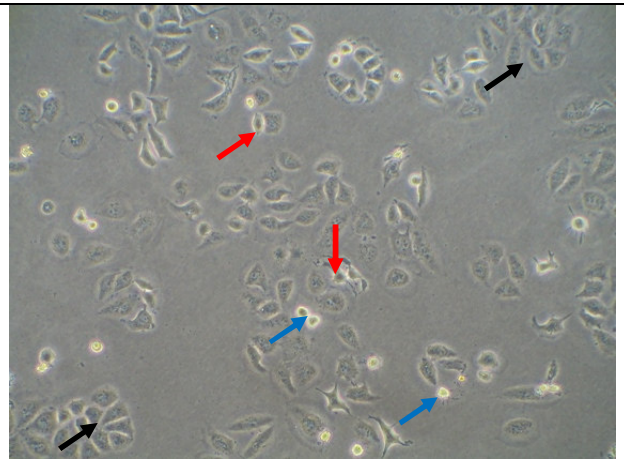 | 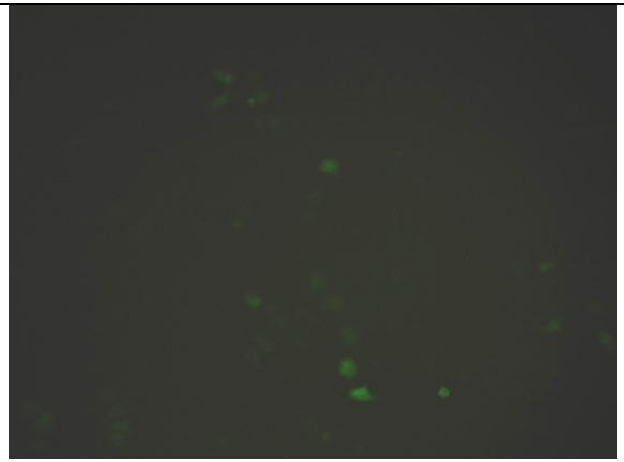 |
| pTracer-RCmICAD-Ldm | 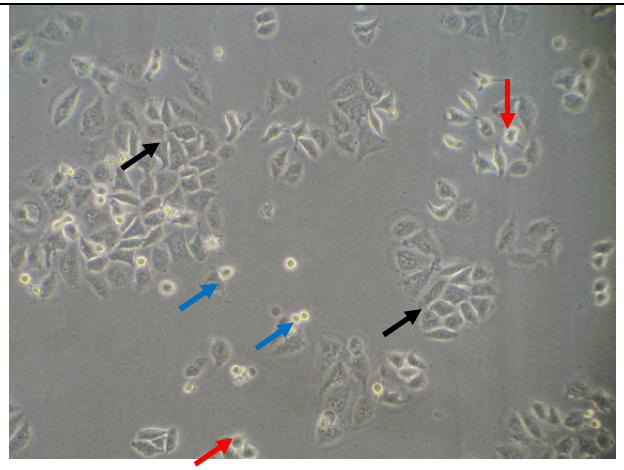 | 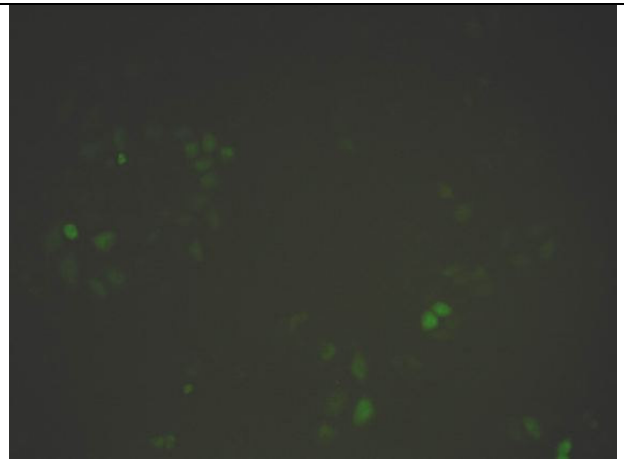 |

| | | |
|---|---|---|
| No DNA (Mock transfection) | 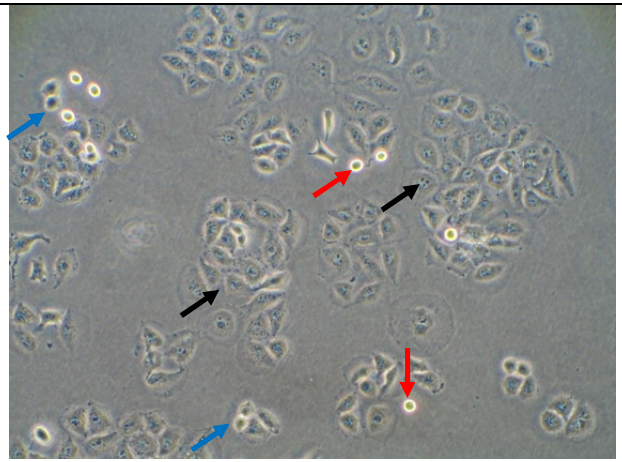 |  |

Table 3.4: Microscopic morphology of transiently transfected SUNE1 cells, treated with 50µM of $H_2O_2$ for 8 hours. Magnification of 100X under bright field and fluorescence light emission. All of the attached cells rounded up and blebbing as indicated by red arrow.

| DNA transfected | Cell Morphology | |
|---|---|---|
| | Bright Field | Fluorescence Light |
| pTracer | 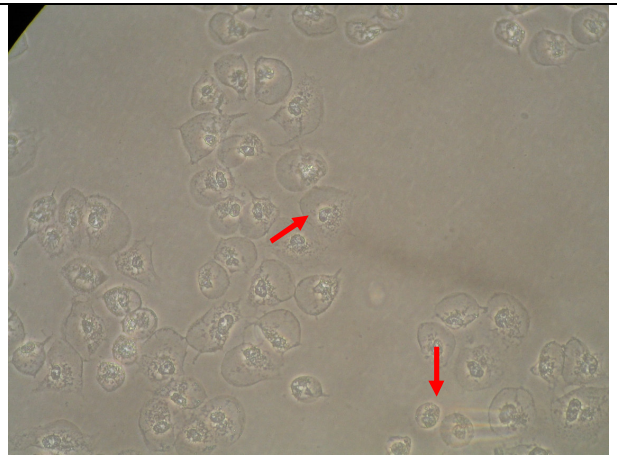 | 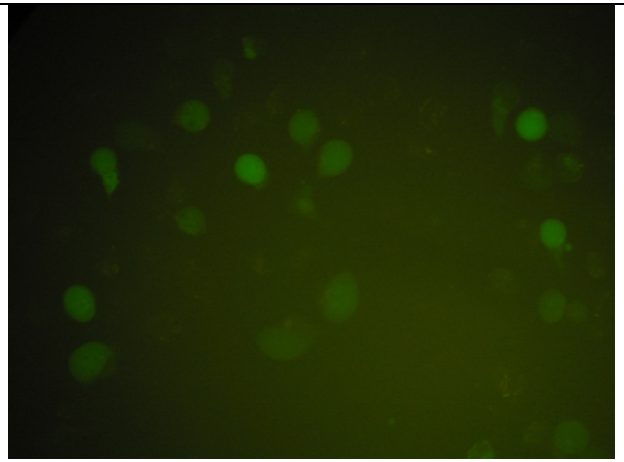 |

| | | |
|---|---|---|
| pTracer-mICAD-Ldm | 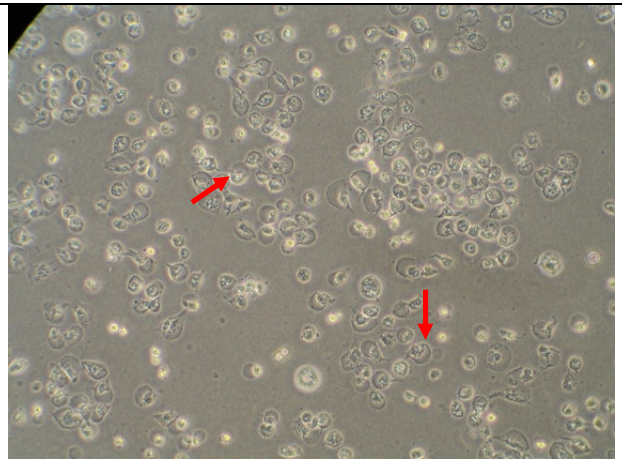 | 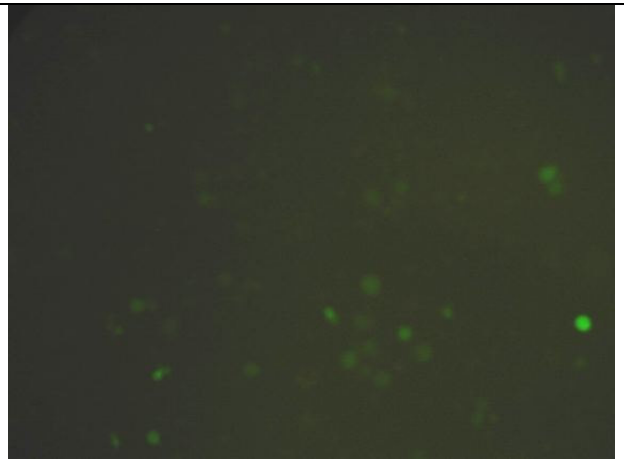 |
| pTracer-RCmICAD-Ldm | 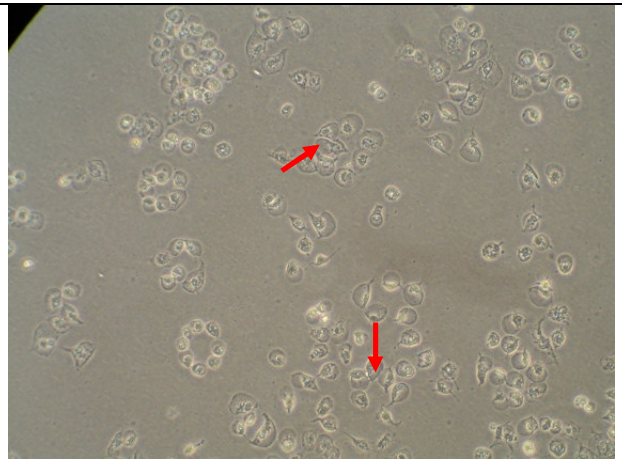 | 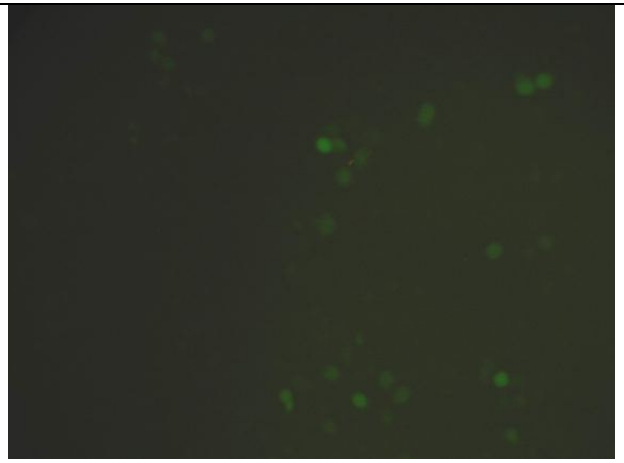 |

| | | |
|---|---|---|
| No DNA (Mock transfection) | 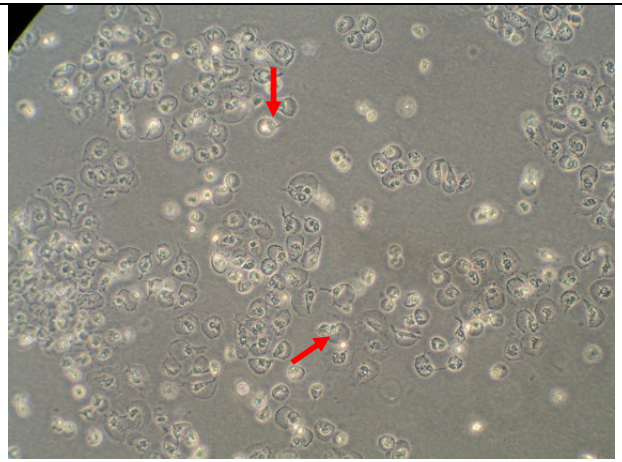 |  |

Genomic DNA was extracted from both the treated and non-treated transiently transfected SUNE1 cells. DNA was modified and IPCR was performed to detect the breaks within the the MLL bcr. It was expected that overexpression of plasmid pTracer-mICAD-Ldm might reduce the cleavage within the MLL bcr as compared to overexpression of pTracer and pTracer-RCmICAD-Ldm. Even though the cells were treated with 50 μM of $H_2O_2$, ICAD double mutant, mICAD-Ldm should remain complexed with CAD and inhibit its DNase activity. Therefore, there should be lesser of the cleaved MLL bcr fragments being amplified as compared to those transfected with pTracer and pTracer-RCmICAD-Ldm.

In this experiment, *Msc* I was used to linearise the circularised DNA fragments before nested IPCR was performed. *Bgl* II was used to linearised circularised DNA and to eliminate amplification of the intact MLL bcr. As shown in Figure 3.4(A) (Lanes 3 – 6), in the absence of treatment, all of the transfectants exhibited the 2.2 kb band, representing the intact MLL bcr. Bands of sizes smaller than 2.2 kb, representing the cleaved MLL bcr, were also detected in all of these samples. Referring to Figure 3.4(A) (Lanes 7 – 10), upon eliminating the amplification of the intact MLL bcr, the 2.2 kb band was clearly absent, while numerous smaller bands were detected. However, in both cases (*Msc* I and *Bgl* II digestion prior to IPCR), cells transfected with pTracer-mICAD-Ldm (Lanes 4 and 8) did not show decreased cleavage within the MLL bcr as compared to pTracer (Lanes 3 and 7), pTracer-RCmICAD-Ldm (Lanes 5 and 9) as well as mock transfected cells (Lanes 6 and 10).

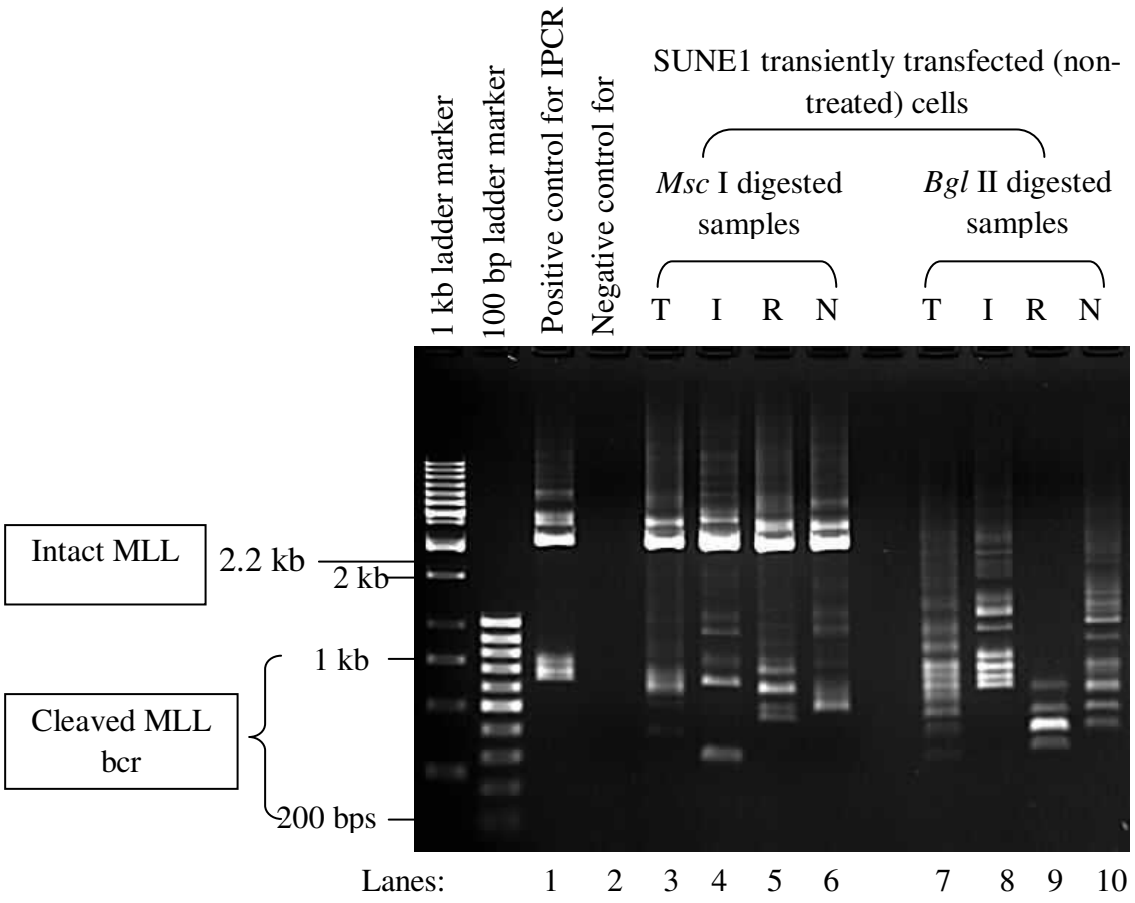


**Figure 3.4(A): Nested IPCR of transiently transfected SUNE1 cells non-treated with $H_2O_2$.** SUNE1 cells were transiently transfected with either pTracer, T (Lanes 3 and 7); pTracer-mICAD-Ldm, I (Lanes 4 and 8) or pTracer-RCmICAD-Ldm, R (Lanes 5 and 9). A mock transfection (no DNA), N (Lanes 6 and 10) was included as control. Genomic DNA extracted was digested with either *Msc* I (Lanes 3 – 6) or *Bgl* II (Lanes 7 – 10). The 2.2 kb band represents the intact MLL bcr whereas smaller fragments of sizes ranging from 250 bps to 1 kb represent the cleaved MLL bcr. As positive control for IPCR, *Msc* I-digested DNA from SUNE1 cells treated with 50 µM of $H_2O_2$ (from previous experiment) was used to ensure that the IPCR condition worked. For negative control of IPCR, no DNA was added for the amplification.

Both *Msc* I and *Bgl* II were also used to digest DNA from transiently transfected SUNE1 cells treated with 50 μM of $H_2O_2$. As shown in Figure 3.4(B) (Lanes 3 – 6), the 2.2 kb band representing the intact MLL bcr was amplified. All of them also showed presence of smaller bands of size smaller than 2.2 kb, representing the cleaved MLL bcr. It was clearly shown in Figure 3.4(B) (Lanes 7 – 10) that upon *Bgl* II digestion to eliminate the amplification of the intact MLL bcr, the 2.2 kb band was absent. Numerous smaller bands were detected. In both cases, *Msc* I and *Bgl* II-digested DNA prior to IPCR showed that cells transfected with pTracer-mICAD-Ldm (Lanes 4 and 8) did not show decreased cleavage of the MLL bcr as compared to cells transfected with pTracer (Lanes 3 and 7), pTracer-RCmICAD-Ldm (Lanes 5 and 9) , as well as mock transfected cells (Lanes 6 and 10). This showed that, with the $H_2O_2$ treatment, cells with overexpression of ICAD-Ldm did not decrease cleavage of the MLL bcr. Cleavage of the MLL bcr was also detected even in mock transfected cells. This suggested that the transient transfection process might be stressful to the cells and could result in apoptosis. Therefore, the transfection process might complicate our analysis.

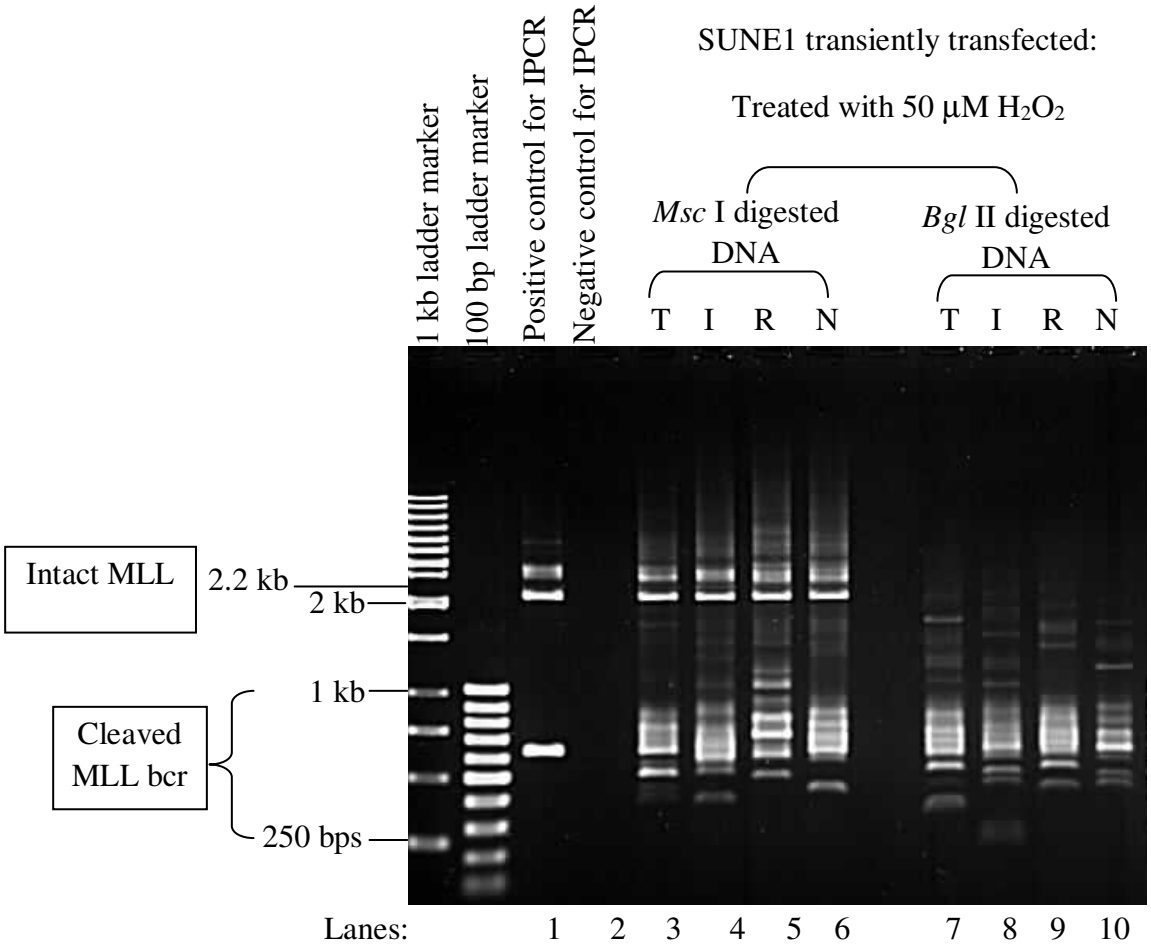


**Figure 3.4(B): Nested IPCR of transiently transfected SUNE1 cells treated with 50 µM of $H_2O_2$.** SUNE1 cells were transiently transfected with either pTracer, T (Lanes 3 and 7); pTracer-mICAD-Ldm, I (Lanes 4 and 8) or pTracer-RCmICAD-Ldm, R (Lanes 5 and 9). A mock transfection (no DNA), N (Lanes 6 and 10) was included as control. Transfected cells were then treated with 50 µM of $H_2O_2$ for 8 hours. Genomic DNA extracted was digested with either *Msc* I (Lanes 3 – 6) or *Bgl* II (Lanes 7 – 10). The 2.2 kb band represents the intact MLL bcr whereas smaller fragments of sizes ranging from 250 bps to 1 kb represent the cleaved MLL bcr. As positive control for IPCR, *Msc* I-digested DNA from SUNE1 cells treated with 50 µM of $H_2O_2$ (from previous experiment) was used to ensure that the IPCR condition worked. For negative control of IPCR, no DNA was added for the amplification.

## 3.4 Discussion

Under normal circumstances, CAD remains complexed with ICAD (Liu *et al.*, 1997; Enari *et al.*, 1998). This ensures that CAD will only become activated when ICAD is cleaved by caspases. Caspases are the apoptotic proteases that only become activated when cells receive apoptotic signals (Cryns and Yuan, 1998). Studies showed that ICAD mutated at the two putative caspsase-3 recognition sites, at amino acid positions 117 and 224 was found to be resistant to cleavage by caspase-3 and thus continue to inhibit CAD's activity regardless of the presence or absence of apoptotic stimuli (Sakahira *et al.*, 1998).

The ICAD double mutant (ICAD-Ldm) overexpressed in this study, was thought to bind to CAD and inhibit its DNase activity. Therefore, there should be a decrease in the level of cleavage within the MLL bcr. From our result, it showed that regardless of the overexpression of ICAD-Ldm or other plasmids as control and whether in the presence or absence of 50 μM $H_2O_2$, cleavage within the MLL bcr was detected. This tally with the observation by McIlroy *et al.* (1999) who showed that ICAD-Ldm remained inactive upon apoptotic induction with UV radiation, etoposide, or γ radiation. The number of Annexin V-positive cells was also found to be increased. This indicated that more cells became apoptotic (McIlroy *et al.*, 1999) even though ICAD-Ldm was overexpressed. In addition, cells that carry ICAD mutant showed identical apoptotic appearance to that of the parental cells (Sakahira *et al.*, 1998). One possible reason is that the overexpressed ICAD-Ldm might not be able to inhibit endogenous CAD which was activated during oxidative stress-induced apoptosis. It could be possible that exogenously expressed ICAD-L mutant was not able to form a complex with endogenous CAD. Studies done by Lechardeur *et al.* (2004) showed that majority of the endogenous CAD complexed with endogenous ICAD while exogenous ICAD-

Ldm was essential for the folding of exogenously expressed CAD (Lechardeur *et al.*, 2004). This may explain our result why expression of ICAD mutant did not show significant reduction in chromosomal breaks within the MLL bcr.

Another possibility is that, there might be other nucleases, other than CAD, that could cleave the DNA upon $H_2O_2$ treatment. Previous study showed that, mICAD-Ldm in Jurkat and TF-1 cells, designated as JLdm and TLdm respectively, did not reduce susceptibility of these cells to apoptotic stimuli. Appearance of these apoptotic transformants was identical to that of the parental cells after 24 hours of treatment with etoposide (McIlroy *et al.*, 1999). This suggests that besides CAD, there might be other nucleases that play a role in DNA fragmentation. Samejima *et al.* (2009) showed that, in DT40 chicken cells with CAD knocked-out, $CAD^{-/-}$, HMW DNA cleavage and early stage apoptotic chromatin condensation were still observed. (Samejima *et al.*, 2009). The involvement of nucleases other than CAD is further supported by Li *et al.* (2001). They found that in fibroblast cells from embryonic mice lacking of CAD/ICAD complex, Endonuclease G (Endo G) was activated upon apoptotic induction and resulted in nucleosomal DNA fragmentation (Li *et al.*, 2001).

Analysis of result was also complicated by the fuzzy bands observed, especially after the transiently transfected SUNE1 cells were treated with $H_2O_2$ as shown in Figure 3.4(B). This could be due to the $H_2O_2$ which has been shown to be able to cause DNA double-stranded breaks in mammalian cells (Birnboim, 1986; Cantoni *et al.*, 1994; Wu *et al.*, 2004). These breaks could be detected in our system and thus added to the background cleavage, complicating the analysis.

## 3.5 Conclusion

As a conclusion, overexpression of ICAD mutant, ICAD-Ldm did not inhibit cleavage of the MLL bcr, indicating that ICAD-Ldm may not form complex with endogenous CAD. In addition, other nuclease may also be involved in MLL bcr cleavage. Overexpression of an unknown gene and the transfection process itself may also introduce stress to the cells.

# CHAPTER FOUR

# INDIRECT INHIBITION OF CAD BY CASPASE INHIBITOR

## 4.1 Introduction

Caspases (cysteinyl aspartate-specific proteinases) was discovered from nematode *Caenorhabditis elegans*. It has been found that, among the genes, the ced-3 gene is essential for all the 131 programmed cell death that occur during the hermaphrodite development (Yuan *et al.*, 1993). This gene encodes a homologue of the independently identified human interleukin-1β converting enzymes (ICE) (Thornberry *et al.*, 1992). In human, the caspase gene (Alnemri *et al.*, 1996) family consists of 14 members, of which 12 of them have been identified (Alnemri *et al.*, 1996; Salvesen and Dixit, 1997; Van de *et al.*, 1997). Caspases can be classified according to their function, namely initiator and executor. The initiator caspases (caspase -1, -2, -4, -5, -8, -9, -10, -11 and -12) possess long prodomains. Among the initiator caspases, caspase -1, -5 and -11 fall into the subclass that control both apoptosis and certain inflammatory responses. The downstream caspases are the executor caspases (caspase -3, -6 and -7) which contain short prodomain (Thornberry *et al.*, 1997). These proteases can also be subdivided according to their substrate specificities which has been defined using a positional scanning combinatorial substrate library (Thornberry *et al.*, 1997; Rano *et al.*, 1997). A distinct feature of caspase family is that, they work specifically and cleave the substrate after an Aspartate, Asp residue (Thornberry *et al.*, 1997). Upon apoptotic stimuli induction, caspase-3 receives the signal and cleaves ICAD at 2 putative recognition sites, hence, releases the activated CAD (Wyllie *et al.*, 1980; Talanian *et al.*, 1997; Thornberry *et al.*, 1997). Studies done by Betti *et al.* (2003) showed that, in the presence of broad spectrum irreversible caspase inhibitor (inhibitor for caspases -3, -6, -7, -8 and -10), both the breaks in the MLL bcr

in leukaemic cells and the expression of MLL fusion products were suppressed and not detected (Betti *et al.*, 2003). Hars and co-workers (2006) also showed that caspase inhibitor increased cell survival (Hars *et al.*, 2006). In addition, variety of cells treated with caspase inhibitor was found to be resistant to various apoptotic inducers (Carmody and Cotter, 2000). It seems that caspase inhibitor can, to a certain extent, prevent chromosomal breaks and enhance cell survival.

It was hypothesised that CAD might be involved in cleavage of the MLL bcr during stress-induced apoptosis in nasopharyngeal carcinoma (NPC) cells. In this experiment, the caspase inhibitor was used. It is a potent, cell-permeable, and irreversible inhibitor of caspase-3 as well as caspase-6, caspase-7, caspase-8, and caspase-10. The molecule can be represented as Z-Asp($OCH_3$)-Glu($OCH_3$)-Val-Asp($OCH_3$)-FMK. Theoretically, it works specifically and binds to the active site of caspases, forming an irreversible linkage. It was thought that when cells were pre-treated with caspase inhibitor before undergoing oxidative stress-induced apoptosis, the activation of caspase-3 should be blocked. The subsequent cleavage of ICAD by the caspase-3 and releasing of CAD should not occur. Therefore, cleavage within the MLL bcr should be reduced.

## 4.2 Materials and Methods

### 4.2.1 Pre-treatment with Caspase Inhibitor and Oxidative Stress-induced Apoptosis in NPC Cells

SUNE1 cells were grown to 70% confluency in a T75 flask. The cells were then trypsinised by adding 2.0 ml of TrypLE Express (Invitrogen). The detached cells were suspended with

13.5 ml of complete culture medium. From a total of 15 ml, 0.2 ml of the cell suspension was seeded into each of the 13 T25 flasks (Nalgene). For positive control, another T25 flask was seeded with 1 ml of cell suspension to allow the cells to be overgrown. Upon reaching confluency of about 70%, cells in 6 of the 13 T25 flasks were treated with 50 µM of caspase inhibitor (Calbiochem) for 2 hours. Simultaneously, another 6 flasks of cells were treated with 2 µl of dimethyl sulfoxide (DMSO), instead of caspase inhibitor. The purpose of using DMSO was as control because it was used as the solvent for caspase inhibitor. Another flask of cells at confluency of 70% was used as negative control where cells were grown at optimal density. Subsequently, both set of cells were treated with 0, 1, 10, 50, 100 and 500 µM of $H_2O_2$ for 8 hours. Cells were collected and genomic DNA was extracted by using Blood and Cell Culture DNA Mini Kit (Qiagen) as described in section 2.2.5.1. Cleavage within the MLL bcr was detected by performing IPCR as described under section 2.2.5.

### 4.2.2 Inverse Polymerase Chain Reaction (IPCR)

In order to detect cleavage within the MLL bcr, IPCR was carried out as described in section 2.2.5.

## 4.3 Result

In the third approach of studying the role of CAD, SUNE1 cells were pre-treated with caspase inhibitor prior to treatment with $H_2O_2$ at varying concentrations. There were 2 sets of cells. One of them was pre-treated with caspase inhibitor for 2 hours while the other set was treated with DMSO as solvent control. Subsequently, both sets were treated with varying concentrations of $H_2O_2$ simultaneously. IPCR was carried out to detect breaks within the

MLL bcr. *Msc* I was used to linearise the circularised DNA for subsequent amplification. In the absence of caspase inhibition, it was expected to see an increased cleavage within the MLL bcr upon treatment with increasing concentrations of $H_2O_2$. In the presence of caspase inhibition, caspase-3 activation will be blocked. The subsequent cleavage of ICAD will not happen and CAD remains inactive. Thus, there should be less cleavage of the MLL bcr.

From the IPCR result, as shown in Figure 4.1(A) (Lanes 3 – 10) and 4.1(B) (Lanes 1 – 6), all of the samples exhibited the 2.2 kb band, representing the intact MLL bcr. Bands of sizes smaller than 2.2 kb, representing the cleaved MLL bcr were also detected in all of the samples. Referring to Figure 4.1(A) and 4.1(B), regardless of whether in the absence [Figure 4.1(A), Lanes 5 – 10] or in the presence [Figure 4.1(B), Lanes 1 – 6] of caspase inhibitor, both the intact and cleaved MLL bcr were detected upon $H_2O_2$ treatment. There was no significant difference between cells pre-treated or without pre-treatment of caspase inhibitor. The result shows that the use of caspase inhibitor did not prevent DNA cleavage within the MLL bcr.

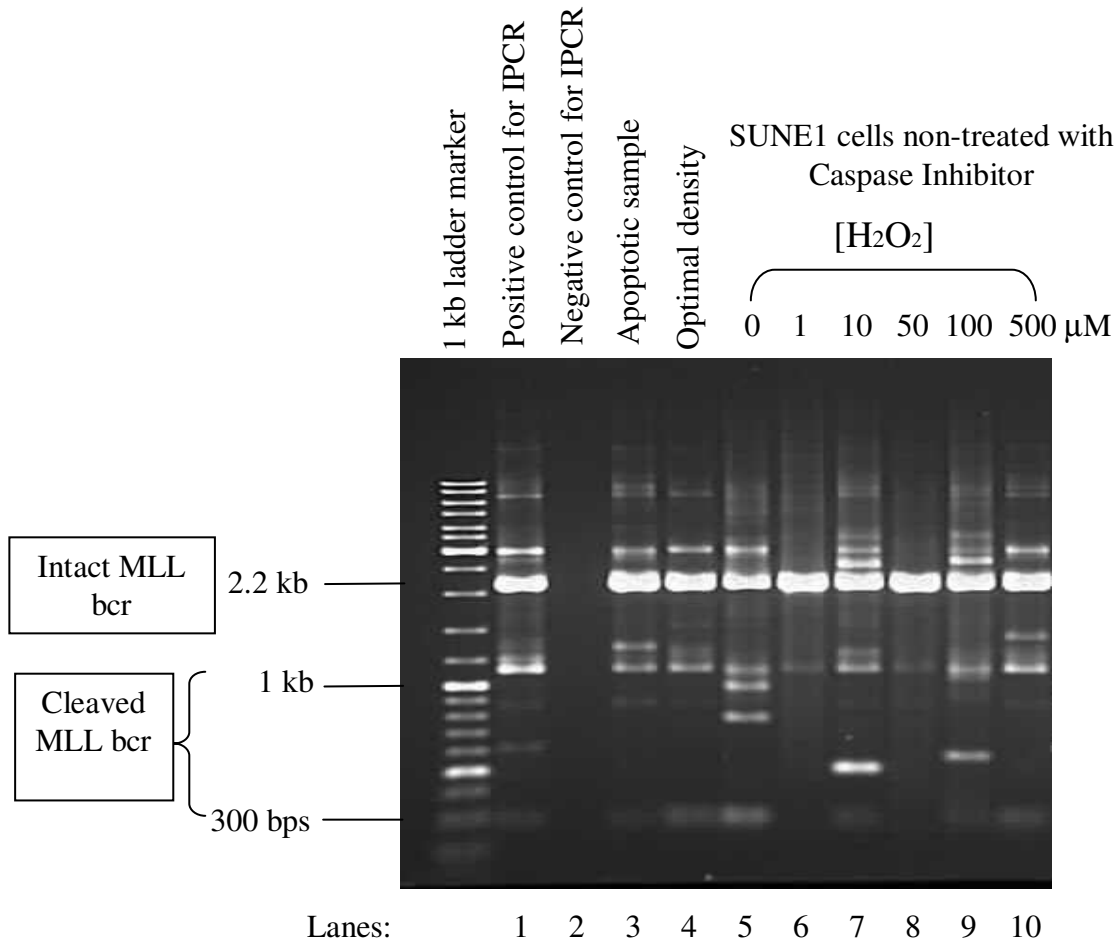


**Figure 4.1(A): Nested IPCR of SUNE1 cells treated with varying concentrations of $H_2O_2$ in the absence of caspase inhibitor.** SUNE1 cells were either grown to the optimal density (70% confluency) (Lane 4) or were overgrown (> 100% confluency) to induce apoptosis (Lane 3). The cells were subsequently treated with 0 µM (Lane 5), 1 µM (Lane 6), 10 µM (Lane 7), 50 µM (Lane 8), 100 µM (Lane 9) or 500 µM (Lane 10) of $H_2O_2$ for 8 hours. Genomic DNA was extracted, modified and digested with *Msc* I. IPCR was performed to detect chromosome break within the MLL bcr. As positive control for IPCR, *Msc* I-digested DNA from SUNE1 cells treated with 50 µM of $H_2O_2$ (from previous experiment) was used to ensure that the IPCR condition worked. For negative control of IPCR, no DNA was added for the amplification. The 2.2 kb band represents the intact MLL bcr whereas smaller fragments of sizes ranging from 250 bps to 1 kb represent the cleaved MLL bcr.

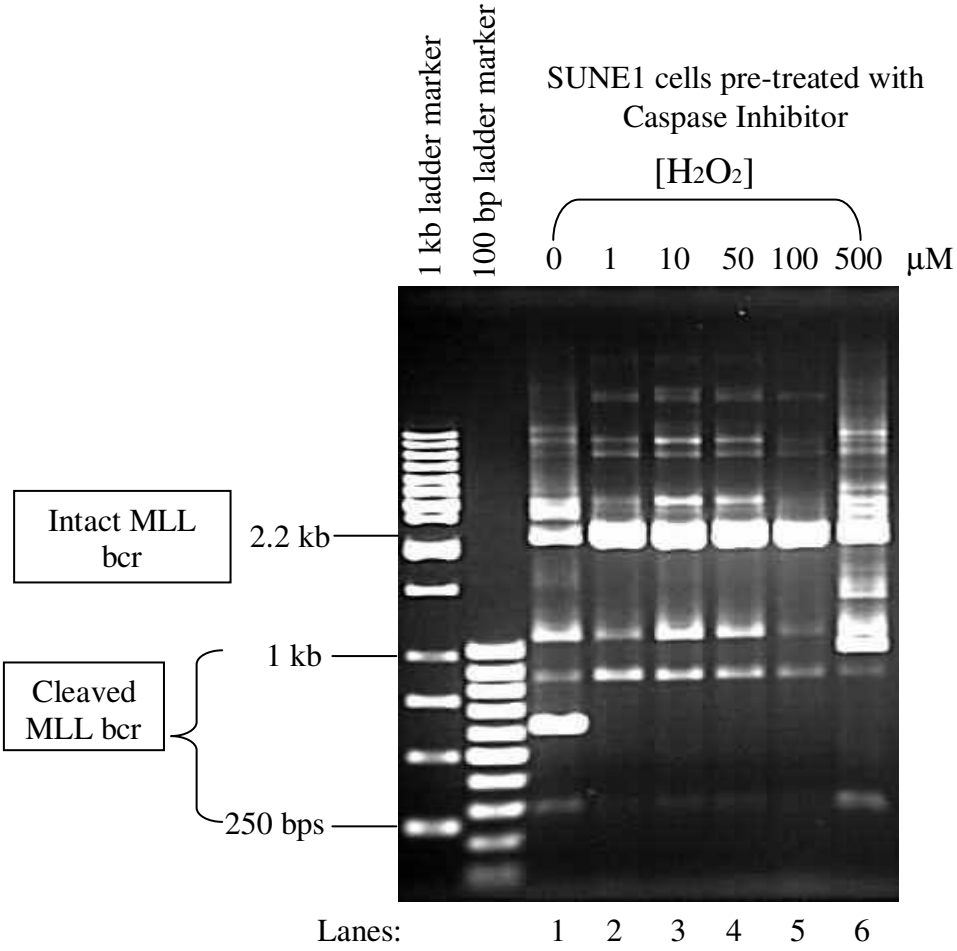


**Figure 4.1(B): Nested IPCR of SUNE1 cells treated with varying concentrations of $H_2O_2$ in the presence of caspase inhibitor.** SUNE1 cells were pre-treated with 50 µM of caspase inhibitor for 2 hour. The cells were subsequently treated with 0 µM (Lane 1), 1 µM (Lane 2), 10 µM (Lane 3), 50 µM (Lane 4), 100 µM (Lane 5) or 500 µM (Lane 6) of $H_2O_2$ for 8 hours. Genomic DNA was extracted, modified and digested with *Msc* I. IPCR was performed to detect chromosome breaks within the MLL bcr. The 2.2 kb band represents intact MLL bcr whereas smaller fragments of sizes ranging from 250 bps to 1 kb represent the cleaved MLL bcr.

## 4.4 Discussion

Caspases play a central role in the apoptotic signaling cascades. Executioner caspases may have their distinct roles in specific pathways. CAD's activity is normally inhibited by ICAD where ICAD binds to CAD, forming a complex (Enari *et al.*, 1998). Only upon ICAD's cleavage by caspase-3, CAD is activated. Caspase inhibitor works to inhibit caspases in the caspase cascade. When caspase-3 is inhibited, ICAD could not be cleaved and hence exists as complex with CAD (Nagata, 2000). Therefore, CAD remains inactive and unable to exert its DNase activity.

It was expected that, upon oxidative stress induction, SUNE1 cells pre-treated with caspase inhibitor should show none or less cleavage within the MLL bcr as compared to cells which were non-treated with caspase inhibitor. This is because, the activation of most of the endogenous CAD should be inhibited by caspase inhibitor. Our result showed that, regardless of with or without caspase inhibition, cleavage within the MLL bcr was detected with no significant difference between both sets of cells. This may suggest that the caspase inhibition did not cancel out the apoptotic effect of $H_2O_2$.

In combination of our result and results from the previous studies, it is suggestive that, when cells underwent oxidative stress, they experienced certain level of assault and were subsequently eliminated. Cell death through caspase-dependent pathway was well studied (Enari *et al.*, 1998; Sakahira *et al.*, 1998). However, it has also been shown that cells undergo apoptosis through caspase-independent pathways (McCarthy *et al.*, 1997; Donovan and Cotter, 2004; Saelens *et al.*, 2004). Caspase-independent pathway has been implicated in Reactive Oxygen Species (ROS)-induced apoptosis. Our result tallied with this observation,

such that the MLL bcr cleavage was detected regardless of the absence or presence of caspase inhibitor. *In vitro* studies done by Carmody and Cotter (2000) showed that ROS was able to induce apoptosis in retinal cells. The apoptotic effect of ROS was eliminated by antioxidants. Cells became apoptotic as confirmed by features such as phosphatidylserine (PS) exposure, DNA nicking and cell shrinkage. However, caspase inhibitor did not affect either the features or the kinetics of apoptosis. Thus their result suggested cell death in a caspase-independent pathway under oxidative stress (Carmody and Cotter, 2000). Several studies have also shown that beside caspases, other proteases, like lysosomal cathepsin proteases and the calcium-dependent cysteine protease calpain that act upstream and downstream of mitochondrial events are also activated during various death stimuli (Choi *et al.*, 2001; Mathiasen and Jaattela, 2002). Moreover, study done by Sanvicens *et al.* (2004) also suggested that both calpains and caspases play a role in apoptosis triggered by sodium nitroprusside (SNP)-induced ROS production. It was shown that caspase inhibitor did not inhibit oxidative stress-induced apoptosis in 661W photoreceptor cells efficiently. On the other hand, CR6, a nitric oxide scavenger could prevent activation of the calpain-mediated apoptotic pathway in 661W photoreceptor cells (Sanvicens *et al.*, 2004).

Our result of MLL bcr cleavage in the presence of caspase inhibitor also suggested another possibility, that is, there could be other nucleases that are carrying out the similar function as CAD. This is supported by the presence of oligonucleosomal DNA fragmentation in nuclei extracted from CAD knockout, $CAD^{-/-}$ cells (Samejima *et al.*, 2001). One of these apoptotic nucleases besides CAD is the Endonuclease G, Endo G (Li *et al.*, 2001). Endo G is one of the nucleases found in mitochondria. This nuclease was suggested to be involved in DNA replication (Cote and Ruiz-Carrillo, 1993). It has also been found that Endo G was released

from mitochondria together with cytochrome C. When incubated with purified nuclei, it caused DNA degradation (van Loo *et al.*, 2001). At high concentration, Endo G possesses the nonspecific nuclease ability (Ohsato *et al.*, 2002) and causes breaks in all nucleic acids species, including double-stranded DNA, single-stranded DNA, single-stranded RNA, and RNA/DNA duplexes (Gerschenson *et al.*, 1995; Widlak *et al.*, 2001). However, at low concentration, Endo G cleaves DNA at more defined sites (Ohsato *et al.*, 2002). Besides Endo G, Apoptotic-inducing Factor (AIF) also plays a role in high molecular weight (HMW) DNA fragmentation (Susin *et al.*, 1999). Upon pro-apoptotic stimuli, AIF is released from mitochondria and caused type I nuclear condensation in a caspase-independent manner (Susin *et al.*, 2000). Susin *et al.* (1999) also suggested that AIF, which lacks the intrinsic nuclease activity, is able to activate an unknown nuclease which is responsible for DNA fragmentation (Susin *et al.*, 1999). These results tally with our observation that caspase inhibitor did not inhibit cleavage within the MLL bcr. The reason could be both CAD and other nucleases are responsible for the cleavage during oxidative stress-induced apoptosis. In addition, even though the caspase inhibitor used in this experiment was cell permeable, uptake of caspase inhibitor into the cells might be inefficient, hence lead to insufficient inhibition of caspase-3. It is suggestive that uptake of caspase inhibitor could be cell type-dependent. From our previous laboratory result, leukaemic cell lines treated with caspase inhibitor under similar condition showed efficient inhibition of cleavage within the MLL bcr. However, when human blood cells were treated with caspase inhibitor prior to apoptotic stimuli, under the similar condition, the caspase inhibition was not as efficient (personal communication).

## 4.3 Conclusion

From the result, it can be concluded that, upon oxidative stress, cells may become apoptotic through caspase-independent pathway. Other than CAD, there might be other nucleases in combination with CAD in causing cleavage within the MLL bcr.

# CHAPTER FIVE

# CO-TRANSFECTION OF CAD AND ICAD-L

## 5.1 Introduction

When cells experience assaults, like stressed, irradiated and so on, these cells will undergo apoptosis. At the molecular level, apoptosis involves a cascade of proteolytic events mediated by caspases, a family of cysteine-aspartate proteases (Nicholson, 1999). The activated caspases possess the abilities to cleave multiple cytoplasmic and nuclear substrates. This process plays a pivotal role in the execution phase of apoptosis (Cohen, 1997). This involves the internucleosomal DNA cleavage, which is the final step of apoptosis since the undigested DNA is able to activate innate immune responses (Mukae *et al.*, 2002). Even though there are several nucleases which have been proposed to be involved in the degradation of genomic DNA during apoptosis, CAD is considered to be the major nuclease in causing chromosomal DNA fragmentation (Scovassi and Torriglia, 2003).

In normal proliferating cells, CAD forms a heterodimer with its inhibitor, ICAD (Liu *et al.*, 1998; Sakahira *et al.*, 1998; Liu *et al.*, 1999). In the presence of ICAD, CAD binds to DNA to form a stable DNA complex (Korn *et al.*, 2005). This complex not only comes in direct contact with the DNA transiently, but also forms indirect contact to its substrate mediated by chromatin-associated proteins such as histone H1 as well as HMGB1 and 2. These proteins have been shown to interact with CAD and stimulate its activity (Toh *et al.*, 1998; Liu *et al.*, 1999; Widlak *et al.*, 2000; Widlak *et al.*, 2005). Studies showed that interrelation of CAD with these proteins may serve an important role for the nuclease to gain access to the linker DNA between nucleosomes and thus might enhance DNA fragmentation in apoptotic cells. In apoptotic cells, CAD cleaves naked DNA as a nonspecific nuclease efficiently. In contrast

to other nonspecific nucleases, both free CAD and the inhibited nucleases are proficient in forming stable DNA complexes ( Widlak, 2000; Korn *et al.*, 2005).

In normal growing cells which do not undergo apoptosis, the activation of CAD is strictly controlled. Stoichiometrically, one molecule of ICAD-L is bound tightly to one molecule of CAD during its synthesis, preventing CAD to degrade DNA (Woo *et al.*, 2004). According to several *in vitro* and *in vivo* studies performed previously, it has been shown that active CAD is produced by synthesising CAD in the presence of ICAD. When synthesised in the absence of ICAD, the CAD protein did not exhibit its DNase ability at all. (Enari *et al.*, 1998; Zhang *et al.*, 1998; Sakahira *et al.*, 1999). The C-terminal half of the CAD protein is responsible for its nuclease activity. However, the N-terminal domain of CAD was found to regulate the optimal nuclease activity of the catalytic C-terminal domain (Inohara *et al.*, 1998). Upon apoptotic induction, ICAD is cleaved by caspase-3 at its two putative cleavage sites, Asp-117 and Asp-224. Cleavage of ICAD at Asp-117, which is adjacent to its N-terminal domain, results in the release of ICAD fragments from CAD. This event leads to the release of N-terminal region of CAD. This in turn, enables the N-terminal of CAD to then activate the C-terminal nuclease domain (Liu *et al.*, 1997; Sakahira *et al.*, 1998).

By referring to the DNA binding properties of CAD and its molecular structure, Reh and colleagues (2005) found that substitution of residues at the active site of the CAD does not affect its ability in forming DNA stable complex. However, substitution of the residues close to or directly from helix-4 of CAD protein has a direct or indirect effect on the formation of stable DNA complex. Alteration of amino acid residues reflect distinct functional regions of a bipartite DNA binding surface which is important for stable DNA complex formation and

DNA cleavage by CAD. This shows that, region close to or at the α-helix 4 is a structurally important region that indirectly contributes to stable DNA complex formation and DNA cleavage by the nuclease (Reh *et al.*, 2005). Lys157 in human (Lys155 in murine), is buried in the protein and is located at the N-terminal end of helix-4 of CAD. These residues are most likely indirectly involved in DNA binding and seem to play an important structural role in stabilising helix-4 (Lys155 and Arg212) (Woo *et al.*, 2004).

In the first approach, as described in Chapter Two, CAD alone was overexpressed. In the second approach, ICAD mutant was overexpressed to inhibit CAD directly. In the third approach, ICAD was inhibited indirectly using caspase inhibitor. The results were inconclusive. In this chapter, the fourth and last approach was carried out to further study the involvement of CAD in the MLL bcr cleavage. In this approach, CAD was co-expressed with its chaperone, ICAD, since the presence of ICAD was shown to be crucial for CAD's nuclease activity. With induction of oxidative stress by $H_2O_2$, an elevation in cleavage within the MLL bcr was expected when CAD and ICAD is co-expressed. When mutant CAD, hCAD(K157Q) was co-expressed with ICAD, there should be less of the MLL bcr cleavage. It has been shown that amino acid at position Lysine 157 in human is involved in maintaining the protein structure and/or DNA binding (Meiss *et al.*, 2001; Widlak *et al.*, 2003; Woo *et al.*, 2004). CAD mutant, CAD(K157Q) was thought to lost its ability to form stable DNA complex and hence unable to execute its DNase activity. Theoretically, when CAD is overexpressed in the presence of ICAD, there should be sufficient ICAD present for CAD, during its polypeptide synthesis. In this way, CAD protein synthesised will be folded in the correct conformation and thus functional. In this experiment, plasmid pTracer-hCAD and pcDNA-mICAD-L were transfected into NPC (SUNE1) cells. As controls, cells were

transfected with vector pTracer and pcDNA. Mock transfection was also included where cells were subjected to the process of transfection in the absence of DNA. Cells were then either treated or not-treated with 50 μM of $H_2O_2$. Expression of the transfected genes were determined by Western blotting. Protein specific antibodies, anti-CAD, anti-ICAD and anti-GAPDH were used to detect CAD, ICAD and GAPDH protein respectively. Nested IPCR was carried out to detect cleavage within the MLL bcr.

## 5.2 Materials and Methods

### 5.2.1 Subcloning of pcDNA-mICAD-L with Stop Codon and Omission of V5 Epitope

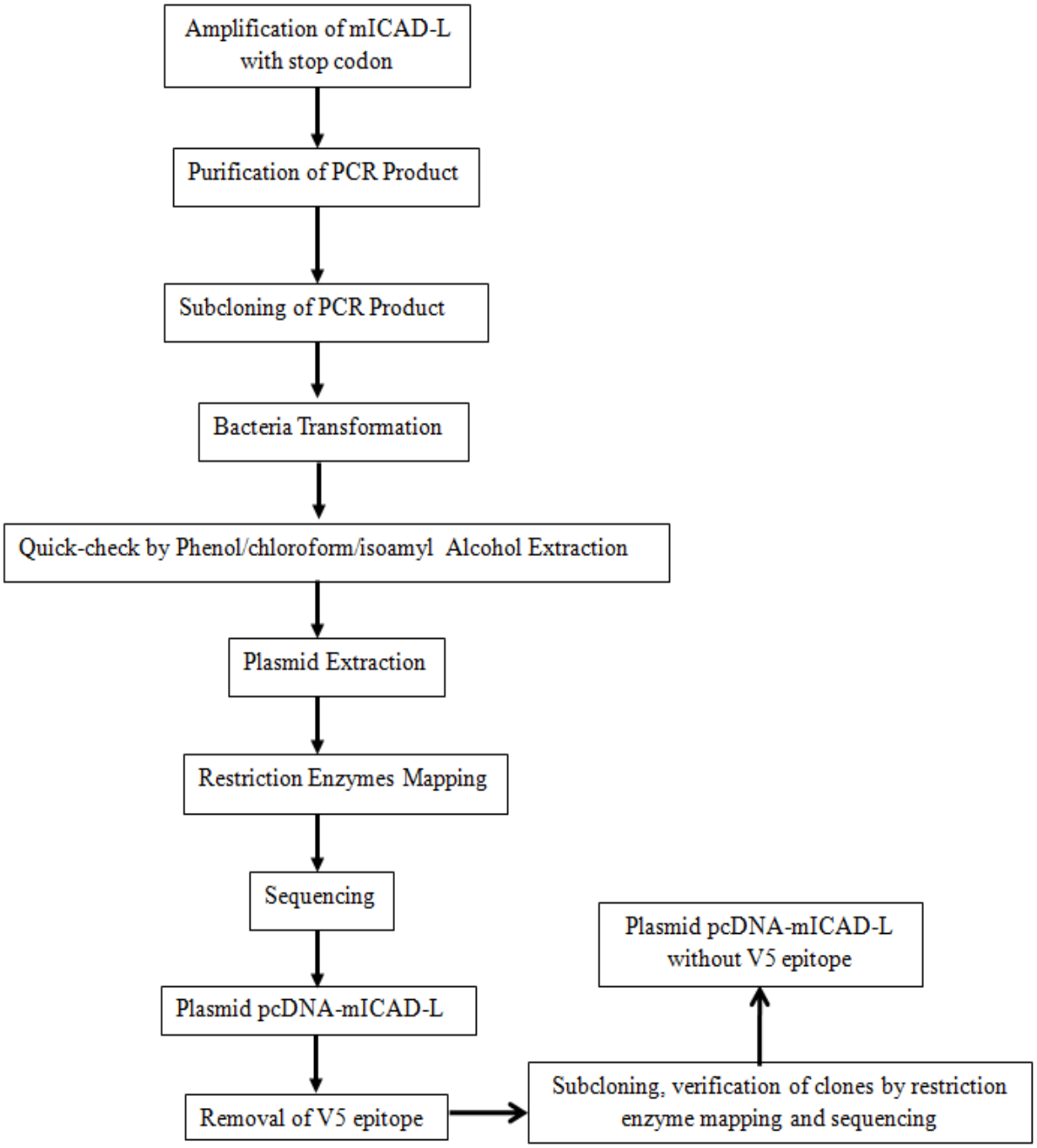


**Figure 5.1:** General flow of subcloning of pcDNA-mICAD-L with stop codon and without the V5 epitope. For transfection purpose, plasmid pcDNA3.1/V5-His-TOPO, as shown in Appendix A, was used as plasmid vector. The mICAD-L gene was amplified via conventional PCR method as described in Section 5.2.1.1. Subsequently, this gene was subcloned into plasmid vector pcDNA3.1/V5-His-TOPO. The stop codon at the 3' end was included, as described in 5.2.1.1. The V5 epitope on the vector was then removed via restriction enzyme digest and religation.

#### 5.2.1.1 Amplification of The mICAD-L Gene with *Kpn* I and *Xba* I Restriction Sites and Stop Codon

The mICAD-L gene with stop codon was amplified by using PCR. Plamid pEF-FL-mICAD-L was used as DNA template. A pair of primers were designed according to mICAD-L sequence reported (GenBank accession number AB009375). The forward mICAD primer, mICAD-K/X(F) (5' – GA**GGTACC**ATGGAGCTGTC – 3') contains a *Kpn* I restriction site as indicated in bold, while the reverse mICAD primer, mICAD-K/X(R) (5' – CG**TCTAGA**CTACGAGGAGTCTC – 3') carries an *Xba* I restriction site as indicated in bold. The expected size of the amplified product was 1 kb. This fragment carries a *Kpn* I restriction site at its 5' end and an *Xba* I restriction site at its 3' end with a stop codon as shown in Figure 5.2.

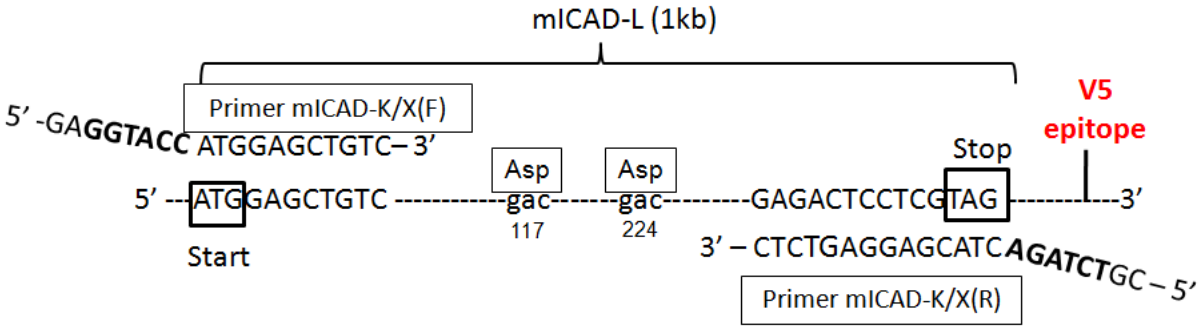


Figure 5.2: Schematic diagram showing primer binding sites in mICAD-L with stop codon. Forward primer, mICAD-K/X(F) contains a *Kpn* I restriction site (GGTACC) as indicated in bold. Reverse primer, mICAD-K/X(R) contains an *Xba* I restriction site (TCTAGA) as indicated in bold. Amplification by using these primers produces a 1 kb fragment of the mICAD gene which includes the start codon (ATG) and the stop codon (TAG). This fragment carries a *Kpn* I restriction site at its 5' end and an *Xba* I restriction site at its 3' end.

#### 5.2.1.2 Purification of PCR Product

PCR product was analysed on 1% agarose gel and product of size 1 kb was excised with clean and sharp scalpel. DNA was purified by using QIAquick Gel Extraction Kit (Qiagen) as described in Section 2.2.1.3.

#### 5.2.1.3 Subcloning of PCR Product

The purified PCR product (mICAD-L with stop codon) was digested with restriction enzymes *Kpn* I and *Xba* I. Ligation was performed as described in Section 3.2.1.4.

#### 5.2.1.4 Bacteria Transformation

The recombinant plasmid was transformed into electrocompetent *E. coli* HB101 cells by electroporation as described in Section 2.2.1.5.

#### 5.2.1.5 Quick-check by Phenol/chloroform/isoamyl Alcohol Extraction

Randomly picked colonies were checked by extraction with phenol/chloroform/isoamyl alcohol (Ratio 25:24:1) as described in Section 2.2.1.6. Suspected clones, which might carry the plasmid of interest, were grown and plasmids were extracted (Section 5.2.1.6) for further confirmation by restriction enzymes mapping as elaborated in Section 5.2.1.7.

#### 5.2.1.6 Plasmid Extraction

The plasmid was isolated from the suspected clones by using S.N.A.P Miniprep Kit as described in Section 2.2.1.7.

#### 5.2.1.7 Restriction Enzymes Mapping

To ensure that the plasmid that was extracted contained the mICAD-L gene, the DNA was digested by restriction enzymes *Kpn* I and *Xba* I, *Bgl* II, *Bam*H I and *Bst*X I as described in Section 3.2.1.8.

#### 5.2.1.8 Sequencing

In order to ensure that there was no alteration in the mICAD-Ldm sequence, the plasmid was sequenced as described in Section 2.2.1.9. However, primers used for sequencing of these plasmids were different. Forward primer, pcDNA-H(F) (5' – AGAACCCACTGCTTACTGGC – 3') was used to sequence the sense strand whereas reverse primer, pcDNA-H (R) (5' – AGGGATAGGCTTACCTTCGA – 3') was used to sequence the anti-sense strand of plasmid pcDNA-mICAD-L. The sequences were analysed with DNASTAR software. The 1 kb sequence is shown in Appendix I.

#### 5.2.1.9 Removal of V5 Epitope

After obtaining plasmid pcDNA-mICAD-L with stop codon, V5 epitope was removed to ensure the mICAD-L expressed does not contain V5 epitope at the C-terminal. Briefly, 10 µg of plasmid pcDNA-mICAD-L was digested with *Sac* II and *Age* I restriction enzymes. Due to the incompatibility of the buffers, sequential restriction digest was performed. Initially, plasmid pcDNA-mICAD-L (10 µg) was digested with 40 units of *Sac* II together with 1X NE Buffer 4 and sUPW in a final volume of 20 µl at 37$^{o}$C for 2 hours. The digested DNA was purified by using QIAquick Nucleotide Removal Kit (Qiagen) as described in Section 2.2.5.3. The procedure is shown in Appendix L. The purified DNA was then digested with 10 units of *Age* I together with 1X NE Buffer 1 and sUPW in a final volume of 30 µl at 37$^{o}$C for 2 hours.

The DNA was subsequently subjected to electrophoresis on 1% agarose gel. The 6.5 kb DNA (pcDNA-mICAD-L without V5 epitope) fragment was excised and purified by using QIAquick Gel Extraction Kit (Qiagen) as described in Section 2.2.1.3. The DNA was filled-in using DNA polymerase I (Large) Klenow Fragment (NEB) to create ligatable blunt ends. Two µg of DNA was filled-in with 4 units of Klenow Fragment in 1X NE Buffer 2, supplemented with 66 µM of each dNTP (Finnzymes) at 25°C for 15 minutes in a total reaction of 50 µl. The reaction was terminated by adding EDTA to a final concentration of 10 mM and heating at 75°C for 20 minutes. The DNA was ligated to form circularised plasmid by using 120 units of T4 DNA ligase, 1X T4 DNA ligase buffer (NEB) and sUPW in a final volume of 60 µl at 16°C overnight. The ligated DNA was digested with 60 units of *Bst*B I in 1X NE Buffer 4 and sUPW in a final volume of 70 µl at 65°C for 2 hours. This is to linearise the plasmid which might still contain V5 epitope due to incomplete digestion, as shown in Figure 5.3. The digested DNA was then transformed into electrocompetent cells, *E. coli* HB101 as described in Section 2.2.1.5. Colonies were picked randomly and extracted with phenol/chloroform/isoamyl alcohol, as described in Section 2.2.1.6, to check the possible clones that might carry the plasmid. Plasmid was isolated from the selected clone(s) by using S.N.A.P Miniprep Kit (Section 2.2.1.7). For further confirmation, plasmid was sent for sequencing as elaborated in Section 2.2.1.9. This pcDNA-mICAD-L without V5 epitope was used in subsequent transfection experiment.

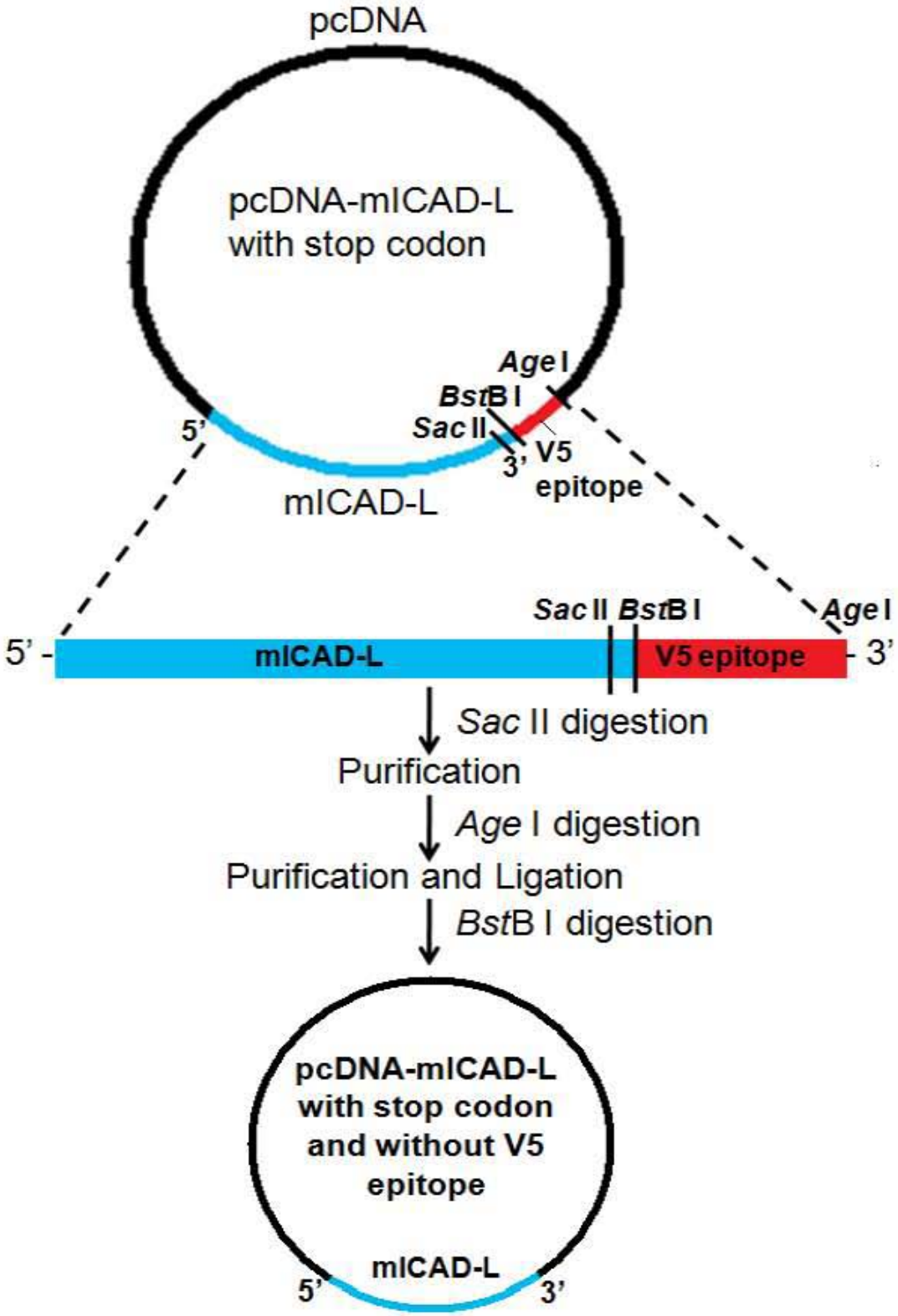


Figure 5.3: Schematic diagram showing removal of V5 epitope from plasmid pcDNA-mICAD-L. Plasmid pcDNA-mICAD-L was digested with *Sac* II. DNA was purified and further digested with *Age* I. DNA was then purified and ligated to form a circularised plasmid pcDNA-mICAD-L with stop codon and without V5 epitope.

### 5.2.2 Transient Transfection of CAD and ICAD-L

#### 5.2.2.1 Plasmid Extraction for Transfection

For the purpose of transfection, a high concentration of plasmid pTracer, pcDNA, pTracer-hCAD, pTracer-hCAD(K157Q) and pcDNA-mICAD-L were extracted using QIAfilter Plasmid Maxi Kits (Qiagen, UK) as described in Section 2.2.4.1.

#### 5.2.2.2 Transient Transfection

In order to study the role of CAD, SUNE1 cells were transfected with 2 μg each of the following: pTracer-hCAD, pcDNA-mICAD-L, pTracer and pcDNA vectors as controls. SUNE1 cells were also co-transfected with the following: pTracer-hCAD and pcDNA-mICAD-L; pTracer-hCAD(k157Q) and pcDNA-mICAD-L in a ratio of 2:1 (1.33 μg: 0.67 μg). Mock transfection was also carried out where cells underwent transfection process in the absence of DNA. As positive control, cells were overgrown to induce apoptosis. As negative control, cells were also grown to optimal density of about 70% confluency. Transient transfection procedure was carried out as elaborated in Section 2.2.4.2.

### 5.2.3 Oxidative Stress-induced Apoptosis in Transiently Transfected Mammalian Cells

Prior to this experiment, a time course optimisation was carried out to determine the optimal time point for treatment of these transfectants. Treatment of 6 hours was chosen. At 17 hours post transfection, the optimal time point when cells were expressing transfected gene, these cells were then either treated with 50 μM $H_2O_2$ or non-treated. This was done to compare the effect of $H_2O_2$ in inducing apoptosis in CAD and ICAD transient transfectants. In order to detect cleavage within the MLL bcr, nested IPCR was done as described in Section 2.2.5.

### 5.2.4 Western Blotting

CAD and ICAD expression were detected by using Western blotting. Crude protein was extracted from transfected cells and analysed on SDS-PAGE. Protein was then transferred onto PVDF membrane or blot. The blot was probed with primary antibodies, Rabbit Anti-CAD and Rabbit anti-ICAD polyclonal antibodies to detect CAD and ICAD protein respectively. Rabbit Anti-GAPDH antibody was also used as internal control to detect the GAPDH house-keeping gene. This is to ensure the amount of protein loaded was comparable. The secondary antibody used to bind with these antibodies was Goat Anti-rabbit IgG Horseradish Peroxidase (HRP). Rabbit Anti-CAD, Rabbit Anti-ICAD polyclonal antibodies, Rabbit Anti-GAPDH polyclonal antibodies and the secondary antibody, Goat Anti-rabbit IgG HRP were purchased from Santa Cruz, USA.

#### 5.2.4.1 Crude Protein Extraction

##### 5.2.4.1.1 Cell Lysis by Triple Detergent Mix

Before crude protein extraction from adherent cells in 60 mm dish (Nalgene, Denmark) (approximately 1.7 x $10^4$ cells), culture medium was removed by aspiration and cells were washed with cold 1X PBS. Cells were then lysed with 0.5 ml triple detergent mix which contained 50 mM Tris.Cl, pH 8, 150 mM sodium chloride, 0.02% sodium azide, 0.1% sodium dodecyl sulphate (SDS), 1% Nonidet P-40 (NP-40) and 0.5% sodium deoxycholate. Five µl of Protease Inhibitor Cocktail for use with mammalian cell and tissue extracts (Sigma, USA) and 5 µg of Phenylmethylsulfonyl fluoride (PMSF) were added fresh to the triple detergent mix prior to lysis. Cells in dishes were lysed on ice for 5 minutes. Subsequently, the lysate were collected in 1.5 ml microcentrifuge tubes (Axygen, USA) by scrapping with an inverted sterile 1 ml pipette tips.

#### 5.2.4.1.2 Cell Lysis by Freeze-thawing Method

The lysate (0.5 ml) was further lysed by freezing and thawing repeatedly. Lysate was frozen in liquid nitrogen (approximately 5 min), then thawed in 37°C waterbath (for approximately 5 min). The lysate was vortexed vigorously at 2,200 rpm for approximately 1 minute. The mixture was spun down briefly by using a benchtop centrifuge. This cycle was repeated for another 4 times to ensure proper lysis of nuclear membrane by the ice crystal.

The lysate was then centrifuged using a refrigerated centrifuge (Eppendorf 5417R) at 4°C, at 20,000x g for 10 minutes. The supernatant, which contained crude protein, was transferred to a sterile 1.5 ml microcentrifuge tubes. The crude protein was then subjected to protein quantification by Brandford Assay as described in Section 5.2.4.2. Samples were either kept in -20°C freezer for longer storage or ran on SDS-PAGE.

### 5.2.4.2 Protein Quantification By Bradford Assay

In order to quantify the concentration of crude protein extracted from each sample, Bradford Assay was performed. This method is used to quantify protein of amount ranging from 1 to 10 µg. The principle of this assay is based on the comparison between the binding of an unknown protein and a standard protein to Coomassie Brilliant Blue dye. A standard curve was constructed based on the known amounts of a standard protein (Bradford, 1976). The standard protein used was gamma (γ)-globulin as the dye binding capacity of this protein is closer to the mean of binding capacity of other proteins, like bovine serum albumin (BSA), ovalbumin, trypsin, myelin basic protein and so on that are being compared (Friedenauer and Berlet, 1989; Stoscheck, 1990). Coomassie Brilliant Blue solution was prepared by dissolving

10 mg of Coomassie Brilliant Blue G-250 (Sigma) in 5 ml of 95% ethanol. Subsequently, 10 ml of 85% phosphoric acid was added. Distilled water was added to a final volume of 100 ml. Prior to use, this dye solution was diluted 5-fold.

#### 5.2.4.2.1 Measuring Concentration of Standard Protein and Construction of Standard Curve

In order to prepare standard protein with a concentration of 2.5 µg, 5 µg, 7.5 µg and 10 µg; 5, 10, 15 and 20 µl of 0.5 mg/ml of γ-globulin was taken and diluted with 0.15 M of NaCl to a final volume of 100 µl. Duplicate of each standard protein samples was prepared. Hundred µl of 0.15 M NaCl was used as blank. Subsequently, 1 ml of Coomassie Brilliant Blue solution was added to each tube and vortexed. The mixture was allowed to stand at room temperature for 5 minutes and the absorbance was determined by using 1 cm-path-length microcuvette (Eppendorf, Germany). Absorbance at 595 nm ($A_{595}$) for each standard protein was taken and recorded. The absorbance value was taken in duplicate and the standard curve was generated by plotting a graph of $A_{595}$ against protein concentration (µg) of the standard protein.

#### 5.2.4.2.2 Measuring Concentration of Sample Protein

To measure the concentration for each sample, 3 µl of crude lysate was taken and added with 97 µl of 0.15 M NaCl as diluent. Subsequently, 1 ml of Coomassie Brilliant Blue was added to each diluted lysate and incubated for 5 minutes at room temperature. Absorbance $A_{595}$ was measured and recorded. Concentration of each sample was calculated from the standard curve plotted as described in Section 5.2.4.2.1.

#### 5.2.4.3 Separation of Crude Protein on Sodium Dodecyl Sulphate-Polyacrylamide Gel Electrophoresis (SDS-PAGE)

##### 5.2.4.3.1 Preparation of SDS-PAGE

In order to prepare sodium dodecyl sulphate-polyacrylamide gel (SDS-PAGE), a denaturing discontinuous gel by Laemmli Gel method, spacer glass plates with 1.5 mm integrated spacer and short plates were assembled using a casting frame. The glass plates were placed on spring-loaded lever in the casting stand to create a tight seal against the rubber gasket. The resolving gel prepared consists of 10% of acrylamide-bis-acrylamide (Sigma), 0.38 M of Tris (pH8.8), 0.1% SDS and 1 mM EDTA in a final volume of 10 ml. Seven µl of TEMED (Amresco, USA) and ammonium persulfate (APS) of a final concentration of 0.1% were added last. Once these 2 components were added, gel mixture was poured immediately into the gap between the 2 glass plates. The resolving gel was poured to the level marked as 1 cm from the edge of the 10-well comb. The gel layer was overlaid with isopropanol to avoid oxidation which may inhibit polymerisation and also to allow the formation of a flat interface. The resolving gel was allowed to solidify for 20 minutes. The stacking gel, which consists of 4% acrylamide/bis-acrylamide (Sigma), 0.38 M of Tris (pH 6.8), 0.1% SDS (Amresco, USA) and 1 mM EDTA (Invitrogen, USA) in a final volume of 5 ml was prepared. To solidify the stacking gel, 3.5 µl of TEMED and APS of a final concentration of 0.1% were added last. The stacking gel mixture was then immediately poured onto the solidified resolving gel between the glass plates. The comb was inserted with care to avoid bubble formation. Preparation for 1 SDS-PAGE mixture is as shown in Table 5.1.

Table 5.1: Preparation of 10% SDS-PAGE mixture.

| | **Resolving gel (10%)** | **Stacking gel (4%)** |
|---|---|---|
| 30% Acrylamide/bis-acrylamide (Sigma) | 3.35 ml | 0.67 ml |
| 1.5M Tris pH 8.8 | 2.5 ml | - |
| 0.5 M Tris pH 6.8 | - | 1.25 ml |
| 20% SDS (Amresco) | 50 µl | 50 µl |
| Distilled water ($dH_2O$) | 4.05 ml | 3.0 ml |
| 10% ammonium persulfate (Amresco) | 100 µl | 50 µl |
| TEMED (Amresco) | 7 µl | 3.5 µl |
| 100 mM EDTA | 100 µl | 50µl |
| TOTAL | ~10 ml | ~5 ml |

#### 5.2.4.3.2 Electrophoresis of SDS-PAGE

After quantification of protein concentration by Bradford Assay, the amount of sample protein (µg) to be loaded in each lane of the gel was determined. The volume of each sample was calculated from the standard curve and transferred into a clean 1.5 microcentrifuge tube. Identical volume of 2X SDS Sample Buffer, containing 1X Tris.Cl/SDS, pH 6.8, 20% glycerol, 4% SDS, 0.2% 2-merchaptoethanol (ME), 0.001% bromophenol blue and $dH_2O$, was added to each sample and mixed thoroughly. The mixture was boiled for 10 minutes. The tubes were then centrifuged at 20,000x g for 5 minutes at room temperature. The supernatant was subsequently loaded into the designated lanes. For each gel, Prestained PageRuler (Fermentas) which was used as protein marker was loaded into the first and the last lanes. Gel cassettes was placed into the assembly and transferred to clamping frame. Electrophoresis was performed at 120 V for approximately one and a half hours by using 1X Running Buffer containing 25 mM Tris(base) (J.T. Baker, UK), 192 mM Glycine (Amresco, USA) and 0.01% SDS.

#### 5.2.4.4 Transferring Protein onto Polyvinylidene Fluoride (PVDF) Membrane

##### 5.2.4.4.1 Equilibration of Gel and PVDF Membrane

After electrophoresis, the gel was removed from the glass plates and rinsed briefly with adequate volume of $dH_2O$ before blotting. Blotting was carried out in blotting buffer [25 mM Tris(base) (J.T.Baker), 192 mM Glycine (Amresco), 20% Methanol and $dH_2O$] and allowed to equilibrate for 20 minutes. Meanwhile, PVDF membrane which was opaque in colour was activated in adequate volume of methanol by mixing gently in rocking motion for about 10 seconds until it turns translucent. The membrane was washed with $dH_2O$ for 2 minutes and then immersed in blotting buffer for 5 minutes. Ice block made of Blotting buffer was prepared earlier on and kept in -80$^{o}$C freezer.

##### 5.2.4.4.2 Protein Transfer

Protein blotting process was performed in cold. Blotting buffer was pre-chilled and the blotting tank was placed in a container surrounded by ice. A magnetic stir bar was put inside the blotting tank to ensure even circulation of cold temperature of the pre-chilled blotting buffer on ice. The blotting sandwich was prepared by putting a piece of fibre pad on the black colour gel holder cassette, followed by 2 pieces of 3 mm Whatman filter papers, protein gel, PVDF membrane, 2 pieces of 3 mm Whatman filter papers and another piece of fibre pad. The sandwich was rolled by using clean glass rod to remove any bubble that was trapped. The transparent side of the gel holder cassette was then closed and tighten. The Blotting sandwich was placed in the lower buffer chamber in such a way that the gel was facing the cathode and PVDF membrane nearer to the anode. This was done so, as the denatured protein is now negatively charged and will move towards positive pole (anode). Hence, protein will be

blotted or trapped on the PVDF membrane. The Blotting process was carried out at 100 V for 1 hour.

#### 5.2.4.5 Protein Gel Staining and Blocking

After the blotting process, the blotting sandwich was disassembled. The gel was briefly rinsed with adequate amount of $dH_2O$ while the PVDF membrane was washed with $dH_2O$ for 2 minutes. The gel was then stained with Gel Code Blue Stain (Pierce,USA). The PVDF membrane or Blot was blocked with a blocking agent containing 5% skimmed milk in 1X Phosphate Buffer Saline-Tween20 (0.05%) (PBST) overnight at $4^oC$.

#### 5.2.4.6 Immunodetection and Image Development

After the overnight incubation, the blot was further immersed in fresh blocking agent for an hour in rocking motion. Subsequently, the blot was incubated with each of the primary antibodies, namely Rabbit anti-CAD (dilution factor of 1:1000), Rabbit anti-ICAD (dilution factor of 1:4000) and Rabbit anti-GAPDH (dilution factor of 1:4000) in blocking agent. After 1 hour of incubation with the primary antibody, the blot was washed with 1X PBST for 10 minutes, further washed with fresh 1X PBST for 5 minutes for 2 times. The blot was subsequently incubated with the secondary antibody Goat anti-rabbit IgG HRP (Santa Cruz, USA) (dilution factor of 1:10,000) in blocking agent. The blot was also washed with 1X PBST for 10 minutes, then washed twice with new 1X PBST for 5 minutes. Chemiluminescent detection was carried out using the WestPico Chemiluminescent Substrate Kit (Pierce, USA). Briefly, the blot was placed on a piece of clean cling wrap, 2 ml of chemiluminescent substrate was added and incubated for 5 minutes. Excess chemiluminescent substrate was removed by dripping. The blot was then covered with cling

wrap, excess chemiluminescent substrate was wiped off carefully to avoid bubbles trapped in between the blot and cling wrap. This blot was then placed inside an X-ray cassette. Protein was detected by placing chemiluminescent sensitive X-ray film (Kodak) on the blot in the cassette for different length of time, ranging from 30 seconds to 10 minutes of exposure.

### 5.2.5 Inverse Polymerase Chain Reaction (IPCR)

In order to detect breaks within the MLL bcr, IPCR was performed. Genomic DNA was extracted using phenol/chloroform/isoamyl alcohol (ratio of 25:24:1) extraction method. This method was used in substitution of commercially available kit due to difficulties in dissolving the DNA pellet. In brief, the culture media in the flasks was removed. Cells were washed with 1X PBS. Then, 1 ml of 1X PBS was added into each dish; cells were scrapped and collected into 1.5 ml microcentrifuge tubes. Centrifugation was carried out at 20,000x g for 5 minutes at 4$^{o}$C. The supernatant was removed and cells were lysed by adding 700 µl of lysis buffer (100 mM NaCl, 25 mM EDTA, 0.5% SDS, 10 mM Tris.Cl, pH8) followed by pipetting up and down thoroughly. Subsequently, Proteinase K was added to a final concentration of 0.1 mg/ml and the cell lysate was agitated continuously at 50$^{o}$C (Stuart Scientific Hybridization Oven/shaker) overnight. The cell lysate was extracted by adding 700 µl of phenol/chloroform/isoamyl alcohol and shaken by hand until the mixture became milky homogenously. The mixture was centrifuged at 20,000x g for 5 minutes. Approximately 450 µl of the aqueous phase was transferred into a clean tube and digested with 20 µg of RNase A at 37$^{o}$C for 1 hour. Lysate was then extracted with 450 µl of phenol/chloroform/isoamyl alcohol and mixed thoroughly by hand until the mixture became milky. The mixture was centrifuged at 20,000x g for 10 minutes. Three hundred and thirty µl of the aqueous phase was transferred to a new 1.5 ml microcentrifuge tube. Genomic DNA was precipitated by

adding 66 µl (0.2 Volume) of 7.5 M ammonium acetate and 660 µl (2 Volumes) of absolute ethanol and mixed by inversion. The mixture was then centrifuged at 20,000x g (Eppendorf 5417R) for 10 minutes. Supernatant was discarded and the DNA pellet was washed with 70% ethanol and centrifuged at 20,000x g for 5 minutes. The supernatant was discarded and the washing was repeated with 70% ethanol. After removing the supernatant, DNA pellet was air-dried for approximately 5 minutes. Hundred µl of TE buffer was added and the tube was incubated at 55$^{o}$C until DNA pellet was dissolved completely. The extracted genomic DNA was digested with 2 µl of FastDigest *Bam*H I (Fermentas) in 1X FastDigest Buffer in a final volume of 100 µl. The DNA was quantified, blunt-ended and circularised as mentioned in Section 2.2.6.2. Free nucleotides were removed (section 2.2.5.3) and the DNA was then subjected to *Msc* I and *Bgl* II (both NEB, UK) restriction enzyme digestion (section 2.2.5.4). Purified DNA was quantified prior to IPCR. Nested IPCR was carried out as described in section 2.2.5.5. The centrifuge used in this protocol was Eppendorf 5417R.

## 5.3 Result

Four approaches were used in this study to investigate the role of CAD in cleavage of the MLL bcr upon oxidative stress-induced apoptosis. The first three approaches were discussed in Chapters Two, Three and Four respectively. In the fourth approach, the role of CAD was further examined by co-expressing CAD together with its natural chaperone, ICAD. In this experiment, SUNE1 cells were either transfected with pTracer, pcDNA, pTracer-hCAD or pcDNA-mICAD-L. Cells were also co-transfected with pTracer-hCAD/pcDNA-mICAD-L and pTracer-hCAD(K157Q)/pcDNA-mICAD-L. As control, cells also underwent mock transfection in the absence of DNA. Cells transfected with pTracer, pTracer-hCAD and

pTracer-hCAD(K157Q) were fluorescing because these plasmids carried the GFP gene. GFP protein expression served as a guide to estimate the transfection efficiency. After three hours of transfection process, cells were allowed to grow in optimal condition for another 17 hours. These transfected cells were either treated with oxidative stress inducer (50 μM of $H_2O_2$) or remained non-treated. Nested IPCR was performed to detect cleavage within the MLL bcr.

A day before the transfection, cells were seeded into 60 mm dishes in such a way that the cell confluency reached 60 to 70% before transfection. Among the attaching cells, 95% of them were healthy and 5% were rounded up. Approximately 5% of floating and blebbing cells were observed (data not shown). Transfection was carried out for three hours. Subsequently, cells were grown under optimal condition for maximum expression of protein for 17 hours. Prior to this, a time course has been done to determine this optimum expression time. Cells were then either treated with 50 μM of $H_2O_2$ or left non-treated. For non-treated samples, as shown in Table 5.2, cells that underwent mock transfection reached cell confluency of 95% where 95% of the attaching cells were healthy, 5% were rounded up and 5% of floating cells were observed. As control, cells were transfected with pcDNA and pTracer. Cells transfected with pcDNA showed better survival as compared to cells transfected with pTracer. Ninety-five percent of cells transfected with pcDNA, which occupied 85% of culture dish surface area, were found healthy even though 5% of them were rounded up. Five percent of floating cells were observed. Cells transfected with pTracer occupied only 70% of culture dish surface area, where 90% of them appeared healthy, 10% rounded up and 10% of floating and blebbing cells were found. Eighty percent of the attaching cells fluoresced strongly. For cells transfected with pTracer-hCAD, cell confluency reached 85%. Among the attaching cells, 90% of them were healthy, 10% were rounded up and 20% of cells were floating and blebbing.

Seventy percent of attaching cells fluoresced strongly. For cells that were transfected with pcDNA-mICAD-L, the observation was similar to cells transfected with pTracer-hCAD, except that these cells did not fluoresce because the pcDNA vector does not carry the GFP gene. Morphologically, cells with co-expression of pTracer-hCAD or pTracer-hCAD(K157Q) with pcDNA-mICAD-L shared the same observation. Cell confluency reached 80% with 90% of these cells appeared healthy, 10% of them rounded up and 10% of floating and blebbing cells were observed. Sixty percent of the attaching cells fluoresced strongly. In Healthy cells are shown by black arrows; red arrows indicate the attached but rounded up cells; whereas blue arrows pointed to show floating and blebbing cells.

Table 5.2: Microscopic morphology of co-transfected SUNE1 cells (non-treated). Magnification of 100X under bright field and fluorescence light emission. Black arrow indicates healthy cells; red arrow indicates attached but rounded up cells; and blue arrow indicates floating cells.

| **DNA transfected** | **Cell morphology** | |
|---|---|---|
| | **Bright Field** | **Fluorescence Light** |
| pTracer | 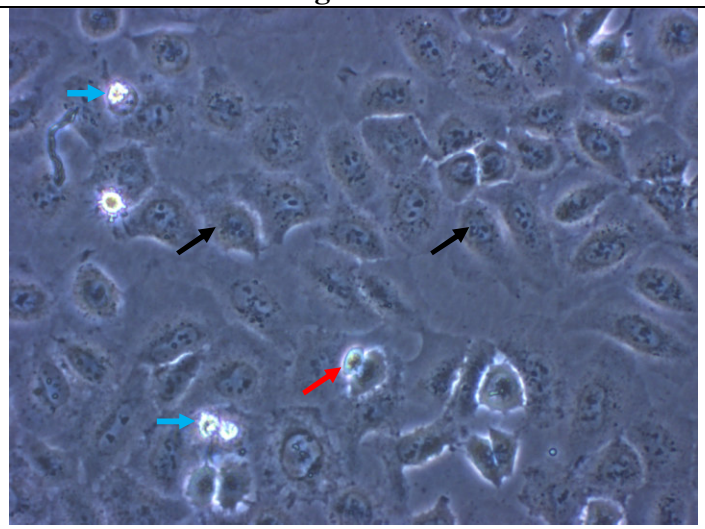 | 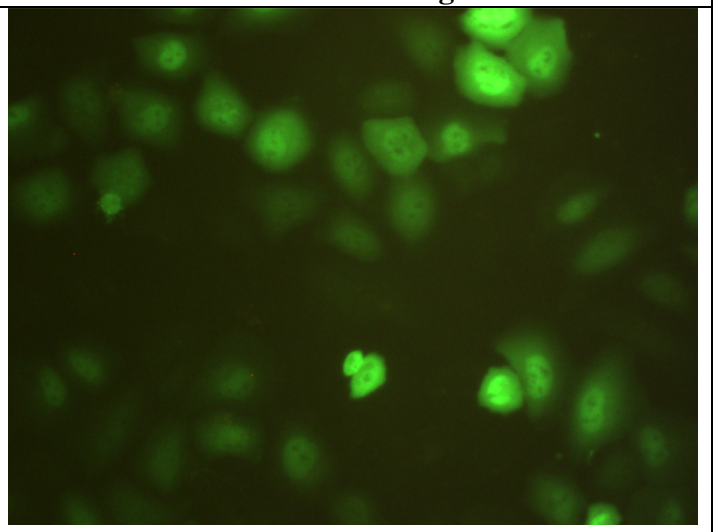 |

| | | |
|---|---|---|
| pcDNA | 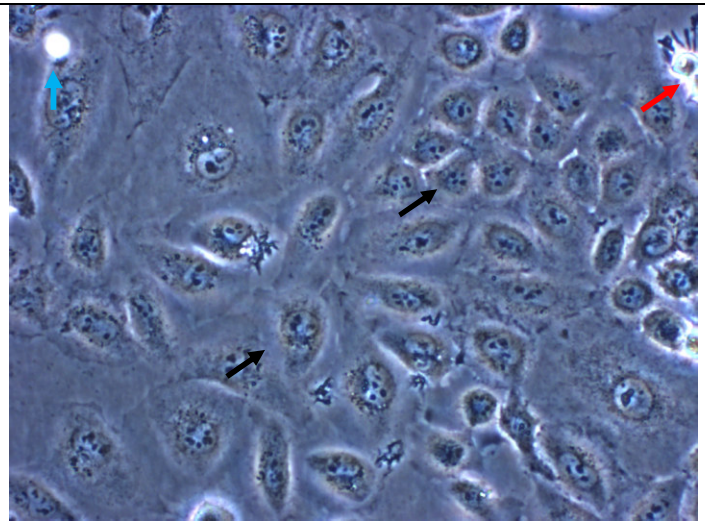 |  |
| pTracer-hCAD | 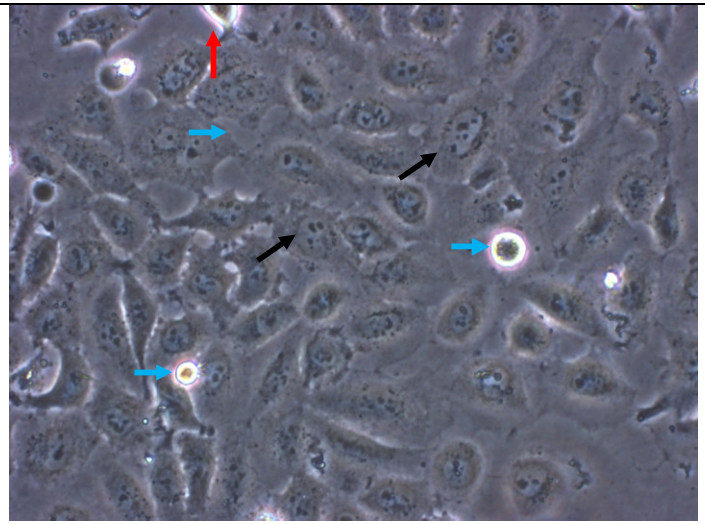 | 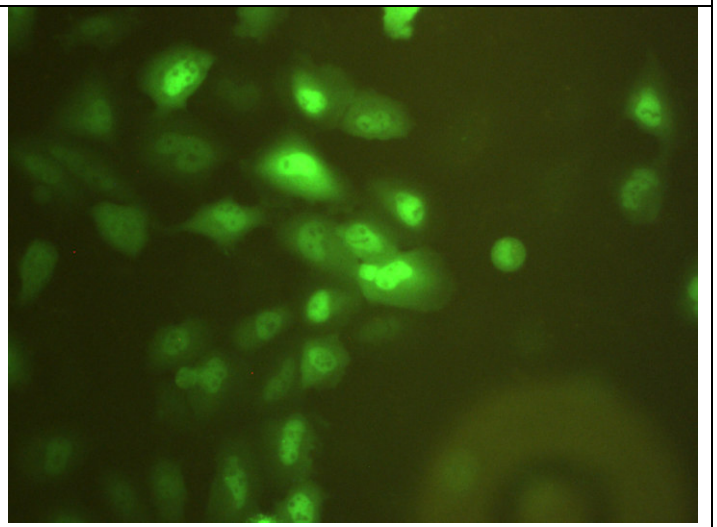 |

| | | |
|---|---|---|
| pcDNA-mICAD-L | 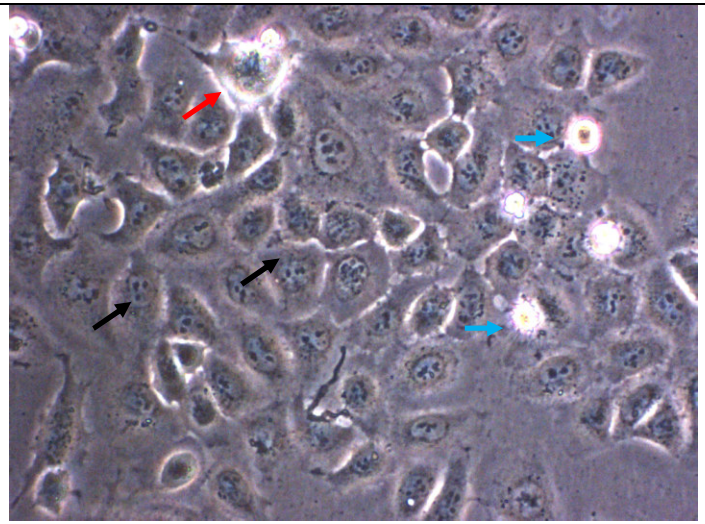 |  |
| pTracer-hCAD/pcDNA-mICAD-L | 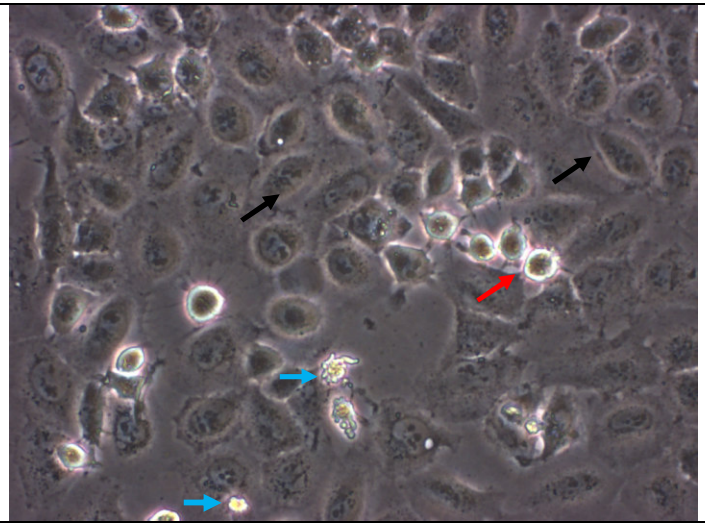 | 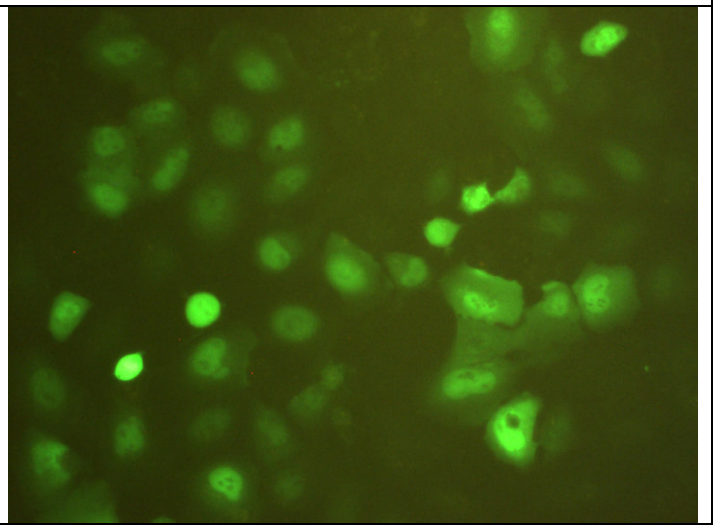 |

| | | |
|---|---|---|
| pTracer-hCAD(K157Q)/pcDNA-mICAD-L | 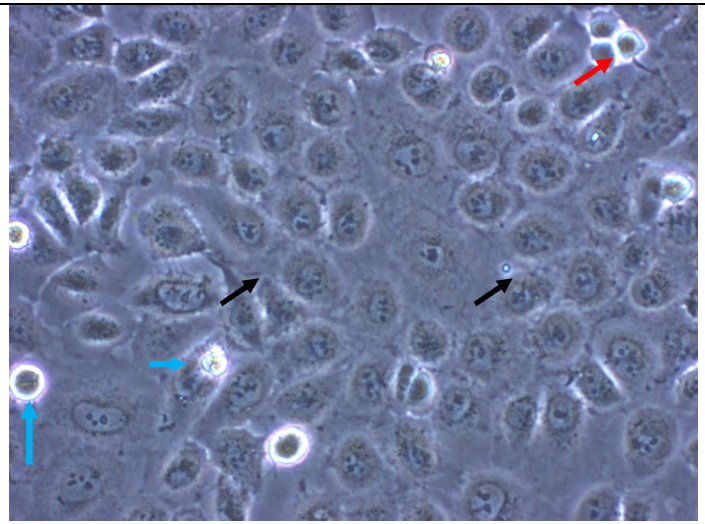 | 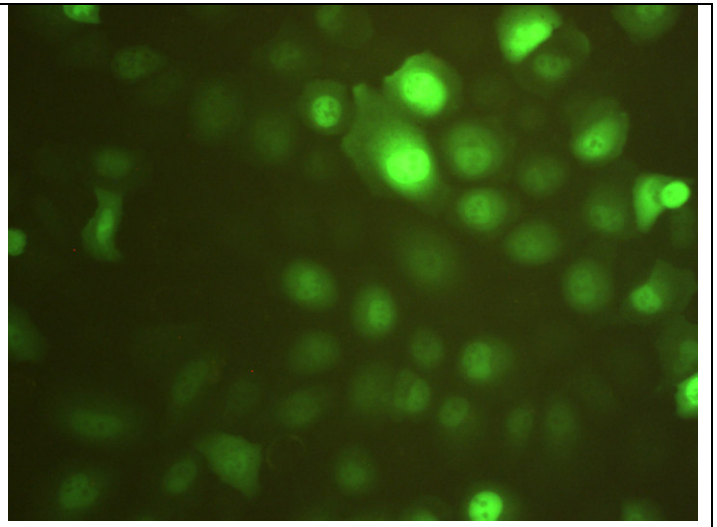 |
| No DNA (Mock Transfection) | 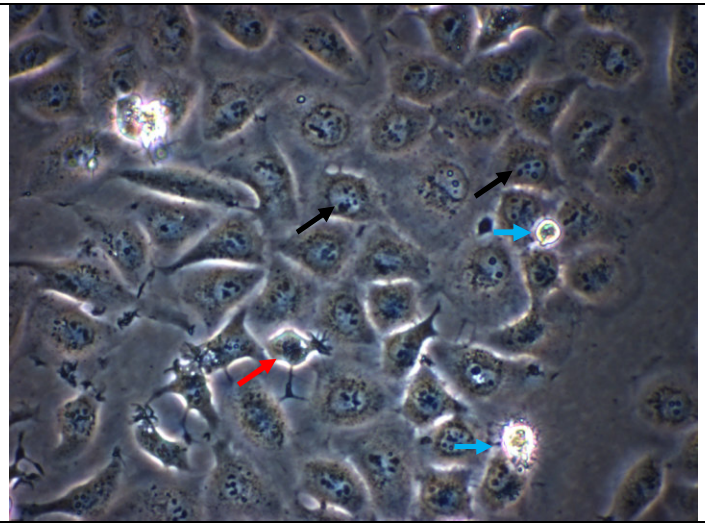 |  |

Prior to this experiment, a time course optimisation was carried out. Transfectants were treated with 50 μM of $H_2O_2$ for 0, 3, 6 and 9 hours. From the morphological observations, IPCR and Western blotting results, treatment of 50 μM of $H_2O_2$ for 6 hours was chosen. After 17 hours of cell growth, another set of the transiently transfected cells were treated with 50 μM of $H_2O_2$ for 6 hours. Prior to treatment, culture media were aspirated and replenished with fresh media. This is to ensure that cells grew at optimal condition and the dead cells were eliminated for estimation of apoptotic cells due to induction of oxidative stress. After 6 hours of treatment, as shown in Table 5.3, cells which underwent mock transfection reached confluency of 98%, where 90% of them were healthy, 5% were rounded up and bright and 5% of the attaching cells with prominent nucleoli. Only one percent of floating cells were found. Cells transfected with pcDNA and pTracer reached a confluency of 95% and 90%, respectively, with 90% of the attaching cells appear healthy, 5% were rounded up and 5% with bright nuclei. Eighty-five percent of cells transfected with pTracer fluoresced strongly. Cells transiently transfected with pTracer-hCAD reached confluency of 90%, 85% of the attaching cells were healthy, 10% were rounded up and bright, and 5% of them with bright nuclei. Approximately 15% of floating and blebbing cells were found. Cells with pcDNA-mICAD-L overexpressed, reached a confluency of 70%, with 80% of the attached cells appeared healthy, 10% of them were rounded up, 10% with bright nuclei and 10% floating and blebbing cells were observed. For cells with co-expression of pTracer-hCAD and pcDNA-mICAD-L, cell confluency was 80%. Among the attaching cells, only 75% were healthy, 10% were rounded up, 15% of the cells with bright nuclei. Twenty percent of floating and blebbing cells were observed. As for cells co-transfected with pTracer-hCAD(K157Q) and pcDNA-mICAD-L, 80% from 80% of the attaching cells appeared to be healthy, 10% rounded up and 10% with bright nuclei. Fifteen percent of floating and

blebbing cells were found. Seventy percent of the SUNE1 cells transiently transfected with pTracer-hCAD, pTracer-hCAD/pcDNA-mICAD-L and pTracer-hCAD/pcDNA-mICAD-L fluoresced strongly. Healthy cells are shown by black arrows; red arrows indicate the attached but rounded up cells; whereas blue arrows pointed to show floating and blebbing cells.

Table 5.3: Microscopic morphology of co-transfected SUNE1 cells (treated). Magnification of 100X under bright field and fluorescence light emission. Black arrow indicates healthy cells; red arrow indicates attached but rounded up cells; and blue arrow indicates floating cells.

| DNA transfected | Cell morphology | |
|---|---|---|
| | **Bright Field** | **Fluorescence Light** |
| pTracer | 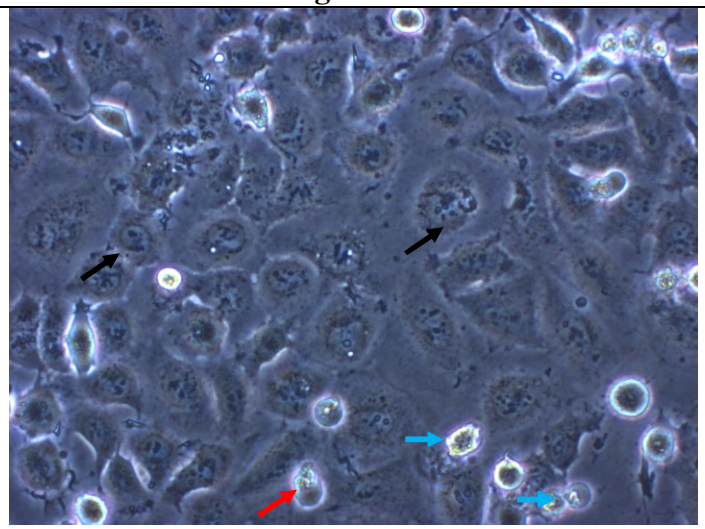 | 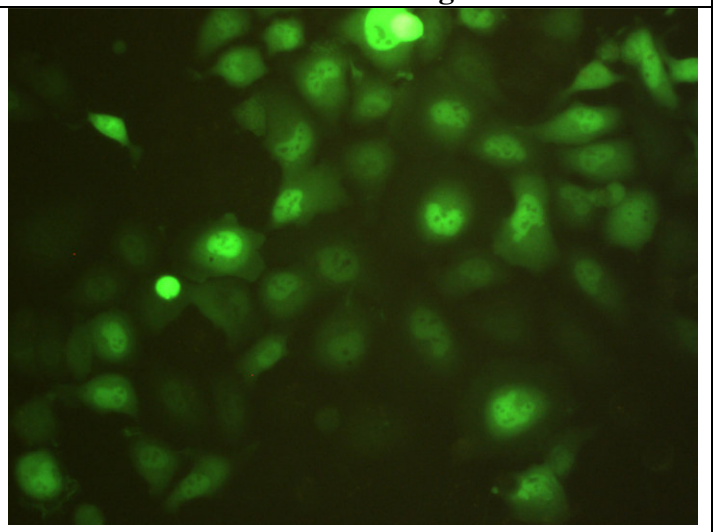 |

| | | |
|---|---|---|
| pcDNA | 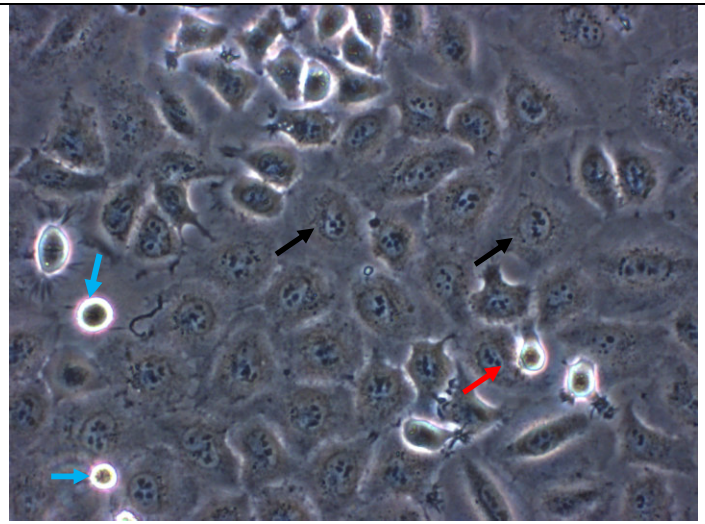 |  |
| pTracer-hCAD | 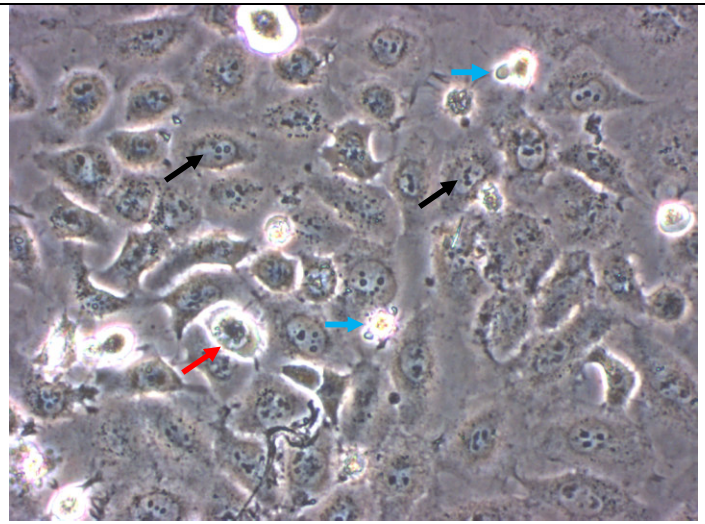 | 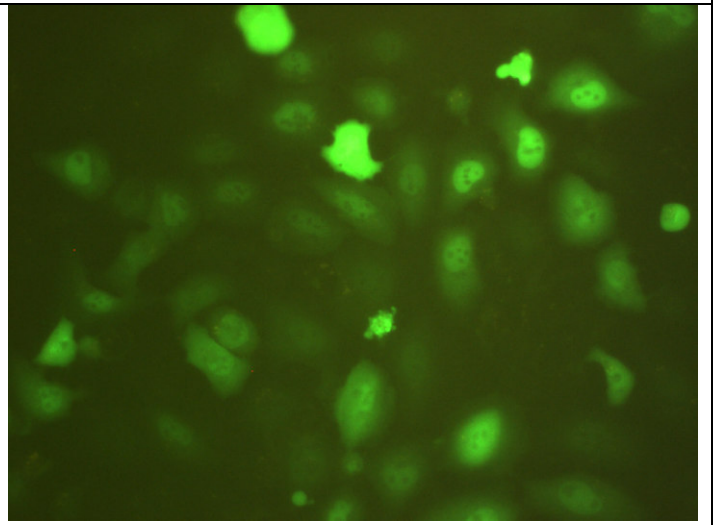 |

| | | |
|---|---|---|
| pcDNA-mICAD-L | 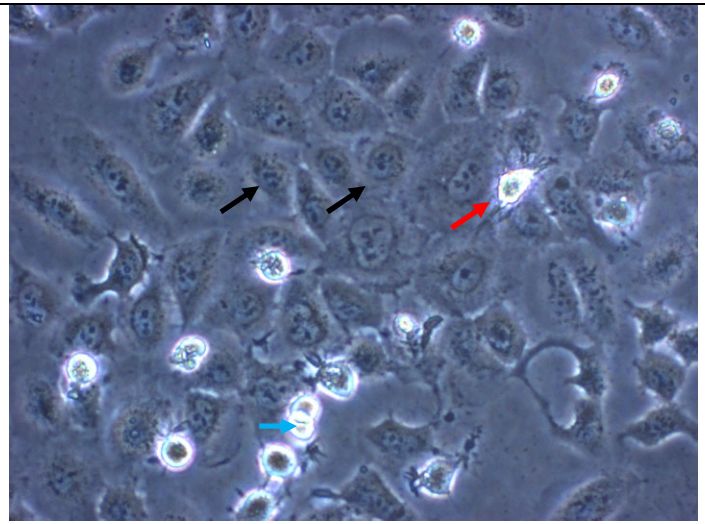 |  |
| pTracer-hCAD/pcDNA-mICAD-L | 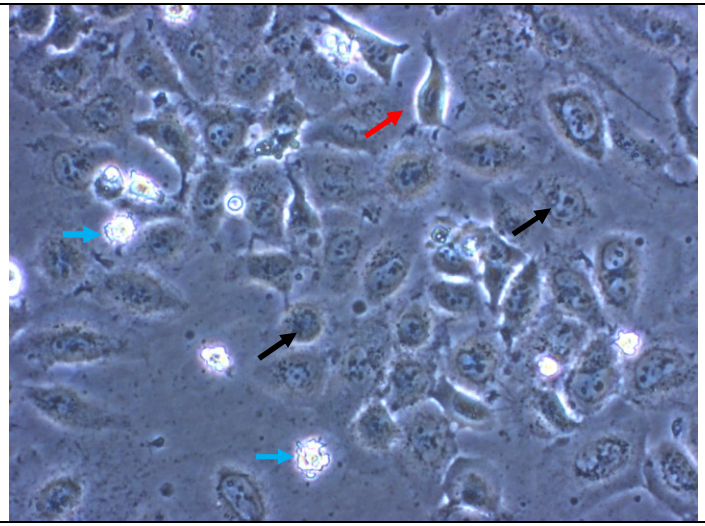 | 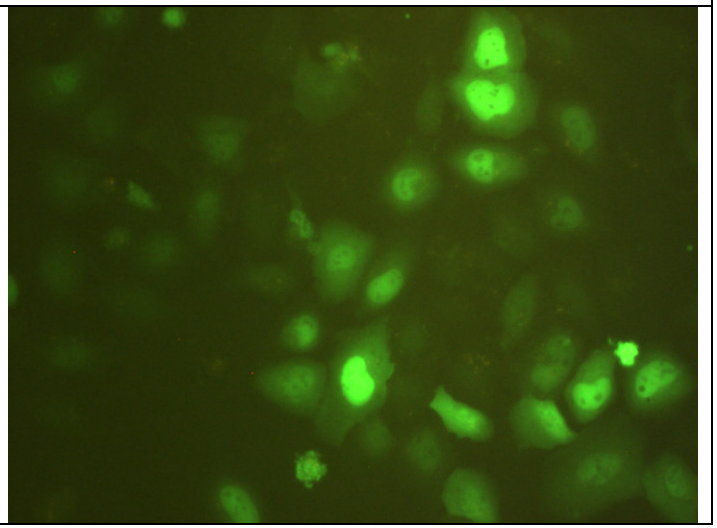 |

| | | |
|---|---|---|
| pTracer-hCAD(K157Q)/pcDNA-mICAD-L | 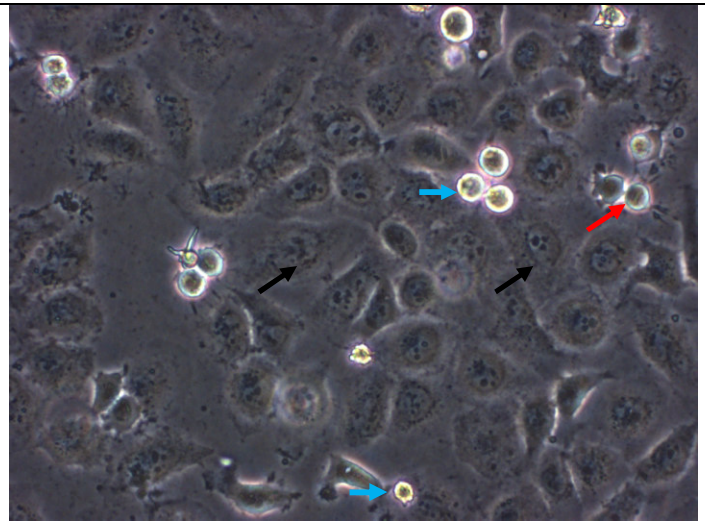 | 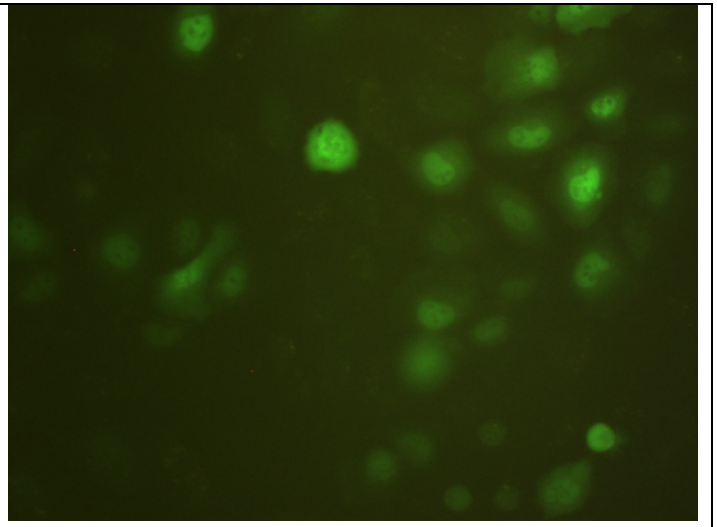 |
| No DNA (Mock Transfection) | 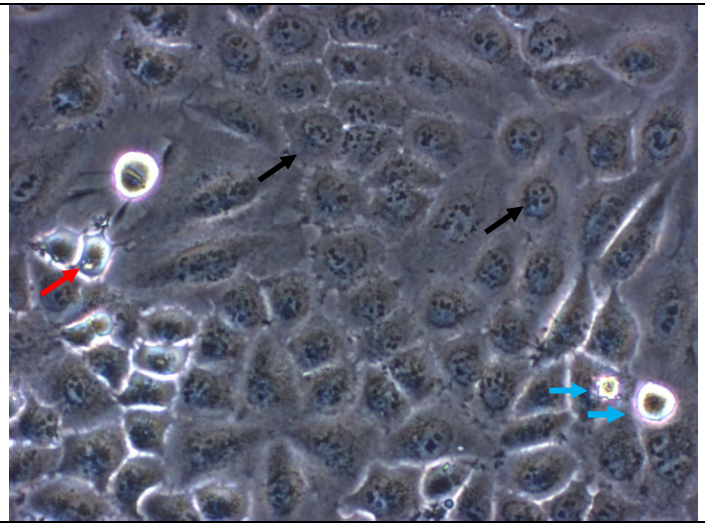 |  |

Expression of the transiently transfected protein in both treated and non-treated samples was detected by using Western blotting prior to IPCR. This is to study the level of expression of CAD in relation to its role in inducing breaks within the MLL bcr. Transfected cells were lysed by repeated freeze-thawing method. Total lysate was quantified by Bradford Assay. Fifty µg of crude protein was separated on 10% SDS-PAGE. Proteins were then transferred onto PVDF membrane for immunodetection. Various antibodies were used for the detection of CAD, ICAD as well as GAPDH protein. GAPDH is a house-keeping gene which is expressed in all cell types. Detection of GAPDH serves as an internal control. A band with a molecular weight of 40 kDa represents the CAD protein when detected with anti-CAD antibody. The 45 kDa ICAD protein was detected with Rabbit Anti-ICAD antibody. GAPDH protein of size 35 kDa was detected with Rabbit Anti-GAPDH.

As shown in Figure 5.4, among the non-treated samples, a band of molecular weight of 40 kDa (indicated by thick arrow), which represents the CAD protein, was detected in cells transfected with pcDNA-mICAD-L (Lane 5) as well as cells co-transfected with pTracer-hCAD/pcDNA-mICAD-L (Lane 6) and pTracer-hCAD(K157Q)/pcDNA-mICAD-L (Lane 7). This was not detected in samples transfected with vector pTracer (Lane 2) and pcDNA (Lane 3), pTracer-hCAD (Lane 4) as well as mock transfected samples (Lane 1). The intensity of the 40 kDa band detected in the pcDNA-mICAD-L transfected sample was higher than both of the co-transfected samples. This may be due to the amount of pcDNA-mICAD-L transfected was double the amount used in cotranfected samples. Our result showed that overexpression of exogenous ICAD could induce the overexpression of endogenous CAD. For samples detected with anti-ICAD antibody, a 45 kDa band, which represents the ICAD protein, was detected in all of the samples (Lanes 1 – 7) as shown in Figure 5.5.

Comparatively, the intensity of the 45 kDa band detected in the samples transfected with pcDNA-mICAD-L (Lane 5) was stronger than samples co-transfected with pTracer-hCAD/pcDNA-mICAD-L (Lane 6) and pTracer-hCAD(K157Q)/pcDNA-mICAD-L (Lane 7). This also may due to the amount of pcDNA-mICAD-L transfected. In cells transfected with pcDNA-mICAD-L alone, 2 µg was used as compared to 0.67 µg used in co-transfected samples. As shown in Figure 5.6 (Lanes 1 – 7), GAPDH protein of 35 kDa was detected in all of the samples. The intensity of the bands detected was almost similar in all of the samples, indicating that the amount of proteins loaded was comparable.

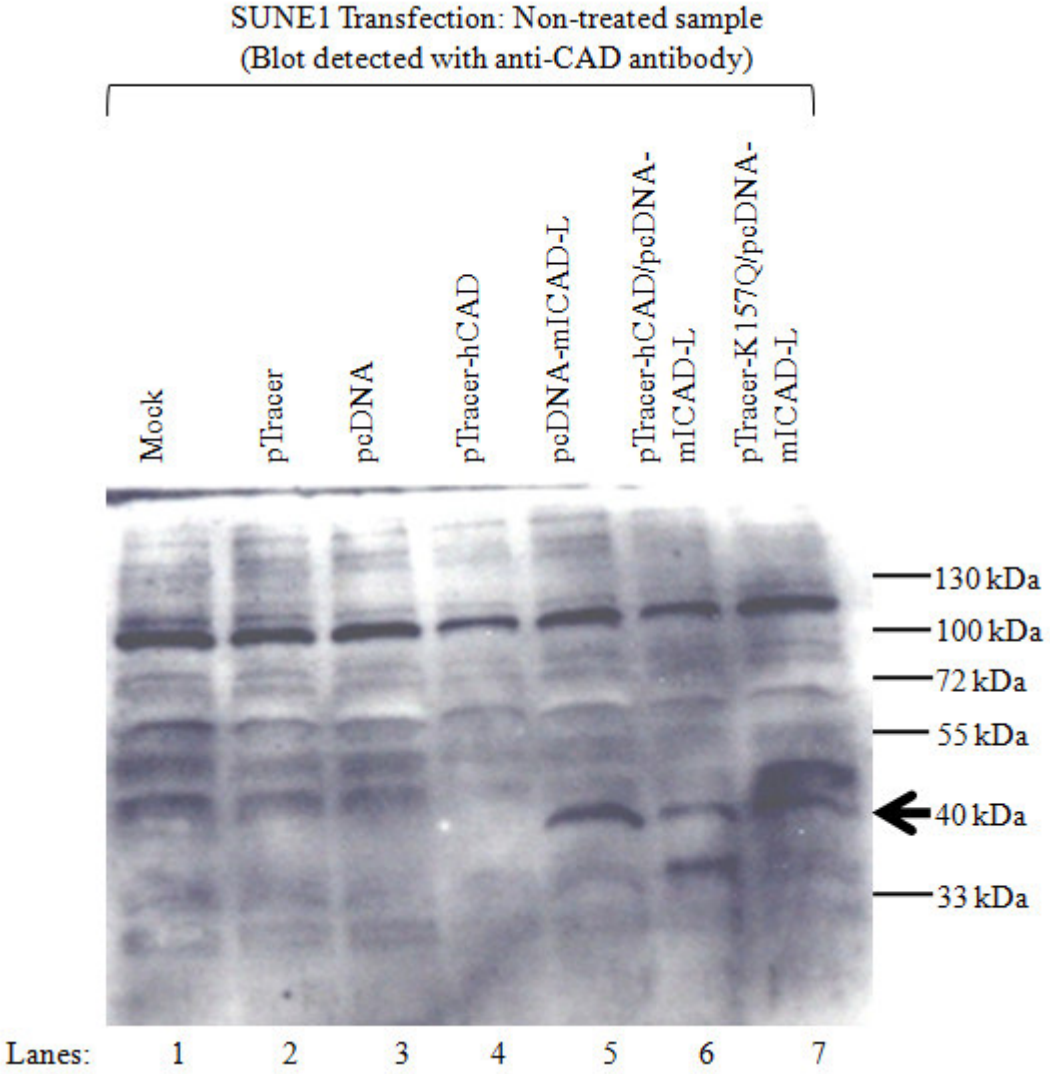


Figure 5.4: Western blot of CAD from transiently transfected SUNE1 cells non-treated with 50 µM of $H_2O_2$. Each lane was loaded with 50 µg of crude protein extracted from SUNE1 cells transiently transfected with pTracer (Lane 2); pcDNA (Lane 3); pTracer-hCAD (Lane 4); pcDNA-mICAD-L (Lane 5); pTracer-hCAD/pcDNA-mICAD-L co-transfection (Lane 6); pTracer-hCAD(K157Q)/pcDNA-mICAD-L co-transfection (Lane 7); and mock transfection (no DNA) (Lane 1). The blot was detected using anti-CAD antibody. Mock transfection was included as a control. The thick arrow indicates the 40 kDa CAD protein.

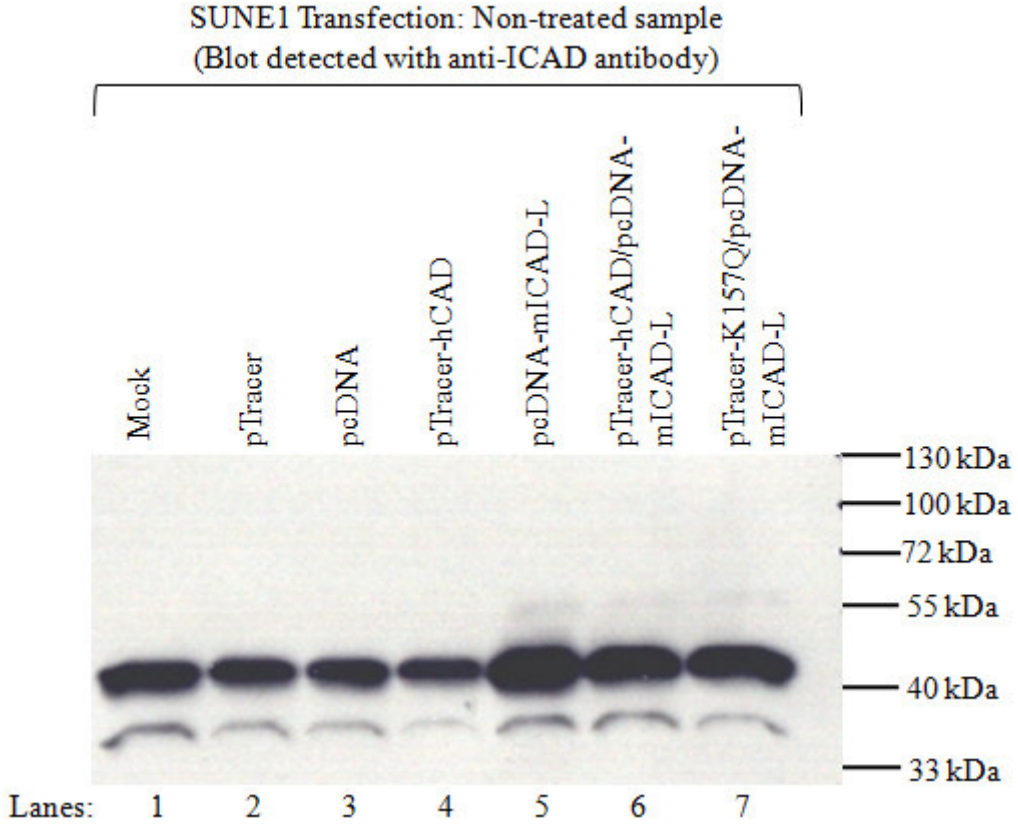


Figure 5.5: Western blot of ICAD from transiently transfected SUNE1 cells non-treated with 50 µM of $H_2O_2$. Each lane was loaded with 50 µg of crude protein extracted from SUNE1 cells transiently transfected with pTracer (Lane 2); pcDNA (Lane 3); pTracer-hCAD (Lane 4); pcDNA-mICAD-L (Lane 5); pTracer-hCAD/pcDNA-mICAD-L co-transfection (Lane 6); pTracer-hCAD(K157Q)/pcDNA-mICAD-L co-transfection (Lane 7); and mock transfection (no DNA) (Lane 1). The blot was detected using anti-ICAD antibody. Mock transfection was included as a control. The 45 kDa protein indicates the ICAD protein.

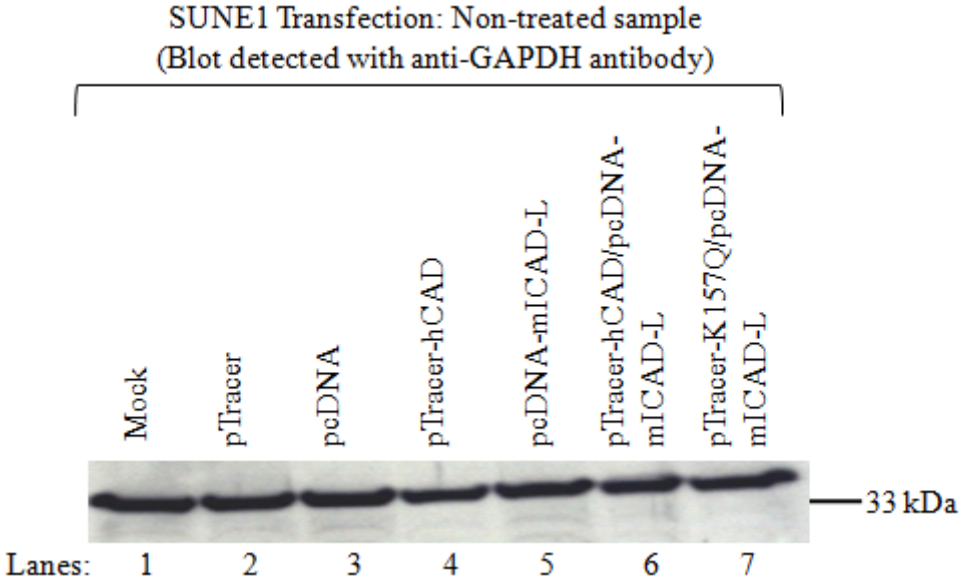


Figure 5.6: Western blot of GAPDH from transiently transfected SUNE1 cells non-treated with 50 µM of $H_2O_2$. Each lane was loaded with 50 µg of crude protein extracted from SUNE1 cells transiently transfected with pTracer (Lane 2); pcDNA (Lane 3); pTracer-hCAD (Lane 4); pcDNA-mICAD-L (Lane 5); pTracer-hCAD/pcDNA-mICAD-L co-transfection (Lane 6); pTracer-hCAD(K157Q)/pcDNA-mICAD-L co-transfection (Lane 7); and mock transfection (no DNA) (Lane 1). The blot was detected using anti-GAPDH antibody. Mock transfection was included as a control. The 35 kDa band represents the GAPDH protein.

After treatment with 50 μM of $H_2O_2$, the expression of CAD was also assessed by using anti-CAD antibody, as shown in Figure 5.7. The 40 kDa band (as indicated by thick arrow) was detected in cells transfected with pcDNA-mICAD-L (Lane 5), pTracer-hCAD/pcDNA-mICAD-L co-transfection (Lane 6) and pTracer-hCAD(K157Q)/pcDNA-mICAD-L co-transfection (Lane 7). The intensity of this band seems to be similar in all of these samples. When the anti-CAD antibody was stripped and re-probed with anti-ICAD antibody, ICAD protein was detected in all of the samples (Figure 5.8, Lanes 1 – 7). The intensity of this band in pcDNA-mICAD-L (Lane 5) transfected sample was the highest, followed by cells which underwent co-transfection with pTracer-hCAD/pcDNA-mICAD-L (Lane 6) and co-transfection with pTracer-hCAD(K157Q)/pcDNA-mICAD-L (Lane 7). For other samples, when cells were transfected with pTracer (Lane 2), pcDNA (Lane 3), pTracer-hCAD (Lane 4) and the mock transfected cells (Lane 1), the intensity of the 45 kDa band seems to be less. This should represent the endogenous ICAD. When detected with the anti-GAPDH antibody, a 35 kDa band was detected in all of the samples (Figure 5.9, Lanes 1 – 7). The intensity of the 35 kDa band was comparable in all of the samples.

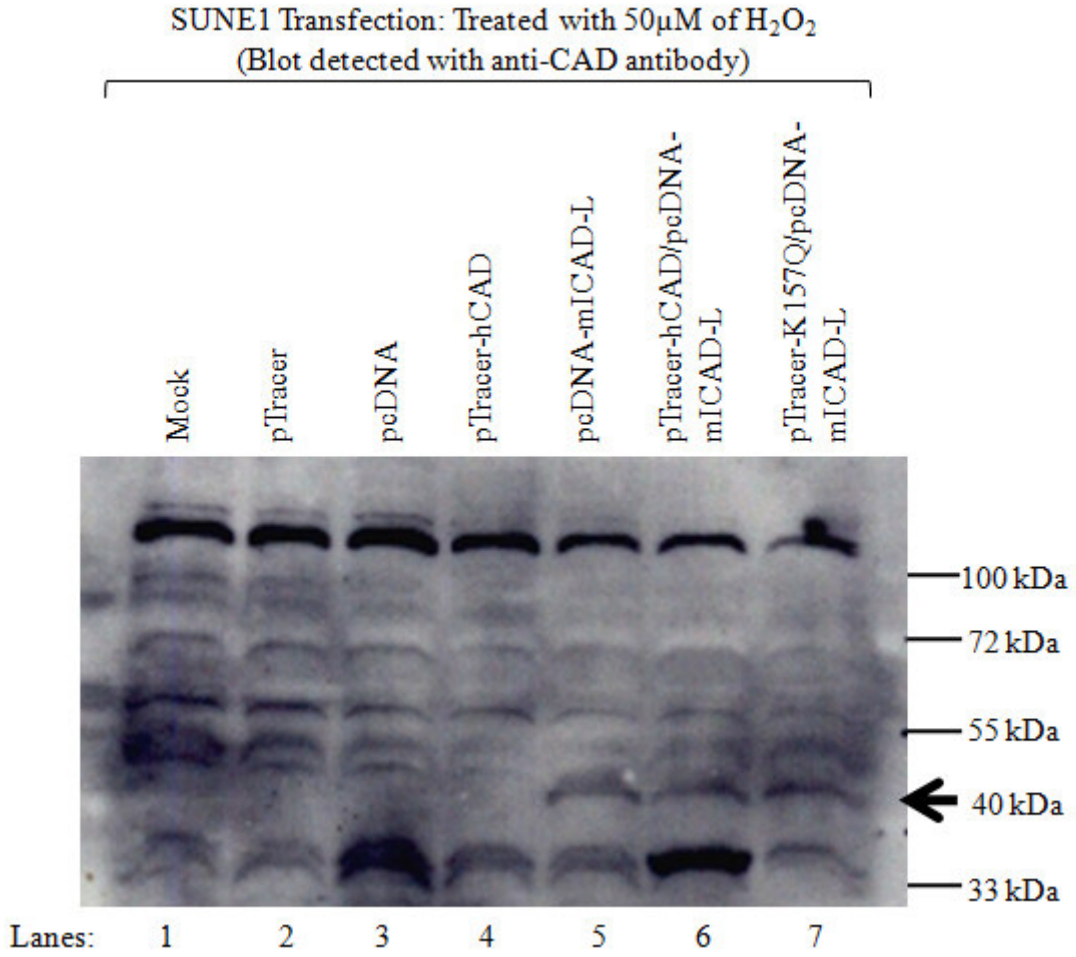


Figure 5.7: Western blot of CAD from transiently transfected SUNE1 cells treated with 50 μM of $H_2O_2$. Each lane was loaded with 50 μg of crude protein extracted from SUNE1 cells transiently transfected with pTracer (Lane 2); pcDNA (Lane 3); pTracer-hCAD (Lane 4); pcDNA-mICAD-L (Lane 5); pTracer-hCAD/pcDNA-mICAD-L co-transfection (Lane 6); pTracer-hCAD(K157Q)/pcDNA-mICAD-L co-transfection (Lane 7); and mock transfection (no DNA) (Lane 1). Blot was detected using anti-CAD antibody. Mock transfection was included as a control. The thick arrow indicates the 40 kDa CAD protein.

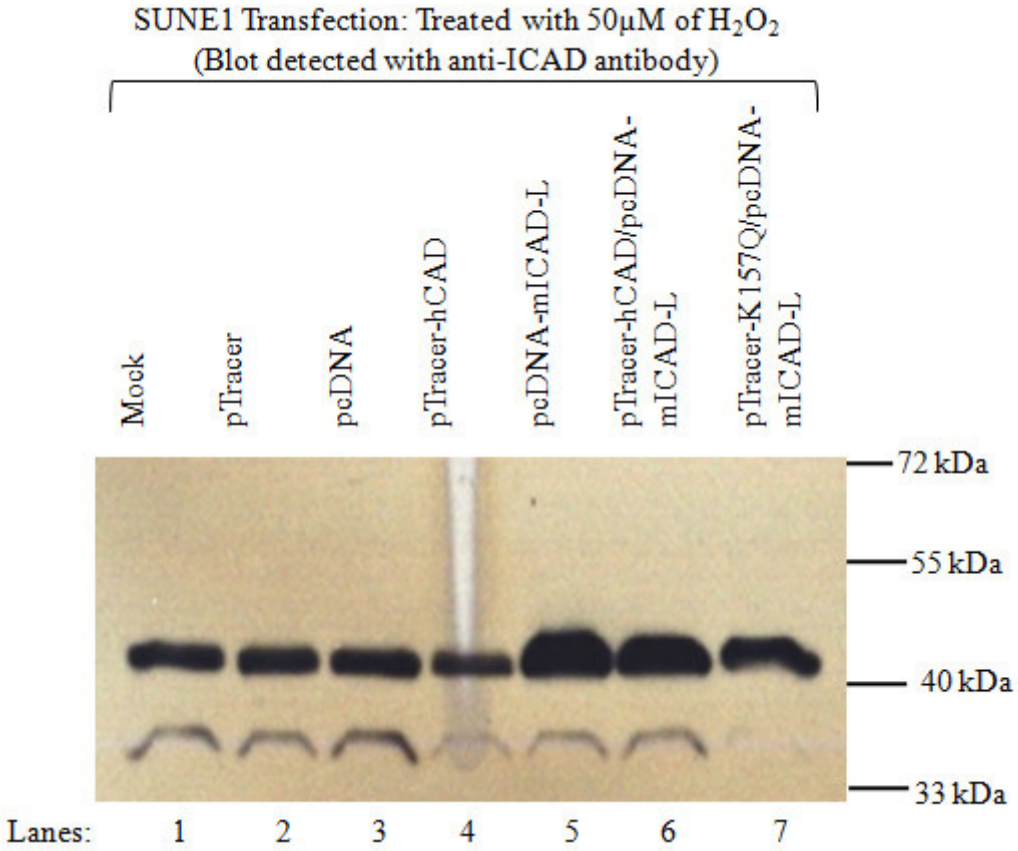


Figure 5.8: Western blot of ICAD from transiently transfected SUNE1 cells treated with 50 μM of $H_2O_2$. Each lane was loaded with 50 μg of crude protein extracted from SUNE1 cells transiently transfected with pTracer (Lane 2); pcDNA (Lane 3); pTracer-hCAD (Lane 4); pcDNA-mICAD-L (Lane 5); pTracer-hCAD/pcDNA-mICAD-L co-transfection (Lane 6); pTracer-hCAD(K157Q)/pcDNA-mICAD-L co-transfection (Lane 7); and mock transfection (no DNA) (Lane 1). Blot was detected using anti-ICAD antibody. Mock transfection was included as a control. The 45 kDa band represents the ICAD protein.

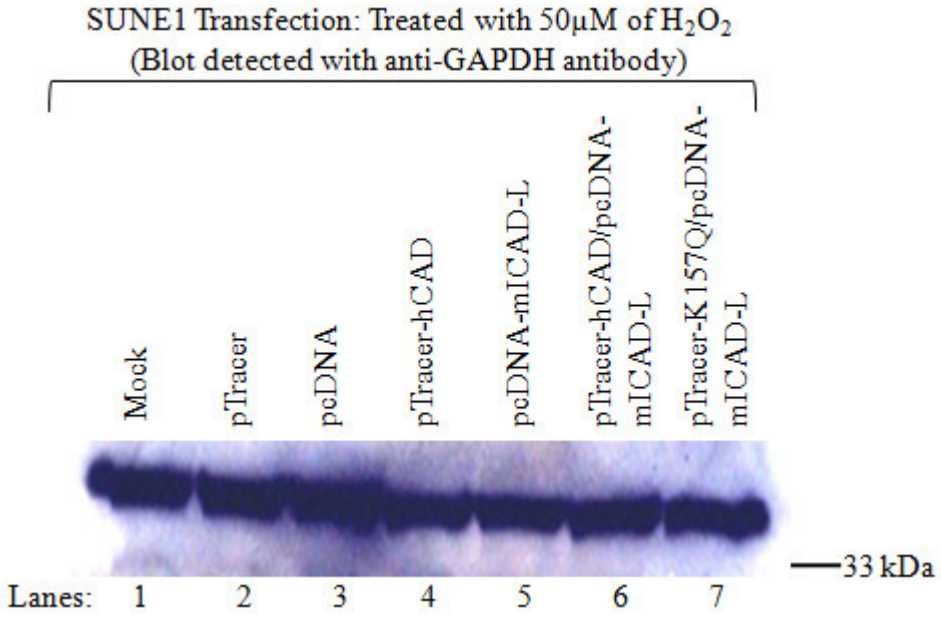


Figure 5.9: Western blot of GAPDH from transiently transfected SUNE1 cells treated with 50 μM of $H_2O_2$. Each lane was loaded with 50 μg of crude protein extracted from SUNE1 cells transiently transfected with pTracer (Lane 2); pcDNA (Lane 3); pTracer-hCAD (Lane 4); pcDNA-mICAD-L (Lane 5); pTracer-hCAD/pcDNA-mICAD-L co-transfection (Lane 6); pTracer-hCAD(K157Q)/pcDNA-mICAD-L co-transfection (Lane 7); and mock transfection (no DNA) (Lane 1). Blot was detected using anti-GAPDH antibody. Mock transfection was included as a control. The 35 kDa band represents the GAPDH protein.

The relative amount of the CAD protein between the treated and non-treated samples was compared, as shown in Figure 5.10. When detected with anti-CAD antibody, the 40 kDa band, which represents the CAD protein, was not observed in pTracer-hCAD transiently transfected sample, regardless of with (Lane 5) or without (Lane 1) treatment with 50 μM of $H_2O_2$. As for cells transfected with pcDNA-mICAD-L (Lanes 2 and 6), the intensity of the 40 kDa band seems to be similar, whether with (Lane 6) or without (Lane 2) treatment. After being treated with 50 μM of $H_2O_2$, the intensity of the 40 kDa band for cells co-transfected with pTracer-hCAD/pcDNA-mICAD-L (Lane 7) seems to have increased as compared to that which was non-treated (Lane 3). For cells co-transfected with pTracer-hCAD(K157Q)/pcDNA-mICAD-L (Lanes 4 and 8), the intensity of the 40 kDa band seems to decrease after treatment with 50 μM of $H_2O_2$ (Lane 8).

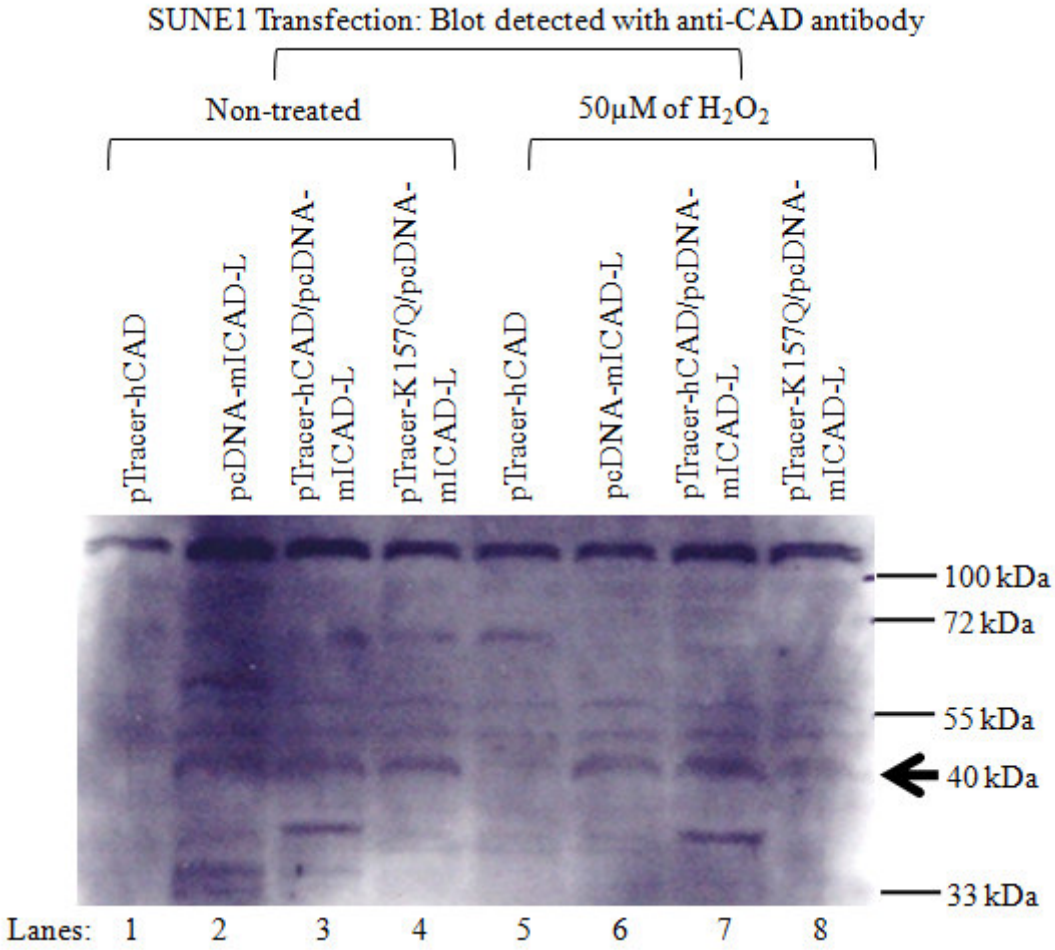


Figure 5.10: Western blot of CAD from transiently transfected SUNE1 cells non-treated and treated with 50 μM of $H_2O_2$. Each lane was loaded with 50 μg of crude protein extracted from SUNE1 cells transiently transfected with pTracer-hCAD (Lanes 1 and 5); pcDNA-mICAD-L (Lanes 2 and 6); pTracer-hCAD/pcDNA-mICAD-L co-transfection (Lanes 3 and 7); and pTracer-hCAD(K157Q)/pcDNA-mICAD-L co-transfection (Lanes 4 and 8). Blot was detected using anti-CAD antibody. The thick arrow indicates the 40 kDa CAD protein.

The same blot was stripped and detected by using anti-ICAD antibody, as shown in Figure 5.11 to compare the level of ICAD expression between treated and non-treated samples. ICAD protein was detected as a band of molecular weight of 45 kDa. Higher intensity of ICAD was detected in cells transiently transfected with pTracer-hCAD after treatment with 50 μM of $H_2O_2$ (Lane 5) as compared to without treatment (Lane 1). Expression of ICAD seems to be similar between cells transiently transfected with pcDNA-mICAD-L (Lanes 2 and 6), regardless of with (Lane 6) or without (Lane 2) treatment. Cells co-transfected with pTracer-hCAD/pcDNA-mICAD-L had more expression of ICAD when treated with 50 μM of $H_2O_2$ (Lane 7) as compared to non-treated (Lane 3) sample. For cells co-transfected with pTracer-hCAD(K157Q)/pcDNA-mICAD-L, the intensity of the 45 kDa band detected was similar between the non-treated (Lane 4) and treated (Lane 8) sample. The same blot was probed with anti-GAPDH antibody. As shown in Figure 5.12, GAPDH protein was detected as a band of molecular weight of 35 kDa in all of the samples.

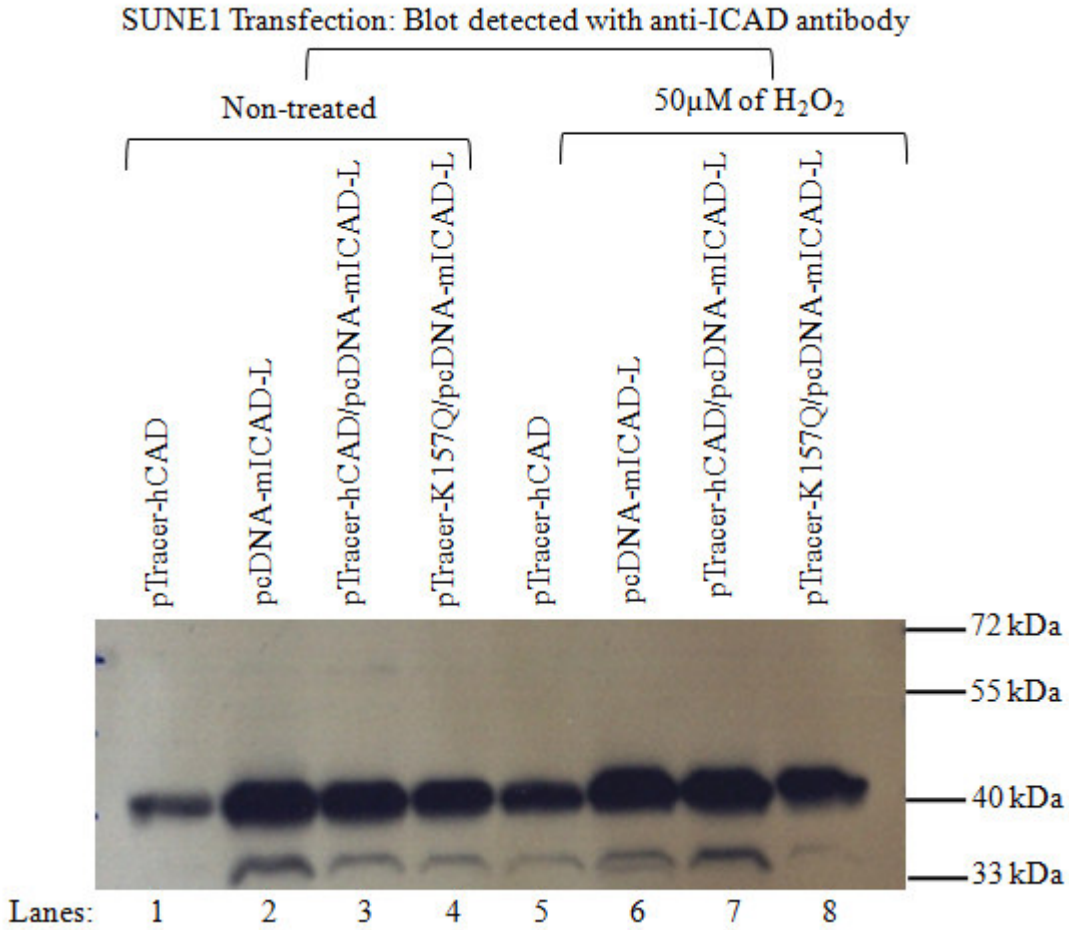


Figure 5.11: Western blot of ICAD from transiently transfected SUNE1 cells non-treated and treated with 50 μM of $H_2O_2$. Each lane was loaded with 50 μg of crude protein extracted from SUNE1 cells transiently transfected with pTracer-hCAD (Lanes 1 and 5); pcDNA-mICAD-L (Lanes 2 and 6); pTracer-hCAD/pcDNA-mICAD-L co-transfection (Lanes 3 and 7); and pTracer-hCAD(K157Q)/pcDNA-mICAD-L co-transfection (Lanes 4 and 8). Blot was detected using anti-ICAD antibody. The 45 kDa band represents the ICAD protein.

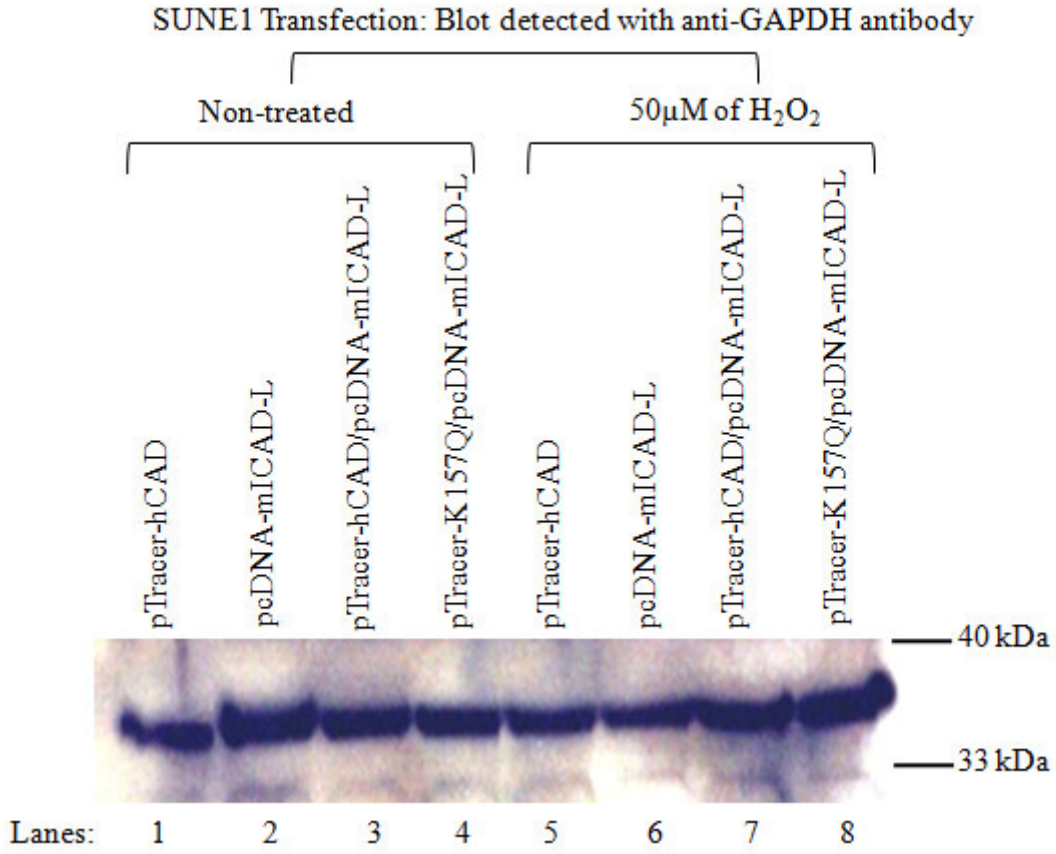


Figure 5.12: Western blot of GAPDH from transiently transfected SUNE1 cells non-treated and treated with 50 μM of $H_2O_2$. Each lane was loaded with 50 μg of crude protein extracted from SUNE1 cells transiently transfected with pTracer-hCAD (Lanes 1 and 5); pcDNA-mICAD-L (Lanes 2 and 6); pTracer-hCAD/pcDNA-mICAD-L co-transfection (Lanes 3 and 7); and pTracer-hCAD(K157Q)/pcDNA-mICAD-L co-transfection (Lanes 4 and 8). Blot was detected by using anti-GAPDH antibody. The 35 kDa band represents the GAPDH protein.

In order to study the role of CAD in chromosome breaks within the MLL bcr during stress-induced apoptosis, IPCR was employed. Genomic DNA extracted from both treated and non-treated samples were modified and used as template for IPCR. Based on the primer position, a 2.2 kb band represents the intact MLL bcr whereas the cleaved MLL bcr fragments are represented by bands of sizes smaller than 2.2 kb. Positive control for IPCR was included to ensure that the PCR reaction worked well. DNA template used in this control was *Msc* I-digested DNA, extracted from SUNE1 cells treated with 50 µM of $H_2O_2$ for 8 hours. As for negative control for IPCR, DNA template was substituted with sterilised $dH_2O$ to ensure the PCR reaction was not contaminated. In this experiment, *Msc* I was used to linearised the circularised DNA template. *Bgl* II was used to linearised the circularised DNA and to eliminate the amplification of the intact MLL bcr fragment. This is to enhance the amplification of the cleaved MLL bcr fragments which are in smaller population.

As shown in Figure 5.13, the 2.2 kb band, representing the intact MLL bcr was detected in all of the transfectants in both treated (Lanes 10 – 16) and non-treated (Lanes 3 – 9) samples. Bands smaller than 2.2 kb were also detected, representing the cleaved MLL bcr in all of the samples. In non-treated samples (Lanes 3 – 9), multiple smaller bands were detected. Intensity of the 2.2 kb band was similar in all of the transfectants.

In samples treated with 50 µM of $H_2O_2$, smaller fragments as well as the 2.2 kb intact band were detected in all of the samples (Lanes 10 to 16) as shown in Figure 5.13. Among the treated samples, the intensity of the intact band for cells transiently transfected with pcDNA-mICAD-L (Lane 14) was the strongest. In addition, it exhibited the least amount of cleaved MLL bcr. Fuzzy and blurry bands were detected for cells transfected with pTracer (Lane 11),

pcDNA (Lane 12), pTracer-hCAD (Lane 13) as well as mock transfected cells (Lane 10). In general, after treatment with 50 µM of $H_2O_2$, there was an increase in cleavage within the MLL bcr as compared to non-treated samples, even though the bands were fuzzy and blurry. This might be contributed by the enhanced cleavage at certain region within the MLL bcr at close proximity in the treated samples. By comparing the intensity of the 2.2 kb band, there was a slight decrease in the intensity when the cells were treated with 50 µM of $H_2O_2$ (Lanes 10 – 16) as compared to the non-treated transfectants (Lanes 3 – 9).

*Bgl* II was used to eliminate amplification of the intact MLL bcr. As shown in Figure 5.14, Lanes 1 to 14, the 2.2 kb band was clearly absent. Numerous smaller bands were detected. Fuzzy bands were detected in both treated (Lanes 8 – 14) and non-treated (Lanes 1 – 7) samples. This was observed in cells transfected with pTracer (Lane 2), pTracer-hCAD (Lane 4) and pcDNA-mICAD-L (Lane 5) in non-treated samples as well as pTracer-hCAD/pcDNA-mICAD-L (Lane 13) in treated samples. Fuzzy and blurry bands were also found even in mock transfected sample, regardless of whether the cells were treated (Lane 8) or non-treated (Lane 1).

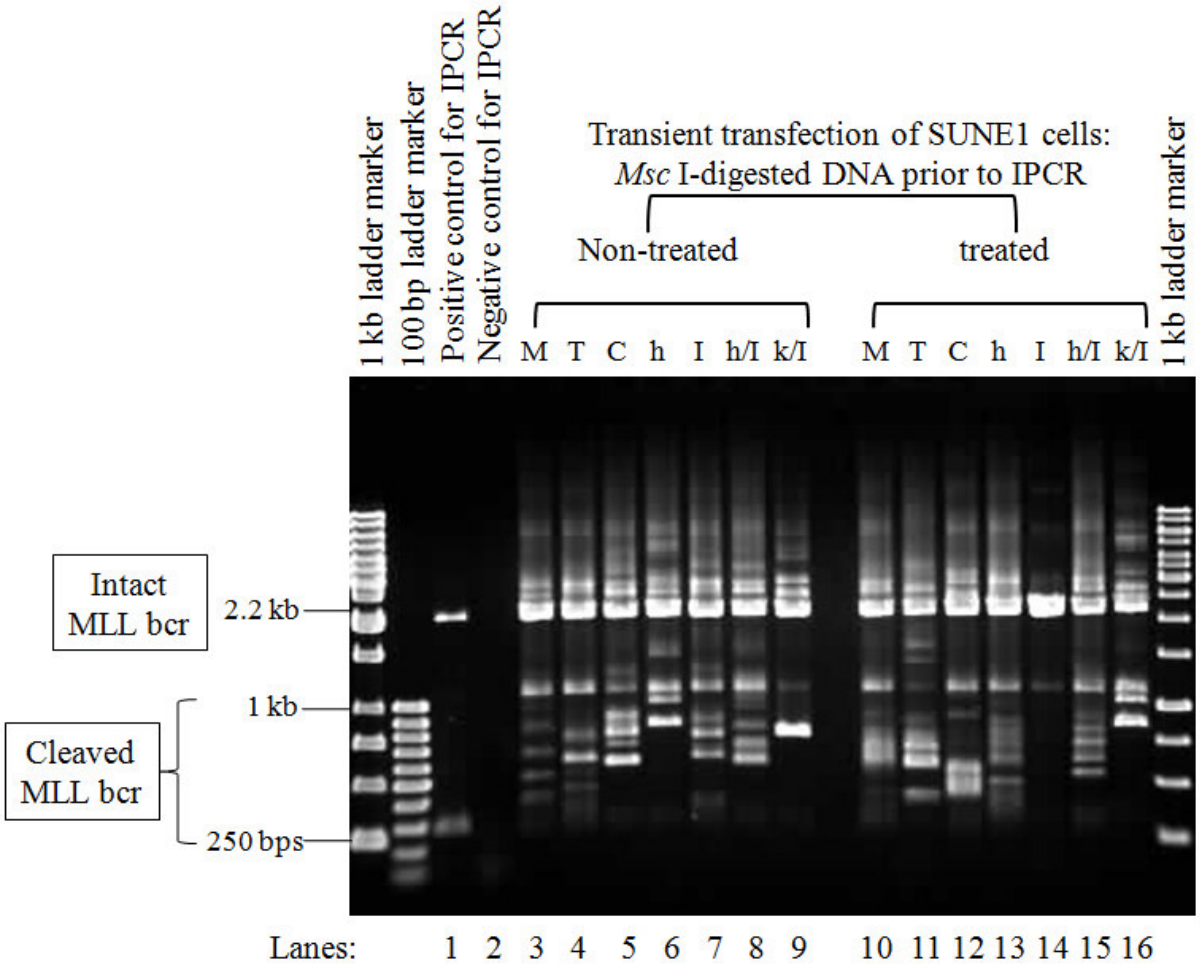


Figure 5.13: Nested IPCR result of transiently transfected SUNE1 cells treated and non-treated with 50 µM of $H_2O_2$, digested with *Msc* I. SUNE1 cells were transiently transfected with pTracer, T (Lanes 4 and 11); pcDNA, C (Lanes 5 and 12); pTracer-hCAD, h (Lanes 6 and 13); pcDNA-mICAD-L, I (Lanes 7 and 14); pTracer-hCAD/pcDNA-mICAD-L co-transfection, h/I (Lanes 8 and 15); and pTracer-hCAD(K157Q)/pcDNA-mICAD-L co-transfection, k/I (Lanes 9 and 16). A mock transfection, M (Lanes 3 and 10) was included as control for the experiment. Cells were either treated with 50 µM of $H_2O_2$ (Lanes 10 to 16) for 6 hours or left untreated (Lanes 3 to 9). The 2.2 kb band represents the intact MLL bcr whereas the bands smaller than 2.2 kb represents the cleaved MLL bcr. Positive control for IPCR (Lane 1) was included, where DNA extracted from SUNE1 cells treated with 50 µM of $H_2O_2$ was used in IPCR. For negative control for IPCR (Lane 2), DNA template was not added.

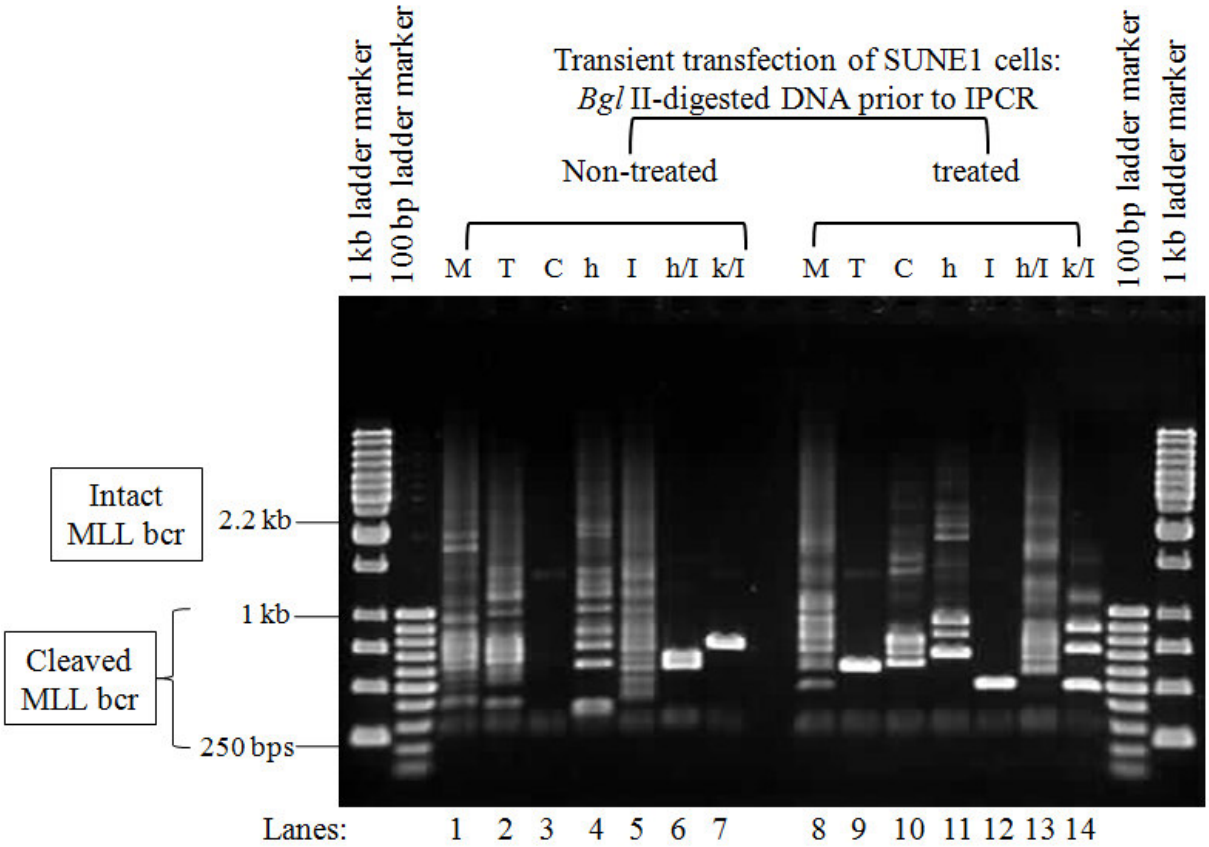


Figure 5.14: Nested IPCR result of transiently transfected SUNE1 cells treated and non-treated with 50 µM of $H_2O_2$, digested with *Bgl* II. SUNE1 cells were transiently transfected with pTracer, T (Lanes 2 and 9); pcDNA, C (Lanes 3 and 10); pTracer-hCAD, h (Lanes 4 and 11); pcDNA-mICAD-L, I (Lanes 5 and 12); pTracer-hCAD/pcDNA-mICAD-L co-transfection, h/I (Lanes 6 and 13); and pTracer-hCAD(K157Q)/pcDNA-mICAD-L co-transfection, k/I (Lanes 7 and 14). A mock transfection, M (Lanes 1 and 8) was included as control for the experiment. Cells were then treated with 50 µM of $H_2O_2$ (Lanes 8 to 14) for 6 hours or left untreated (Lanes 1 to 7). The 2.2 kb band represents the intact MLL bcr whereas the bands smaller than 2.2 kb represents the cleaved MLL bcr.

## 5.4 Discussion

The role of CAD in causing DNA fragmentation has been well studied (Enari *et al.*, 1998; Sakahira *et al.*, 1998; Susin *et al.*, 1999). However, the involvement of CAD in chromosomal breaks within the MLL bcr during oxidative stress is not established. The MLL bcr is located at chromosome 11q23. It has been found that chromosome 11q23 is a common deletion site in NPC (Hui *et al.*, 1996; Mutirangura *et al.*, 1997; Hui *et al.*, 2003) and the MLL gene is also found to be translocated in *de novo* (Hayashi *et al.*, 1988; Kaneko *et al.*, 1988) and therapy-related leukaemia patients (Le Beau *et al.*, 1986). The most common 11q23 translocations are the t(4;11) and t(11;19) in ALL and the t(9;11), t(6;11) and t(11;19) in *de novo* AML (Raimondi, 1993; Kaneko *et al.*, 1998). Recently, the apoptotic nucleases have been implicated in the 11q23 translocation involving the MLL gene (Betti *et al.*, 2003). In addition, CAD is also found to be the major nuclease in causing nucleosomal DNA ladder formation (Nagata, 2000; Hars *et al.*, 2006). Hence, overexpression of CAD and ICAD was conducted to look at the role of CAD in chromosome breaks within the MLL bcr during stress-induced apoptosis.

Our result showed that regardless of the presence or absence of oxidative stress, when ICAD alone was overexpressed, endogenous CAD was detected. However, when CAD alone was overexpressed, CAD was not detected. Most likely the CAD could be expressed but in the absence of its chaperone (ICAD), this CAD was misfolded and rapidly removed. It is known that co-translational folding of protein is an important mechanism to avoid the intramolecular misfolding which in turn, will lead to aggregation (Netzer and Hartl, 1998). Misfolding and aggregation of proteins could be cytotoxic and causes apoptosis (Kakizuka, 1998). However, Sakahira and Nagata (2002) suggested that the misfolded CAD could be rapidly removed

because they observed that in the absence of ICAD, CAD was not detected and cells were growing healthily (Sakahira and Nagata, 2002). On the other hand, when CAD was co-expressed with ICAD, soluble and functional CAD which exists as a complex with ICAD was detected (Sakahira and Nagata, 2002). This observation is also suggested by other study, whereby in ICAD-knockout mice, there was no functional CAD produced (Zhang *et al.*, 1998). This showed that ICAD helps in producing functional CAD by assisting co-translational folding of CAD. This may explain the reason why in our IPCR result, SUNE1 cells with CAD overexpressed did not show enhanced cleavage within the MLL bcr after being treated with 50 μM of $H_2O_2$ as shown in this chapter and in Chapter Two. It is not because of CAD is not involved in causing the chromosomal breaks within the MLL bcr, but it is because of CAD expressed in the absence of ICAD was not functional and most likely rapidly removed.

CAD and ICAD proteins were detected in cells with CAD mutant, CAD(K157Q) co-expressed with ICAD. Fewer breaks were detected in cells with CAD mutant co-expressed with ICAD as compared to the wild type CAD co-expressed with ICAD. A decrease in DNase activity of the mutant CAD is not due to the inability of caspase-3 in cleaving the ICAD that is bound to the mutant CAD (Inohara *et al.*, 1999) but due to the inability of mutant CAD itself in cleaving DNA (Meiss *et al.*, 2001; Widlak *et al.*, 2003; Woo *et al.*, 2004). Lys157 is situated at the N-terminal of CAD. Even though it is not an active site, it is important in maintaining the α-helix 4 structure of the protein. Mutation at this site could lead to inability of CAD mutant to bind to the major groove of DNA as what the wild type protein did. This in turn disable the CAD mutant to form stable complex with the DNA (Woo *et al.*, 2004).

Our result showed that both CAD and ICAD proteins were detected in cells with CAD and ICAD co-expressed. It was found that only a minute amount of ICAD-L was sufficient to inhibit CAD's activity efficiently in cells induced to undergo apoptosis by treating with anti-Fas antibody (Enari *et al.* 1998). Protein purified from the native gel showed the stoichiometry of 1:1 binding of ICAD to CAD (Woo *et al.*, 2004). When cells underwent oxidative stress-induced apoptosis, cleavage within the MLL bcr was detected. However, the involvement of CAD was not distinct. This could be contributed by the stressful transfection process, $H_2O_2$ derived-hydroxyl radicals and the involvement of other nucleases. After treatment, the 2.2 kb intact MLL bcr band in CAD co-expressed with ICAD showed a slight decrease in intensity as compared to non-treated samples. This indicates an increased cleavage within the MLL bcr. This is in agreement with a study done by Enari *et al.* (1998). They found that when CAD was co-expressed with ICAD, the lysate had strong CAD activity. In the *in vitro* treatment with caspase-3, chromosomal DNA in nuclei and plasmid were fragmented. As compared to control samples transfected with plasmid vector, CAD activity in the presence of ICAD was approximately 1,000 times higher in cells overexpressed with CAD. CAD produced was not fully functional without co-existance with ICAD. When CAD was co-expressed with ICAD, CAD was fully functional with caspase-3 activation (Enari *et al.*, 1998).

From our Western blotting result, it was shown that when ICAD alone was overexpressed, there was an increased expression of ICAD as well as CAD. This suggests that exogenous expression of ICAD enhances the expression of the endogenous CAD. Although endogenous CAD expression was enhanced, cleavage within the MLL bcr was not enhanced, instead, it was reduced. It could be possible that when undergoing oxidative stress, endogenous CAD

was freed from ICAD upon ICAD's cleavage by caspase-3. Due to the presence of abundant exogenous ICAD, these freed endogenous CAD might complex with both the endogenous and exogenous ICAD, which in turn, inhibits DNA cleavage by CAD. As described in Chapter Three, it has been shown that when cells with mICAD-Ldm overexpressed underwent oxidative stress, this caspase-3 resistant ICAD did not inhibit cleavage within the MLL bcr. This suggested that mICAD-Ldm did not bind to the freed endogenous CAD. It could be explained by the exogenous mICAD-Ldm binds to the exogenous CAD and endogenous ICAD tends to bind to the endogenous CAD as being suggested by Lechardeur *et al.* (2004). On the other hand, our result here clearly suggests that the exogenous wild type ICAD may act as chaperone for CAD. It is able to complex with CAD and thus inhibits the CAD's activity. Similarly co-expression of ICAD with wild type or mutant CAD exhibited CAD expression. However, in this case, the expressed CAD could be a mixture of both endogenous and exogenous CAD. Since the stoichiometry of ICAD:CAD is 1:1 (Woo *et al.*, 2004), co-expression of CAD titers out the availability of ICAD, thus cleavage of the MLL bcr was still detected. Our result of ICAD and CAD mutant co-expression exhibited less cleavage compare to ICAD and CAD co-expression. Thus, this tally with the previous study that CAD mutant could not bind to the major groove of DNA and not able to form stable complex with DNA (Woo *et al.*, 2004). Our result supported the hypothesis that CAD is involved in cleavage of the MLL bcr during oxidative stress-induced apoptosis. This is in line with the observation by Sakahira and colleagues that, DNA fragmentation was inhibited in Jurkat cells which were overexpressed with ICAD when treated with staurosporine or anti-Fas antibody (Sakahira *et al.*, 1998).

ICAD inhibits CAD through protein-protein interaction. It interacts with CAD through the CAD domain (Uegaki *et al.*, 2000). Both CAD and ICAD share a homologous domain, called the CAD/CIDE domain, which consists of about 80 amino acids at their N terminal (Inohara *et al.*, 1998; Mukae *et al.*, 1998). These homologous domains interact with each other in forming a heterodimeric complex, and is important in leading to the correct folding of CAD (Otomo *et al.*, 2000). Based on Woo and colleagues (2004) investigations of the molecular structure of CAD and ICAD proteins and their interaction during apoptosis, the CAD molecule is folded in serial manner. CAD can be divided into three distinct domains, namely Domain C1 (1 – 85), Domain C2 (residues 86 – 131) and Domain C3 (132 – 328). Similarly, ICAD molecule is folded serially into three domains, namely Domain I1 (residues 1 – 117), Domain I2 (residues 118 – 224) and Domain I3 (residues 225 – 331). Domain C1 interacts with Domain I1; Domain C2 binds to Domain I2; whereas Domain C3 interacts with Domain I3. During apoptosis, ICAD-L is cleaved by caspase-3 at Asp 117 and Asp 224, releasing 3 domains of ICAD-L from the latent CAD monomer. The CAD molecules then self-assemble into active dimers. In this dimer, the C3 domains exist as a large and deep crevice which resembles the shape of the two blades of an open pair of scissors. The width of the crevice is the right size for accommodating double-stranded DNA. Domain I2 plays a critical role in the CAD dimer formation as well as the disassembly of the CAD dimer. When Domain I2 dissociates from Domain C2, the Domain C2 is unlocked. This subsequently leads to the assembly of inactive CAD monomers to form active CAD dimer. Therefore, Domain I2 is required to assemble the CAD dimer (Woo *et al.*, 2004). For CAD and ICAD protein, the overall structure is categorised in the ubiquitin superfold. CAD domain binds strongly with its ICAD domain. It has been suggested that, when ICAD co-translated with CAD, the first step of the correct folding of CAD protein involved the interaction between these two proteins.

The CAD domain is immediately folded as soon as translational process starts from its mRNA. During the translation process, Hsp70 and Hsp40 bind to the elongating CAD at the C-terminal to assist the partial folding. This generates a "molten globule"-like status of CAD (Kuwajima, 1989; Ewbank and Creighton, 1991). Subsequently, ICAD then recognises the *quasi*native state of CAD (Sakahira and Nagata, 2002) through the C-terminal of CAD. It recognises the partially folded CAD and completes the folding of CAD polypeptide correctly (Liu *et al.*, 1997). CAD-ICAD complex is formed due to the ICAD's chaperon-like activity (Uegaki *et al.*, 2000).

Cleavage within the MLL bcr was detected in all of the samples. Band of size 1.5 kb was also detected in all of the samples. This may be due to the background cleavage. Transfection process by itself is a stressful process to the cells. It has been shown that calcium ion, an essential factor in transfection process, is cytotoxic. It leads to increased number of damaged mitochondria (Cartier *et al.*, 2003). Besides, $H_2O_2$ which often exists as hydroxyl radical ($OH\cdot$) could lead to chromosomal breaks that could be detected by our system. In addition, other hydroxyl-derived products could also react with cellular DNA to cause DNA damage. $H_2O_2$ may also cause influx of calcium ions and hence increase intracellular calcium concentration which has the cytotoxic effect. As a result, endonucleases will be activated and subsequently causes DNA fragmentation (Halliwell and Aruoma, 1991; Ueda and Shah, 1992). Besides CAD, there might be other nucleases that are involved in the cleavage of the MLL bcr. In staurosporine- and Fas-induced Jurkat cells, chromosomal breaks were detected even though ICAD was overexpressed (Sakahira *et al.*, 1998).

## 5.5 Conclusion

Exogenous ICAD expression enhances expression of endogenous CAD. ICAD is required for the expression of functional CAD. Overexpression of ICAD reduced cleavage of the MLL bcr, supporting our hypothesis that CAD is involved in the MLL bcr cleavage during stress-induced apoptosis.

# CHAPTER SIX

# GENERAL DISCUSSION, CONCLUSION AND FUTURE WORK

## 6.1 General Discussion

In order to study the role of CAD in cleaving the MLL bcr upon oxidative stress induction, 4 approaches were designed. The first approach was designed to overexpress CAD exogenously so that there is abundant CAD to cleave within the MLL bcr upon apoptotic induction. This was to investigate if CAD is responsible for cleavage within the MLL bcr. In the second approach, mutant ICAD, ICAD-Ldm was overexpressed instead of the wild type. ICAD-Ldm should bind to CAD and inactivate CAD even in the presence of oxidative stress. This approach was to inhibit CAD directly. In the third approach, activation of CAD was inhibited indirectly by using caspase inhibitor. Caspase inhibitor inhibits the activation of caspase-3 upon oxidative stress-induced apoptosis. This in turn, inhibits the activation of CAD. In the last approach, CAD and ICAD were co-expressed. Knowing the fact that ICAD is essential for the production of functional CAD, exogenous wild type ICAD was expressed with CAD simultaneously. This was to study the importance of ICAD for the proper folding of CAD, and the involvement of activated functional CAD in cleavage within the MLL bcr.

### 6.1.1 Cells became apoptotic when treated with hydrogen peroxide ($H_2O_2$)

Under normal condition, cells are programmed to die. This is a homeostasis event to eliminate the harmful and aging cells (Zakeri *et al.*, 1995). Apoptosis can also be induced by various agents, including reactive oxygen species (ROS). ROS is a by-product, which is being continuously produced during aerobic metabolism process (Benhar *et al.*, 2002). $H_2O_2$, is one

of the ROS, which was used in this study to treat the cancer cells to undergo oxidative stress-induced apoptosis.

In this study, it was shown that concentration of $H_2O_2$ ranging from 10 to 500 µM was sufficient to induce cells to undergo oxidative stress-induced apoptosis. Our IPCR result suggested that concentration of $H_2O_2$ of more than 1 mM might cause an extensive cleavage within the MLL bcr. After the optimisation, concentration of $H_2O_2$ of 50 µM was chosen to treat the leukaemia and nasopharyngeal carcinoma (NPC) cell lines for 8 hours. This concentration was chosen based on the obtained from the morphological observation and IPCR result. This observation is in line with another study done by Li *et al*. They found that when U937 cells were treated with $H_2O_2$, DNA was fragmented into high molecular weight (HMW) DNA. Increase in exogenous ROS could lead to the disturbance of the redox balance in the cells. This in turn, could lead to damage of the nuclear and mitochondrial DNA (mtDNA). Damage of the mitochondrial DNA causes the cellular respiration function affected. This in turn, leads to the increase production of ROS in the cells (Spitz *et al.*, 2004;Wallace, 1992), resembling the positive feedback mechanism.

### 6.1.2 Overexpression of Caspase-activated DNase (CAD) alone was insufficient to cleave chromosomal DNA.

A study done by Susin *et al*. (2002) showed that when cells were injected with exogenous CAD, chromatin were condensed and fragmented (Susin *et al.*, 2000). It has been well studied that CAD possesses intrinsic DNase activity (Liu *et al.*, 1999) and introduces double stranded breaks within the chromosomes (Liu *et al.*, 1998). It was initially thought that

overexpression of CAD could enhance cleavage within the MLL bcr. When the cells were treated with 50 μM of $H_2O_2$, apoptotic pathway will be initiated where caspase-3 is activated. Such activation could lead to activation of the exogenously overexpressed, as well as endogenous CAD. These activated CAD will in turn, cleave the MLL bcr. Due to the presence of abundance of CAD, there should be an increase in cleavage within the MLL bcr. However, from the result described in Chapter Two and Five, CAD was overexpressed as shown by Western blot, there was no enhancement of cleavage within the MLL bcr. This suggests that overexpression of exogenous CAD alone could not execute its DNase activity. This observation was supported by a study that overexpression of CAD alone, in the absence of its natural chaperone cum inhibitor, ICAD, was inactive (Enari *et al.*, 1998). It could be possible that the endogenous ICAD could not assist the proper folding of the exogenous CAD.

Both laboratory and clinical studies have shown that ICAD plays an important role in the formation of functional CAD. Zhang *et al.* (1998) showed that cell extracts prepared from DFF45 knockout mice, upon apoptotic induction, DNA fragmentation was not observed (Zhang *et al.*, 1998). A later finding demonstrated that esophageal carcinoma patients with low endogenous ICAD expression were diagnosed with poor prognosis (Konishi *et al.*, 2002). These show that the absence of ICAD could lead to absence of functional CAD.

### 6.1.3 Mutant ICAD, ICAD-Ldm did not inhibit the effect of CAD completely

As the native inhibitor of CAD, ICAD could bind to CAD and inhibit its DNase property. Besides working as inhibitor, ICAD is also functioning as the chaperone of CAD. During the

synthesis of the nascent polypeptide of CAD, ICAD binds to it to assist the proper folding of CAD. In other word, the presence of ICAD is essential for the production of functional CAD to execute its DNase activity. Thereafter, ICAD binds to CAD to form CAD/ICAD complex (Enari *et al.*, 1998; Halenbeck *et al.*, 1998; Zhang J *et al.*, 1998) in the absence of apoptotic stimuli. Upon receiving apoptotic stimuli, caspase-3 will be activated and subsequently lead to the cleavage of ICAD at 2 putative caspase-3 recognition sites, namely at amino acid positions 117 and 224. This will inactivate ICAD and release activated CAD (Sakahira *et al.*, 1998; Nagata, 2000). The freed CAD now could bind and cleave chromosomal DNA which leads to the formation of HMW DNA (Samejima *et al.*, 2001) and subsequently leads to internucleosomal DNA ladder formation (Enari *et al.*, 1998; Nagata, 2000).

When ICAD is mutated at the 2 putative caspase-3 recognition sites, ICAD-Ldm will not be inactivated upon the apoptotic induction as caspase-3 could not cleave these sites. It binds tightly to CAD and hence, the freely available activated CAD is absent (Enari *et al.*, 1998; McCarty *et al.*, 1999). It was hypothesised that, when ICAD-Ldm was overexpressed, upon oxidative stress induction, the activated endogenous CAD will bind to ICAD-Ldm and remain inactive. Due to the mutated caspase-3 recognition sites, ICAD-Ldm will be insensitive to caspase-3 cleavage.

Our result showed that, the overexpression of ICAD-Ldm did not reduce the cleavage within the MLL bcr. Cleaved MLL bcr fragments were detected. This observation tallied with another study which showed that, upon various apoptotic inductions, in the presence of ICAD-Ldm, cells became apoptotic (McIlroy *et al.*, 1999). This could be explained by the possibility that the exogenous ICAD-Ldm could not inhibit the activated endogenous CAD

efficiently. Lechardeur *et al.* (2004) suggested that majority of endogenous CAD coupled with endogenous ICAD (Lechardeur *et al.*, 2004). In this case, there might be insufficient exogenous ICAD to assist the correct folding of exogenously expressed CAD when exogenous ICAD-Ldm was overexpressed. The endogenous ICAD works as chaperone for the folding of the endogenous ICAD. Additionally, there was insufficient endogenous ICAD to work as chaperone of CAD when CAD alone was overexpressed. This could lead to the function of exogenous CAD being severely impaired without the presence of ICAD.

### 6.1.4 Wild type ICAD is essential for the production of functional CAD

From our result, when CAD was overexpressed in the absence of ICAD, CAD seems to be non functional. When ICAD-Ldm was overexpressed alone, it did not inhibit the activated endogenous CAD efficiently. As there is a possibility that the endogenous ICAD aids the correct folding of the endogenous CAD, so as the exogenous ICAD to work as a chaperone for the exogenous ICAD, thus the forth approach was designed. In this approach, the exogenous wild type ICAD was co-expressed with the exogenous CAD in a ratio of CAD to ICAD of 2 to 1. This is also to ensure that there were sufficient of ICAD for the production of functional CAD. With the presence of abundant functional CAD in the cells, when these cells underwent oxidative stress, they were activated and able to execute their DNase activity. From our Western blot result, when ICAD co-expressed with CAD, both ICAD and CAD protein were detected. When exogenous CAD alone was overexpressed, CAD protein was not detected even though the endogenous CAD protein was detected. These observations suggested that ICAD is essential for the correct folding of CAD. Without the presence of exogenous ICAD, exogenous CAD expressed was not folded properly and thus degraded

(Sakahira and Nagata, 2002). It has been shown in the IPCR result that, in the presence of ICAD, CAD could cleave the MLL bcr as being indicated with the decreased of the intact MLL bcr. This observation is in agreement with the study done by Enari *et al.* (1998). They found that, when CAD co-expressed with ICAD, the cell lysate showed strong DNase activity (Enari *et al.*, 1998).

In the presence of ICAD, ICAD binds to the nascent polypeptide chain of CAD during its synthesis. The CAD domain is immediately folded as soon as translational process starts from its mRNA. Besides ICAD, Hsp70 and Hsp40 are also involved in the folding of Cad. During the translation process, Hsp70 and Hsp40 bind to the elongating CAD at the C-terminal to assist the partial folding. This generates a "molten globule"-like status of CAD (Ewbank and Creighton, 1991; Kuwajima, 1989). ICAD will be in-charged in the subsequent event. As ICAD recognises the *quasi*native state of CAD (Sakahira and Nagata, 2002) through the C-terminal of CAD, it completes the folding of CAD polypeptide correctly (Liu *et al.*, 1997). CAD-ICAD complex is formed due to the ICAD's chaperon-like activity (Uegaki *et al.*, 2000).

### 6.1.5 Overexpression of wild type ICAD induces the overexproduction of endogenous CAD

From our Western blot result, it was found that when exogenous ICAD was overexpressed, endogenous CAD was overexpressed. This result suggested that the expression of ICAD is closely related to the expression of CAD as it works as its chaperone (Enari *et al.*, 1998; Uegaki *et al.*, 2000). This is an interesting finding where it suggested that overexpression of ICAD was sufficient to work as "cellular signal" to produce more functional endogenous

CAD. There is a possibility that these "cellular signal" could enhance the transcription of CAD mRNA and subsequently, translated to produce more CAD polypeptide chains. There was abundant ICAD-L to bind to these CAD polypeptide chains. Subsequently, ICAD-L assists the partially folded CAD to its complete conformation (Liu *et al.*, 1997)

### 6.1.6 Overexpression of the wild type ICAD, ICAD-L exogenously could inhibit the DNase activity of both the endogenous and exogenous CAD

As being described in Section 6.1.3 and 6.1.4, our result suggested that overexpression of exogenous ICAD is essential for the correct folding of the overexpressed exogenous CAD. ICAD possesses another important function, where it works as the natural inhibitor of CAD. Even though it has been shown that the ICAD-Ldm might not be able to bind to the freed endogenous CAD, the wild type ICAD, ICAD-L exhibited another characteristic of inhibition. From our result, exogenously expressed ICAD-L inhibited the activation of the endogenous CAD. It is clearly shown in the IPCR result that, the intensity of the intact MLL bcr band was increased when cells with ICAD-L overexpressed underwent oxidative stress-induced apoptosis. This could be explained by the presence of abundant ICAD to bind to the freed CAD upon apoptotic induction. It has been found that ICAD inhibits CAD through protein-protein interaction by binding to its CAD domain (Uegaki *et al.*, 2000). Both CAD and ICAD share a homologous domain, called the CAD/CIDE domain, which consists of about 80 amino acids at their N terminal (Inohara *et al.*, 1998; Mukae *et al.*, 1998). These homologous domains interact with each other to form a CAD/ICAD heterodimeric complex. This interaction is also important in leading to the correct folding of CAD (Otomo T *et al.*, 2000). On the other hand, when cells were co-expressed with CAD and ICAD, the cleavage within the MLL bcr was still detected. This is because there was abundant functional CAD present

in the cells. Even though the ICAD was present, the presence of both endogenous and exogenous CAD out-numbered the amount of ICAD existed in the cells.

### 6.1.7 Mutant CAD could not exhibit its DNase activity

The wild type CAD, in the presence of ICAD showed its DNase activity. When CAD which was mutated at its amino acid position 157, designated as CAD(k157Q), co-expressed with ICAD-L, fewer breaks were detected as compared to the wild type CAD co-expressed with ICAD-L. From the Western blot result, both CAD and ICAD proteins were detected in cells with CAD mutant, CAD(K157Q) co-expressed with ICAD. This result suggested that CAD(K157Q) protein was expressed in the presence of ICAD-L. Upon oxidative stess-induced apoptosis, CAD(K157Q) could not cleave the MLL bcr efficiently. Exogenously introduced CAD(K157Q) on its own, was not able to cleave DNA (Meiss *et al.*, 2001; Widlak *et al.*, 2003; Woo *et al.*, 2004) even though exogenous ICAD was cleaved by caspase-3 (Inohara *et al.*, 1999). Lys157 is located at the N-terminal of CAD. This amino acid at this location is crucial in maintaining the α-helix 4 structure of the protein even though it is not an active site. This mutation could cause CAD(K157Q) to lost its binding ability to the major groove of DNA as what the wild type protein did. Therefore, CAD(K157Q) was not able to form stable complex with the DNA (Woo *et al.*, 2004).

### 6.1.8 Possibility of involvement of other nucleases in cleaving the MLL bcr.

Upon apoptotic induction, cell die through caspase-dependent pathway (Enari *et al.*, 1998; Sakahira *et al.*, 1998). Cell death in caspase-independent manner was also observed (McCarthy *et al.*, 1997; Donovan M and Cotter TG, 2004; Saelens *et al.*, 2004). Reactive Oxygen Species (ROS) could induce cells to undergo apoptosis through caspase-independent

pathways. This tally with our result which showed that, regardless of absence or presence of caspase inhibitor, cleavage within the MLL bcr was detected. Carmody and Cotter (2000) had performed an *in vitro* study which showed that, when retinal cells were exposed to ROS even with the presence of caspase inhibitor, these cells became apoptotic and presented with a few apoptotic features. These features were phosphatidylserine (PS) exposure, DNA nicking and cell shrinkage which are the common features of apoptosis (Carmody and Cotter, 2000).

There might be other nuclease, besides CAD that could cleave the MLL bcr upon apoptotic stimuli as being shown by our result. Samejima *et al.* (2001) showed that oligonucleosomal DNA fragmentation was detected in nuclei extracted from CAD knockout, $CAD^{-/-}$ cells (Samejima *et al.*, 2001). Besides CAD, Endonuclease G, Endo G is also an apoptotic nuclease (Li *et al.*, 2001). Endo G is one of the nucleases found in mitochondria (Cote and Ruiz-Carrillo, 1993). This protein was released from mitochondria together with cytochrome C. When Endo G was incubated with purified nuclei, it caused DNA degradation (van Loo *et al.*, 2001). This DNase also possesses the ability to cleave various kind of nucleic acids, including double-stranded DNA, single-stranded DNA, single-stranded RNA, and RNA/DNA duplexes (Gerschenson *et al.*, 1995; Widlak *et al.*, 2001). When large amount of Endo G present, it cleaves in a nonspecific manner. However, at low concentration, Endo G cleaves DNA at more defined sites (Ohsato *et al.*, 2002).

Besides Endo G, another DNase that play a role in caspase-independent manner is Apoptotic-inducing Factor (AIF). Its cleaving leads to the formation of high molecular weight (HMW) DNA fragmentation (Susin *et al.*, 1999). Upon pro-apoptotic stimuli, AIF is released from mitochondria and caused type I nuclear condensation in a caspase-independent manner (Susin

*et al.*, 2000). Susin *et al.* (1999) also suggested that AIF is responsible for the DNA fragmentation process. Due to the fact that it lacks an intrinsic nuclease activity, it can perhaps activate an unknown nuclease. This unknown nuclease, in turn, cleaves chromosomal DNA (Susin *et al.*, 1999). Besides these possibilities, it could be possible that the caspase inhibition was insufficient. Hence, cleavage within the MLL bcr in the presence of caspase inhibitor was still detected.

### 6.1.9 Transfection is a stressful process for the cells

Throughout the whole study, CAD and/or ICAD were overexpressed in cancer cell lines through transient transfection. After obtaining the IPCR result, fuzzy and blurry bands were often observed. For DNA extracted from cells which did not undergo the transfection process, the IPCR bands obtained were clearer and more defined. This indicates that transient transfection process could contribute to the formation of fuzzy and blurry bands. Cartier *et al.* (2003) observed the movement of cationic polymer/DNA complexes (polyplexes) during transfection process by using electron microscope. The polyplexes were stained with uranyl acetate on a formvar-coated grid (Bremer and Rasquin, 1998). Formation of these polyplexes during the transfection process is a critical issue. The main concern was on the physicochemical properties of transfection active complexes as well as the internalisation process. In addition, calcium ion, which is an essential factor for the transfection process could be cytotoxic. This compound could lead to elevated number of damaged mitochondria regardless of presence or absence of DNA complexes (Cartier R *et al.*, 2003). Sakurai *et al.* showed that mitochondrial damage resulted in apoptosis as indicated by DNA ladder formation and externalisation of phosphatidylserine of plasma membrane (Sakurai *et al.*, 2001). Thus, the elevated number of damaged mitochondria seen during gene transfer may

indicate that the transfer process could exert certain level of damage to the cells. This could explain our observation that transfection process could be a stressful process for the cells and contributed to the background cleavage within the MLL bcr.

### 6.2 Conclusion and future work

Our result indicates that, $H_2O_2$ could cause mammalian cell lines, namely HeLa and SUNE1 cells to undergo oxidative stress-induced apoptosis. In the absence of exogenous ICAD, both wild type CAD and its mutant, hCAD(K157Q) were not functional. In the presence of ICAD, the functional CAD involves in the MLL bcr cleavage. hCAD(K157Q) is unable to cleave the MLL bcr. Exogenous ICAD-Ldm did not inhibit cleavage of the MLL bcr, indicating that ICAD-Ldm may not form complex with endogenous CAD. Unlike ICAD-Ldm, overexpression of exogenous ICAD reduced cleavage of the MLL bcr. Besides working as inhibitor, ICAD also works as CAD's chaperone. Exogenous ICAD enhances expression of endogenous CAD. Besides CAD, other nuclease may also be involved in MLL bcr cleavage through caspase-independent pathway. Overexpression of an unknown gene and the transfection process itself may also introduce stress to the cells.

Overexpression of ICAD that may induce the overexpression of endogenous CAD is an interesting finding. The presence of abundant of ICAD may improve prognosis of cancer patients. In this experiment, only two types of mammalian cell lines were studied. In future, other kind of mammalian cell lines could be tested to examine if similar result could be reproduced. Besides, involvement of CAD in cleaving other genes should also be studied. This is to gather more information to know the preference cleavage site of CAD in relation to the chromosomal structure. Breakpoints induced by CAD should be mapped through

conventional sequencing method. Paired End diTag (PET) method can be adapted to sequence larger fragments of approximately 5 to 10 kb. This method allows researcher to identify insertion and deletion with remarkable reproducibility. In order to further elucidate the role of CAD, endogenous CAD or ICAD could be "silenced" by using RNA interference, RNAi method. This could be a more promising method to study a particular gene of interest. These could further elucidate the contribution of CAD in chromosome rearrangement.

## REFERENCES


Abello, P.A., Buchman T.G., Bukley, G.B, & Fidler, S.A. (1994). Antioxidants modulate induction of programmed endothelial cell death (apoptosis) by endotoxin. *Arch Surg* 129:134-141.

Alnemri, E.S., Livingston, D.J., Nicholson, D.W., Salvesen, G., Thornberry, N.A., Wong, W.W. & Yuan, J. (1996). Human ICE/CED-3 protease nomenclature. *Cell* 87:171.

Ames, B.N., Shigenaga, M.K., & Hagen, T.M. (1993). Oxidants, antioxidants, and the degenerative diseases of aging. *Proc Natl Acad Sci U S A* 90:7915-7922.

Antunes, F. & Cadenas. E. (2000). Estimation of $H_2O_2$ gradients across biomembranes. *FEBS Lett* 475:121-126.

Antunes, F., Cadenas, E. & Brunk, U.T. (2001). Apoptosis induced by exposure to a low steady-state concentration of H2O2 is a consequence of lysosomal rupture. *Biochem J* 356:549-555.

Aplan, P.D. (2006). Causes of oncogenic chromosomal translocation. *Trends Genet.* 22:46-55.

Artandi, S.E. & DePinho, R.A. (2000). A critical role for telomeres in suppressing and facilitating carcinogenesis. *Curr. Opin. Genet. Dev.* 10:39-46.

Ashkenazi, A. & Dixit, V.M. (1998). Death receptors: Signaling and modulation. *Science* 281:1305-1308.

Benhar, M., Engelberg, D. & Levitzki. A. (2002). ROS, stress-activated kinases and stress signaling in cancer. *EMBO Rep.* 3:420-425.

Bernard, O. & Berger, R. (1995). Molecular basis of 11q23 rearrangements in hematopoietic malignant proliferations. *Genes Chromosomes Cance :* 13:75.

Betti, C.J., Villalobos, M.J., Diaz, M.O., & Vaughan, A.T.M. (2001). Apoptotic triggers initiate translocations within the MLL gene involving the nonhomologous endjoining repair system. *Cancer Res.* 61:4550-4555.

Betti, C.J., Villalobos, M.J., Diaz, M.O. & Vaughan, .A.T.M. (2003). Apoptotic stimuli initiate MLL-AF9 translocations that are transcribed in cells capable of division. *Cancer Res.* 63:1377-1381.

Birnboim, H.C. (1986). DNA strand breaks in human leukocytes induced by superoxide anion, hydrogen peroxide and tumor promoters are repaired slowly compared to breaks induced by ionizing radiation. *Carcinogenesis* 7:1511-1517.

Bradford, M.M. (1976). A rapid and sensitive method for the quantitation of microgram quantities of protein utilizing the principle of protein-dye binding. *Anal Biochem.* 72:248-254.

Branda, R.F., Sullivan, L.M., O'Neill, J.P., Falta, M.T., Nicles, J.A., Hirsch, B., Vacek, P.M. & Albertina, R.J. (1993). Measurement of HPRT mutant frequencies in T-lymphocytes from healthy human populations. *Mutat. Res.* 285:267-279.

Brar, S.S., Kennedy, T.P., Sturrock, A.B., Huecksteadt, T.P., Quinn, M.T., Whorton, A.R. & Hoidal, J.R. (2002). An NAD(P)H oxidase regulates growth and transcription in melanoma cells. *Am. J Physiol Cell Physiol* 282:C1212-C1224.

Bremer, F.M. & Rasquin, F. (1998). Histochemical localization of hyaluronic acid in vitreous during embryonic development. *Invest Ophthalmol. Vis. Sci* 39:2466-2469.

Broeker, P.L., Super, H.G., Thirman, M.J., Pomykala, H., Yonebayashi, Y., Tanabe, S., Zeleznik-Le, N., & Rowley, J.D. (1996). Distribution of 11q23 breakpoints within the MLL breakpoint cluster region in de novo acute leukemia and in treatment-related acute myeloid leukemia: correlation with scaffold attachment regions and topoisomerase II consensus binding sites. *Blood* 87:1912.

Budihardjo, I.H., Oliver, M., Lutter, X. & Luo, X.W. (1999). Biochemical pathways of caspase activation during apoptosis. *Annu. Rev. Cell Dev. Biol.* 15:269-290.

Burdon, R.H. (1995). Superoxide and hydrogen peroxide in relation to mammalian cell proliferation. *Free Radic. Biol. Med.* 18:794.

Burdon, R.H., Alliangana, D. & Gill, V. (1995). Hydrogen peroxide and the proliferation of BHK-21 cells. *Free Radic Res* 23:471-486.

Burdon, R.H., Gill, V., Boyd, P.A. & Rahim. R.A. (1996). Hydrogen peroxide and sequence-specific DNA damage in human cells. *FEBS Lett* 383:150-154.

Burks, R.T., Kessis, T.D., Cho, K.R., & Hedrick. L. (1994). Microsatellite instability in endometrial carcinoma. *Oncogene* 9:1163-1166.

Burmeister, T. & Thiel. E. (2001). Molecular genetics in acute and chronic leukemias. *J Cancer Res Clin Oncol.* 127:80-90.

Bustin, M. & Reeves, R. (1996). High-mobility-group chromosomal proteins: architectural components that facilitate chromatin function. *Prog. Nucleic Acid Res. Mol. Biol.* 54:35-100.

Cadet, J. & Berger, M. (1985). Radiation-induced decomposition of the purine bases within DNA and related model compounds. *Int. J Radiat. Biol Relat Stud. Phys. Chem Med* 47:127-143.

Cantoni, O., Guidarelli, A., Sestili, P., Mannello, F., Gazzanelli, G. & Cattabeni, F. (1994). Hydrogen peroxide cytotoxicity under conditions of normal or reduced catalase activity in $H_2O_2$-sensitive and -resistant Chinese hamster ovary (CHO) cell variants. *Toxicol. Lett* 73:193-199.

Cao, G., Pei, W., Lan, J., Stetler, R.A., Luo, Y., Nagayama, T., Graham, S.H., Yin, X.M., Simon, R.P., & Chen, J. (2001). Caspase-activated DNase/DNA fragmentation factor 40 mediates apoptotic DNA fragmentation in transient cerebral ischemia and in neuronal cultures. *J Neurosci.* 21:4678-4690.

Carmody, R.J. & Cotter, T.G. (2000). Oxidative stress induces caspase-independent retinal apoptosis in vitro. *Cell Death Differ.* 7:282-291.

Cartier, R., Velinova, M., Lehman, C., & Erdmann, B. & Reszka, R. (2003). Ultrastructural analysis of DNA complexes during transfection and intracellular transport. *The Journal of Histochemistry & Cytochemistry* 51:1237-1240.

Chance, B., Sies H., & Boveris A. (1979). Hydroperoxide metabolism in mammalian organs. *Physiol Rev.* 59:527-605.

Chandra, J., Samali, A. & Orrenius, S. (2000). Triffering and modulation of apoptosis by oxidative stress. *Free Radic Biol. Med.* 29:323-333.

Chien, G., Yuen, P.W., Kwong, D., & Kwong, Y.L. (2001). Comparative genomic hybridization analysis of nasopharygeal carcinoma: consistent patterns of genetic aberrations and clinicopathological correlations. *Cancer Genet. Cytogenet.* 126:63-67.

Chien, Y.C. & Chen, C.J. (2003). Epidemiology and etiology of nasopharyngeal carcinoma. *Cancer Reviews: Asia Pacific* 1:1-19.

Choi, W.S., Lee, E.H., Chung, C.W., Jung, Y.K., Jin, B.K., Kim, S.U., Oh, T.H., Saido, T.C., & Oh, Y.J. (2001). Cleavage of Bax is mediated by caspase-dependent or -independent calpain activation in dopaminergic neuronal cells: protective role of Bcl-2. *J Neurochem.* 77:1531-1541.

Clarke, A.R., Purdie, C.A., Harrison, D.J., Morris, R.G., Bird, C.C., Hooper, M.L., & Wyllie, A.H. (1993). Thymocyte apoptosis induced by p53-dependent and independent pathways. *Nature* 362:849-852.

Cohen, G.M. (1997). Caspases: the executioners of apoptosis. *Biochem J* 326 ( Pt 1):1-16.

Collins, E.C. & Rabbitts, T.H. (2002). The promiscuous MLL gene links chromosomal translocations to cellular differentiation and tumour tropism. *Trends Mol Med* 8:436-442.

Cote, J. & Ruiz-Carrillo, A. (1993). Primers for mitochondrial DNA replication generated by endonuclease G. *Science* 261:765-769.

Crawley, J.J. & Furge, K.A. (2002). Identification of frequent cytogenetic aberrations in hepatocellular carcinoma using gene-expression microarray data. *Genome Biol* 3:RESEARCH0075.

Cryns, V. & Yuan, J. (1998). Proteases to die for. *Genes Dev.* 12:1551-1570.

Dalluge, R., Haberland, A., Zaitsev, S., Schneider, M., Zastrow, H., Sukhorukov, G. & Bottger, M. (2002). Characterization of structure and mechanism of transfection-active peptide-DNA complexes. *Biochim Biophys Acta* 1576:45-52.

Degterev, A., Boyce, M., & Yuan J. (2003). A decade of caspases. *Oncogene* 22:8543-8567.

DeVore, R., Whitlock, J., Hainsworth, J.D. & Johnson, D.H. (1989). Therapy-related acute nonlymphocytic leukemia with monocytic features and rearrangement of chromosome 11q. *Ann. Intern. Med* 110:740-742.

Dimartino, J.F. & Cleary, M.L. (1999). MLL rearrangements in haematological malignancies: lessons from clinical and biological studies. *Br. J Haematol.* 106:614-626.

DiPietrantonio, A.M., Hsieh, T., & Wu, J.M. (1999). Activation of caspase 3 in HL-60 cells exposed to hydrogen peroxide. *Biochem Biophys Res Commun.* 255:477-482.

Donovan, M. & Cotter, T.G. (2004). Control of mitochondrial integrity by Bcl-2 family members and caspase-independent cell death. *Biochim Biophys Acta.* 1644:133-147.

Ellis, R.E., Yuan, J.Y., & Horvitz, H.R. (1991). Mechanisms and functions of cell death. *Annu. Rev. Cell Biol* 7:663-698.

Enari, M., Sakahira, H., Yokoyama, H., Okawa, K., Iwamatsu, A., & Nagata, S. (1998). A caspase-activated DNase that degrades DNA during apoptosis and its inhibitor ICAD. *Nature* 391:43-50.

Evan, G. & Littlewood, T. (1998). A matter of life and cell death. *Science* 281:1317-1322.

Ewbank, J.J. & Creighton, T.E. (1991). The molten globule protein conformation probed by disulphide bonds. *Nature* 350:518-520.

Fan, C.S., Wong, N., Leung, S.F., To, K.F., Lo, K.W., Lee, S.W., Mok, T.S., Johnson, P.J., & Huang, D.P. (2000). Frequent c-myc and Int-2 overrepresentations in nasopharyngeal carcinoma. *Hum Pathol.* 31:169-178.

Fang Y., Guan X., Guo Y., Sham J., Deng M., Liang, Q., Zhang, H., Zhou, H., & Trent, J. (2001). Analysis of genetic alterations in primary nasopharyngeal carcinoma by comparative genomic hybridization. *Genes Chromosomes Cancer.* 30:254-260.

Fang, W., Rivard, J.J., Ganser, J.A., LeBien, T.W., Nath, K.A., Mueller, D.L. & Behrens, T.W. (1995). Bcl-xL rescues WEHI 231 B lymphocytes from oxidant-mediated death following diverse apoptotic stimuli. *J Immunol* 155:66-75.

Felix, C.A., Winick, N.J., Negrini, M., Bowman, W.P., Croce, C.M. & Lange, B.J. (1993). Common region of ALL-1 gene disrupted in epipodophyllotoxin-related secondary acute myeloid leukemia. *Cancer Res* 53:2954-2956.

Fesus, L. (1991). Apoptosis: molecular mechanisms in programmed cell death. *Eur. J. Cell Biol.* 56:177.

Finkel, T. & Holbrook, N.J. (2000). Oxidants, oxidative stress and biology of aging. *Nature* 408:247.

Floyd, R.A. (1995). Measurement of oxidative stress *in vivo*. In *The oxygen paradox*. (Daview KJA & Ursini F, ed.). p. 89-103, Cleup University Press, Padova.

Friedenauer, S. & Berlet, H.H. (1989). Sensitivity and variability of the Bradford protein assay in the presence of detergents. *Anal Biochem* 178:263-268.

Garcia-Calvo, M., Peterson, E.P., Leiting, B., Ruel, R., Nicholson, D.W., & Thornberry, N.A. (1998). Inhibition of human caspases by peptide-based and macromolecular inhibitors. *J Biol Chem* 273:32608-32613.

Gerschenson, M., Houmiel, K.L. & Low, R.L. (1995). Endonuclease G from mammalian nuclei is identical to the major endonuclease of mitochondria. *Nucleic Acids Res* 23:88-97.

Gibbons, B., Katz, F.E., Ganly,P. & Chessells, J.M. (1990). Infant acute lymphoblastic leukaemia with t(11; 19). *Br. J Haematol.* 74:264-269.

Gonzalez-Zulueta, M., Ruppert, J.M., Tokino, K., Tsai, Y.C., Spruck, C.H., Miyao, N., Nichols, P.W., Hermann, G.G., Horn, T. & Steven, K. (1993). Microsatellite instability in bladder cancer. *Cancer Res* 53:5620-5623.

Gorman, A., McGowan, A. & Cotter, T.G. (1997). Role of peroxide and superoxide anion during tumour cell apoptosis. *FEBS Lett* 404:27-33.

Green, D.R. (2000). Apoptotic pathways: paper wraps stone blunts scissors. *Cell* 102:1-4.

Green, D.R. & Reed, J.C. (1998). Mitochondria and apoptosi. *Science* 281:1309-1312.

Gu, J., Dong, R.P., Zhang, C., McLaughlin, D.F., Wu, M.X. & Schlossman, S.F. (1999). Functional interaction of DFF35 and DFF45 with caspase-aWu,M.X.,and Schlossman,S.F.ctivated DNA fragmentation nuclease DFF40. *J. Biol. Chem.* 274:20762.

Gu, S.Y., Tang, W.P., Zeng, Y., Zhao, E.W., Deng, W.H. & Li, K. (1983). An epithelial cell line established from poorly differentiated nasopharyngeal carcinoma. *Chinese J. Cancer,* 2:272.

Halenbeck, R., MacDonald, H., Roulston, A., Chen, T.T., Conroy, L., & Williams, L.T. (1998). CPAN, a human nuclease regulated by the caspase-sensitive inhibitor DFF45. *Curr. Biol.* 8:537-540.

Halliwell, B. & Aruoma, O.I. (1991). DNA damage by oxygen-derived species. Its mechanism and measurement in mammalian systems. *FEBS Lett* 281:9-19.

Hanahan, D. & Weinberg, R.A. (2000). The hallmarks of cancer. *Cell* 100:57-70.

Hansson, M., Asea, A., Ersson, U., Hermodsson, S. & Hellstrand, K. (1996). Induction of apoptosis in NK cells by monocyte-derived reactive oxygen metabolites. *J. Immunol* 156:42-47.

Hars, E.S., Lyu, Y.L., Lin, C.P. & Liu, L.F. (2006). Role of apoptotic nuclease caspase-activated DNase in etoposide-induced treatment-related acute myelogenous leukemia. *Cancer Res* 66:8975-8979.

Hayashi, Y., Kobayashi, Y., Hirai, H., Hanada, R., Yamamoto, K., Abe, T., Sugita, K., Nakazawa, S., Suetake, N., Hoshino, H., Kuroume, T., Bessho, F., Hayakawa, H. & Takaku, F. (1988). Immunoglobulin heavy chain gene rearrangements and mixed lineage characteristics in acute leukemias with the 11;19 translocation. *Cancer* 61:712-720.

Hearne, C.M., Ghosh, S. & Todd, J.A. (1992). Microsatellites for linkage analysis of genetic traits. *Trends Genet.* 8:288-294.

Heim, S. & Mitelman, F. (1995). *Cancer Cytogenetics: Chromosomal and Molecular Aberrations of Tumor Cells*. 2nd Ed. New York: John Wiley & Sons.

Heim, S. & Mitelman, F. (1987). Cancer Cytogenetics. (Alan, R., ed.). pp. 224 - 261. Liss, Inc, New York.

Hildesheim, A. & Levine, P.H. (1993). Etiology of nasopharyngeal carcinoma: a review. *Epidemiol. Rev.* 15:466-485.

Ho, J.H.C. (1971). Recent Advances in Human Tumor Virology and Immunology. In *Genetic and environmental factors in nasopharyngeal carcinoma*. (Nakahara W., Nishioka K, & Hirayama T., ed.). p. 257-295. University of Tokyo Press, Tokyo.

Ho, J.H.C. (1972). Nasopharyngeal carcinoma (NPC). *Adv. Cancer Res.* 15:547-582.

Hsieh, S.Y., Liaw, S.F., Lee, S.N., Hsieh, P.S., Lin, K.H., Chu, C.M. & Liaw, Y.F. (2003). Aberrant caspase-activated DNase (CAD) transcripts in human hepatoma cells. *Br. J. Cancer* 88:210-216.

Hu, L.F., Eiriksdottir, G., Lebedeva, T., Kholodniouk, I., Alimov, A., Chen, F., Luo, Y., Zabarovsky, E.R., Ingvarsson, S., Klein, G. & Ernberg, I. (1996). Loss of heterozygosity on chromosome arm 3p in nasopharyngeal carcinoma. *Genes Chromosomes Cancer* 17:118-126.

Huang, D.P., Lo, K.W., van Hasselt, C.A., Woo, J.K., Choi, P.H., Leung, S.F., Cheung, S.T., Cairns, Sidransky, P. D. & Lee, J.C. (1994). A region of homozygous deletion on chromosome 9p21-22 in primary nasopharyngeal carcinoma. *Cancer Res* 54:4003-4006.

Huang, P., Ballal, K. & Plunkett, W. (1997). Biochemical characterization of the protein activity responsible for high molecular weight DNA fragmentation during drug-induced apoptosis. *Cancer Res* 57:3407-3414.

Hudson, M.M., Raimondi, S.C., Behm, F.G., & Pui, C.H. (1991). Childhood acute leukemia with t(11;19) (q23;p13). *Leukemia* 5:1064-1068.

Hui, A.B., Lo, K.W., Leung, S.F., Choi, P.H., Fong, Y., Lee, J.C. & Huang, D.P. (1996). Loss of heterozygosity on the long arm of chromosome 11 in nasopharyngeal carcinoma. *Cancer Res* 56:3225-3229.

Hui, A.B., Lo, K.W., Leung, S.F., Teo, P., Fung, M.K., To, K.F., Wong, N., Choi, P.H., Lee, J.C. & Huang, D.P. (1999). Detection of recurrent chromosomal gains and losses in primary nasopharyngeal carcinoma by comparative genomic hybridisation. *Int. J Cancer* 82:498-503.

Hui, A.B., Lo, K.W., Chan, S.Y., Kwong, J., Chan, A.S., & Huang, D.P. (2002). Absence of SDHD mutations in primary nasopharyngeal carcinomas. *Int. J Cancer* 97:875-877.

Hui, A.B., Lo, K.W., Kwong, J., Lam, E.C., Chan, S.Y., Chow, L.S., Chan, A.S., Teo, P.M. & Huang, D.P. (2003). Epigenetic inactivation of TSLC1 gene in nasopharyngeal carcinoma. *Mol Carcinog.* 38:170-178.

Hunger, S.P., Tkachuk, D.C., Amylon, M.D., Link, M.P., Carroll, A.J., Welborn, J.L., Willman, C.L., & Cleary, M.L. (1993). HRX involvement in de novo and secondary leukemias with diverse chromosome 11q23 abnormalities. *Blood* 81:3197-3203.

Hutchinson, F. (1985). Chemical changes induced in DNA by ionizing radiation. *Prog. Nucleic Acid Res Mol Biol* 32:115-154.

Inohara, N., Koseki, T., Chen, S., Benedict, M.A. & Nunez, G. (1999). Identification of regulatory and catalytic domains in the apoptosis nuclease DFF40/CAD. *J Biol Chem* 274:270-274.

Inohara, N., Koseki, T., Chen, S., Wu, X. & Nunez, G. (1998). CIDE, a novel family of cell death activators with homology to the 45 kDa subunit of the DNA fragmentation factor. *EMBO J.* 17:2526-2533.

Jacobson, M.D., Raff, M.C., & Weil, M. (1997). Programmed cell death in animal development. *Cell* 88:347-354.

Jeannel, D., Bouvier, G., & Huber, A. (1999). Nasopharyngeal carcinoma: an epidemiological approach to carcinogenesis. *Cancer Surv* 33:125-155.

Jen, J., Kim, H., Piantadosi, S., Liu, Z.F., Levitt, R.C., Sistonen, P., Kinzler, K.W., Vogelstein, B. & Hamilton, S.R. (1994). Allelic loss of chromosome 18q and prognosis in colorectal cancer. *N. Engl. J Med* 331:213-221.

Jia, W.H., Shao, J.Y., Feng, B.J., & Zeng, Y.X. (2003). Genetic component involved in nasopharyngeal carcinoma development. *Cancer Reviews: Asia Pacific* 1:31-49.

Johansson, B., Bardi, G., Heim, S., Mandahl, N., Mertens, F., Bak-Jensen, E., Andren-Sandberg, A. & Mitelman, F. (1992). Nonrandom chromosomal rearrangements in pancreatic carcinomas. *Cancer* 69:1674-1681.

Kakizuka, A. (1998). Protein precipitation: a common etiology in neurodegenerative disorders? *Trends Genet.* 14:396-402.

Kaneko, Y., Maseki, N., Takasaki, N., Sakurai, M., Hayashi, Y., Nakazawa, S., Mori, T., Sakurai, M., Takeda, T., Shikano, T. & Hiyoshi, Y. (1986). Clinical and hematologic characteristics in acute leukemia with 11q23 translocations. *Blood* 67:484-491.

Kaneko, Y., Shikano, T., Maseki, N., Sakurai, M., Sakurai, M., Takeda, T., Hiyoshi,Y., Mimaya, J. & Fujimoto, T. (1988). Clinical characteristics of infant acute leukemia with or without 11q23 translocations. *Leukemia* 2:672-676.

Kanno, S., Ishikawa, M., Takayanagi, M., Takayanagi, Y. & Sasaki, K. (1999). Exposure to hydrogen peroxide induces cell death via apoptosis in primary cultured mouse hepatocytes. *Biol Pharm. Bull.* 22:1296-1300.

Kasai, T., Ohguchi, K., Nakashima, S., Ito, Y., Naganawa, T., Kondo, N., & Nozawa, Y. (1998). Increased activity of oleate-dependent type phospholipase D during actinomycin D-induced apoptosis in Jurkat T cells. *J Immunol* 161:6469-6474.

Katoh, S., Mitsui, Y., Kitani, K. & Suzuki, T. (1999). Hyperoxia induces the neuronal differentiated phenotype of PC12 cells via a sustained activity of mitogen-activated protein kinase induced by Bcl-2. *Biochem J* 338 ( Pt 2):465-470.

Kawane, K., Fukuyama, H., Adachi, S.H.M., Copeland, N.G., Gilbert, D.J., Jenkins, N.A. & Nagata, S. (1999). Structure and promoter analysis of murine CAD and ICAD genes. *Cell Death Differ.* 6:745-752.

Khodarev, N.N., Bennett, T., Shearing, N., Sokolova, I., Koudelik, J., Walter, S., Villalobos, M. & Vaughan, A.T. (2000). LINE L1 retrotransposable element is targeted during the initial stages of apoptotic DNA fragmentation. *J. Cell. Biochem. 79*: 486-495.

Klebanoff S.J. (1988). Phagocytic cells: products of oxygen metabolism. *In* Inflammation: Basic Principles and Clinical Correlates. Gallin JI, Goldstein IM, & Synderman R, editors. Raven Press, New York, 391-444.

Koeffler, H.P., McCormick, F. & Denny, C. (1991). Molecular mechanisms of cancer. *West J Med* 155:505-514.

Konishi, S., Ishiguro, S.Y.H., Kudo, J., Terashita, Y., Sugiura, H., Koyama, H., Kimura, M., Sato, A. & Shinoda N. (2002). Decreased expression of *DFF45*/ICAD is correlated with a poor prognosis in patients with esophageal carcinoma. *Cancer* 95:2473-2478.

Korn, C., Scholz, S.R., Gimadutdinow, O., Pingoud, A. & Meiss, G. (2002). Involvement of conserved histidine, lysine and tyrosine residues in the mechanism of DNA cleavage by the caspase-3 activated DNase CAD. *Nucleic Acids Res* 30:1325-1332.

Korn, C., Scholz, S.R., Gimadutdinow, O., Lurz, R., Pingoud, A. & Meiss, G. (2005). Interaction of DNA fragmentation factor (DFF) with DNA reveals an unprecedented mechanism for nuclease inhibition and suggests that DFF can be activated in a DNA-bound state. *J Biol Chem* 280:6005-6015.

Krieser, R.J. & Eastman, A. (1998). The cloning and expression of human deoxyribonuclease II. A possible role in apoptosis. *J Biol Chem* 273:30909-30914.

Kuwajima, K. (1989). The molten globule state as a clue for understanding the folding and cooperativity of globular-protein structure. *Proteins* 6:87-103.

Le Beau, M.M., Albain, K.S., Larson, R.A., Vardiman, J.W., Davis, E.M., Blough, R.R., Golomb, H.M., & Rowley, J.D. (1986). Clinical and cytogenetic correlations in 63 patients with therapy-related myelodysplastic syndromes and acute nonlymphocytic leukemia: further evidence for characteristic abnormalities of chromosomes no. 5 and 7. *J Clin Oncol.* 4:325-345.

Lechardeur, D., Drzymala, L., Sharma, M., Zylka, D., Kinach, R., Pacia, J., Hicks, C., Usmani, N., Rommens, J.M., & Lukacs, G.L. (2000). Determinants of the nuclear localization of the heterodimeric DNA fragmentation factor (ICAD/CAD). *J Cell Biol* 150:321-334.

Lennon, S.V., Martin, S.J., & Cotter, T.G. (1991). Dose-dependent induction of apoptosis in human tumour cell lines by widely divergent stimuli. *Cell Prolif* 24:203-214.

Lennon, S.V., Kilfeather, S.A., Hallett, M.B., Campbell, A.K. & Cotter, T.G. (1992). Elevations in cytosolic free $Ca^{2+}$ are not required to trigger apoptosis in human leukaemia cells. *Clin Exp Immunol* 87:465-471.

Leroy, X., Leteurtre, E., Mahe, P.H., Gosselin, B., Delobel, B. & Croquette, M.F. (2002). Renal oncocytoma with a novel chromosomal rearrangement, der(13)t(13;16)(p11;p11), associated with a renal cell carcinoma. *J Clin Pathol.* 55:157-158.

Li, P.F., Dietz, R. & von Harsdorf, R. (1997). Reactive oxygen species induce apoptosis of vascular smooth muscle cell. *FEBS Lett* 404:252.

Li, L.Y., Luo, X. & Wang, X. (2001). Endonuclease G is an apoptotic DNase when released from mitochondria. *Nature* 412:95-99.

Li, T.K., Chen, A.Y., Yu, Mao, C.Y., Wang, H. & Liu. L.F. (1999). Activation of topoisomerase II-mediated excision of chromosomal DNA loops during oxidative stress. *Genes Dev.* 13:1553-1560.

Li, X., Wang, E., Zhao, Y.D., Ren, J.Q., Jin, P., Yao, K.T. & Marincola, F.M. (2006). Chromosomal imbalances in nasopharyngeal carcinoma: a meta-analysis of comparative genomic hybridization results. *J Transl. Med* 4:4.

Li, Z. & Zong, Y. (1999). Effects of LMP-1 expression on neoplastic cell proliferation and apoptosis in nasopharyngeal carcinoma. *Zhonghua Bing. Li Xue. Za Zhi.* 28:340-343.

Liu, X., Zou, H., Slaughter, C. & Wang, X. (1997). DFF, a heterodimeric protein that functions downstream of caspase-3 to trigger DNA fragmentation during apoptosis. *Cell* 89:174.

Liu, X., Li, P., Widlak, P., Zou, H., Luo, X., Garrard, W.T. & Wang, X. (1998). The 40-kDa subunit of DNA fragmentation factor induces DNA fragmentation and chromatin condensation during apoptosis. *Proc. Natl. Acad. Sci. U. S. A* 95:8461-8466.

Liu, X., Zou, H., Widlak, P., Garrard, W. & Wang, X. (1999). Activation of the apoptotic endonuclease DFF40 (caspase-activated DNase or nuclease). Oligomerization and direct interaction with histone H1. *J. Biol. Chem.* 274:13836-13840.

Lo, K.W. & Huang, D.P. (2002). Genetic and epigenetic changes in nasopharyngeal carcinoma. *Semin. Cancer Biol* 12:451-462.

Lo, K.W., Teo, P.M., Hui, A.B., To, K.F., Tsang, Y.S., Chan, S.Y., Mak, K.F., Lee, J.C. & Huang, D.P. (2000). High resolution allelotype of microdissected primary nasopharyngeal carcinoma. *Cancer Res* 60:3348-3353.

Lo, K.W., Tsao, S.W. & Huang, D.P. (1994). Detail deletion mapping on the short arm of chromosome 3 in nasopharyngeal carcinoma. *Proc. Am. Assoc. Cancer Res.* 35:571.

Lugovskoy, A.A., Zhou, P., Chou, J.J., McCarty, J.S., Li, P. & Wagner, G. (1999). Solution structure of the CIDE-N domain of CIDE-B and a model for CIDE-N/CIDE-N interactions in the DNA fragmentation pathway of apoptosis. *Cell* 99:747-755.

Lundqvist-Gustafsson, H. & Bengtsson, T. (1999). Activation of the granule pool of the NADPH oxidase accelerates apoptosis in human neutrophils. *J Leukoc. Biol* 65:196-204.

Mathiasen, I.S. & Jaattela, M. (2002). Triggering caspase-independent cell death to combat cancer. *Trends Mol Med* 8:212-220.

McCarthy, N.J., Whyte, M.K., Gilbert, C.S., Ivan, G.I. (1997). Inhibition of Ced-3/IDE-related proteases does not prevent cell death induced by oncogenes, DNA damage, or the Bcl-2 homologoue Bak. *J. Cell Biol.* 136:215-227.

McCarty, J.S., Toh, S.Y. & Li, P. (1999). Multiple domains of DFF45 bind synergistically to DFF40: Roles of caspase cleavage and sequestration of activator domain of DFF40. *Biochem. Biophys. Res. Commun.* 264:181-185.

McDermott, A.L., Dutt, S.N. & Watkinson, J.C. (2001). The aetiology of nasopharyngeal carcinoma. *Clin Otolaryngol. Allied Sci* 26:82-92.

McIlroy, D., Sakahira, H., Talanian, R.V. & Nagata, S. (1999). Involvement of caspase 3-activated DNase in internucleosomal DNA cleavage induced by diverse apoptotic stimuli. *Oncogene* 18:4401-4408.

Meiss, G., Scholz, S.R., Korn, C., Gimadutdinow, O., Knoblauch, M. & Pingoud, A. (2001). Identification of functionally relevant histidine residues in the apoptotic nuclease CAD. *Nucleic Acids Res.* 29:3901-3909.

Meneghini, R., & Martin, E.L. (1993). Hydrogen peroxide and DNA damage. In *DNA and Free Radicals*. (Halliwell B. and Aruoma, ed.). pp. 83 -93. Ellis Horwood.

Merlo, A., Gabrielson, E., Askin, F. & Sidransky, D. (1994). Frequent loss of chromosome 9 in human primary non-small cell lung cancer. *Cancer Res* 54:640-642.

Meyer, C., Kowarz, E., Schneider, B., Oehm, C., Klingebiel, T., Dingermann, T. & Marschalek, R. (2006). Genomic DNA of leukemic patients: target for clinical diagnosis of MLL rearrangements. *Biotechnol. J* 1:656-663.

Meza-Junco, J., Montano-Loza, A. & Aguayo-Gonzalez A. (2006). Molecular basis of cancer. *Rev. Invest Clin* 58:56-70.

Mirro, J., Kitchingman, G., Williams, D., Lauzon, G.J., Lin, C.C., Callihan, T. & Zipf, T.F. (1986). Clinical and laboratory characteristics of acute leukemia with the 4;11 translocation. *Blood* 67:689-697.

Mitelman, F., Mertens, F. & Johansson, B. (1997). A breakpoint map of recurrent chromosomal rearrangements in human neoplasia. *Nat. Genet.* 15 Spec No:417-474.

Mukae, N., Enari, M., Sakahira, H., Fukuda, Y., Inazawa, J., Toh, H. & Nagata, S. (1998). Molecular cloning and characterization of human caspase-activated DNase. *Proc. Natl. Acad. Sci. USA* 95:9123-9128.

Mukae, N., Yokoyama, H., Yokokura, T., Sakoyama, Y. & Nagata, S. (2002). Activation of the innate immunity in Drosophila by endogenous chromosomal DNA that escaped apoptotic degradation. *Genes Dev.* 16:2662-2671.

Murnane, J.P. (2006). Telomeres and chromosome instability. *DNA Repair (Amst)* 5:1082-1092.

Mutirangura, A., Pornthanakasem, W., Sriuranpong, V., Supiyaphun, P. & Voravud, N. (1998). Loss of heterozygosity on chromosome 14 in nasopharyngeal carcinoma. *Int. J Cancer* 78:153-156.

Mutirangura, A., Tanunyutthawongese, C., Pornthanakasem, W., Kerekhanjanarong, V., Sriuranpong, V., Yenrudi, S., Supiyaphun, P. & Voravud, N. (1997). Genomic alterations in nasopharyngeal carcinoma: loss of heterozygosity and Epstein-Barr virus infection. *Br. J Cancer* 76:770-776.

Mutirangura, A., Tanunyutthawongese, C., Kerekhanjanarong, V., Sriuranpong, V., Pornthanakasem, W., Yenrudi, S., Supiyaphun, P. & Voravud, N. (1996). Loss of heterozygosity for chromosome 11 in Epstein-Barr-virus associated nasopharyngeal carcinoma. *J Med Assoc. Thai.* 79 Suppl 1:S65-S70.

Nagata, S. (2005). DNA degradation in development and programmed cell death. *Annu. Rev. Immunol* 23:853-875.

Nagata, S., Nagase, H., Kawane, K., Mukae, N., & Fukuyamam, H. (2003). Degradation of chromosomal DNA during apoptosis. *Cell Death and Differentiation* 10:108-116.

Nagata, S. (2000). Minireview Apoptotic DNA Fragmentation. *Experimental Cell Research* 256:12-18.

Nagata, S. (1997). Apoptosis by death factor. *Cell* 88:365.

Netzer, W.J. & Hartl, F.U. (1998). Protein folding in the cytosol: chaperonin-dependent and -independent mechanisms. *Trends Biochem Sci* 23:68-73.

Nicholson, D.W. (1999). Caspase structure, proteolytic substrates, and function during apoptotic cell death. *Cell Death Differ.* 6:1028-1042.

Oberhammer, F., Wilson, J.W., Dive, C., Morris, I.D., Hickman, J.A., Wakeling, A.E., Walker, P.R. & Sikorska, M. (1993). Apoptotic death in epithelial cells: Cleavage of DNA to 300 and/or 50 kb fragments prior to or in the absence of internucleosoma fragmentation. *EMBO J.* 12:3679-3684.

Ohira, M., Kageyama, H., Mihara, M., Furuta,S., Machida, T., Shishikura, T., Takayasu, H., Islam, A., Nakamura, Y. & Takahashi, M. (2000). Identification and characterization of a 500-kb homozygously deleted region at 1p36.2-p36.3 in a neuroblastoma cell line. *Oncogene* 19:4302-4307.

Ohsato, T., Ishihara, N., Muta, Umeda, T. S., Ikeda, S., Mihara, K., Hamasaki, N. & Kang, D. (2002). Mammalian mitochondrial endonuclease G. Digestion of R-loops and localization in intermembrane space. *Eur. J Biochem* 269:5765-5770.

Otomo, T., Sakahira, H, Uegaki, K., Nagata, S. & Yamazaki, T. (2000). Structure of the heterodimeric complex between CAD domains of CAD and ICAD. *Nat. Struct. Biol.* 7: 658-662.

Pais, A., Amare, K.P., Raje, G., Sawant, M., Kabre, S., Jain, H., Advani, S. & Banavali, S. (2005). Identification of various MLL gene aberrations that lead to MLL gene mutation in patients with acute lymphoblastic leukemia (ALL) and infants with acute leukemia. *Leuk. Res* 29:517-526.

Parkin, D.M. & Muir, C.S. (1992). Cancer Incidence in Five Continents. Comparability and quality of data. *IARC Sci Publ.*45-173.

Parman, T., Wiley, M.J. & Wells, P.G. (1999). Free radical-mediated oxidative DNA damage in the mechanism of thalidomide teretogenicity. *Nat. Med.* 5:582-585.

Pearse, M.J., O'Bryan, M., Fisicaro, N., Rogers, L., Murphy, B. & d'Apice, A.J. (1992). Differential expression of clusterin in inducible models of apoptosis. . *Int. Immunol.* 4:1225-1231.

Pearson, G.R., Johansson, B., & Klein, G. (1978). Antibody-dependent cellular cytotoxicity against Epstein-Barr virus-associated antigens in African patients with nasopharyngeal carcinoma. *Int. J Cancer* 22:120-125.

Pearson, G.R., Neel, H.B., Weiland, L.H., Mulroney, S.E., Taylor, W., Goepfert, H., Huang, A., Levine, P., Lanier, A. & Pilch, B. (1984). Antibody-dependent cellular cytotoxicity and disease course in North American patients with nasopharyngeal carcinoma: a prospective study. *Int. J Cancer* 33:777-782.

Pearson, G.R., Weiland, L.H., Neel, H.B., Taylor, W., Earle, J., Mulroney, S.E., Goepfert, H., Lanier, A., Talvot, M.L., Pilch, B., Goodman, M., Huang, A., Levine, P.H., Hyams, V., Moran, E., Henle, G. & Henle, W. (1983). Application of Epstein-Barr virus (EBV) serology to the diagnosis of North American nasopharyngeal carcinoma. *Cancer* 51:260-268.

Pierce, G.B., Parchment, R.E. & Lewellyn, A.L. (1991). Hydrogen peroxide as a mediator of programmed cell death in the blastocyst. *Differentiation* 46:181-186.

Rabbitts, T.H. (1994). Chromosomal translocations in human cancer. *Nature* 372:143-149.

Raff, M. (1998). Cell suicide for beginners. *Nature* 396:119-122.

Raimondi, S.C. (1993). Current status of cytogenetic research in childhood acute lymphoblastic leukemia. . *Blood* 81:2237-2251.

Raimondi, S.C., Peiper, S.C., Kitchingman, G.R., Behm, F.G., Williams, D.L., Hancock, M.L. & Mirro Jr, J. (1989). Childhood acute lymphoblastic leukemia with chromosomal breakpoints at 11q23. *Blood* 73:1627-1634.

Rano, T.A., Timkey, T., Peterson, E.P., Rotonda, J., Nicholson, D.W., Becker, J.W., Chapman, K.T. & Thornberry, N.A. (1997). A combinatorial approach for determining protease specificities: application to interleukin-1beta converting enzyme (ICE). *Chem Biol* 4:149-155.

Ratain, M.J. & Rowley, J.D. (1992). Therapy-related acute myeloid leukemia secondary to inhibitors of topoisomerase II: from the bedside to the target genes. *Ann. Oncol.* 3:107-111.

Reh, S., Korn, C., Gimadutdinow, O. & Meiss, G. (2005). Structural basis for stable DNA complex formation by the caspase-activated DNase. *J Biol Chem* 280:41707-41715.

Rennstam, K., Baldetorp, B., Kytola, S., Tanner, M. & Isola, J. (2001). Chromosomal rearrangements and oncogene amplification precede aneuploidization in the genetic evolution of breast cancer. *Cancer Res* 61:1214-1219.

Rhee, S.G. (1999). Redox signaling: hydrogen peroxide as intracellular messenger. *Exp Mol Med* 31:53-59.

Rowley, J.D. (1993). Rearrangements involving chromosome band 11q23 in acute leukemia. *Cancer Biol.* 4:377-385.

Sabol, S.L., Li, R., Lee, T.Y. & Abdul-Khalek, R. (1999). Inhibition of apoptosis-associated DNA fragmentation activity in nonapoptotic cells: The role of DNA fragmentation factor-45 (DFF45/ICAD). *Biochem. Biophys. Res. Commun.* 253:151-158.

Saelens, X., Festjens, N., Vande, W.L., van Gurp, M., van Loo, G. & Vandenabeele, P. (2004). Toxic proteins released from mitochondria in cell death. *Oncogene* 23:2861-2874.

Sakahira, H. & Nagata, S. (2002). Co-translational folding of caspase-activated DNase with Hsp70, Hsp40, and inhibitor of caspase-activated DNase. *J Biol Chem* 277:3364-3370.

Sakahira, H., Takemura, Y. & Nagata, S. (2001). Enzymatic active site of caspase-activated DNase (CAD) and its inhibition by inhibitor of CAD. *Arch. Biochem. Biophys.* 388:91-99.

Sakahira, H., Iwamatsu, A., Nagata, S. (2000). Specific Chaperone-like Activity of Inhibitor of Caspase-activated DNase for Caspase-activated DNase. *J. Biol. Chem.* 275: 8091-8096.

Sakahira, H., Enari, M. & Nagata, S. (1999). Functional differences of two forms of the inhibitor of caspase-activated DNase, ICAD-L, and ICAD-S. *J Biol Chem* 274:15740-15744.

Sakahira, H., Enari, M., Ohsawa, Y., Uchiyama, Y. & Nagata, S. (1999). Apoptotic nuclear morphological change without DNA fragmentation. *Curr. Biol.* 9:543-546.

Sakahira, H., Enari, M. & Nagata, S. (1998). Cleavage of CAD inhibitor in CAD activation and DNA degradation during apoptosis. *Nature* 391:96-99.

Sakurai, K., Katoh, M., Someno, K. & Fujimoto, Y. (2001). Apoptosis and mitochondrial damage in INS-1 cells treated with alloxan. *Biol Pharm. Bull.* 24:876-882.

Salvesen, G.S. & Dixit, V.M. (1997). Caspases: intracellular signaling by proteolysis. *Cell* 91:443-446.

Samejima, K., Tone, S. & Earnshaw, W.C. (2001). CAD/DFF40 nuclease is dispensable for high molecular weight DNA cleavage and stage I chromatin condensation in apoptosis. *J Biol Chem* 276:45427-45432.

Samejima, K. & Earnshaw, W.C. (1998). ICAD/DFF regulator of apoptotic nuclease is nuclear. *Exp Cell Res.* 243:453-459.

Hemmer, S., Wasenius, V.M., Knuutila, S., Franssila, K. & Joensuu, H. (1999). DNA Copy Number Changes in Thyroid Carcinoma. *Am J Pathol.* 154(5):1539-1547.

Sanvicens, N., Gomez-Vicente, V., Masip, I., Messeguer, A. & Cotter, T.G. (2004). Oxidative stress-induced apoptosis in retinal photoreceptor cells is mediated by calpains and caspases and blocked by the oxygen radical scavenger CR-6. *J Biol Chem* 279:39268-39278.

Scholz, S.R., Korn, C., Gimadutdinow, O., Knoblauch, M., Pingoud, A. & Meiss, G. (2002). The effect of ICAD-S on the formation and intracellular distribution of a nucleolytically active caspase-activated DNase . *Nucleic Acids Research* Vol. 30:3045-3051.

Scovassi, A.I. & Torriglia, A. (2003). Activation of DNA-degrading enzymes during apoptosis. *Eur. J Histochem.* 47:185-194.

Sestili, P., Cattabeni, F. & Cantoni, O. (1995). Simultaneous determination of DNA double strand breaks and DNA fragment size in cultured mammalian cells exposed to hydrogen peroxide/histidine or etoposide with CHEF electrophoresis. *Carcinogenesis* 16:703-706.

Shanmugaratnam, K. & Sobin, L.H. (1993). The World Health Organization histological classification of tumours of the upper respiratory tract and ear. A commentary on the second edition. *Cancer* 71:2689-2697.

Shao, J.Y., Huang, X.M., Yu, X.J., Huang, L.X., Wu, Q.L., Xia, J.C., Wang, H.Y., Feng, Q.S. Ren, Z.F., Ernberg, I., Hu, L.F. & Zeng, Y.X. (2001). Loss of heterozygosity and its correlation with clinical outcome and Epstein-Barr virus infection in nasopharyngeal carcinoma. *Anticancer Res* 21:3021-3029.

Shao, J.Y., Li, Y.H., Wu, Q.L., Liang, X., Yu, X., Huang, L., Hou , J., Huang, X., Ernberg, I., Hu, L.F., & Zeng, Y. (2002). High frequency loss of heterozygosity on the long arm of chromosome 13 and 14 in nasopharyngeal carcinoma in Southern China. *Chinese Med. J.* 115:571-575.

Shao, J.Y., Wang, H.Y., Huang, X.M., Feng, Q.S., Huang, P., Feng, B.J., Huang, L.X., Yu, X.J., Li, J.T., Hu, L.F., Ernberg, I. & Zeng, Y.X. (2000). Genome-wide allelotype analysis of sporadic primary nasopharyngeal carcinoma from southern China. *Int. J Oncol.* 17:1267-1275.

Shiokawa, D. & Tanuma, S. (2001). Characterization of human DNase I family endonucleases and activation of DNase c during apoptosis. *Biochemistry* 40:432-152.

Sim, S.P. & Liu, L.F. (2001). Nucleolytic cleavage of the mixed lineage leukemia breakpoint cluster region during apoptosis. *J. Biol. Chem.* 276:31590-31595.

Simon, R., Desper, R., Papadimitriou, C.H., Peng, A., Alberts, D.S., Taetle, R., Trent, J.M. & Schaffer, A.A. (2000). Chromosome abnormalities in ovarian adenocarcinoma: III. Using breakpoint data to infer and test mathematical models for oncogenesis. *Genes Chromosomes Cancer* 28:106-120.

Smith, S., Hwang, J.Y., Banerjee, S., Majeed, A., Gupta, A. & Myung, K. (2004). Mutator genes for suppression of gross chromosomal rearrangements identified by a genome-wide screening in Saccharomyces cerevisiae. *Proc Natl Acad Sci U S A* 101:9039-9044.

Spitz, D.R., Azzam, E.I., Li, J.J. & Gius, D. (2004). Metabolic oxidation/reduction reactions and cellular responses to ionizing radiation: a unifying concept in stress response biology. *Cancer Metastasis Rev.* 23:311-322.

Stangel, M., Zettl, U.K., Mix, E., Zielasek, Toyka, J. K.V., Hartung, H.P. & Gold, R. (1996). H2O2 and nitric oxide-mediated oxidative stress induce apoptosis in rat skeletal muscle myoblasts. *J Neuropathol. Exp Neurol.* 55:36-43.

Stanulla, M., Wang, J., Chervinsky, D.S., Thandla, S. & Aplan, P.D. (1997). DNA cleavage within the MLL breakpoint cluster region is a specific event which occurs as part of higher-order chromatin fragmentation during the initial stages of apoptosis. *Mol. Cell. Biol.* 17:4070-4079.

Steinbeck, M.J., Kim, J.K., Trudeau, M.J., Hauschka, P.V. & Karnovsky, M.J. (1998). Involvement of hydrogen peroxide in the differentiation of clonal HD-11EM cells into osteoclast-like cells. *J Cell Physiol* 176:574-587.

Steller, H. (1995). Mechanisms and genes of cellular suicide. *Science 267* 267:1445-1449.

Stoscheck C.M. (1990). Increased uniformity in the response of the coomassie blue G protein assay to different proteins. *Anal Biochem.* 184:111-116.

Strissel, P.L., Strick, R., Rowley, J.D. & Zeleznik-Le, N.J. (1998). An in vivo topoisomerase II cleavage site and a DNase I hypersensitive site colocalize near exon 9 in the MLL breakpoint cluster region. *Blood* 92:3793-3803.

Stroh, C. & Schulze-Osthoff, K. (1998). Death by a thousand cuts: an ever increasing list of caspase substrates. *Cell Death Differ.* 5:997-1000.

Sun, X.M. & Cohen, G.M. (1994). $Mg^{2+}$-dependent cleavage of DNA into kilobase pair fragments is responsible for the initial degradation of DNA in apoptosis. *J Biol Chem* 269:14857-14860.

Sung, N.S., Zeng, Y. & Raab-Traub, N. (2000). Alterations on chromosome 3 in endemic and nonendemic nasopharyngeal carcinoma. *Int. J Cancer* 86:244-250.

Super, H.G., Strissel, P.L., Sobulo, O.M., Burian, D., Reshmi, S.C., Roe, B., Zeleznik, L., Diaz, M.O., & Rowley, J.D. (1997). Identification of complex genomic breakpoint junctions in the t(9;11) MLL-AF9 fusion gene in acute leukemia. *Genes Chromosomes Cancer* 20:185-195.

Super, H.J., McCabe, N.R., Thirman, M.J., Larson, R.A., Le Beau, M.M., Pedersen-Bjergaard, J., Philip, P., Diaz, M.O. & Rowley, J.D. (1993). Rearrangements of the MLL gene in therapy-related acute myeloid leukemia in patients previously treated with agents targeting DNA-topoisomerase II. *Blood* 82:3705-3711.

Susin, S.A., Daugas, E., Ravagnan, L., Samejima, K., Zamzami, N., Loeffler, M., Costantini, F.K.P., Irinopoulou, T., Prevost, M.C., Brothers, G., Mak, T.W., Penninger, J., Earnshaw, W.C. & Kroemer, G. (2000). Two distinct pathways leading to nuclear apoptosis. *J. Exp. Med.* 192:571-580.

Susin, S.A., Lorenzo, H.K., Zamzami, N., Marzo, I., Snow, B.E., Brothers, G.M., Mangion, J., Jacotot, E., Costantini, P., Loeffler, M., Larochette, N., Goodlett, D.R., Aebersold, R., Siderovski, D.P., Penninger, J.M. & Kroemer, G. (1999). Molecular characterization of mitochondrial apoptosis-inducing factor. *Nature* 397:441-446.

Talanian, R.V., Quinlan, C., Trautz, S., Hackett, M.C., Mankovich, J.A., Banach, D., Ghayur, T., Brady, K.D. & Wong, W.W. (1997). Substrate specificities of caspase family proteases. *J Biol Chem* 272:9677-9682.

ter Elst, A., Hiemstra, B.E., d.van, V, Kamminga, W., van der Veen, A.Y., Davelaar, I., Terpstra, P., Te Meerman, G.J., Gerbens, F., Kok, K. & Buys, C.H. (2006). Functional analysis of lung tumor suppressor activity at 3p21.3. *Genes Chromosomes Cancer* 45:1077-1093.

Thornberry, N.A. (1998). Caspases: key mediators of apoptosis. *Chem Biol* 5:R97-103.

Thornberry, N.A., Bull, H.G., Calaycay, J.R. Chapman, K.T., Howard, A.D., Kostura, M.J. Miller, D.K., Molineaux, S.M., Weidner, J.R., Aunins, J. (1992). A novel heterodimeric cysteine protease is required for interleukin-1 beta processing in monocytes. *Nature* 356:768-774.

Thornberry, N.A., Rano, T.A., Peterson, E.P., Rasper, D.M., Timkey, T., Garcia-Calvo, M. Houtzager, V.M., Nordstrom, P.A., Roy, S., Vaillancourt, J.P., Chapman, K.T. & Nicholson, D.W. (1997). A combinatorial approach defines specificities of members of the caspase family and granzyme B. Functional relationships established for key mediators of apoptosis. *J Biol Chem* 272:17907-17911.

Tkeshelashvili, L.K., McBride, T., Spence, K. & Loeb, L.A. (1992). Mutation spectrum of copper-induced DNA damage. *J Biol Chem* 267:13778.

Toh, S.Y., Wang, X. & Li, P. (1998). Identification of the nuclear factor HMG2 as an activator for DFF nuclease activity. *Biochem. Biophys. Res. Commun.* 250:598-601.

Ueda, N. & Shah, S.V. (1992). Endonuclease-induced DNA damage and cell death in oxidant injury to renal epithelial cells. *J Clin Invest* 90:2593-2597.

Uegaki, K., Otomo, T., Sakahira, H., Shimizu, M., Yumoto, N., Kyogoku, Y., Nagata, S. & Yamazaki T. (2000). Structure of the CAD domain of caspase-activated DNase and interaction with the CAD domain of its inhibitor. *J Mol Biol* 297:1121-1128.

Umanskaia, O.N., Bystritskii, A.A. & Razin, S.V. (2005). Chromosomal rearrangements breakpoints clusterization: is the clonal selection involved. *Mol Biol (Mosk)* 39:355-363.

Van de, C.M., Vandenabeele, P., Declercq, W., Van, D.B., van Loo, G., Molemans, F., Schotte, P., Van Criekinge, W., Beyaert, R. & Fiers, W. (1997). Characterization of seven murine caspase family members. *FEBS Lett* 403:61-69.

van Holde, K.E. (1989). *Chromatin*. Series in Molecular Biology. Springer-Verlag New York Inc., New York. 198-288.

van Loo, G., Schotte, P., van Gurp, M., Demol, H., Hoorelbeke, B., Gevaert, K., Rodriguez, I., Ruiz-Carrillo, A., Vandekerckhove, J., Declercq, W., Beyaert, R. & Vandenabeele, P. (2001). Endonuclease G: a mitochondrial protein released in apoptosis and involved in caspase-independent DNA degradation. *Cell Death Differ.* 8:1136-1142.

Vaux, D.L. & Korsmeyer, S.J. (1999). Cell death in development. *Cell* **96**:245-254.

Wallace, D.C. (1992). Mitochondrial genetics: a paradigm for aging and degenerative diseases? *Science* 256:628-632.

Wang, X. (2001). The expanding role of mitochondria in apoptosis. *Gene Dev* 15:2922-2933.

Widlak, P., Kalinowska, M., Parseghian, M.H., Lu, X., Hansen, J.C. & Garrard, W.T. (2005). The histone H1 C-terminal domain binds to the apoptotic nuclease, DNA fragmentation factor (DFF40/CAD) and stimulates DNA cleavage. *Biochemistry* 44:7871-7878.

Widlak, P., Lanuszewska, J., Cary, R.B. & Garrard, W.T. (2003). Subunit structures and stoichiometries of human DNA Fragmentation Factor proteins before and after induction of apoptosis. *J. Biol. Chem.* 278:26915-26922.

Widlak, P., Li, L.Y., Wang, X. & Garrard, W.T. (2001). Action of recombinant human apoptotic endonuclease G on naked DNA and chromatin substrates: cooperation with exonuclease and DNase I. *J Biol Chem* 276:48404-48409.

Widlak, P., Li, P., Wang, X. & Garrard, W.T. (2000). Cleavage Preferences of the Apoptotic Endonuclease DFF40 (Caspase-activated DNase or Nuclease) on Naked DNA and Chromatin Substrates. *J. Biol. Chem* 275:8226-8232.

Widlak, P. (2000). The DFF40/CAD endonuclease and its role in apoptosis. *Acta Biochim. Pol.* 47:1037-1044.

Wolf, B.B., Schuler, M., Echeverri, F. & Green, D.R. (1999). Caspase-3 is the primary activator of apoptotic DNA fragmentation via DNA fragmentation factor-45/inhibitor of caspase-activated DNase inactivation. *J Biol Chem* 274:30651-30656.

Woo, E.J., Kim, Y.G., Kim, M.S., Han, W.D., Shin, S., Robinson, H., Park, S.Y. & Oh, B.H. (2004). Structural mechanism for inactivation and activation of CAD/DFF40 in the apoptotic pathway. *Mol Cell.* 14:531-539.

Wu, L.T., Chu, C.C., Chung, J.G., Chen, C.H., Hsu, L.S., Liu, J.K. & Chen, S.C. (2004). Effects of tannic acid and its related compounds on food mutagens or hydrogen peroxide-induced DNA strands breaks in human lymphocytes. *Mutat. Res* 556:75-82.

Wyllie, A.H., Kerr, J.F.R. & Currie, A.R. (1980). Cell death: The significance of apoptosis. *Int. Rev. Cytol.* 68:251-306.

Yan, B., Wang, H., Peng, Y., Hu, Y., Wang, H., Zhang, X., Chen, Q., Bedford, J.S., Dewhirst, M.W., & Li, C.Y. (2006). A unique role of the DNA fragmentation factor in maintaining genomic stability. *Proc Natl Acad Sci U S A* 103:1504-1509.

Yu, M.C. & Henderson, B.E. (1996). Cancer Epidemiology and Prevention. *In* Nasopharyngel Cancer. Schottenfeld D. and Fraumeni J.F., editors. Oxford University Press, New York. 603-618.

Yuan, J., Shaham, S., Ledoux, S., Ellis, H.M. & Horvitz, H.R. (1993). The C. elegans cell death gene ced-3 encodes a protein similar to mammalian interleukin-1 beta-converting enzyme. *Cell. 1993 Nov 19;():-* 75:641-652.

Zakeri, Z., Bursch, W., Tenniswood, M., & Lockshin, R.A. (1995). Cell death: programmed, apoptosis, necrosis, or other? *Cell Death Differ.* 2:296.

Zhang, J., Liu, X., Scherer, D.C., van Kaer, L., Wang, X. & Xu, M. (1998). Resistance to DNA fragmentation and chromatin condensation in mice lacking the DNA fragmentation factor 45. *Proc. Natl. Acad. Sci. USA* 95:12480-12485.

Zhang, J.H. & Xu, M. (2000). DNA fragmentation in apoptosis. *Cell Res.* 10:205-211.

Zhou, P., Lugovskoy, A.A., McCarty, J.S., Li, P. & Wagner, G. (2001). Solution structure of DFF40 and DFF45 N-terminal domain complex and mutual chaperone activity of DFF40 and DFF45. *Proc. Natl. Acad. Sci. U. S. A* 98:6051-6055.

Zulian, G.B., Jotterand, B.M., Cabrol, C., Beris, P., Mermillod, B. & Alberto, P. (1993). Etoposide and secondary haematological malignancies: coincidence or causality? *Ann. Oncol.* 4:559-566.

http://www.biochem.northwestern.edu/

**APPENDIX A:**

**MAP OF PLASMID VECTORS**

## A.1 pTracer-EF/V5-HisB

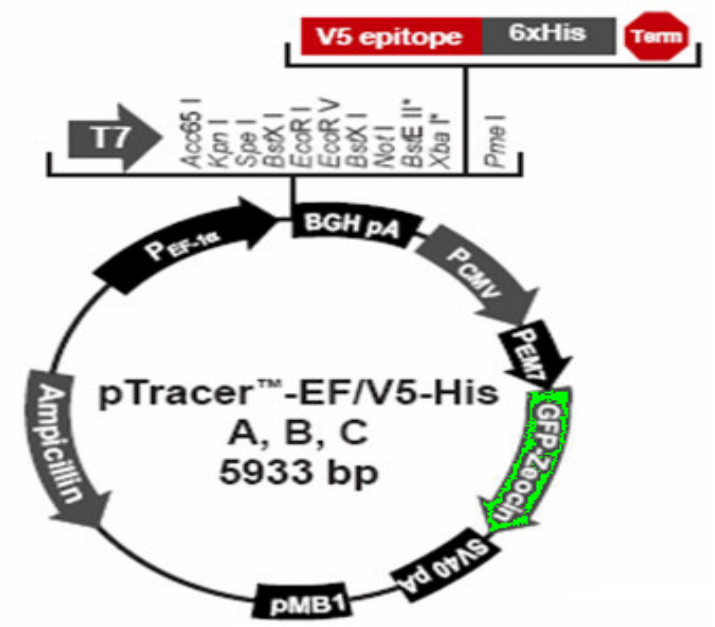


## A.2 pcDNA3.1/V5-His-TOPO

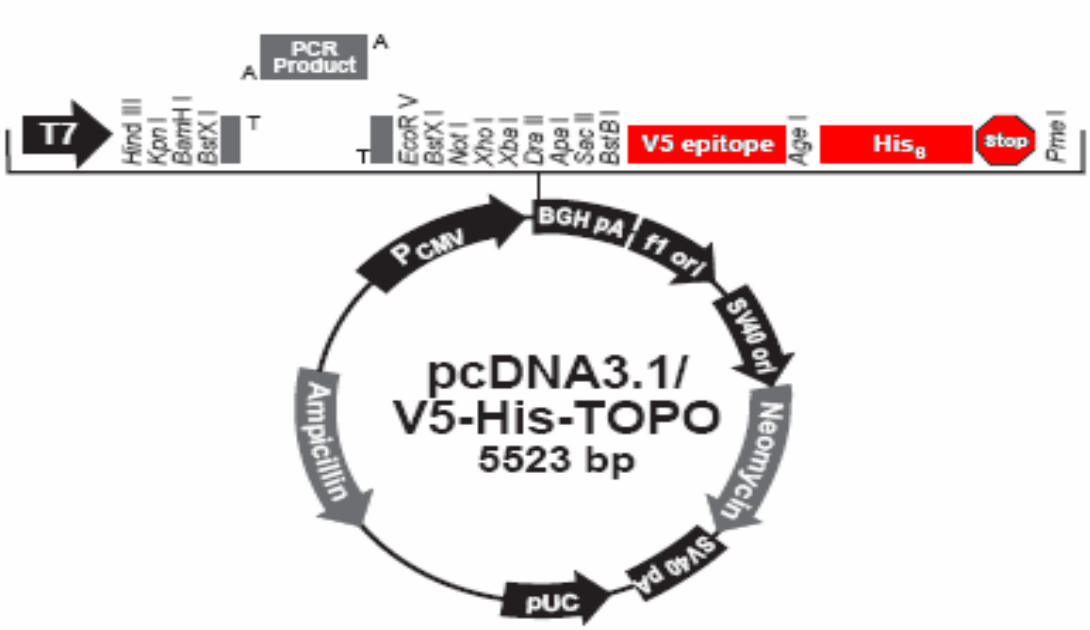

## APPENDIX B

## DNA SEQUENCES FROM GENBANK

Human Strain of Caspase-activated DNase (hCAD) Sequence From GenBank (AB013918)

```
GGTACCATGCTCCAGAAGCCCAAGAGCGTGAAGCTGCGGGCCCTGCGCAGCCCGAGGAAGTTCGGCGTGGCTGGCCGGAG 80

CTGCCAGGAGGTGCTGCGCAAGGGCTGTCTCCGCTTCCAGCTCCCTGAGCGCGGTTCCCGGCTGTGCCTGTACGAGGATG 160

GCACGGAGCTGACGGAAGATTACTTCCCCAGTGTTCCCGACAACGCCGAGCTGGTGCTGCTCACCTTGGGCCAGGCCTGG 240

CAGGGCTATGTGAGCGACATCAGGCGCTTCCTCAGTGCATTTCACGAGCCACAGGTGGGGCTCATCCAGGCCGCCCAGCA 320

GCTGCTGTGTGATGAGCAGGCCCCACAGAGGCAGAGGCTGCTGGCTGACCTCCTGCACAACGTCAGCCAGAACATCGCGG 400

CCGAGACCCGGGCTGAGGACCCGCCGTGGTTTGAAGGCTTGGAGTCCCGATTTCAGAGCAAGTCTGGCTATCTGAGATAC 480

AGCTGTGAGAGCCGGATCCGGAGTTACCTGAGGGAGGTGAGCTCCTACCCCTCCACGGTGGGTGCGGAGGCTCAGGAGGA 560

ATTCCTGCGGGTCCTCGGCTCCATGTGCCAGAGGCTCCGGTCCATGCAGTACAATGGCAGCTACTTCGACAGAGGAGCCA 640

AGGGCGGCAGCCGCCTCTGCACACCGGAAGGCTGGTTCTCCTGCCAGGGTCCCTTTGACATGGACAGCTGCTTATCAAGA 720

CACTCCATCAACCCCTACAGTAACAGGGAGAGCAGGATCCTCTTCAGCACCTGGAACCTGGATCACATAATAGAAAAGAA 800

ACGCACCATCATTCCTACACTGGTGGAAGCAATTAAGGAACAAGATGGAAGAGAAGTGGACTGGGAGTATTTTTATGGCC 880

TGCTTTTTACCTCAGAGAACCTAAAACTAGTGCACATTGTCTGCCATAAGAAAACCACCCACAAGCTCAACTGTGACCCA 960

AGCAGAATCTACAAACCCCAGACAAGGTTGAAGCGGAAGCAGCCTGTGCGGAAACGCCAGTCTAGA 1026
```

Human Strain of CAD mutant, hCAD(K157Q) – Modified from hCAD (AB013918) in GenBank

```
GGTACCATGCTCCAGAAGCCCAAGAGCGTGAAGCTGCGGGCCCTGCGCAGCCCGAGGAAGTTCGGCGTGGCTGGCCGGAG 80

CTGCCAGGAGGTGCTGCGCAAGGGCTGTCTCCGCTTCCAGCTCCCTGAGCGCGGTTCCCGGCTGTGCCTGTACGAGGATG 160

GCACGGAGCTGACGGAAGATTACTTCCCCAGTGTTCCCGACAACGCCGAGCTGGTGCTGCTCACCTTGGGCCAGGCCTGG 240

CAGGGCTATGTGAGCGACATCAGGCGCTTCCTCAGTGCATTTCACGAGCCACAGGTGGGGCTCATCCAGGCCGCCCAGCA 320

GCTGCTGTGTGATGAGCAGGCCCCACAGAGGCAGAGGCTGCTGGCTGACCTCCTGCACAACGTCAGCCAGAACATCGCGG 400

CCGAGACCCGGGCTGAGGACCCGCCGTGGTTTGAAGGCTTGGAGTCCCGATTTCAGAGCCAGTCTGGCTATCTGAGATAC 480

AGCTGTGAGAGCCGGATCCGGAGTTACCTGAGGGAGGTGAGCTCCTACCCCTCCACGGTGGGTGCGGAGGCTCAGGAGGA 560

ATTCCTGCGGGTCCTCGGCTCCATGTGCCAGAGGCTCCGGTCCATGCAGTACAATGGCAGCTACTTCGACAGAGGAGCCA 640

AGGGCGGCAGCCGCCTCTGCACACCGGAAGGCTGGTTCTCCTGCCAGGGTCCCTTTGACATGGACAGCTGCTTATCAAGA 720

CACTCCATCAACCCCTACAGTAACAGGGAGAGCAGGATCCTCTTCAGCACCTGGAACCTGGATCACATAATAGAAAAGAA 800

ACGCACCATCATTCCTACACTGGTGGAAGCAATTAAGGAACAAGATGGAAGAGAAGTGGACTGGGAGTATTTTTATGGCC 880

TGCTTTTTACCTCAGAGAACCTAAAACTAGTGCACATTGTCTGCCATAAGAAAACCACCCACAAGCTCAACTGTGACCCA 960

AGCAGAATCTACAAACCCCAGACAAGGTTGAAGCGGAAGCAGCCTGTGCGGAAACGCCAGTCTAGA 1026
```

Mouse Strain of Caspase-activated DNase (mCAD) Sequence From GenBank (AB009377)

GATATCATGTGCGCGGTGCTCCGCCAACCCAAATGCGTCAAGTTGCGAGCCCTACATAGCGCCTGCAAGTTCGGCGTGGC 80

GGCCCGGAGCTGCCAGGAGCTGCTGCGTAAGGGCTGCGTCCGCTTCCAGCTCCCGATGCCCGGTTCCCGGCTGTGCCTGT 160

ACGAAGATGGCACGGAGGTGACGGACGACTGCTTCCCGGGCCTTCCCAACGACGCTGAGCTCCTATTGCTCACCGCTGGC 240

GAGACCTGGCATGGCTATGTGAGTGACATCACACGTTTCCTCAGTGTGTTTAATGAGCCACATGCCGGCGTCATCCAGGC 320

TGCACGGCAACTGCTGTCAGATGAGCAGGCCCCACTGAGGCAAAAGCTGCTGGCCGATCTTCTGCATCACGTGAGCCAGA 400

ATATTACTGCAGAGACCCGGGAGCAGGACCCATCCTGGTTTGAAGGTTTGGAGTCGAGATTCAGGAATAAGTCGGGCTAT 480

CTGAGATACAGCTGTGAGAGTCGGATCCGGGGTTACCTAAGAGAGGTGAGCGCTTACACCTCTATGGTGGATGAAGCAGC 560

TCAAGAAGAGTACCTGCGAGTCCTTGGCTCCATGTGCCAGAAGCTCAAATCGGTGCAGTACAATGGCAGCTATTTCGACA 640

GAGGTGCAGAGGCCAGCAGCCGCCTCTGTACTCCAGAAGGATGGTTCTCCTGCCAGGGCCCCTTTGACCTGGAGAGCTGT 720

CTTTCCAAGCACTCCATCAACCCCTATGGCAACAGAGAGAGCCGGATCCTCTTCAGTACCTGGAACCTGGATCATATAAT 800

AGAGAAGAAGCGCACCGTGGTACCCACGCTGGCTGAAGCCATCCAGGATGGGAGGGAGGTGAACTGGGAGTACTTCTACA 880

GCCTGCTCTTCACTGCCGAGAACCTGAAGCTGGTGCACATCGCCTGCCACAAGAAGACCACACACAAGCTGGAGTGCGAC 960

CGCAGTAGGATCTATCGGCCTCAGACAGGATCCAGGAGGAAGCAGCCTGCTCGGAAGAAGCGCCCTGCTCGGAAGCGCTA 1040

GTGAGAATTCCTGCAGCCCGGGGGATCCACTCTAGA 1076

Mouse Strain of Inhibitor of Caspase-activated DNase (mICAD-L) Sequence From GenBank

(AB009375)

ATGGAGCTGTCGCGGGGAGCCAGCGCCCCAGACCCGGACGATGTCCGGCCTCTCAAACCGTGTCTGCTACGCCGCAACCA 80

CAGCCGCGATCAGCACGGCGTGGCAGCCTCCAGTCTCGAGGAGCTGAGGAGCAAAGCCTGTGAACTCCTGGCCATTGATA 160

AGTCCCTGACGCCGATCACCCTGGTCCTGGCTGAGGACGGGACCATAGTGGATGACGATGACTACTTCCTCTGCCTTCCT 240

TCCAATACGAAGTTTGTGGCGTTGGCCTGCAATGAGAAGTGGACTTATAATGATTCCGATGGAGGGACGGCTTGGGTTTC 320

CCAAGAGTCCTTTGAGGCAGATGAGCCGGACAGCAGGGCAGGGGTGAAGTGGAAGAATGTGGCCAGGCAGCTGAAAGAAG 400

ATCTGTCCAGCATCATCCTGCTGTCAGAAGAGGACCTCCAAGCGCTCATCGACATCCCATGTGCAGAGCTGGCTCAGGAA 480

CTCTGCCAAAGCTGTGCCACTGTCCAGGGGCTGCAGAGCACACTCCAGCAGGTGCTTGACCAGAGAGAGGAAGCCCGCCA 560

GTCCAAGCAGCTCCTGGAACTTTACCTCCAGGCCTTGGAGAAAGAGGGCAACATCTTGTCCAACCAGAAAGAGTCCAAAG 640

CTGCCCTCAGTGAAGAGCTGGATGCAGTTGACACAGGCGTCGGCAGAGAGATGGCTTCGGAAGTGCTGCTCAGAAGCCAG 720

ATCCTTACCACACTGAAGGAGAAGCCTGCCCCAGAGCTGAGTTTATCTAGTCAGGATTTGGAGTCTGTCTCCAAGGAGGA 800

TCCCAAAGCCCTGGCTGTCGCTCTGAGCTGGGACATAAGGAAGGCAGAGACAGTCCAGCAGGCCTGCACCACGGAGCTCG 880

CCCTGCGGCTGCAGCAAGTGCAGAGCTTGCATTCACTCAGGAATCTATCAGCAAGGAGGAGCCCACTGCCTGGGGAACCA 960

CAGCGACCCAAACGAGCCAAACGAGACTCCTCGTAG 996

Mouse Strain of Inhibitor of Caspase-activated DNase double mutant (mICAD-Ldm)

Sequence – Modified from mICAD-Ldm (AB009375) in GenBank

```
ATGGAGCTGTCGCGGGGAGCCAGCGCCCCAGACCCGGACGATGTCCGGCCTCTCAAACCGTGTCTGCTACGCCGCAACCA 80

CAGCCGCGATCAGCACGGCGTGGCAGCCTCCAGTCTCGAGGAGCTGAGGAGCAAAGCCTGTGAACTCCTGGCCATTGATA 160

AGTCCCTGACGCCGATCACCCTGGTCCTGGCTGAGGACGGGACCATAGTGGATGACGATGACTACTTCCTCTGCCTTCCT 240

TCCAATACGAAGTTTGTGGCGTTGGCCTGCAATGAGAAGTGGACTTATAATGATTCCGATGGAGGGACGGCTTGGGTTTC 320

CCAAGAGTCCTTTGAGGCAGATGAGCCGGAAAGCAGGGCAGGGGTGAAGTGGAAGAATGTGGCCAGGCAGCTGAAAGAAG 400

ATCTGTCCAGCATCATCCTGCTGTCAGAAGAGGACCTCCAAGCGCTCATCGACATCCCATGTGCAGAGCTGGCTCAGGAA 480

CTCTGCCAAAGCTGTGCCACTGTCCAGGGGCTGCAGAGCACACTCCAGCAGGTGCTTGACCAGAGAGAGGAAGCCCGCCA 560

GTCCAAGCAGCTCCTGGAACTTTACCTCCAGGCCTTGGAGAAAGAGGGCAACATCTTGTCCAACCAGAAAGAGTCCAAAG 640

CTGCCCTCAGTGAAGAGCTGGATGCAGTTGAAACAGGCGTCGGCAGAGAGATGGCTTCGGAAGTGCTGCTCAGAAGCCAG 720

ATCCTTACCACACTGAAGGAGAAGCCTGCCCCAGAGCTGAGTTTATCTAGTCAGGATTTGGAGTCTGTCTCCAAGGAGGA 800

TCCCAAAGCCCTGGCTGTCGCTCTGAGCTGGGACATAAGGAAGGCAGAGACAGTCCAGCAGGCCTGCACCACGGAGCTCG 880

CCCTGCGGCTGCAGCAAGTGCAGAGCTTGCATTCACTCAGGAATCTATCAGCAAGGAGGAGCCCACTGCCTGGGGAACCA 960

CAGCGACCCAAACGAGCCAAACGAGACTCCTCGTAG 996
```

**APPENDIX C:**

**QIAquick GEL EXTRACTION KIT (QIAGEN) PROTOCOL**

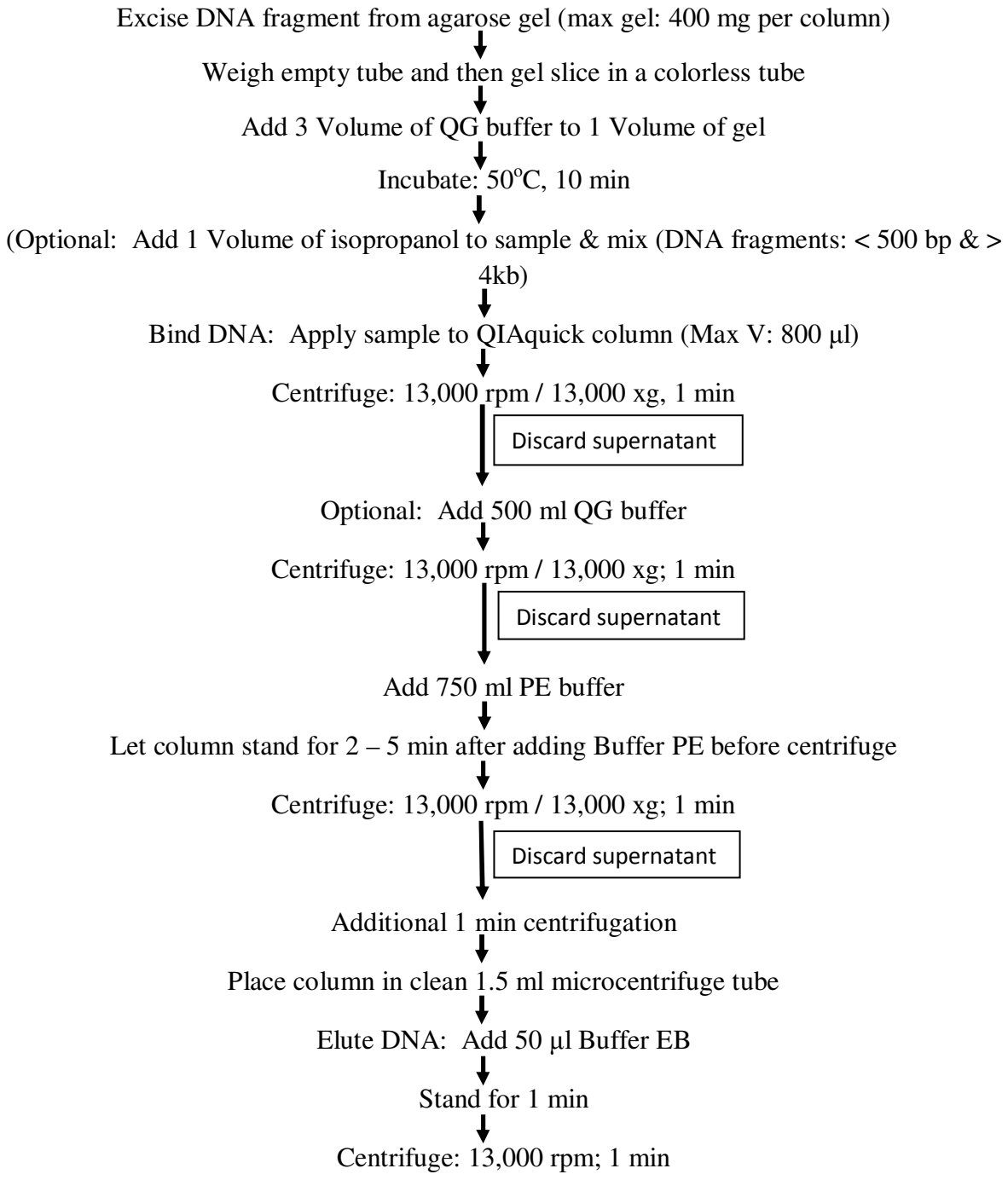

## APPENDIX D

### PREPARATION OF ELECTROCOMPETENT CELLS (*E. COLI* HB101)

1. Select single colony and grow 5 ml starter culture O/N at 37 $^{o}$C (200-250 rpm).
2. Inoculate 500 ml of LB media and place culture in 37 $^{o}$C shaker. (*Note: 500 ml culture can be separated into 3 flasks each containing 170 ml of LB media)*
3. Measure $OD_{600}$ every 45 min-1 hr (usually after 2 hr incubation). When $OD_{600}$ equals 0.6-0.9 (log phase). Remove cells from shaker and place on ice.
4. Split the 500 ml culture into 10 equal parts by pouring 50 ml of culture into each chilled 50 ml tube.
5. Spin (in centrifuge Eppondorf 5810 R) at 4,000 rpm, 25 min at 4 $^{o}$C.
6. Place tubes on ice. Remove supernatant immediately and gently resuspend each pellet in 40 ml ice-cooled $dH_2O$.
7. Spin (in centrifuge Eppondorf 5810 R) at 4,000 rpm, 25 min at 4 $^{o}$C.
8. Place tubes on ice. Remove supernatant immediately and gently resuspend each pellet in 20 ml ice-cooled $dH_2O$.
9. Pool the 10 tubes of culture into 5 tubes each containing 40 ml of culture
10. Spin (in centrifuge Eppondorf 5810 R) at 4,000 rpm, 25 min at 4 $^{o}$C.
11. Place tubes on ice. Remove supernatant immediately and gently resuspend each pellet in 8 ml ice-cooled 10% glycerol.
12. Pool 5 tubes into 1 tube (1 tube = 40 ml).
13. Spin (in centrifuge Eppondorf 5810 R) at 4,000 rpm, 10 min at 4 $^{o}$C.
14. Place tubes on ice. Remove supernatant immediately and gently resuspend each pellet in 1 ml ice-cooled 10% glycerol. Final $OD_{600}$ of resuspend cells ~ 200-250.

15. With cell-suspensions on ice, prepare 50-70 ml of cells in pre-chilled 1.5 ml tubes. Snap freeze tubes containing cells and store at -80 $^{o}$C.

## APPENDIX E

## ELECTROPORATION PROTOCOL

1 ng/µl of plasmid (in TE pH 8.0) [recommended 1 ng in 1-10 µl] (from ligation)

↓

Add 2 µl of plasmid into 50 µl electrocompetant HB101

(Add the plasmid within ≤ 5 min after take out from the -86°C freezer)

↓

Chill on ice for < 1 min prior to electroporation (or electroporate directly)

↓ Pipette the ligation mixture & competent cells into the electroporation cuvette

Electroporation (press pulse button twice)

Chamber Gap: BTX Disposable Cuvette P/N 610 (1 mm gap) [Eppendorf]

Charging Voltage: 2,000 V

Desired Fired Strength: 20 kV/cm

Desired Pulse Length: 5-6 msc (fixed)

↓

Add in 700 µl of pre-warmed SOC medium (37°C, ~30 min) and suspend immediately

↓

Transfer to clean tube and incubate at 37°C for ~1 hr 30 min, ~200 rpm

(Use snap cap culture tube)

↓

Spread the culture on LB-Ampicillin plate (50 µg/ml)

(30, 60 and 100 µl in each LB agar plate)

↓

Incubate at 37°C O/N (≤16 hr)

## APPENDIX F

## QUICK-CHECK (PHENOL/CHLOROFORM/ISOAMYL ALCOHOL EXTRACTION) PROTOCOL

*Quick-check determine which single colony contained the plasmid with expected insert*

Phenol/chloroform/isoamyl alcohol - thaw at 37$^{o}$C waterbath

↓

Spin at 2000 rpm, 3 min, room temperature (Eppendorf 5810)

↓

Spin down 1 ml of bacterial culture 4000 rpm, 3 min

↓

Pipette away 900 µl supernatant, left 100 µl of bacteria culture

↓

Add 100 µl phenol/chloroform/isoamyl alcohol

↓

Vortex vigorously until homogeneous (2200/min, 1 min)

↓

Centrifuge: max speed, 14,000 rpm, 5 min

↓

Load 10 µl of clear supernatant for gel electrophoresis

Add 3 µl 6X loading dye

## APPENDIX G

## SNAP MINIPREP KIT (INVITROGEN) PROTOCOL

**1. Lysis & Precipitation**

Centrifuge 1-3 ml Overnight bacteria culture to pellet cells

↓

Resuspend cell pellet in 150 µl of Resuspension Buffer (4°C)

↓ Vortex / Pipetting up and down

Add 150 µl of Lysis Buffer and mix gently (invert 5-6x)

↓

Incubate 3 min at RT

↓

Add 150 µl of ice-cold Precipitation Salt (4°C) [invert 6-8x]

↓

Centrifuge at 14,000 xg, RT for 5 min

↓

**2. Plasmid Binding**

Pipette supernatant into a sterile tube

↓ Discard gelatinous

Add 600 µl of Binding Buffer (mix by inverting 5-6x)

↓

Pipette/pour entire solution into the SNAP miniprep column

↓

Centrifuge SNAP miniprep column/collection tube (1,500 rcf, RT, 30 sc)

↓ Discard

Add 500 µl of Wash Buffer

↓ Discard flow

Centrifuge SNAP miniprep column/collection tube (1,500 rcf, RT, 30 sc)

↓ Discard flow

Add 900 µl of 1x Final Wash

↓

Centrifuge at 1,500 rcf, RT , 30 sc

↓ Discard flow

Centrifuge SNAP Miniprep column (max speed, room temperature, 1 min)

**3. Plasmid Elution**

Transfer SNAP miniprep column to the sterile microcentrifuge tube

Add 50 µl of TE buffer pH 8.0 directly onto the resin

Incubate 3 min at RT

Centrifuge SNAP miniprep column/sterile new tube

(max speed, room temperature, 30 seconds)

Remove and discard column

## APPENDIX H

## DYENamic ET TERMINATOR CYCLE SEQUENCING KIT (AMERSHAM) PROTOCOL

| | Forward Reaction (µl) | Reverse Reaction (µl) |
|---|---|---|
| DNA Template | 2 | 2 |
| Forwar primer | 2 | - |
| Reverse primer | - | 2 |
| SUPW | 2 | 2 |
| Sequencing premix | 4 | 4 |
| **Total** | **10** | **10** |

Mix contents thoroughly by gentle pipetting

↓

Centrifuge briefly (bring contents to the bottom of the tubes)

↓

Place in thermocycler

↓

Programme: 95°C, 20 sc
50°C, 15 sc
60°C, 60 sc
} 25 cycles (~1 hr)

↓

Add 1 µl (1/10V) of sodium acetate/EDTA buffer into new 1.5 ml tube

↓

Add 80 µl of 95% ethanol & mix well

↓

Incubate on ice for 15 min

↓

Centrifuge at ~12,000 rpm, R.T. for 15 min

↓

Remove supernatant by aspiration

↓

Add 300 µl of 70% ethanol

↓

Centrifuge at ~12,000 rpm, R.T. for 5 min

↓

Remove supernatant

↓

Air dry (preferably) or vacuum-dry (in a vacuum centrifuge 2 – 5 min)

# APPENDIX I

## SEQUENCING RESULT

Sequencing Result for Plasmid pTracer-hCAD

AGTCCCGATTTCAGAGCAAGTCTGGCTATCTGAGATACAGCTGTGAGAGCCGGATCCGGAGTTACCTGAGGGAGGTGAGC 80

TCCTACCCCTCCACGGTGGGTGCGGAGGCTCAGGAGGAATTCCTGCGGGTCCTCGGCTCCATGTGCCAGAGGCTCCGGTC 160

CATGCAGTACAATGGCAGCTACTTCGACAGAGGAGCCAAGGGCGGCAGCCGCCTCTGCACACCGGAAGGCTGGTTCTCCT 240

GCCAGGGTCCCTTTGACATGGACAGCTGCTTATCAAGACACTCCATCAACCCCTACAGTAANCAGGGAGAGCAGGATCCT 320

CTTCAGCACCTGGAACCTGGATCACATAATAGAAAAGAAACGCACCATCATTCCTACACTGGTGGAAGCAATTAAGGAAC 400

CAAGATGGAAGAGAAGTGGACTGGGAGTATTTTTATGGCCTGCTTTTTACCTCAGAGAACCTAAAACTAGTGCACATTGT 480

CTGCCATAAGAAAACCACCCACAAGCTCAACTGTGACCCAAGCAGAATCTACAAACCCCAGACCAAGGTTGAAGCGGAAG 560

CAGCCTGTGCGGAAACGCCAGTCTAGAGGGCCCGCGGTTCGAAGGTAAGCCTATTCCCTAACCCTCTCCCTCGGTCNTCA 640

GTTTCTACNGCGTAGCCGGCACACCGGAAGGCTGGTTCTCCTGCCAGGGTCCCTTTGACATGGACAGCTGCTTATCAAGA 720

CACTCCATCAACCCCTACAGTAACAGGGAGAGCAGGATCCTCTTCAGCACCTGGAACCTGGATCACATAATAGAAAAGAA 800

ACGCACCATCATTCCTACACTGGTGGAAGCAATTAAGGAACAAGATGGAAGAGAAGTGGACTGGGAGTATTTTTATGGCC 880

TGCTTTTTACCTCAGAGAACCTAAAACTAGTGCACATTGTCTGCCATAAGAAAACCACCCACAAGCTCAACTGTGACCCA 960

AGCAGAATCTACAAACCCCAGACCAAGGTTGAAGCGGAAGCAGCCTGTGCGGAAACGCCAGTCTAGAGGGCCCGCGGTTC 1040

GAAGGTAAGCCTATTCCCTAACCCTCTCCCTCGGTCNTCAGTTTCTACNGCGTAGCCG 1098

Sequencing Result for Plasmid pTracer-hCAD(K155Q)

```
TACGACTCACTATAGGGAGACCCAAGCTGGCTAGGTAAGCTTGGTACCATGCTCCAGAAGCCCAAGAGCGTGAAGCTGCG 80

GGCCCTGCGCAGCCCGAGGAAGTTCGGCGTGGCTGGCCGGAGCTGCCAGGAGGTGCTGCGCAAGGGCTGTCTCCGCTTCC 160

AGCTCCCTGAGCGCGGTTCCCGGCCTGTGCCTGTACGAGGATGGCACGGAGCTGACGGAAGATTACTTCCCCAGTGTTCC 240

CGACAACGCCGAGCTGGTGCTGCTCACCTTGGGCCAGGCCTGGCAGGGCTATGTGAGCGACATCAGGCGCTTCCTCAGTG 320

CATTTCACGAGCCACAGGTGGGGCTCATCCAGGCCGCCCAGCAGCTGCTGTGTGATGAGCAGGCCCCACAGAGGCAGAGG 400

CTGCTGGCTGACCTCCTGCACAACGTCAGCCAGAACATCGCGGCCGAGACCCGGGCTGAGGACCCGCCGTGGTTTGAAGG 480

CTTGGAGTCCCGATTTCAGAGCMAGTCTGGCTATCTGAGATACAGCTGTGAGAGCCGGATCCGGAGTTACCTGAGGGAGG 560

TGAGCTCCTACCCCTCCACGGTGGGTGCGGAGGCTCAGGAGGAATTCCTGCGGGTCCTCGGCTCCATGTGCCAGAGGCTC 640

CGGTCCATGCAGTACAATGGCAGCTACTTCGACAGAGGAGCCAAGGGCGGCAGCCGCCTCTGCACACCGGAAGGCTGGTT 720

CTCCTGCCAGGGTCCCTTTGACATGGACAGCTGCTTATCAAGACACTCCATCAACCCCTACAGTAACAGGGAGAGCAGGA 800

TCCTCTTCAGCACCTGGAACCTGGATCACATAATAGAAAAGAAACGCACCATCATTCCTACACTGGTGGAAGCAATTAAG 880

GAACAAGATGGAAGAGAAGTGGACTGGGAGTATTTTTATGGCCTGCTTTTTACCTCAGAGAACCTAAAACTAGTGCACAT 960

TGTCTGCCATAAGAAAACCACCCACAAGCTCAACTGTGACCCAAGCAGAATCTACAAACCCCAGACAAGGTTGAAGCGGA 1040

AGCAGCCTGTGCGGAAACGCCAGTCTAGA 1069
```

Sequencing Result for Plasmid pTracer-mCAD

GATTCAGGAATAAGTCGGGCTATCTGAGATACAGCTGTGAGAGTCGGATCCGGGGTTACCTAAGAGAGGTGAGCGCTTAC 80

ACCTCTATGGTGGATGAAGCAGCTCAAGAAGAGTACCTGCGAGTCCTTGGCTCCATGTGCCAGAAGCTCAAATCGGTGCA 160

GTACAATGGCAGCTATTTCGACAGAGGTGCAGAGGCCAGCAGCCGCCTCTGTACTCCAGAAGGATGGTTCTCCTGCCAGG 240

GCCCCTTTGACCTGGAGAGCTGTCTTTCCAAGCACTCCATCAACCCCTATGGCAACAGAGAGAGCCGGATCCTCTTCAGT 320

ACCTGGAACCTGGATCATATAATAGAGAAGAAGCGCACCGTGGTACCCACGCTGGCTGAAGCCATCCAGGATGGGAGGGA 400

GGTGAACTGGGAGTACTTCTACAGCCTGCTCTTCACTGCCGAGAACCTGAAGCTGGTGCACATCGCCTGCCANCAAGAAG 480

ACCACACACAAGCTGGAGTGCGACCGCAGTAGGATCTATCGGCCTCAGACAGGATCCAGGAGGAAGCAGCCTGCTCGGAA 560

GAAGCGCCCTGCTCGGAAGCGCTCTAGAGGGCCCGCGGTTCGAAGGTAAGCCTATCCCTAACCCTCTCCTCGGTCTCGAT 640

TCTACGCGTANCCGG 655

Sequencing Result for Plasmid pTracer-mICAD-Ldm

CNGGTACGCGGTAGAATCGAGACCGAGGAGAGGGTTAGGGATAGGCTTACCTTCGAACCGSGGGCCCTCTAGACGAGGAG 80

TCTCGGTTTGGCTCGTTTGGGTCGCTGTGGTTCCCCAGGCAGTGGGCTCCTCCGTTGGCTGATAGATTCCTGAGGTGAAT 160

GCAAGCTCTGCACTTGGCTGCAGCCGCAGGGCGAGCTCCGTGGTGCAGGCCTGCTGGACTGTCTCTGCCTTCCTTATGTC 240

CCAGCTCAGAGCGACAGCCAGGGNCTTTGGGATCCTCCTTGGNAGACAGACTCCAAATCCTGACTAGATAAACTCAGCTC 320

TGGGGCAGGCTTCTCCTTCAGTGTGGTAAGGATCTGGCTTCTGAGCAGCACTTCCGAAGCCATCTCTCTGCCGACGCCTG 400

TTTCAACTGCATCCAGCTCTTCACTGAGGGCAGCTTTGGACTCTTTCTGGTTGGACAAGATGTTGCCCTCTTTCTCCAAG 480

GCCTGGAGGTAAAGTTCCAGGAGCTGCTTGGACTGGCGGGCTTCCTCTCTCTGGTCAAGCACCTGCTGGAGTGTGCTCTG 560

CAGCCCCTGGACAGTGGCACAGCTTTGGCAGAGTTCCTGAGCCAGCTCTGCACATGGGATGTCGATGAGCGCTTGGAGGT 640

CCTCTTCTGACAGCAGGATGATGCTGGACAGATCTTCTTTCAGCTGCCTGGCCACATTCTTCCACTTCACCCCTGCCCTG 720

CTTNCGGCTCATCTGCCTCAAAGGACTCTTGGGNA 755

Sequencing Result for Plasmid pcDNA-mICAD-L

```
ACTCCTATAGGGAGACCAAGCTGGCTAGTTAAGCTTGGTACCATGGAGCTGTCGCGGGGAGCCAGCGCCCCAGACCCGGA 80

CGATGTCCGGCCTCTCAAACCGTGTCTGCTACGCCGCAACCACAGCCGCGATCAGCACGGCGTGGCAGCCTCCAGTCTCG 160

AGGAGCTGAGGAGCAAAGCCTGTGAACTCCTGGCCATTGATAAGTCCCTGACGCCGATCACCCTGGTCCTGGCTGAGGAC 240

GGGACCATAGTGGATGACGATGACTACTTCCTCTGCCTTCCTTCCAATACGAAGTTTGTGGCGTTGGCCTGCAATGAGAA 320

GTGGACTTATAATGATTCCGATGGAGGGACGGCTTGGGTTTCCCAAGAGTCCTTTGAGGCAGATGAGCCGGACAGCAGGG 400

CAGGGGTGAAGTGGAAGAATGTGGCCAGGCAGCTGAAAGAAGATCTGTCCAGCATCATCCTGCTGTCAGAAGAGGACCTC 480

CAAGCGCTCATCGACATCCCATGTGCAGAGCTGGCTCAGGAACTCTGCCAAAGCTGTGCCACTGTCCAGGGGCTGCAGAG 560

CACACTCCAGCAGGTGCTTGACCAGAGAGAGGAAGCCCGCCAGTCCAAGCAGCTCCTGGAACTTTACCTCCAGGCCTTGG 640

AGAAAGAGGGCAACATCTTGTCCAACCAGAAAGAGTCCAAAGCTGCCCTCAGTGAAGAGCTGGATGCAGTTGACACAGGC 720

GTCGGCAGAGAGATGGCTTCGGAAGTGCTGCTCAGAAGCCAGATCCTTACCACACTGAAGGAGAAGCCTGCCCCAGAGCT 800

GAGTTTATCTAGTCAGGATTTGGAGTCTGTCTCCAAGGAGGATCCCAAAGCCCTGGCTGTCGCTCTGAGCTGGGACATAA 880

GGAAGGCAGAGACAGTCCAGCAGGCCTGCACCACGGAGCTCGCCCTGCGGCTGCAGCAAGTGCAGAGCTTGCATTCACTC 960

AGGAATCTATCAGCAAGGAGGAGCCCACTGCCTGGGGAACCACAGCGACCCAAACGAGCCAAACGAGACTCCTCGTAGTC 1040

TAGAGGGCCCGCGGTTCGAAGGTAAGCCTATCCCTAACCCTCTCCTCGGTCTCGATTCTACGCGTACCGGTCATCATCAC 1120

CATCACCATTTGAGTTTAAACCCGCCTGATCA 1152
```

**APPENDIX J**

**SIMPLIFIED BLOOD AND CELL CULTURE DNA MINI KIT (QIAGEN) PROTOCOL**

**Dislodged cells in 15 ml screw cap tube**

↓

**Centrifuge (in Eppondorf 5810 R) at 1,500 xg/rcf, 7 min, 4°C**

↓ Discard supernatant

**Add in 3 ml of cold PBS onto the cell pellet**

↓

**Vortex at 1600/min to resuspend the cell pellet**

↓

**Centrifuge at 1,500 xg/rcf, 10 min, 4°C**

↓ Discard supernatant

**Add in 0.5 ml of cold PBS to resuspend the cell pellet**

↓

In 15 ml screw cap tube: **Add in 0.5 ml cold C1** (- lyse cells but preserves nuclei)

↓

**Add in 1.5 ml cold sdH2O** (invert to mix)

↓

**Incubation on ice for 10 min**

↓

**Centrifuge at 1,300 xg/rcf, 15 min, 4°C**

↓ Discard supernatant

**Add in 0.25 ml cold C1 and 0.75 ml cold sdH2O (vortex to resuspend)**

↓

**Centrifuge at 1,300 xg/rcf, 15 min, 4°C (discard supernatant)**

↓ Thaw Qiagen protesase

Purification**:** **Add in 1 ml G2 (vortex 2,200/min, 10 sc)**

↓

**Add in 25 µl of QIAGEN protease (vortex 1,400/min)**

↓

**Incubation at 50°C for 30 – 60 min**

↓ Warm up QF buffer at 55°C to increase yield

**Equilibrate QIAGEN-Tip with 2 ml of QBT (by gravity flow)**

↓

**Vortex sample at 2,200/min and load to Q-Tip immediately**

↓

**Wash sample with 3 times of 1 ml buffer QC by gravity flow**

↓

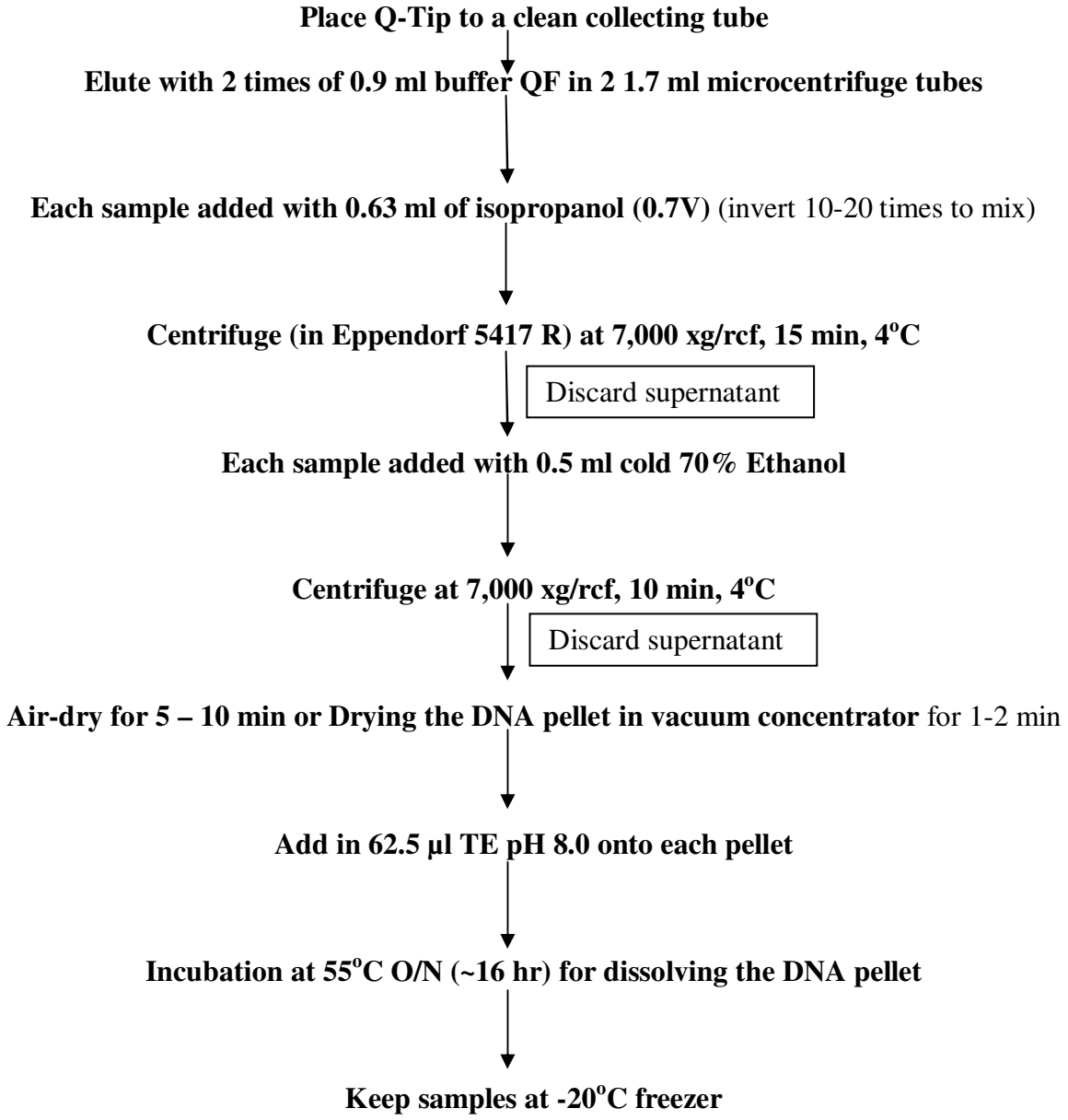
Place Q-Tip to a clean collecting tube
Elute with 2 times of 0.9 ml buffer QF in 2 1.7 ml microcentrifuge tubes
Each sample added with 0.63 ml of isopropanol (0.7V) (invert 10-20 times to mix)
Centrifuge (in Eppendorf 5417 R) at 7,000 xg/rcf, 15 min, 4°C
Discard supernatant
Each sample added with 0.5 ml cold 70% Ethanol
Centrifuge at 7,000 xg/rcf, 10 min, 4°C
Discard supernatant
Air-dry for 5 – 10 min or Drying the DNA pellet in vacuum concentrator for 1-2 min
Add in 62.5 µl TE pH 8.0 onto each pellet
Incubation at 55°C O/N (~16 hr) for dissolving the DNA pellet
Keep samples at -20°C freezer

## APPENDIX K

## ETHANOL PRECIPITATION PROTOCOL

From klenow and ligation:

300 µl sample gDNA

+ 30 µl 3M NaAcetate (pH 5.2) (0.1V)

+ 750 µl ice cold absolute ethanol (2.5µl)

↓

flicking several times / vortexing

↓

-70$^{o}$C freezer for 15 min

↓

Centrifuge: max. speed – 14,000 rpm, 10 - 15 min

↓

Remove supernatant

↓

+ 1 ml rt 70% EtOH, invert few times

↓

Centrifuge: max. speed – 14,000 rpm, 10 min

*(Note: Pour supernatant/ pipette out. Subsequently, spin briefly and pipette the remaining supernatant away and air dry for about 5 min to avoid over drying)*

↓

Air-dry / or in concentrator

↓

Redissolve in 50 µl TE buffer

**APPENDIX L**

**QIAquick NUCLEOTIDE REMOVAL KIT PROTOCOL**

**Add 10V of Buffer PN to 1V reaction sample & mix**

↓

**Place a QIAquick spin column in a provided 2 ml collection tube**

↓

**Bind DNA: Apply the sample to the QIAquick column**

↓

**Centrifuge: 6000 rpm, 1 min**

↓

**Wash QIAquick column**

↓

**Add 750 µl of Buffer PE**

↓

**Centrifuge: 6000 rpm, 1 min**

↓

**Discard flow-through**

↓

**Place the QIAquick column back in the same empty tube**

↓

**Centrifuge: 13,000 rpm, 1 min**

↓

**Place the QIAquick column in a clean 1.5 ml microcentrifuge tube.**

↓

**<u>Elute DNA:</u> Add 100 – 200 µl of Buffer EB or $H_2O$ to the center of the QIAquick membrane.**

↓

**Centrifuge: 13,000 rpm, 1 min.**